The University Of Sheffield.

Impacts of sub-ambient and elevated CO_2 on above- and below-ground microbial interactions with Arabidopsis.

Alex Williams

Department of Animal and Plant Science,

The University of Sheffield

Thesis submitted for the degree of Doctor of Philosophy

Submitted: December 2017

This work is dedicated to Pauline Williams.

The most beautiful life I knew.

Abstract

Over recent years, an increasing body of evidence has suggested that elevated atmospheric CO_2 concentrations can alter plant microbial interactions. However, there is limited consensus whether these impacts will be positive or negative for plants in terms of disease resistance. Accordingly, there is a pressing need to gain a better understanding of the molecular and physiological mechanisms by which CO_2 shapes the plant's ability to interact with its biotic environment, which is essential to predict impacts of future climate scenarios on crop production.

The work described in this thesis has used a range of CO_2 concentrations, from past through present to future predicted concentrations, to study the immune response of the model plant *Arabidopsis thaliana* to aboveground pathogens and belowground rhizosphere bacteria. Furthermore, a novel developmental correction was established, which enables assessing the direct immunological effects of CO_2 on microbial interactions without bias from age-related resistance arising from the stimulatory effects of CO_2 on plant development.

Changes in disease resistance at elevated CO_2 (eCO_2), against the necrotrophic fungus *Plectosphaerella cucumerina* (*Pc*) and the obligate biotrophic oomycete *Hyaloperonospora arabidopsidis* (*Hpa*) were associated with changes in production and sensitivity of the phytohormones jasmonic acid (JA and salicylic acid (SA), respectively. However, priming of SA-dependent defence was not the only mechanisms contributing to eCO_2-induced resistance against *Hpa*. The increased resistance to *Hpa* at sub-ambient CO_2 ($saCO_2$) against *Hpa* operated independently of SA signaling and was associated with changes in cellular redox state and priming of pathogen-inducible intracellular ROS. Based on the defence phenotypes of knock-down mutants in glycolate oxidase, the H_2O_2-generating enzyme of the photorespiration cycle, and transcriptional profiling of the peroxisomal catalase gene *CAT2*, it is proposed that the enhanced *Hpa* resistance at $saCO_2$ is controlled by photorespiratory ROS.

Below-ground, the root colonisation of a specialised rhizobacterial strain *Pseudomonas simiae* WCS417 was found to be dependent on CO_2 concentration

and soil-nutritional status, whereas root colonisation by the soil saprophytic strain *Pseudomonas putida* KT2440 was largely unaffected by these variables. Hence, changes in atmospheric CO_2 have a greater impact on specialist rhizosphere microbes. Furthermore, the ability of *P. simiae* WCS417 to promote plant growth and elicit an induced systemic resistance (ISR) was highly dependent on CO_2 and nutritional status of the soil. These results suggest that the effects of atmospheric CO_2 on rhizosphere microbes depend on the rhizosphere species in question and the nutritional status of the soil.

To obtain a more global impression of the impacts of CO_2 on rhizosphere interactions, rhizosphere soil was studied for bacterial community diversity and composition using PCR-based community profiling techniques. This revealed that CO_2 has a measurable impact on microbial communities in a time-point dependent manner, whereby the effects of *e*CO_2 are more pronounced at earlier stages and the effects of *sa*CO_2 are more pronounced at later stages. To study the biochemical basis of these CO_2 effects on the rhizosphere effect, a new mass spectrometry-based method was developed to study quantitative and qualitative impacts of CO_2 on non-sterile rhizosphere chemistry. These experiments revealed that the diversity of chemical signals greatly increases with rising CO_2 concentrations, and that *sa*CO_2 and *e*CO_2 are associated with rhizosphere enrichment of different classes of chemicals.

Together, the results presented in this thesis provide novel insights into the mechanisms by which plants have adapted to past CO_2 climates, and the potential impacts by which future CO_2 scenarios will affect interactions with hostile and beneficial microbes. Further research is required to explore the combined impacts of *e*CO_2 and other environmental changes due to global climate change, such as elevated temperatures and drought.

Table of Contents

Abbreviations and nomenclature

ABA	Abscisic acid
a- e - saCO_2	Ambient, elevated, sub-ambient CO_2
AMF	Arbuscular mycorrhizal fungi
ARR	Age-related resistance
C	Carbon
CFC	Chlorofluorocarbon
CFU	Colony forming unit
DAB	3,3'-diaminobenzidine
DAMP	Damage associated molecular pattern
DC	Devlopmental correction
DCFH-DA	2',7'-dichlorofluorescein diacetate
DIMBOA	2,4-dihydroxy-7-methoxy-2H-1,4-benzoxazin-3(4H)-one
DNA	Deoxyribonucleic acid
dpg	Days post germination
dpi	Days post inoculation
DW	Dry weight
eCO_2	Elevated CO_2
ESI	Electropray (positive or negative mode)
ET	Ethylene
ETI	Effector triggered immunity
ETS	Effector triggered susceptibility
FACE	Free air CO_2 enrichment
FAM	6-fluorescein amidite
FDR	False discovery rate
FW	Fresh weight
GFP	Green fluorescent protein
GHG	Green-house gas
gs	Stomatal conductance
Hpa	*Hyaloperonospora arabidopsidis*
hpi	Hours post infection
HR	Hypersensitive response
IPCC	International panel on climate change
ISR	Induced systemic resistance
JA	Jasmonic acid
LB	Lysogeny broth
LN	Leaf number
MS	Mass spectrometry
mya	Million years ago
N	Nitrogen
NAD	Nicotinamide adenine
NB-LRR	Nucleotide binding lucine rich repeats

nMDS	Non-parametric multi-dimensional scaling
NO	Nitrous oxide
NSC	Non-structural carbohydrates
nt	Nucleotide
OTC	Open top chamber
OTU	Operational taxonomic unit
P	Phosphorous
PAL	Phenylalanine ammonia lyase
PAMP	Pathogen associated molecular pattern
Pc	*Plectospharella cucumerina*
PCA	Principal component analysis
PCR	Polymerase chain reaction
PDA	Potato dextrose agar
PGPF	Plant growth promoting fungi
PGPR	Plant growth promoting rhizobacteria
PR	Pathogenesis related
PRR	Pattern recognition receptors
Pst	*Pseudomonas syringae*
PTI	Pattern triggered immunity
Q-TOF	Quadrupole time-of-flight
R	Resistance protein
RCP	Representative concentration pathway
RH	Relative humidity
RNA	Ribonucleic acid
ROS	Reactive oxygen species
RT-qPCR	Reverse transcription quantitative PCR
SA	Salicylic acid
saCO_2	Sub-ambient CO_2
SAR	Systemic acquired resistance
SD	Stomatal density
TAE	Tris acetate ethylenediaminetetraacetic acid
TIC	Total ion current
T-RF	Terminal-restriction fragment
T-RFLP	Terminal-restriction fragment length polymorphism
TYLCV	Tomato yellow leaf curl virus
UPLC	Ultra Performance Liquid Chromatography
YFP	Yellow fluorescent protein

List of tables and figures

Chapter 1: General Introduction

1.1 Introduction

Plants employ their immune system to manage interactions with a wide range of microorganisms, above- and below-ground. These interactions can be beneficial or detrimental to plant health, depending on the microbe in question, the host plant and the prevailing environmental conditions (Newton et al., 2010). Over the last few decades, the molecular mechanisms driving these processes have been investigated extensively, but knowledge gaps remain. A central component of these interactions involves immune regulation by phytohormonal signalling networks. For instance, the phytohormones salicylic acid (SA), jasmonic acid (JA), ethylene (ET) and abscisic acid (ABA) all play major roles in the maintenance of plant immunity, through complex, and interlinked, signalling networks (Bari and Jones, 2009; Pieterse et al., 2009). Many of these phytohormones are involved in interactions with pathogens and beneficial rhizosphere microorganisms (Carvalhais et al., 2013). However, the identity of root-exuded chemical signals that govern the recruitment and/or selection of beneficial microbes in the rhizosphere are less clear (Haldar and Sengupta, 2015). Furthermore, our knowledge about how environmental factors, such as those imposed by anthropogenic changes to the global climate, will affect plant hormonal signalling, and how this will alter the plant's immune function and its communication with pathogens and rhizosphere microbiota, remains poorly understood.

Rising levels of carbon dioxide (CO_2) are caused directly by combustion of fossil fuel and indirectly through land use changes, such as deforestation (Pielke, 2005; Cook et al., 2016). Increases in CO_2 have generally stimulatory effects on plant growth, yield, reproductive fitness and photosynthetic efficiency, known as the CO_2 fertilisation effect (Ainsworth and Rogers, 2007). However, rising CO_2 will also increase the occurrence of extreme weather events, such as heat waves and drought (Hansen et al., 2012), which are detrimental to crop development and yield (Gray and Brady, 2016). The beneficial effects of CO_2 fertilisation are not predicted to sufficiently offset the negative impacts of climate

change (Long et al., 2006). Consequently, in socio-economic terms, the negative effects of climate change will be of global significance, resulting in widespread malnutrition from unsuitable or unproductive agricultural land (Fischer et al., 2005). Most future emission scenarios, modelled and published by the intergovernmental panel on climate change (IPCC, 2013), predict a stark decline in agricultural land, due to longer and more widespread periods of aridity, as well as rising sea levels encroaching on coastal areas (United Nations, 2015). Possible increases in global crop prices will focus economic pressure on developing countries and could result in widespread civil conflict (Hanjra and Qureshi, 2010). Moreover, an increasing body of evidence suggests that rising CO_2 concentrations will influence the outcome of plant-pathogen interactions (Eastburn et al., 2011) and interactions with rhizosphere-inhabiting microbes (Gschwendtner et al., 2015), thereby affecting plant development and crop yield. This introduction aims to highlight the current knowledge about impacts of atmospheric CO_2 on plant-microbe interactions, and identify knowledge gaps regarding the effects of CO_2 on plant immunity and rhizosphere interactions.

1.2 Shifting global climate.

1.2.1 The greenhouse effect and the importance of CO_2.

To predict how plants respond to changes in global atmospheric CO_2, it is important to understand *i)* how plants have adapted to past atmospheric CO_2 concentrations and *ii)* how plants respond to future CO_2 concentrations. CO_2 is an important gas for global temperature regulation. The Earth warms due to the constant exposure to short-wave solar energy. Subsequent long-wave radiation, emitted by Earth, is 'trapped' and redirected by atmospheric 'greenhouse' gases (GHGs), causing tropospheric warming via the greenhouse effect (Donohoe et al., 2014). Without this greenhouse effect, our planet would maintain a global temperature of -18°C, which is 33°C colder than the current average temperature of 15°C (Lacis et al., 2010). A few major atmospheric gases are involved in the greenhouse effect, predominantly water (which contributes 75% of the warming effect) and CO_2 (which contributes 20%), with the remaining contributions from methane, ozone, N_2O and chlorofluorocarbons (together, 5%; Lacis et al., 2010). Once present in the atmosphere, GHGs can have a long-lasting contribution to

global climate (Archer et al., 2009). Furthermore, their warming effect will modulate the influence of the hydrological cycle on the global climate (Lacis et al., 2010).

1.2.2 Past CO_2 concentrations.

Deuterium ratios and CO_2 measurements from the Vostock ice-cores, indicate that cycles of CO_2 and temperature are strongly coupled over the last 800 k years (Petit et al., 1999; Fig. 1.1 a). Within this time-frame, the Earth has consistently experienced periods of interglacial warming and glacial cooling every 100 k years (Fig. 1.1 a). These cycles are thought to occur through the combined influence of solar insolation, changes in biosphere and ocean chemistry (with resultant carbon-cycle feedbacks) and orbital forcing (Ganopolski and Calov, 2011). Switches are often followed by increases in global CO_2 concentration, due to release of CO_2 from deglaciation (Shakun et al., 2012), which then drives further increases in global temperature. The importance of CO_2 as a GHG has been further demonstrated through radiative forcing models where removal of CO_2 from the atmosphere results in rapid global cooling (Lacis et al., 2010).

To understand plant responses to CO_2, it is important to consider their evolution in context of Earth's CO_2 history. Land plants evolved around 476 million years ago (mya) in the mid Ordovician period (Gray, 1993; Kenrick and Crane, 1997). Flowering plants became prevalent in the Cretaceous around 90mya, but diversified much earlier (Qiu et al., 1999). This means that modern plant species have repeatedly been exposed to periods of extreme global warming and high CO_2, alternated with glacial periods of low CO_2 (see Fig. 1.1 c). For instance, the flowering plant *Arabidopsis thaliana*, which is commonly used to study molecular-genetic mechanisms of plant development and plant-environment interactions, diverged in a period of relatively low CO_2 (~ 200 ppm) during the Miocene (Beilstein et al., 2010; Beerling and Royer, 2011). Experiments at sub-ambient CO_2 (*sa*CO_2) conditions can reveal new insights about the physiological and metabolic plant functions that were necessary to adapt and survive over past glacial periods (Ward and Gerhart, 2010).

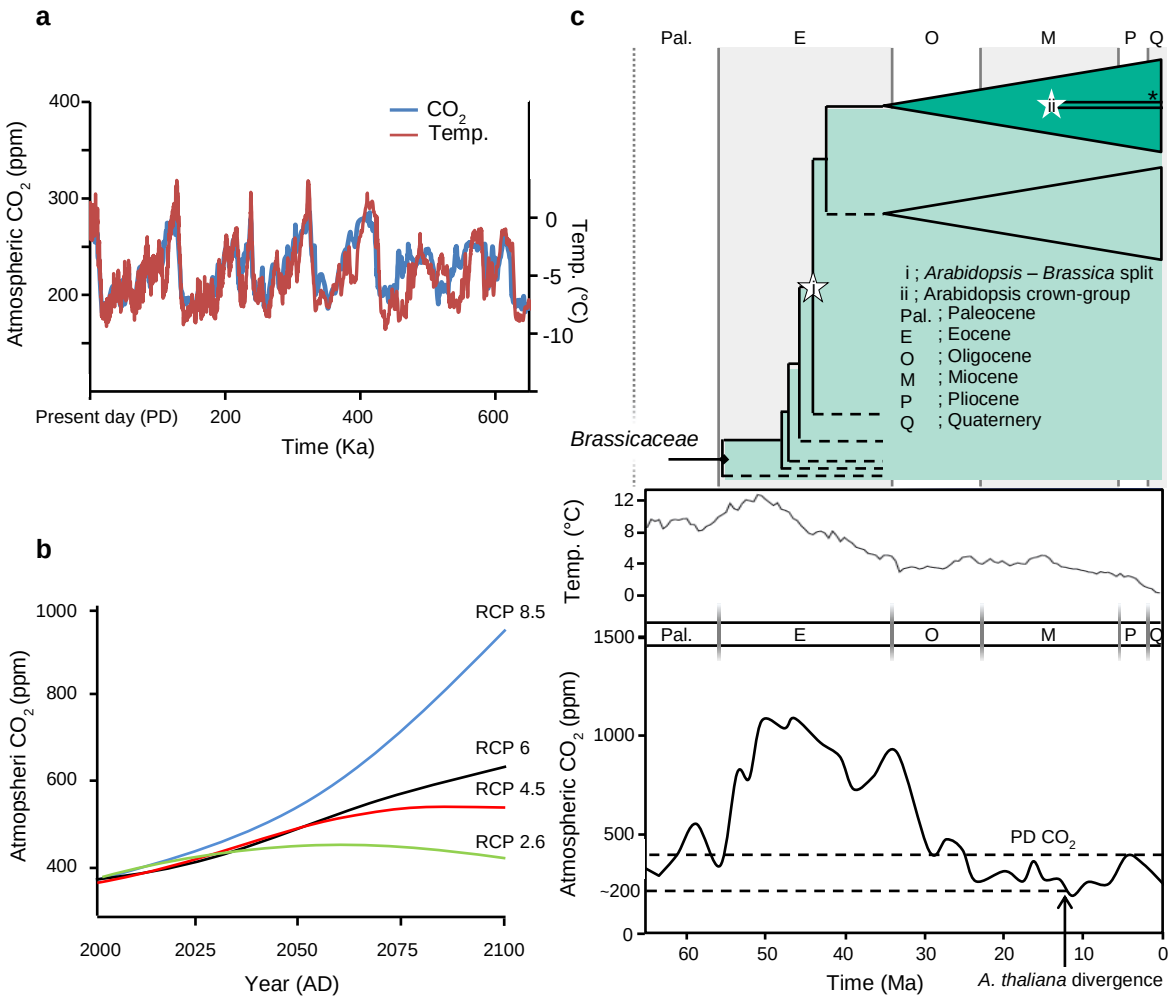

Figure 1.1. Ancestral and future atmospheric CO_2 and global temperature in relation to *Brassicaceae* divergence. **a**, Past atmospheric CO_2 concentration over the Quatenary period (adapted from publicly available Vostock data - www.ncdc.noaa.gov; Petit et al., 1999). The data illustrates the Pleistocene's characteristic 100kyr punctuations of cooling and warming for the last 600 k years, directly influenced by temporally fluctuating CO_2. **b**, Present day CO_2 exceeds 400 ppm, higher than any level within the Quaternary period. A multi-model summary of projected CO_2 levels is presented. These representative concentration scenarios use economic and social predictions to estimate the future climate. These attribute different weights to population expansion, equality, economic growth, advancement of technology, public education and emphasis on sustainability and environment. RCP8.5 is representative of scenarios that result in high GHG concentrations (Riahi et al., 2011). RCP6 is a stabilisation scenario where the application of a range of technologies and strategies reduce GHG emissions (Masui et al., 2011). RCP4.5 is a scenario where stabilisation occurs after 2100, without exceeding global targets (Thomson et al., 2011). RCP2.6 is a scenario where GHGs are reduced considerably (van Vuuren et al., 2011b). **c**, Ancestral climatic levels of CO_2 estimated from proxy data, temperature and *Brassicaceae* evolution from molecular data have been amalgamated to produce a 'consensus' of historic CO_2 values (adapted from Beilstein et al., 2010; Beerling and Royer, 2011). CO_2 data are largely in agreement, despite there being a high level of variance at some of the earlier time periods. Around 13mya, during the divergence of *A. thaliana* from its close relative *Arabidopsis lyrata*, the consensus of atmospheric CO_2 in this time-period is ~200ppm, compared to 400ppm of present day (PD).

1.2.3 Current and future CO_2 projections.

Since 1852, the concentration of atmospheric CO_2 has risen steeply from ~280 ppm to over 400 ppm (IPCC, 2013). As the population of the world increases, so does the demand for energy to fuel economic development. Due to government subsidies for coal power, and storage restrictions for sustainable

alternatives, current energy supplies are provided predominantly through combustion of fossil fuels (Goldemberg, 2006). Although there is a global government initiative to reduce international carbon emissions, this falls short of what is required to meet warming targets, partly because they ignore long-term feedbacks (Hansen et al. 2007; Hansen et al. 2008). Thus, phasing down emissions is as much a political issue as it is a humanitarian necessity (Obama, 2017). In the UK, policy includes energy based carbon budgets which are implemented to reduce the carbon cost of buildings, industry, transport and the implication of renewable sources of energy production (Department of Energy and Climate Change, 2011). The current target in the EU is at 2°C above pre-industrial levels (EU, 2005), which implies an atmospheric concentration of 450 ppm CO_2 should not be exceeded (Hansen et al. 2007). Depending on international adherence to such carbon targets, there are various projections of future CO_2 concentrations and the climate (Fig. 1.1 b; van Vuuren et al., 2011a). These scenarios stipulate that to stay within CO_2 and temperature targets, fossil-fuel based power needs to be globally phased out within the next decade (Hansen et al., 2008). Currently, renewable sources of energy are becoming cheaper and more viable solutions (REN 21, 2017), and many countries are already generating a significant proportion of their domestic energy through renewables (for instance the share for the UK is 22.2% with 28.8% for the EU and 8.4% in the US). Adherence to warming targets would result in a more positive future climate scenario (Fig. 1.1b), and may provide a better opportunity to effectively manage global agriculture and food production. In addition, if handled correctly, policy informing adherence to these targets should not be a detriment to economic growth (Obama, 2017). Without such measures, atmospheric CO_2 will likely exceed 1000 ppm over the next century (van Vuuren et al., 2011a).

Nevertheless, if atmospheric CO_2 concentrations exceed 1000 ppm, it will be critical to understand the direct impacts of increasing CO_2 on plant development and environmental interactions, such as resistance to pathogens. Accurate predictions of the ways by which increased CO_2 affect plant life and agricultural efficacy will determine how well people can adapt to an uncertain future (Hanjra and Qureshi, 2010). Of major interest are the effects of CO_2 on disease resistance, singularly and in unison with extreme weather events

(Rosenzweig et al., 2014). For instance, it is estimated that a loss of approximately $5 billion USD in annual crop revenue can be attributed to global warming (Lobell and Field, 2007), but how much of this is due to altered plant-pathogen interactions remains undefined. Certainly, range, duration of infection, and disease severity have been reported to increase for many economically important crop diseases due to warming (Sharma et al., 2007; Evans et al., 2008; Laine, 2008). Although most studies agree that rising CO_2 will have an effect on plant-pathogen interactions, there is little consensus whether these impacts will be positive or negative on crop production, especially when considering other factors associated with global climate change (Eastburn et al., 2011). Hence, there are pressing social and financial incentives to understand the effects of increasing CO_2 levels on both natural and agricultural plant production systems.

1.3 Plant perception, recognition and responses to pathogenic microbes.

The current thesis focuses on the interactive effects of CO_2 concentration and plant responses to microorganisms, both pathogenic and beneficial. A critical factor in plant survival is strict transcriptional control used to manage and alleviate biotic stresses, such as pathogen challenge. Activation of stress-inducible defences are costly and often occur at the expense of growth or other cellular functions (Herms and Mattson, 1992; Walters and Heil, 2007). As such, regulation is stringently controlled and tolerant to minor stress (Heil, 2002). Depending on the type and perceived severity of the threat, plants can tailor the amplitude and timing of their immune response though specialised defence signalling cascades. Plant pathogens are often categorised by their trophic mode; necrotrophic pathogens lyse and feed off living cells, whereas biotrophic pathogens require living cells for sustenance. The majority of attackers are hemibiotrophic pathogens, which employ an initial biotrophic stage, followed by the necrotrophic infection strategy.

Biotrophic pathogens are predominantly detected by recognition of pathogen associated molecular patterns (PAMPs; (Zipfel and Felix, 2005). Typically, PAMPs are highly conserved molecules shared between a range of microbial taxa. A well-known example is flg22, which is a highly conserved 22 amino acid fragment of flagellin, the structural protein in flagellar filaments of

bacteria (Felix et al., 1999; Boller and Felix, 2009). Recognition of PAMPs results in pattern-triggered immunity (PTI), which confers a broad-spectrum protection against many potentially hostile microbes. Some pathogens produce effectors that actively subvert the PTI response, resulting in effector-triggered susceptibility (ETS). The plant counteracts ETS through the production of resistance proteins, which can recognise and bind to specific effectors, or act to protect the molecular target on which the pathogen effectors acts (McDowell and Woffenden, 2003). Effector-triggered immunity (ETI) invariably results in resistance through the hypersensitive response (HR; Greenberg, 1997). Many of the downstream defences contributing to ETI are controlled by, or associated with, the phytohormone salicylic acid (SA; Vlot et al., 2009), which has been implicated multiple times in enhanced resistance at *e*CO_2 (*e.g.* Mhamdi & Noctor 2016). Unlike PTI, whose targets are highly conserved, ETI is subject to adaptive diversification as pathogens shed or adapt ineffective effectors, or synthesise novel ones that suppress ETI. Plants are therefore under selection to evolve new R proteins to combat these ETI-suppressing effectors (Abramovitch et al., 2006; Fu et al., 2007; Cui et al., 2009; Houterman et al., 2009). Hence, plants and pathogens maintain an evolutionary 'arms race', the outcome of which depends on the equilibrium between the pathogen's ability to supress the immune system and plant's capacity to recognise the pathogen. As a result, the frequency of resistance (R) proteins and effectors in any given host-pathogen population are in constant flux (Dangl and Jones, 2001; Jones and Dangl, 2006).

ETI confers no protection against necrotrophic organisms, which destroy and feed from lysed host cells. HR response causes cell lysis which can further facilitate necrotrophic infection (Glazebrook, 2005). To resist necrotrophs, plants have evolved an alternative immune strategy that is largely under control by the phytohormone JA (Pozo et al., 2005; Bari and Jones, 2009). Local recognition of damaged-self, through damage associated molecular patterns (DAMPs), results in a systemic activation and priming of JA-dependent defences (Wasternack and Hause, 2013). Despite the differences in recognition, both DAMP- and PAMP-triggered immunity are dependent, to an extent, on the co-receptor BAK1 (Chinchilla et al., 2009), indicating that these processes share common signalling steps. The spatially regulated suppression of JA by SA and the downstream

defence regulator NPR1 (Koornneef et al., 2008) illustrated that the activation of SA- and JA-dependent defences is carefully controlled (Glazebrook et al., 2003). Another hormone, ABA, is linked to plant growth and the regulation of defence responses to abiotic stress, such as drought and high temperatures, as well as responses to *e*CO_2 (Sah et al., 2016; Zhou et al., 2017). ABA is also involved in early immune responses to pathogens, where it controls PAMP-induced stomatal closure, as well as the localised accumulation of reactive oxygen species (ROS) and callose. At later stages of infection, ABA modulates the intensity and specificity of SA- and JA-dependent defence responses (Ton et al., 2009). The fact that all of these hormones play an active role in immunity, while also controlling elements of plant development, highlights the importance of hormonal networks to simultaneously coordinate growth and defence.

1.4 Elevated CO_2 effects on plant pathogen interactions.

1.4.1 Impacts of eCO_2 on plant physiology.

Direct effects of climate change on plants are multifaceted. For instance, many crops produce sub-optimal yields when grown outside of a certain temperature range (*e.g.* in rice and maize (Amthor, 2001; Luo, 2011). Furthermore, RuBisCO activity can be drastically reduced by elevated levels of O_3 (Krupa et al., 2000), while drought can have severe impacts on plant both above- and below-ground physiology and development (Farooq et al., 2009; Song et al., 2012). Furthermore, plant interactions with pathogens can be exacerbated by changing environmental conditions (Boyer, 1995; Mcelrone et al., 2005).

Elevated CO_2 (*e*CO_2) promotes above- and below-ground generation of biomass (Hovenden and Williams, 2010) and development. This includes the initiation of flowering (Pritchard et al., 1999; Springer and Ward, 2007) and developmental changes in foliar nutrient composition (Conroy, 1992; Teng et al., 2006). Generally, *e*CO_2 benefits reproductive fitness through increased production of flowers and fruit (~19% and 18% respectively), as well as increased seed mass (4%; Jablonski et al., 2002). Free air CO_2 enrichment (FACE) experiments have shown that augmentation of developmental and reproductive traits are linked to enhanced C sequestering due to increased rates of

photosynthesis and enhanced water use efficiency (Leakey et al., 2009). Although *e*CO_2 boosts biomass as a result of greater C sequestering, the nutritional value of the foliar material may decline, as C:N increases. Decreased tissue N generally reduces palatability of foliar tissues to herbivores and pathogens (Taub and Wang, 2008); although see Robinson et al., 2012). Changes in C:N also present a problem agriculturally, as the nutritional value of seed and fruit are compromised by *e*CO_2 (seed N decreases by 14%; (Jablonski et al., 2002). Below-ground, *e*CO_2 is often reported to decrease root:shoot ratio, suggesting much of the additionally sequestered C is used to boost leaf development (Miri et al., 2012).

1.4.2 A meta-analysis of the impacts of eCO_2 on plant disease.

Despite the wealth of information about the effects of CO_2 on plant morphology and physiology, there is currently limited consensus about the impacts of CO_2 on plant resistance to pathogens. To date, 72 studies have tested various host-plant interactions with multiple different pathogens (Table 1.1; plant-herbivore interactions have also been studied in detail, but these are outside the scope of this project – reviewed by Robinson et al., 2012). Of those, 31 plant-pathogen interactions have positive outcomes for host resistance, 19 have negative outcomes and 22 report no change in host resistance (Table 1.1). Some studies link the disease phenotype to altered leaf development. For example, at *e*CO_2 *Stylosanthes scabra* develops twice as many lesions from the canker causing fungus, *Colletotrichum gloeosporioides,* than at ambient CO_2 (aCO_2; Pangga et al. 2004), which is related to an increased canopy size and catchment surface for spore attachment. Interestingly, these data contrasted with reports that *C. gloeosporioides* shows reduced virulence at *e*CO_2 (Chakraborty & Datta 2003). Plant size and leaf surface area are often reported as factors contributing to increased disease incidence at *e*CO_2 (*e.g.* Eastburn et al., 2010; Melloy et al., 2014), although biomass and surface area have been shown to increase in instances where disease severity was reduced (Kretzschmar et al., 2009; Runion et al., 2010; dos Santos et al., 2013). Hence, plant responses to pathogens at *e*CO_2 likely involve other aspects of pre- and post-invasive immunity. For example, reduced stomatal density and stomatal aperture, have been reported to

play a role in pathogen resistance at *e*CO_2 (Lake and Wade, 2009; Eastburn et al., 2010; Li et al., 2014b; Zhang et al., 2015; Zhou et al., 2017)

1.4.3 CO_2 and pre-invasive resistance.

Although leaf traits, such as surface area, biomass and RGR, increase at *e*CO_2, stomatal development is reduced. Furthermore, stomatal conductance (g_s) decreases at increasing CO_2 levels, due to an over-abundance of C (Ainsworth and Rogers, 2007). This occurs either through a reduction in stomatal density, or through reduced stomatal aperture. Early work has established an inverse relationship between stomatal density and CO_2 concentration (Beerling & Kelly 1997; Penuelas & Matamala 1990; Woodward & Kelly 1995). This correlation was so strong that stomatal measurements on fossil plants are now commonly used as a proxy method for gathering data on paleo-CO_2 (Royer, 2001). The relationship between CO_2 and stomatal density is reliant on the action of the *HIC* gene (High Carbon Dioxide), which acts as negative regulator of stomatal development at *e*CO_2 (Gray et al., 2000). Interestingly, some experimental data indicate no change, or even an increase in stomatal density at eCO_2 under more complex scenarios (Estiarte et al., 1994; Bettarini et al., 1998; Lake and Wade, 2009). For many foliar pathogens, natural openings, like stomata and hydathodes, are an important entry point into the leaf (Melotto et al., 2006; Sawinski et al., 2013). So, the higher the stomatal density, the more opportunity there is for pathogen invasion (Jordá et al., 2016). Strict control over stomatal development and aperture in response to infection is therefore an important feature of pre-invasive defence, which may increase by higher concentrations of atmospheric CO_2. However, there is a great deal of inconsistency in the literature about the contribution of pre-invasive stomatal defence to disease resistance. For instance, increased resistance to *Pseudomonas syringae* pv. *tomato* DC3000 (*Pst*) in tomato at *e*CO_2, was associated with smaller stomatal apertures (Li et al., 2014b; Zhang et al., 2015), while another study revealed reduced resistance to *Pst* at eCO2 (Zhou et al., 2017). Counterintuitively, at eCO_2, significant increases in stomatal density and trichrome numbers after *Erysiphe cichoracearum* (powdery mildew) infection are linked to increased susceptibility (Lake and Wade, 2009), even though this pathogen is not known to infect via stomata (Schulze-Lefert and Vogel, 2000). While both partial closure, and decreased stomatal

density, can limit pathogen entry, reduced g_s at *e*CO_2 has also been shown to increase canopy temperatures through decreased transpirational cooling (Ziska and Bunce, 1997). This additional factor may act as an compounding factor on disease severity (Garrett et al., 2006). In tomato, bypassing stomatal immunity by syringe infiltration of *Pst*, resulted in elevated levels of *Pst* resistance at *e*CO_2 (Li et al., 2014b), whereas Zhou et al. (2017) reported enhanced *Pst* susceptibly under these conditions in Arabidopsis. In summary, it is difficult to gauge a consistent pattern from the literature about the potential impacts of *e*CO_2 on pre-invasive defence. However, the majority of studies suggest that *e*CO_2 may increase the effectiveness of pre-invasive defence by boosting stomatal immunity.

1.4.4 CO_2: an enhancer or suppressor of post-invasive defences?

Plant exposure to *e*CO_2 results in changes in resource allocation (Berger et al., 2007), which influences profiles of secondary metabolites (Lavola et al., 2000; Kuokkanen et al., 2001; Matros et al., 2006) that in turn play an important role in post-invasive defence against pathogens. Changes in leaf chemistry at *e*CO_2 have been linked to a decrease in *Phyllosticta minima* disease in *Acer rubrum* (Mcelrone et al. 2005). Specifically, increases in leaf tannins and phenolic content were recorded at *e*CO_2. Furthermore, enhanced production of defence-related secondary metabolites, such as phenolics, flavonoids and glucosinolates, as well as increases in phenylalanine ammonia lyase (PAL) activity, have been associated with *e*CO_2 in various plant species (Matros et al., 2006; Kretzschmar et al., 2009; Mathur et al., 2013). As PAL is a key enzyme in alternate SA biosynthesis (Seyfferth and Tsuda, 2014), the dominant view supports that increased defence against biotrophic pathogens at *e*CO_2 is associated with SA. Indeed, SA-controlled defence-related (*PR*) genes, such as *PR-1*, *PR-2* and *PR-5*, have been shown to be expressed to higher levels in Arabidopsis at *e*CO_2, including the SA isochorismate biosynthesis gene, *ICS1* (Mhamdi and Noctor, 2016). Increased *PR* gene expression at *e*CO_2 was also reported in tomato leaves and roots (Jwa and Walling, 2001), while increased activity of the PR protein β-1,3-glucanase and osmotin were found during infection of potato by *Phytophthora* pathosystem (Plessl et al., 2007; Liu et al., 2013). Moreover, multiple studies have recorded increased levels of total SA in different plant

species, including Arabidopsis, tobacco, tomato, maize, barley and wild bean (Jwa and Walling, 2001; Matros et al., 2006; Huang et al., 2012; Zhang et al., 2015; Mhamdi and Noctor, 2016). Together, these data indicate that *e*CO_2 augments basal and/or pathogen-inducible SA levels. Other defence hormones have received considerably less attention, such as jasmonic acid (JA) signalling, which controls post-invasive defences against necrotrophs (Turner et al., 2002).

Remarkably, of the 19 cases reporting a repressive effect of *e*CO_2 on plant resistance, 7 involve necrotrophic pathogens (24%; Table 1.1). By contrast, of the 29 cases reporting a stimulatory effect of *e*CO_2 in resistance, only 3 involve necrotrophic pathogens (10%; Table 1.1). This disparity suggests that *e*CO_2 generally represses host resistance against necrotrophic infection. Nevertheless, some studies on tomato reported enhanced JA accumulation at *e*CO_2 during infection by *Pst* and tomato yellow leaf curl virus (TYLCV), respectively (Huang et al., 2012; Zhang et al., 2015). However, *Pst* is a (hemi)biotroph that uses coronatine to activate JA signalling and suppress SA (Block et al., 2005), which may become more effective at *e*CO_2 (Zhou et al., 2017), whereas the mechanisms of resistance against TYLCV, although not fully understood, involve SA and not JA (Moshe et al., 2012). Furthermore, basal transcription of JA related genes, *LOX3*, *OPR3*, *JAZ10* and *PDF1.2*, in Arabidopsis correlated with resistance against the necrotrophic fungus *Botrytis cinerea* at *e*CO_2 (Mhamdi and Noctor, 2016). However, more conclusive evidence from basal resistance phenotypes of JA signalling mutants remained absent. In contrast to these studies with tomato and Arabidopsis, exposure of maize and tea to *e*CO_2 was found to suppress JA signalling and increase susceptibility to *Fusarium* rot and *Colletotrichum* blight, respectively (Vaughan et al., 2014; Li et al., 2014b). Lipoxygenase, which is involved in the initial steps of JA synthesis, is encoded by a diverse family of *LOX* genes (Turner et al., 2002). In maize, immune suppression against *Fusarium* was associated with a decrease in *LOX* gene expression, with the notable exception of *LOX2*, the function of which is undetermined, and *LOX10*, which only has a putative function in JA production (Chauvin et al., 2013). In addition, JA production to infection, as well as downstream production of the anti-fungal phytoalexins, zealexin and kaualexin, were lower at *e*CO_2. In tea, LOX activity and associated gene expression

Table 1.1. A summary of the known changes in disease response in plants at eCO_2.

Disease severity		Observations	Set.[c]	CO_2 (p.pm)	Pathogen	Type[d]	Reference
Decreased							
Hyaloperonospora brassicae (downy mildew) and *Alternaria brassicae* (blight)	*Brassica juncea* (mustard)[a]	C, C:N, S:N increase, N decrease. Increase in sugar, phenolics, glucosinolates and PAL activity	FACE	550	Biotroph, necrotroph	Constant	Mathur *et al.* 2013
Puccinia psidii (rust)	*Eucalyptus globulus* (blue gum)[a]	Decreased C:N, increased growth. Essential oils unaffected	CEF/ OTC	750	Biotroph	Constant	Ghini *et al.* 2014
Ampelomyces quisqualis (leaf spot) and *Podosphaera xanthii* (powdery mildew)	Cucurbita pepo (Zucchini)[a]	Fungicides unaffected by CO_2	CEF	800	Biotroph	Semi-constant	Gilardi *et al.* 2017
Ceratocystis fimbriata (wilt)	*Eucalyptus urophylla* (rose gum)[a]	Growth increased, C increased, N decreased	CEF	553;878	Necrotroph	Constant	dos Santos *et al.* 2013
Erysiphe graminis (powdery mildew)	*Hordeum vulgare* (barley)[a]	Reduction in photosynthesis; decline in carboxylation efficiency; silicon accumulation (contrasting results). Leaf age affects response	CEF	700	Biotroph	Constant	Hibberd *et al.* 1996a, 1996b
Pseudomonas syrinage (DC3000)	*Solanum lycopersicum* (tomato)[a]	Lower stomatal aperture, controlled by NO. Increased SA and JA accumulation	CEF	800	Biotroph	Pulse	Li *et al.* 2014; Zhang *et al.* 2015
Pseudomonas syrinage (DC3000)	*Arabidopsis thaliana* (thale cress)[a]	Increased SA accumulation and transcripts. Evidence for a role of redox activity	CEF	1000	Biotroph	Constant	Mhamdi & Noctor 2016
Tomato mosaic virus (TMV)	*Solanum lycopersicum* (tomato)[a]	Increased SA and JA accumulation	CEF	800	Biotroph	Pulse	Huang *et al.* 2012; Zhang *et al.* 2015
Blumeria graminis (powdery mildew)	Hordeum vulgare (barley)[a]	Decreased stomatal conductance	CEF	700	Biotroph	Constant	Mikkelsen *et al.* 2014
Potato virus Y (PVY)	*Nicotiana tabacum* (tobacco)[a]	Increased phenylpropanoids; PAL; altered C:N; and SA production, as well as lignification. Decreased nicotine production.	CEF	1000	Biotroph	Constant	Matros *et al.* 2006
Puccinia sparganioides (rust)	*Scirpus olneyi* (sedge)[a]	Reduced N	FACE	700	Biotroph	Constant	Thompson & Drake 1994
Peronospora manshurica (downy mildew)	*Glycine max* (soybean)[a]	No changes in stomatal density; defence expression not measured. No noted changes in N, C:N or phenolics	FACE	550	Biotroph	Constant	Eastburn *et al.* 2010
Cronartium quercuum (fusiforme rust)	*Pinus taeda* (loblolly pine)[a] and Quercus rubra (northern red oak)[a]	Increased height and stem diameter	FACE	720	Biotroph	Constant	Runion *et al.* 2010
Fusarium circinatum (pitch canker)	*Pinus taeda* (loblolly pine)[a]	As above	FACE	720	Biotroph	Constant	Runion *et al.* 2010
Erysiphe alphitoides (powdery mildew)	*Quercus mongolica* (Japanese oak)[a]	Increased height, diameter and mass, as well as carboxylation and electron transport rates	FACE	500	Biotroph	Semi-constant	Watanabe *et al.* 2014
Phythophthora sojae (root rot elicitor)	*Glycine max* (soybean)[a]	Increased leaf areas and photosynthesis, glyceollin (phytoalexin) but only in resistant cultivar	FACE	720	Biotroph	Constant	Braga *et al.* 2006
Phythophthora sojae (root rot elicitor)	*Glycine max* (soybean)[a]	Increased growth, photosynthetic assimilation, altered C:N, defence related flavonoids and intermediates	FACE	760	Biotroph	Constant	dos Santos Kretzschmar *et al.* 2009
Phytophthora parasitica (black shank)	Lycopersicon esculentum (tomato)[a]	Increased PR mRNAs in roots. Slight changes in PR mRNAs and wound response genes in leaves and slight changes in SA and ABA levels.	CEF	700	Hemibiotroph	Pulse	Jwa & Walling 2002
Phytophthora infestans (late blight)	*Solanum tuberosum* (potato)[a]	Increased expression of PR-proteins 3-1,3-glucanase and osmotin in leaves	CEF	700	Hemibiotroph	Constant	Plessl *et al.* 2007
Colletotrichum gloeosporioides (anthracnose)	*Stylosanthes scabra* (legume)[a]	Reduced incubation period, germtube growth, appressoria production. Increased disease severity in field conditions	CEF	700	Hemibiotroph	Constant	Chakraborty *et al.* 2000; Chakraborty & Datta 2003
Phyllosticta minima (leaf spot)	*Acer rubrum* (maple)[a]	Reduced stomatal conductance and aperture; Reduced N; Increased C:N ratio, phenolics and tannins.	FACE	600	Hemibiotroph	Semi-constant	Mcelrone *et al.* 2005
Cercospora species	*Solidago rigida* (goldenrod)[a]	Reduced N; Reduced photosynthetic rate	FACE	560	Hemibiotroph	Constant	Strengbom & Reich 2006
Cylindrocladium candelabrum (leaf spot)	*Eucalyptus urophylla* (eucalypt)[a]	Increases in height, shoot and root weight	CEF	645; 904 1147	Hemibiotroph	Pulse	Silva *et al.* 2014
Potato virus Y (PVY)	*Nicotiana benthamiana* (tobacco)[a]		OTC	750	Virus	Constant	Ye *et al.* 2010
Fusarium pseudograminearum (crown rot)	*Triticum aestivum* (wheat – various cultivars)[a]	Increased dry weight and size. Severity very dependent on cultivar used	CEF	690	Hemibiotroph	Constant	Melloy *et al.* 2014
Potato virus X (PVX)	*Nicotiana benthamiana* (tobacco)[a]	Temp increased resistance, ROS production increased and pathogen virulence proteins decreased	CEF	970	Virus	Constant	Aguilar *et al.* 2015

[a] – C_3 photosynthesis; [b] – C_4 photosynthesis; [c] - Setting refers to the type of facility used where CEF is controlled environment facility, FACE is free air CO_2 enrichment and OTC is open topped chambers in field sites;

[d] - Constant CO_2, plants grown from seed; Pulse, plants moved to high CO_2 before experiment; Semi-constant, plants were grown initially in ambient before relocation to eCO_2 for between 2 weeks and 4 years depending on the species and experimental design.

Disease severity		Observations	Set.[c]	CO_2 (ppm)	Pathogen	Type[d]	Reference
Botrytis cinerea (grey mould)	*A. thaliana* (thale cress)[a]	Increased JA transcripts. Evidence for a role of redox activity	CEF	1000	Necrotroph	Constant	Mhamdi & Noctor 2016
Increased							
Pseudomonas syringae (DC3000)	*Arabidopsis thaliana* (thale cress)[a]	Decreased stomatal aperture. Disease symptoms unaffected.	CEF	800	Biotroph	Semi-constant	Zhou *et al.* 2017
Erysiphe cichoracearum (powdery mildew)	*Arabidopsis thaliana* (thale cress)[a]	Increased stomatal density; increased guard cell length; increased trichrome numbers	CEF	800	Biotroph	Constant	Lake & Wade 2009
Albugo candida (rust)	*Brassica juncea* (mustard)[a]	Increase carbohydrates.	FACE	550	Biotroph	Constant	Mathur *et al.* 2013
Pyricularia oryzae (blast)	*Oryza sativa* (rice)[a]	Lower silicon content	FACE	650	Biotroph	Constant	Kobayashi *et al.* 2006
Phytophthora cactorum, P. plurivo (root rot)	*Fagus sylvatica* (beech)[a]	Root pathogen – interesting question, poorly executed	CEF	800	Hemibiotroph	Constant	Tkaczyk *et al.* 2014
C. gloeosporioides (anthracnose)	Stylosanthes scabra (shrubby stylo)[a]	Increased canopy size	CEF/ FACE	700	Hemibiotroph	Constant	Pangga *et al.* 2004
Cercospora (leaf spot)	*Cercis canadensis* (redbud) and Liquidambar styraciflu (sweet gum)[a]	Increased photosynthetic efficiency mitigating effects.	FACE	580	Hemibiotroph	Semi-constant	McElrone *et al.* 2010
Various fungal pathogens (leaf spot)	various C_3 grasses[a]	More prominent at low community diversity	FACE	560	Hemibiotroph	Constant	Mitchell *et al.* 2003
F. pseudograminearum (crown rot)	*Triticum aestivum* (wheat – various cultivars)[a]	Increased dry weight and size. Severity very dependent on cultivar used	CEF	690	Necrotroph	Constant	Melloy *et al.* 2014
F. verticillioides (rot)	*Zea mays* (maize)[b]	Decreased fumonisin production, increased intracellular CO_2, decreased stomatal conductance, decreased JA, LOX activity and phytoalexin production in response to infection	CEF	720	Hemibiotroph	Constant	Vaughan *et al.* 2014
Septoria glycines (brown spot)	*Glycine max* (soybean)[a]	Increased plant height and canopy density. Barely passable increase in disease severity	FACE	550	Necrotroph	Constant	Eastburn *et al.* 2010
Rhizoctonia solani (sheath blight)	*Oryza sativa* (rice)[a]	Increased number of tillers	FACE	560	Necrotroph	Constant	Kobayashi *et al.* 2006
Phytophthora citricola (root rot)	*Fagus sylvatica* (beech)	Increased biomass when N increases. Infection slightly mitigated by N. Survivors more resistant in F2	FACE		Necrotroph	Constant	Fleischmann & Oswald 2010
F. pseudograminearum (crown rot)	*Triticum aestivum* (wheat)	Pathogen fitness drastically increases, could effect F2	CEF/ FACE	550	Necrotroph	Constant	Melloy *et al.* 2010
C. gloeosporioides (brown blight)	*Camellia sinensis* (tea)a	Suppresses JA and caffeine accumulation	CEF	800	Necrotroph	Pulse	Li et al 2016
Unknown fungal pathogen	*Spartina patens* (C_4 grass)[b]	Increased water content	FACE	700	Unknown	Constant	Thompson & Drake 1994
Barley yellow dwarf virus (BYDV)	*Triticum aestivum* (wheat)[a]	Increased virus titre. Growth parameters less affected by infection at eCO2	CEF	650	Virus	Pulse	Trębicki et al. 2015
F. graminearum (blight)	Triticum aestivum (wheat)[a]	*Fusarium* acclimated to eCO_2 was effective against resistant cultivar	CEF	780	Hemibiotroph	Constant	Váry *et al.* 2015
Septoria tritici (blotch)	*Triticum aestivum* (wheat)[a]	Both pathosystems enhanced yield loss particularly when acclimated	CEF	780	Necrotroph	Constant	Váry *et al.* 2015
No Change							
Erysiphe graminis (powdery mildew)	Triticum aestivum (wheat)[a]	Reduced Nitrogen content; increased water content	CEF	700	Biotroph	Constant	Thompson *et al.* 1993
Erysiphe necatrix (powdery mildew)	*Vitis vinifera* (grapevine)[a]	Increased chlorophyll content, intercellular carbon and photosynthesis.	CEF	799	Biotroph	Constant	Pugliese *et al.* 2010
Podosphaera xanthii (powdery mildew)	*Cucurbita pepo* (zucchini cv. Genovese)[a]	Increased intercellular carbon and photosynthesis. Decreased chlorophyll content	CEF	800	Biotroph	Constant	Pugliese *et al.* 2012
Melampsora medusae (leaf rust)	Populus tremuloides (aspen)[a]	Increased growth; changes in cuticular wax deposition and composition	FACE	550	Biotroph	Constant	Karnosky *et al.* 2002; Percy *et al.* 2002
Bipolaris sorokiniana (spot blotch)	Hordeum vulgare (barley)[a]	Decreased stomatal conductance	CEF	700	Hemibiotroph	Constant	Mikkelsen *et al.* 2014
Pyrenopeziza betulicola (leaf spot)	*Betula pendula* (silver birch)[a]	Reduction in stomatal conductance	FACE	700	Hemibiotroph	Pulse	Riikonen *et al.* 2008
Various fungal pathogens (leaf spot, rust, powdery mildew)	various C_4 grasses, forbs and legumes[b]	Increased infection with added N	FACE	560	(Hemi)biotroph	Constant	Mitchell *et al.* 2003

[a] – C_3 photosynthesis; [b] – C_4 photosynthesis; [c] - Setting refers to the type of facility used where CEF is controlled environment facility, FACE is free air CO_2 enrichment and OTC is open topped chambers in field sites;

[d] - Constant CO_2, plants grown from seed; Pulse, plants moved to high CO_2 before experiment; Semi-constant, plants were grown initially in ambient before relocation to eCO_2 for between 2 weeks and 4 years depending on the species and experimental design.

Disease severity		Observations	Set.[c]	CO_2 (p.pm)	Pathogen	Type[d]	Reference
Phytophthora cajani (blight)	Cajanus cajan (pigeonpea)a	Incubation period delayed eCO_2, lower colonisation	CEF	500-700	Hemibiotroph	Constant	Sharma *et al.* 2015
F. virguliforme (sudden death syndrome)	*Glycine max* (soybean)[a]	No reported changes	FACE	550	Hemibiotroph	Constant	Eastburn *et al.* 2010
F. pseudograminearum (crown rot)	Triticum aestivum (wheat)[a]	Increased *F. pseugograminearum* biomass. Sacrophytic capacity unaffected	FACE	550	Hemibiotroph	Constant	Melloy *et al.* 2010
Septoria glycines (brown spot)	*Glycine max* (soybean) [a]	Increased plant height and canopy density. More severe in combination with O_3	FACE	550	Necrotroph	Constant	Eastburn *et al.* 2010
F. culmorum and *F. pseudograminearum* (crown rot)	Triticum aestivum (wheat – various cultivars)[a]	Huge effect of successive cycles. Susceptible cultivar more effected. Huge amount of inherent variation.	FACE	700	Hemibiotroph	Constant	Khudhair *et al.* 2014
Various fungi	*Ambrosia artemisiifolia* (ragweed)[a]	Decreased association with penicillium	FACE	550	Various	Semi-constant	Ruion *et al.* 2014
F. pseudograminearum (crown rot)	Triticum aestivum (wheat – various cultivars)[a]	Increased dry weight and size. Severity very dependent on cultivar used	CEF	690	Hemibiotroph	Constant	Melloy *et al.* 2014
Various pathogens	Prairie legume	Generalist herbivores associated with height, negatively correlated with pubescence. Opposite for specialists.r	FACE	560	Various	Constant	Lau *et al.* 2008
Puccinia striiformis (stripe rust)	*Triticum aestivum* (wheat)[a]		FACE	820	Biotroph	Constant	Chakraborty *et al.* 2011
Various fungal pathogens	*Coffea arabica* (coffee)[a]	N decreased, photosynthetic rate increased	FACE	550	Various	Constant	Ghini *et al.* 2015
Collectotrichum gloeosporioides (anthracnose)	*Stylosanthes scabra* (pencilflower)[a]	Increased leaf canopy affect production and dispersal of spores	CEF/ FACE	700	Hemibiotroph	Constant	Chakraborty *et al.* 2000
Erysiphe graminis (powdery mildew), *Puccinia* species (rust) *Septoria tritici* (leaf blotch)	*Triticum aestivum* (wheat)[a] and *Brassica napus* (rapeseed)[a]	Bioass, N and C unaffected	FACE	550	Biotroph	Constant	Oehme *et al.* 2013
F. oxysporum (wilt)	*Lactuca sativa* (lettuce)[a]	Total bacterial abundance reduced. Temp increased disease	CEF	800	Necrotroph	Constant	Feroccino *et al.* 2013
Puccinia recondite (leaf rust)	*Triticum aestivum* (wheat)[a]	Increased photosynthetic rate, WUE, biomass, conductance. Decreased ozone sensitivity	FACE	610	Biotroph	Constant	Tiedemann & Firshing 2000

[a] – C_3 photosynthesis; [b] – C_4 photosynthesis; [c] - Setting refers to the type of facility used where CEF is controlled environment facility, FACE is free air CO_2 enrichment and OTC is open topped chambers in field sites;

[d] - Constant CO_2, plants grown from seed; Pulse, plants moved to high CO_2 before experiment; Semi-constant, plants were grown initially in ambient before relocation to eCO_2 for between 2 weeks and 4 years depending on the species and experimental design.

were decreased at *e*CO_2 (Li et al., 2016). Furthermore, soybean showed reduced levels of *LOX7* and *LOX8* gene expression at *e*CO_2, which was associated with increased herbivory by the Japanese beetle and corn root worm (Zavala et al., 2008). It has been proposed that elevated SA levels at *e*CO_2 can suppress JA-dependent defences against herbivores (DeLucia et al., 2012). However, this hypothesis has not been validated and it remains unclear whether this type of signalling cross-talk could affect resistance against necrotrophic pathogens at *e*CO_2. Thus, the majority of studies suggest that *e*CO_2 represses resistance against necrotrophic pathogens, but contrasting reports about the effects of *e*CO_2 on JA signalling merits further investigation.

The signalling pathways controlled by defence regulatory hormones interact strongly with primary metabolism (Rojas et al., 2014), which could have a contribution to *e*CO_2-induced resistance. For instance, a recent study demonstrated that *e*CO_2-induced increased resistance in Arabidopsis against *Pst* is associated with altered redox status (Mhamdi and Noctor, 2016). At *e*CO_2, the metabolic profiles were radically different from air-grown plants and, upon further analysis, it became clear that transcription of genes controlling antioxidants and ROS homeostasis, such ascorbate and glutathione, were enhanced at *e*CO_2. Furthermore, mutants in NADH generating enzymes (*i.e. np-gapdh* and *nadp-me2*), which play important roles in redox homeostasis, were impaired in *e*CO_2-induced resistance against *Pst*. Changes in primary metabolite profiles of the plants, such as enhanced amino acid profiles and non-structural carbohydrate (NSC) contents (Mathur et al., 2013; Mhamdi and Noctor, 2016), may have a contribution to this process. For instance, sugar signalling has been shown to regulate redox homeostasis and (a)biotic stress responses (Keunen et al., 2013). Together, these data highlight the need for further research that focuses specifically on the link between plant development and primary metabolism, on the one hand, and post-invasive defences, on the other hand.

1.4.5 Host defence responses to sub-ambient CO_2.

The effects of sub-ambient CO_2 (*sa*CO_2) on disease resistance is less well studied than the effects of *e*CO_2. Over shorter than evolutionary time scales, CO_2 has been relatively constant, although fluctuations occur along altitude gradients,

seasons and day/night cycles (Brooks et al., 1997). However, due to anthropogenic climate change, plants are currently experiencing unprecedented rates by which atmospheric CO_2 is changing, potentially outpacing the evolutionary adaptation of plant metabolism. This is highlighted in Arabidopsis, where no changes in developmental responses were reported over 15 generations of exposure to *e*CO_2 (Teng et al., 2009). On the other hand, herbarium records show that stomatal density has decreased in response to post-industrial rises in CO_2 (Woodward and Kelly, 1995). Whether such CO_2-related changes are the result of genetic adaptation or phenotypic plasticity, remains a matter of debate (Ward and Gerhart, 2010). Despite the physiological ability of plants to adapt to changing CO_2 concentrations, our current crops are genetically very similar to their ancestral species that survived under the low atmospheric CO_2 concentrations of relatively recent glacial periods (Badr and El-Shazly, 2012). Accordingly, one could argue that our current crop germplasm is genetically adapted to cope with *sa*CO_2 conditions, rather than the predicted *e*CO_2 levels in the near future.

The impacts of *sa*CO_2 on plant immune signalling and disease resistance remain poorly understood. A transcriptomic analysis of Arabidopsis at *sa*CO_2 (Li et al., 2014c) uncovered increased expression of photorespiration-related genes at *sa*CO_2. Interestingly, in addition to redox regulatory genes (*e.g. CAT2, APX1, GST, AOX1D*), plants at *sa*CO_2 also displayed increased transcription of defence-related genes, such as *ICS1, PR1, LOX3, MYC2, ERF1-1*. Although these data are too preliminary to support conclusions about effects of *sa*CO_2 on disease resistance, they indicate changes in primary metabolism that favour immunity, which is supported by other studies. For instance, in peppermint, it was shown that secondary metabolites, such as terpenoids, were increased at *sa*CO_2 (Forkelova et al., 2016). Moreover, the relative investment of winter wheat in non-structural carbohydrates and phenylalanine-derived secondary metabolites, such as ferulic acid, luteolin, chrysoeriol, tricin, apigenin and putrescine, is enhanced at *sa*CO_2, indicating that stress tolerance takes priority over development at *sa*CO_2 (Huang et al., 2017). Such trade-offs between primary and secondary metabolism may have aided plants in reaching an optimum balance between growth and stress tolerance in a carbon-limited environment over recent

glacial periods. In contrast to the above studies, a study on *Sequoia sempervirens* reported reduced investment in foliar phenolic defence compounds, which may repress pathogen resistance at *sa*CO_2 (Quirk et al., 2013). Remarkably, there is only one study that has directly addressed the impacts of *sa*CO_2 on disease resistance: Zhou et al. (2017) showed in Arabidopsis that *sa*CO_2 increases resistance to *Pst* (Zhou et al., 2017). This resistance was associated with reduced levels of ABA that cause insensitivity to the *Pst* effector coronatine, which counters pre-invasive defence by inducing stomatal re-opening. While enhanced stomatal immunity may explain part of this *sa*CO_2-induced resistance, *sa*CO_2-exposed plants were still more resistant after leaf infiltration with *Pst* (Zhou et al., 2017), suggesting involvement of additional post-invasive defences. As ABA acts as a repressor of SA-dependent defences (Moeder et al., 2010), the observed reduction in ABA signalling at *sa*CO_2 may play a role in *sa*CO_2-induced resistance against (hemi)biotrophic pathogens (Zhou et al., 2017). Whether attenuation of infection at *sa*CO_2 is specific to Arabidopsis and/or (hemi)biotrophic pathogens, and whether other defence regulatory mechanisms than ABA and stomatal immunity are involved as well, remains to be investigated. In particular, further research is required to better understand plant metabolic responses to *sa*CO_2, which would allow greater insight into the conditions under which plant metabolism evolved over recent glacial periods.

1.5 Interactions with below-ground beneficial microbes.

The rhizosphere can be defined as the thin layer of root-surrounding soil that is under direct physio-chemical and biological influence from plant roots (Bakker et al., 2013). From a biological and biochemical perspective, the rhizosphere is a dynamic system, shaped not only by soil type, plant species and associated microbes (Berg and Smalla, 2009), but also influenced by the environmental conditions to which the plant is exposed (Classen et al., 2015). The rhizosphere often contains higher microbial titres than the surrounding soil as it contains higher concentration of plant-derived organic matter, which provides substrate for microbial growth (Lugtenberg and Kamilova, 2009). In particular, carbon (C) is present in higher concentrations in plant root exudates and occurs in more digestible forms than other soil-based C, including organic acids such as malate and citrate (Rengel and Marschner, 2005). The beneficial

association between plants and mutualistic rhizosphere organisms relies mostly on plant-derived C and requires intricate coordination between both organisms. For instance, plants recognise plant-growth promoting rhizobacteria (PGPR) through microbe-associated molecular patterns (MAMPs; often equivalent to PAMPs), which can result in PTI (Millet et al., 2010). However, the intensity of PTI during beneficial interactions can be subdued, either by plant-mediated suppression of the immune response (Maunoury et al., 2010), or by PTI-suppressing effectors from the mutualist (Zamioudis and Pieterse, 2012). There is increasing evidence that JA and ET signalling play important roles in mediating associations with beneficial microbes (Van Wees et al., 2008; Van der Ent et al., 2009; Jung et al., 2012), indicating that plants use defence hormones to coordinate long-range responses and gain selective control of the extent and expense of the association. For example, plants can limit endophytic colonisation by nitrogen-fixing rhizobia through JA-mediated autoregulation of nodulation (Nakagawa and Kawaguchi, 2006; Oka-Kira and Kawaguchi, 2006).

PGPR benefit plant development through a combination of mechanisms. Apart from mobilising insoluble phosphates and nitrates (Vessey, 2003; Vassilev et al., 2006), growth stimulation can occur directly through microbial production of growth hormone homologues, such as auxin, brassinolids and cytokinins (Ping and Boland, 2004), suppression of ethylene production (Glick et al., 2007), and manipulation of ABA signalling to stimulate photosynthesis (Zhang et al., 2008). Growth stimulation can also occur indirectly through competitive exclusion of soil-borne pathogens (Bolwerk et al., 2003; Kamilova et al., 2007), including the production of antibiotics (Lugtenberg and Kamilova, 2009), competition for micro-nutrients, such as iron, and signal disruption by degradation of quorum sensing molecules (Lin et al., 2003). Importantly, certain PGPR and plant-growth promoting fungi (PGPF), such as mycorrhiza, elicit an induced systemic resistance (ISR) response (van Loon et al., 1998; Van Wees et al., 2008; Pineda et al., 2010; Lakshmanan et al., 2013). ISR can provide an advantage to plants, especially in environments with heightened disease pressure or limiting nutrient availability. Research on the Arabidopsis - *Pseudomonas simiae* WCS417 interaction has revealed important regulatory mechanisms driving the ISR response. WCS417-mediated ISR in Arabidopsis relies on an ethylene- and JA-

dependent signalling pathway (van Loon et al., 1998) and results in systemic priming of SA-independent defences (Verhagen et al., 2004; Van der Ent et al., 2009). More recent work on this model system has revealed that root colonisation by *P. simiae* WCS417 triggers a MYB72-dependent iron starvation response that results in the synthesis of iron-mobilizing phenolic metabolites and their release into the rhizosphere through activity of the beta-glucosidase BGLU42 (Zamioudis et al., 2014). In a subsequent paper, Zamioudis et al (2015) showed that the onset of ISR and the accompanying iron deficiency response is triggered by WCS417-produced volatile organic compounds (VOCs). Interestingly, the associated gene expression response to WCS417 in roots was dependent on CO_2 and photosynthesis, indicating that atmospheric CO_2 controls the rhizosphere interaction with ISR-eliciting PGPRs (Zamioudis et al., 2015).

Effective communication between plants and rhizosphere microbes requires specialised chemical signals (semiochemcials) that are produced and perceived by both plants and microbes. The chemical exudation profile from plant roots is complex (Uren, 2007), and varies according to plant species, plant age, microbiome context, and physiochemical soil properties (Gregory, 2007). The role of root-exuded primary and secondary metabolites as chemo-attractants is well established (Barbour et al., 1991; Dharmatilake and Bauer, 1992; Kape et al., 1992; Pandya et al., 1999). Flavonoids, strigolactones, organic acids, and benzoxazinoids have been reported to stimulate colonisation by beneficial PGPRs, rhizobia and PGPFs (Dharmatilake and Bauer, 1992; Steinkellner et al., 2007; Neal et al., 2012; Lakshmanan et al., 2013). Despite this knowledge, the specificity of chemotaxis-inducing and/or biocidal secondary metabolites to beneficial rhizosphere microbes remains relatively unknown. Organic acids have been demonstrated to trigger positive chemotaxis in PGPR. One example from root-exuded malic acid, which recruits the beneficial PGPR *Bacillus subtilis* F17 (Lakshmanan et al., 2013). As malic acid is a primary metabolite and, therefore, an easily accessible C source, it seems unlikely that this chemical has a specific signalling function in the rhizosphere. Benzoxazinoids, such as DIMBOA, have also been shown to recruit beneficial *Pseudomonas putida* KT2440 to the rhizoplane of maize (Neal et al., 2012). DIMBOA is a tryptophan-derived secondary metabolite with antibacterial activity (Guo et al., 2016). In contrast to

other soil bacteria, *P. putida* KT2440 is highly tolerant to the biocidal activity of DIMBOA and activates genes controlling a positive chemotactic response when exposed to DIMBOA (Neal et al., 2012). Although KT2440 can persist saprophytically in soil without roots, it colonises the rhizosphere of plants, where it can elicit an ISR response (Matilla et al., 2010) and prime JA-dependent defences (Neal and Ton, 2013).

Systematic studies of rhizosphere chemistry present practical problems due to the difficulty in defining the rhizosphere in spatial terms, which makes it difficult to obtain chemical extracts from rhizosphere soil without mechanically damaging delicate root tissues. This explains why most profiling studies of root exudation chemistry are based on sterile, hydroponically cultivated, root systems (van Dam and Bouwmeester, 2016), even though these profiles will be fundamentally different than the *in situ* chemistry of microbially diverse, non-sterile, rhizosphere soil, which is arguably the most important factor for biological interactions in the rhizosphere.

1.6 Effects of CO_2 on belowground interactions in rhizosphere.

1.6.1 Effects of CO_2 on rhizosphere chemistry.

Knowledge regarding the effects of CO_2 on root exudation profiles remains fragmented. Most studies are limited to specific classes of chemicals or global estimations of total C budget. Moreover, many reports seem to contradict each other (Rice et al., 1994; Ross et al., 1995; Kassem et al., 2008; Eisenhauer et al., 2012).. At ambient CO_2 concentrations, it has been estimated that up to 30% of all assimilated C is exuded by the plant in ambient conditions (Bais et al., 2006). Although concrete evidence remains scarce, it is generally assumed that increasing CO_2 concentrations stimulate exudation of C-based chemistry into the rhizosphere (Phillips et al., 2009; Eisenhauer et al., 2012). Clearly, more research is needed to validate these assumptions and identify the quantitative and qualitative changes in root exudation and/or rhizosphere chemistry at changing atmospheric CO_2 concentrations.

The impact of *e*CO_2 on root-exuded primary metabolites has been investigated in rye grass (*Lolium multiflorum*), bean (*Phaseolus vulgaris*) and barley (*Hordeum vulgare*), where it was found that exuded amino acid profiles remained unaffected by *e*CO_2 (Phillips et al., 2006; Haase et al., 2007). By contrast, Calvo et al. (2017) reported reduced levels of amino acids in root exudates of barley at *e*CO_2 (Calvo et al., 2017), which occurred in a growth-stage dependent manner. The latter findings may be relevant for the composition of the microbial community in the rhizosphere, since rhizobacteria commonly respond to amino acids with positive chemotaxis (Nelson, 2004). Additionally, Calvo et al. (2017) reported cultivar-dependent changes at *e*CO_2 in phytohormones, including indole acetic acid, IAA, cytokinins and auxin, (Calvo et al., 2017). Many rhizosphere microbes manipulate these hormones to aid in root colonisation and growth promotion, indicating that they may play a key role in rhizosphere communication at *e*CO_2 (Garcia de Salamone et al., 2001; Khalid et al., 2004; Ahmad et al., 2005). Notably, most analyses of root exudation chemistry at *e*CO_2 involve targeted quantifications of specific classes of metabolites (*i.e.* amino acids, sugars or hormones), whereas a more comprehensive un-targeted profiling of rhizosphere chemistry at *e*CO_2 has never been conducted.

Untargeted metabolite profiling by tandem mass spectrometry provides a powerful and accurate tool to identify a range of primary and secondary metabolites that could potentially influence rhizosphere interactions, including amino acids, phytohormones, coumarins, flavonoids, organic acids, glucosinolates and oxylipins (Strehmel et al., 2014). However, these profiling techniques are typically performed on plants grown in hydroponic sterile conditions. Considering that active semio-chemcials in the rhizosphere can be microbial products that are derived from root exudates or produced *de novo* by rhizosphere-inhabiting microbes, the chemical exudation profiles from sterile roots might miss important chemical signals (van Dam and Bouwmeester, 2016). Recently, Pétriacq et al. (2017) have developed a non-sterile cultivation system that allows for the collection of extracts from plant-free and plant-containing soils (Pétriacq et al., 2017; Appendix 1). This method is based on comparisons between untargeted mass-spectrometry-based profiles from extracts of plant-free and plant-containing soils. Subsequent statistical filtering for markers that are

statistically enriched in extracts from plant-containing pots, allows for quantitative and qualitative analysis of rhizosphere chemistry from different plant-soil combinations. A further advantage of the method developed by Pétriacq et al. (2017) is that it enables profiling of microbial communities. The possibility of simultaneously profiling rhizosphere chemicals and rhizosphere microbes entails a powerful new technique to establish causal relationships between rhizosphere chemistry to rhizosphere microbiota. In this context, the method by Pétriacq et al. (2017) would provide a very attractive approach to study the impacts of CO_2 on the chemical and microbial composition of the rhizosphere.

1.6.2 Effects of eCO_2 on rhizosphere microbes.

The influence of *e*CO_2 on total microbial biomass, colonisation, and community composition can be either positive or negative (Paterson et al., 1997; Wiemken et al., 2001; Montealegre et al., 2002). This variability has been attributed to complex interactions between biotic and abiotic environmental conditions, as well as host plant genotype (Classen et al., 2015). As outlined earlier, root-associated microbes can form functional symbioses with plants and rely largely on root-exuded C, which changes under varying CO_2 conditions (Denef et al., 2007). Hence, CO_2 can be expected to have far-reaching impacts on the beneficial root-associated microbes. Indeed, ample research has shown mostly positive impacts of *e*CO_2 on rhizobium-plant and mycorrhiza-plant associations (summarised in Compant et al., 2010). By contrast, little is known about the effects of atmospheric CO_2 on PGPR (Drigo et al., 2008), the known published interactions since 2010 are summarised in Table 1.2 (pre 2010 can be found in Compant et al., 2010). This knowledge gap justifies future research to determine the effects of future CO_2 climates on PGPR colonisation and plant responses to PGPR, such a growth promotion and ISR.

Table 1.2. A summary of the known changes in PGPR response at eCO_2.

Species		Observations	Set.[c,d]	CO_2 (ppm)	Reference
Burkholderia sp.	*Phytolacca americana* (pokeweed)[a] and *Amaranthus cruentus* (purple amaranth)[b]	Increased tissue Cs and phytoremediation effects	OTC	860	Tang *et al.,* 2011
Pseudomonas fluorescens	*Medicago truncatula* (barrelclover)[a]	Increased development, vegetative growth and C/N content. Lower bacteiral colonisation.	CEF	750	Lepinay *et al.,* 2012
Burkholderia sp.	Lolium multiflorum (ryegrass)[a]	Growth stimulation through regulation of photosynthesis. Decreased toxic metal in shoots.	OTC	860	Guo *et al.,* 2014
Pseudomonas fluorescens	*Bouteloua gracilis* (blue grama)[b]	Increased productivity, increased capacity to store C, decreased C loss via microbial respiration	CEF	703	Nie *et al.,* 2015
Cyanobacteria	*Vigna unguiculata* (cowpea)[a]	Enhanced root growth and nitrogen fixation	FACE	550	Dey *et al.,* 2017

[a] – C_3 photosynthesis; [b] – C_4 photosynthesis; [c] - Setting refers to the type of facility used where CEF is controlled environment facility, FACE is free air CO_2 enrichment and OTC is open topped chambers in field sites; [d] - All plants were grown from seed in constant CO_2.

1.6.2 Effects of saCO_2 on rhizosphere microbes.

Studies concerning the effects of *sa*CO_2 on rhizosphere microbes are rare. One study about the effect of *sa*CO_2 and *e*CO_2 on fungal species in grassland rhizospheres reported soil type-dependent relationships between CO_2 concentration and fungal species richness and abundance (Procter et al., 2014). Depending on the soil type, certain fungal clades, such as *Chytridomycota* and *Glomeromycota*, responded positively to increases in CO_2 while others, such as *Basidiomycota* and *Ascomycota*, were unaffected. Similarly, in an *Adenostoma fasciculatum* dominated, natural chaparral community exposed to an *sa*CO_2-to-*e*CO_2 gradient, positive correlations were found between rising CO_2 levels and fungal hyphal length, spore volume and a change in fungal species dominance (Treseder et al., 2003). In contrast, in a C_3/C_4 grassland communities exposed to *sa*CO_2-to-*e*CO_2 gradient, microbial biomass was decreased at both *sa*CO_2 and *e*CO_2 (Gill et al., 2006). These studies illustrate that the effects of reduced CO_2 concentrations on soil and rhizosphere microbes remain largely unclear, probably due the complexity of different interacting factors, such as nutrient content, soil type, and plant species. A global assessment of the effects of *sa*CO_2 on microbial communities in relation to the associated chemistry would cast more light on the role of rhizosphere interactions in plant adaptation to past *sa*CO_2 climates.

1.7 Thesis outline.

This introductory Chapter has highlighted the need for more research concerning the effects of atmospheric CO_2 on plant microbial interactions, with a greater focus on the role of plant development, metabolism and physiology. If performed over a range of past-to-future CO_2 concentrations, this data will aid in understanding how plants have adapted to historic CO_2 concentrations and how plants are likely to respond to future concentrations.

The aim of this PhD research was to determine how different CO_2 concentrations affect the plant's ability to interact with above- and below-ground microbes.

Chapter 2 is the methods chapter of this thesis and provides a detailed description of all techniques, materials and equipment used for the experiments that are outlined in the experimental **Chapters 3 - 5**. The technique to profile

simultaneously chemistry and microbial populations in the rhizosphere (applied in **Chapter 5**) is further detailed in Appendix 1, presenting the recently published technical advance paper by Petriacq et al. (2017), to which I have made a substantial contribution during my PhD.

Chapter 3 is the first experimental chapter of this thesis, which describes the effects of glacial-to-future CO_2 concentrations on aboveground Arabidopsis-pathogen interactions. As atmospheric CO_2 affects growth stage (Ainsworth et al., 2002; Mhamdi and Noctor, 2016), I hypothesised that plants that are continuously cultivated at *e*CO_2 or *sa*CO_2 show altered developmental rates, which in turn would have indirect effects on plant-pathogen interactions. Because resource allocation changes throughout a plant's life-cycle (Boege and Marquis, 2005), it can be expected that the developmental stage has an impact on plant-microbe interactions. Indeed, the stimulatory effects of plant age on disease resistance, generally referred to as age-related resistance, is a common phenomenon in plants (Garcia-Ruiz and Murphy, 2001; Kus et al., 2002; Rusterucci et al., 2005; Shibata et al., 2010). To address these differences, a developmental correction is required to ensure that physiological plant age is similar at the time of pathogen challenge. Surprisingly, very few previous studies have considered plant development as an influencing factor on CO_2-induced effects on plant-microbe interactions. A notable exception is the study by Staddon et al. (1998), who reported that the stimulatory effect of *e*CO_2 on root development largely drives the increase in AMF colonization at eCO2. Using a developmental correction, **Chapter 3** of this thesis describes the direct impacts of *e*CO_2 and *sa*CO_2 on post-invasive immunity in Arabidopsis and the resulting effects on interactions with biotrophic and necrotrophic pathogens. Subsequent molecular and biochemical characterization of CO_2-dependent resistance phenotypes uncovered different mechanisms by which CO_2 shapes plant immunity. Apart from priming effects of *e*CO_2 on hormone-dependent defences, this Chapter provides evidence that enhanced photorespiration contributes to plant defence against biotrophic pathogens at *sa*CO_2.

Chapters 4 focuses on the effects of glacial-to-future CO_2 levels on belowground interactions in the rhizosphere of Arabidopsis. This Chapter investigates the effects of CO_2 and soil type on two previously characterised

soil bacteria was investigated. These experiments revealed that CO_2 has differential impacts on rhizosphere colonisation by the specialised rhizobacterial strain *P. simiae* WCS417 and the generalist saprophytic soil coloniser *P. putida* KT2440. Moreover, plant growth and systemic resistance (ISR) responses to *P. simiae* WCS417 were altered at different CO_2 regimes and dependent on the soil nutritional status. Together, this Chapter provides evidence that the impacts of atmospheric CO_2 on plant-rhizosphere interactions are highly dependent on the microbial species and the nutritional status of the soil.

Chapter 5, has employed the profiling technique described by Pétriacq et al (2017; Appendix 1) to obtain a global impression of the impacts of past-to-future CO_2 on rhizosphere microbial communities and rhizosphere chemistry. Using T-RFLP profiling, this Chapter reveals that atmospheric CO_2 has a measurable impact on microbial community structures in a plant development-dependent manner. Using un-targeted mass-spectrometry-based metabolite profiling, this Chapter furthermore reveals quantitative and qualitative impacts of CO_2 on rhizosphere chemistry. Together, this Chapter provides evidence that both the microbial and chemical diversity increased with rising CO_2 concentrations.

Finally, **Chapter 6** of this thesis, the general Discussion, provides a wider reflection on the experimental results of my PhD. The results of the experimental **Chapters 3 - 5** are discussed in the context of future climate change and plant evolution during recent glacial periods.

Chapter 2: Materials and Methods

2.1 Reagents and chemicals.

All chemicals, solvents and reagents (analytical grade) used throughout this project were purchased from Sigma-Aldrich, (UK), unless stated otherwise. Jasmonic acid (JA) was obtained from OlChemim (CZ; http://www.olchemim.cz/).

2.2 Plant cultivation and growth conditions.

Arabidopsis thaliana (Arabidopsis) was cultivated in mx flow 6000 cabinets (Sanyo, UK) under ambient conditions (*a*CO_2; 400 ppm, *i.e.* µL L^{-1}), sub-ambient CO_2 (*sa*CO_2; 200 ppm), or elevated CO_2 (*e*CO_2; 1200 ppm). Growth chambers were supplemented with compressed CO_2 (BOC, UK) or scrubbed with Sofnolime 797 (AP diving, UK) to maintain constant CO_2 levels at indicated concentrations. For experiments with plant-free control soils, pots of unseeded soil were set-up and maintained in the same growth conditions as samples. Most plants were grown in 'standard' pots, but various experiments were undertaken in 'specialised' pots, as detailed below. Arabidopsis wild-type accession Columbia 0 (Col-0), was used throughout these studies along with the Col-0 mutant lines *npr1-1* (Cao et al., 1997), *sid2-1* (Wildermuth et al., 2001), *jar1-1* (Staswick, 2002), *aos1-1* (Przybyla et al., 2008), *rbohD/F* (Torres et al., 2002), *gox1-2* (SALK_051930; Alonso et al., 2003) and *haox1-2* (SALK_022285; Alonso et al., 2003). Plants were cultivated under short-day conditions (8.5: 15.5 h light: dark; 20 °C light, 18 °C dark; 65% relative humidity). For 'standard' pots, seeds were stratified for 2 days (d) in the dark at 4 °C and planted in 60-mL pots, containing a sand (silica CH52) : dry compost (Levington M3) mixture, in a ratio of 2 : 3 for nutrient rich soil, or 1 : 9 for nutrient poor soil (v:v in both instances). Pots were transferred to trays to allow for bi-weekly watering. At 7 d post-germination (dpg), seedlings were thinned to prevent crowding.

2.3 Experimental set-up of growth system for metabolite collection.

For metabolite extractions and sampling of soil bacterial communities, 'specialised' pots were used. This method, detailed in Appendix 1, involves custom-made 30-mL collection tubes (Starlab, UK), plugged with micracloth (VWR, UK) and filled with nutrient poor soil. To prevent cross contamination

between samples, tubes were placed in individual petri-dishes (Nunclon™ Delta, 8.8 cm^2 ThermoScientific, UK) and subsequently wrapped in aluminium foil to limit algal growth in the soil matrix. Growth conditions of Arabidopsis were then as described above. All pots were watered twice weekly with 5 mL of autoclaved distilled water applied to the petri-dishes, using a 5-mL pipette (Starlab, UK). The final watering date was set at 3 d before sampling, which resulted in consistent soil water contents at the time of sampling (Pétriacq et al., 2017; Appendix 1).

2.4 Development measurements and correction.

Developmental stage of plants was evaluated by counting the number of leaves. To determine the size of the plants, rosette area was estimated non-destructively from digital photographs (Canon EOS 500D) of rosettes, taken with a size standard. Image analysis involved converting pixels per rosette into area (mm^2), using imaging software (Corel Paintshop Pro, ver. X7). To determine root growth, root material plus soil was collected carefully and oven dried using an economy incubator 2 (Weiss Technik, UK; 60°C). Subsequently, soil was carefully extracted from surrounding soil and weighed using an analytical balance (Mettler Toledo AJ100).

2.5 Plant developmental correction (DC).

CO_2 directly impacts plant growth-stage. To compare plants with similar developmental stages, a correction was applied. Using leaf numbers of 3- and 4.5-week old plants as a proxy of development stage at different CO_2 regimes (Boyes et al., 2001), seed germination at *sa*CO_2 was started 7 days earlier than at *a*CO_2, whereas seed germination at *e*CO_2 was delayed by 3 days in comparison to *a*CO_2. DC resulted in plants with equal number of leaves at all three CO_2 concentrations at the day of pathogen inoculation (8-leaf stage for *Hyaloperonospora arabidopsidis*, *Hpa*, and 18-leaf stage for *Plectosphaerella cucumerina*, *Pc*; see below).

2.6 Pathogenicity assays using Hpa and Pc.

To determine disease resistance, plants were grown in ‘standard’ 60-mL pots and either inoculated with the obligate biotroph, *Hpa*, or the fungal necrotroph, *Pc*. Due to its sensitivity to age-related resistance (ARR), assays with

Hpa, (strain WACO9) were conducted with relatively young plants (3-week old at *a*CO_2 for non-DC experiments or 8-leaf stage for DC experiments). Plants were spray-inoculated with 5×10^4 conidiospores mL^{-1} and left at high humidity (100% relative humidity, RH) by placing transparent lids on trays. Subsequently, whole-plant tissues were collected at 6 or 7 days post inoculation (dpi) to determine the extent of hyphal colonization by trypan-blue staining and microscopy analysis (Optika LAB-30), as described previously (Luna et al., 2012). Levels of *Hpa* colonisation were assigned to four distinct classes, as is illustrated in Fig. 2.2. I, no pathogen development; II, presence of hyphal colonisation; III, extensive colonisation and presence of conidiophores; IV, extensive colonisation and the presence of conidiophores and > 10 oospores. At least 50 leaves from more than 15 plants per treatment were used to determine distributions of inoculated leaves across the four *Hpa* colonization classes. Images of disease symptoms were taken on an Olympus SZX12 binocular microscope and a Leica MZ FLIII. Differences in distribution of leaves across *Hpa* colonization classes were analysed for statistical significance, using Chi-square tests (using R, v. 3.1.2).

To ensure necrotrophic infection, assays with *Pc* (strain BMM) were based on droplet inoculation (6 µL, 5×10^6 spores mL^{-1}) on 4 to 6 fully expanded leaves of plants (n = 8) at the 18-leaf stage (4.5-week old at *a*CO_2), as described previously (Pétriacq et al., 2016a). Disease progression was measured as lesion diameters at 8 and 13 dpi. Four lesion diameters per plant were averaged and treated as one biological replicate (n = 8). Differences in average lesion diameter between treatments were analysed for statistical significance by ANOVA (using R, v. 3.1.2).

2.07 Gene expression analysis by reverse-transcriptase quantitative PCR.

RNA extraction a trizol-containing extraction buffer, cDNA synthesis and real-time quantitative qPCR (RT-qPCR) were performed to determine relative gene expression levels, as described previously (Pétriacq et al., 2016a). Gene-specific primers for RT-qPCR are listed in Table 2.1. Basal expression of *CAT2* (*A*T4G35090), *GOX1* (AT3G14420) and *HAOX1* (AT3G14130) were determined in shoot material of plants at the 8-leaf stage. Each biological replicate consisted of shoot material from one plant (n = 5). Basal and hormone-induced expression of *PR1* (AT2G14610) and *VSP2* (AT5G24770) were determined in plants of the

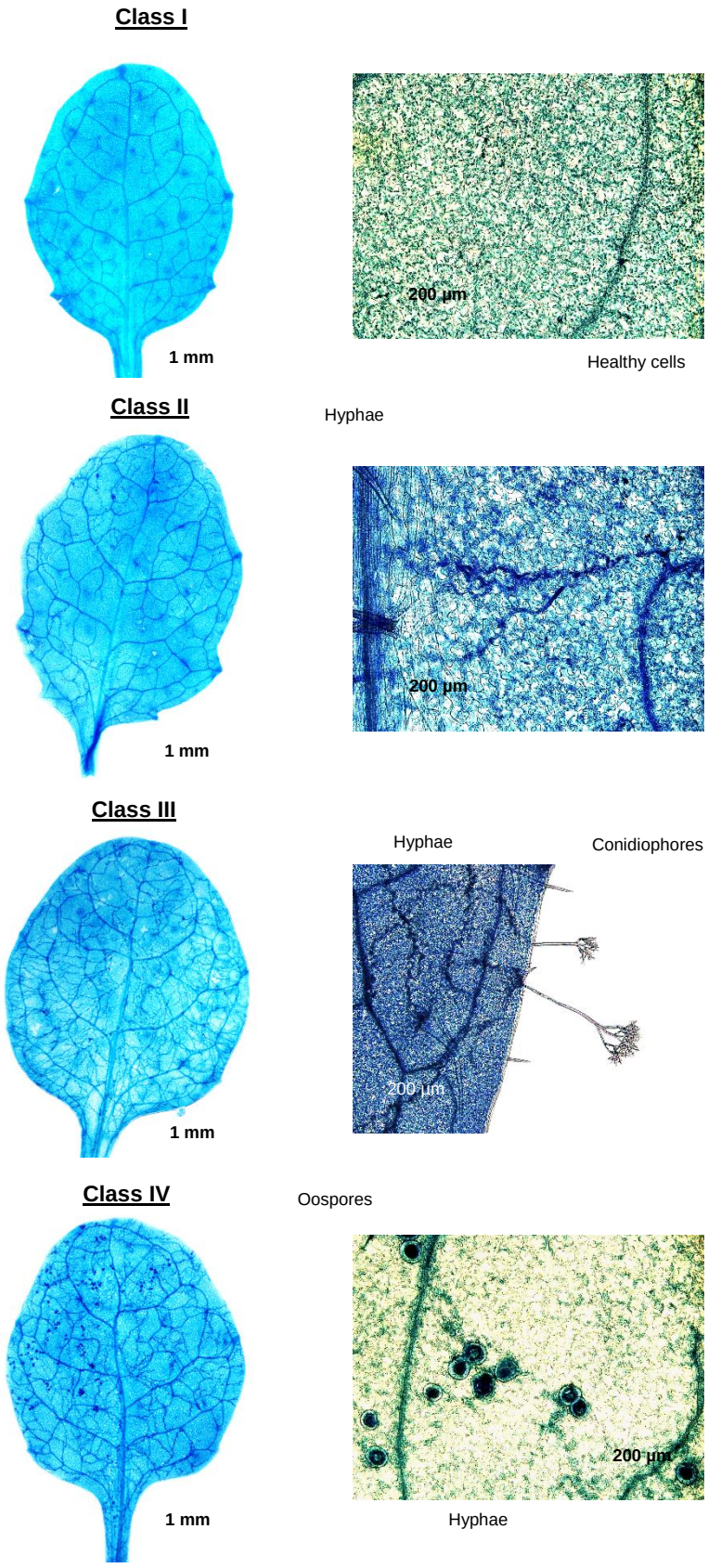

Fig. 2.1 Representative examples of the four different *Hpa* colonization classes that were used to quantify Arabidopsis resistance. To visualise *Hpa* colonisation, leaves were stained with lactophenol trypan-blue, as described previously (Luna et al. 2012). Class I is defined by a lack of hyphal growth; Class II sustains hyphal development, but not the production of asexual conidiospores; Class III is characterised by extensive hyphal colonisation and the formation of conidiophores and asexual condiospores; Class IV is similar as class III, but with additional formation of sexual oospores (> 10 per leaf). Black bars indicate scales.

8-leaf stage after spraying shoots with double-distilled water, 0.1 mM JA, or 0.5 mM salicylic acid (SA), supplemented with 0.01% Silwet L-77 until imminent runoff. Each biological replicate in these assays consisted of 4 leaves from 4 different plants (n = 3). In all cases, gene expression was normalised against Arabidopsis house-keeping genes, At5g25760 (*SAND*) and At2g28390 (*UBC*; Czechowski et al., 2005). Pipetting was performed with a QIAgility robot and RT-qPCR using a Rotor-Gene Q instrument (QIAGEN), SYBR Green (Thermo-Fisher) and a three-step cycle setting, 30s 95°C, 20s 58°C and 20s 62°C for 40 cycles. Differences in relative transcript levels were analysed for statistical significance, using Welch's t-test (R, v. 3.1.2). Assays to quantify *CAT2*, *GOX1* and *HAOX1* (At3g14420, At3g14130 and At4g35090, respectively) gene expression were repeated once with similar results.

Table 2.1 Primers used for mutant genotyping and RT-qPCR analysis of gene expression

	Gene	Gene locus	Forward primer sequence (5' - 3')	Reverse primer sequence (5' - 3')
Genotyping	*GOX1*	AT3G14420	CCG AAA GCT ATT AAA CAG CCC	CTT ACA TTG CAC CCA ACT TCC
	HAOX1	AT3G14130	GCA GAA TGG AGG GGT TTA GTC	CAT GCA AGA ATC TTG CTC CTC
	SALK Insert (LBb1.3)		-	ATT TTG CCG ATT TCG GAA C
qRT-PCR primers	Gene expression			
	GOX1	AT3G14420	AGA ACA GCA GCA ACA CAG AAC	CAC TAG GCT TGG TTT GTG ATC TGA TA
	HAOX1	AT3G14130	GAA TTA AAT CTA TGC TCT GAT CCT AAA ACC	GAA CAA GTC CAA CGT ACT ATT GTC TT
	CAT2	AT4G35090	CGA GGT ATG ACC AGG TTC GT	CTT CCA GGC TCC TTG AAG TTG
	PR1	AT2G14610	GTC TCC GCC GTG AAC ATG T	CGT GTT CGC AGC GTA GTT GT
	VSP2	AT5G24770	GGA CTT GCC CTA AAG AAC GAC ACC	GTC GGT CTT CTC TGT TCC GTA TCC
	UBC 9	AT5G25760	TCA CAA TTT CCA AG^ GTG CTG C	TCA TCT GGG TTT GGA TCC GT
	SAND	AT2G28390	AAC TCT ATG CAG CAT T	GGT GGT ACT AGC ACA A
	DNA quantification			
	HpaACT	g_ID_807716	GTG TCG CAC ACT GTA CCC ATT TAT	ATC TTC ATC ATG TAG TCG GTC AAG T
	Pcβ-Tub		CAA GTA TGT TCC CCG AGC CGT	GAA GAG CTG ACC GAA GGG ACC
	AtACT2	AT3G18780	AAT CAC AGC ACT TGC ACC A	GAG GGA AGC AAG AAT GGA AC

2.7 RT-PCR quantification of pathogen DNA.

The results of both the *Hpa* and the *Pc* assays were verified in independent DC experiments with wild-type plants (Col-0), using quantitative PCR (Fig. S3). Shoot material was collected at 6 dpi (n = 4) for quantification of *Hpa* biomass; fully expanded leaves were collected at 8 dpi (n = 4) for quantification of *Pc* biomass. For DNA quantification of *Hpa* and *Pc* infection, DNA was extracted from infected plants (n = 5) using CTAB extraction protocol (2% CTAB; 100mM

Tris-HCl pH 8, 1.4M NaCl; 20mM EDTA; 1% PVP- 40; 2µ ml-1 2-Mercaptoethanol) and subsequent chloroform-isopropanol precipitation, as described previously (López Sánchez et al., 2016). The qPCR quantifications of *Hpa* and *Pc* biomass were performed with pathogen-specific primers (Table S2), using the PCR conditions described by Anderson and McDowell (2015) and Sanchez-Vallet et al., (2010), respectively. Relative levels of pathogen DNA were calculated by normalisation against genomic DNA of the Arabidopsis *ACT2* gene (AT3g18780).

2.8 In situ detection of reactive oxygen species.

Extracellular reactive oxygen species (ROS) were analysed by 3,3'-diaminobenzidine (DAB) staining (Daudi and O'Brien, 2012), whereas intracellular ROS were quantified by 2′,7′-dichlorofluorescein diacetate (DCFH-DA; Pétriacq et al., 2016b). Each biological replicate in these assays consisted of one individual leaf collected from different plants (n = 10 for DCFH-DA, n = 5 for DAB). In both cases, mock- or *Hpa*-treated leaves were sampled at 48 hours post inoculation (hpi). ROS intensities from DAB or DCFH-DA images were obtained with an Olympus SZX12 binocular microscope (using a HQ510 1p emission filter for DCFA-DA fluorescence; Ex/Em: 492-495/517-527 nm) and quantified using Photoshop (v CS.5), by calculating fluorescent pixels relative to dark leaf area (Luna et al., 2011; Pétriacq et al., 2016b). Statistical evaluation was performed using ANOVA (R, v. 3.1.2).

2.9 Targeted quantification of hormones.

Salicylic acid (SA) and jasmonic acid (JA) were quantified by ultra-pure liquid chromatography quadrapole time of flight mass spectrometry (UPLC-Q-TOF-MS) with MS^E, using the methods detailed in Pétriacq et al., 2016b. Briefly, phytohormones were double- extracted from freeze-dried leaf material (10 mg dry weight) in a total volume of 1.5 mL of ethyl acetate. Each biologically replicated sample (n =5) consisted of four pooled leaves of similar size and age from different plants. Hormones were quantified by UPLC-Q-TOF-MS^E in negative electrospray ionization mode (ESI^-), using standard curves of pure SA and JA.

Compound identity was verified by the following fragmentation patterns: SA, 137→93; and JA, 209→59.

2.10 Metabolite extraction for untargeted profiling.

Metabolic profiles of leaves at *sa*CO_2 or *a*CO_2 were analysed after application of DC. To this end, plants in the 8-leaf stage were inoculated with *Hpa* or water, after which leaf tissues of 4 plants from each pot were pooled as one biological replicate. Replicates (n = 3) were collected in the middle of the photoperiod and snap frozen in liquid nitrogen at 24 hpi and 72 hpi. For the analysis of rhizoshere chemcials, extracts from plant-containing pots and plant-free pots were collected by applying ice-cold extraction solution (5 mL) 50% (v/v) with 0.05% formic acid (v/v) to the top of the pots. After 1 min, 4 - 4.5 mL, the extract was recovered from the hole in the pot's base. Extracts were centrifuged to pellet soil residues (5 min, 3500 *g*), and 4 mL of supernatant was transferred into a centrifuge tube and flash-frozen in liquid nitrogen, freeze-dried for 48 hours (Modulyo benchtop freeze dryer, Edwards, UK), and stored at -80 °C. Dried aliquots, from either collection method (*i.e.* foliar material or soil chemicals), were re-suspended in 100 µL of methanol: water: formic acid (50: 49.9: 0.1, v/v) and prior to UPLC-Q-TOF analysis they were sonicated at 4 °C for 20 min, vortexed and centrifuged (15 min, 14000 *g*, 4 °C) to remove any large particles. Supernatants (80 µL) were aliquoted into glass vials containing a glass insert before injection through the UPLC system.

2.11 Untargeted metabolic profiling by UPLC-qTOF-MS^E.

To determine metabolic profiles, UPLC-Q-TOF-MS^E analysis of methanol extracts was carried out as described previously (Pétriacq et al., 2016b), using the following modifications: high-resolution full-scan mass spectrometry was performed with a SYNAPT G2 HDMS Q-TOF mass spectrometer (Waters), coupled to a UPLC BEH C18 column (2.1 × 50 mm, 1.7 µm, Waters) with a guard column (VanGuard, 2.1 x 5 mm, 1.7 µm, Waters) for separation of compounds at a flow rate of 400 µL min^{-1}. The mobile phase consisted of A; water with 0.05% formic acid, and B; acetonitrile with 0.05% formic acid with a gradient applied: 0 – 3 min 5 – 35 % B, 3 – 6 min 35 – 100 % B, holding at 100 % B for 2 min, 8 – 10 min, 100 – 5 % B. The column temperature was kept at 45 °C with an injection

volume of 10 µL. Buffer (50% methanol) was injected between treatments and between ESI^- and ESI^+ ionization modes for stabilization of the electrospray ionization source. Ions were detected over a mass range of 50 – 1200 Da, using a scan time of 0.2 s (ESI^- and ESI^+) with the instrument operating in sensitivity mode for the MS full scan (*i.e.* without collision energy). Collision energy was ramped in the transfer cell from 5 to 45 eV (MS^E), using the conditions highlighted in Table 2.2. Prior to analysis, the Q-TOF detector was calibrated with a solution of sodium formate. During each run, accurate mass measurements were ensured by infusing leucine enkephalin peptide as an internal reference, or lock mass (10 s scan frequency, cone voltage of 40 V and a capillary voltage of 3 kV). The system was piloted by MassLynx v. 4.1 software (Waters).

Table 2.2 UPLC-Q-TOF-MS settings

Setting	**ESI^-**	**ESI^+**
Capillary voltage (kV)	- 3	+ 3
Sampling cone voltage (V)	- 25	+ 25
Extraction cone voltage (V)	4.5	+ 10
Source Temperature (°C)	120	120
Desolvation Temperature (°C)	350	350
Desolvation gas flow (L h^{-1})	800	800
Cone gas flow (L h^{-1})	60	60

2.12 Data preparation of MS data for statistical analysis.

Raw files obtained from MassLynx, were converted into CDF format, using the Databridge function in MassLynx (v. 4.1). Subsequent alignment and integration of metabolic peaks were performed in R (v 3.1.2), using XCMS (Smith et al., 2006). Peaks were retained for analysis when present in all bio-replicates (k = 3 when used in **Chapter 3** and k = 5 when used in **Chapter 5**), at a threshold intensity of 10 (I = 10) and at maximum resolution range of 20 ppm. Peak values from each run were normalised for total ion current (TIC). For each sample, normalised peak values were corrected for dry weight, generating separate datasets in ESI^+ and in ESI^- ionisation modes.

2.13 Analysis of soil chemistry and statistical analysis of MS data.

Unless stated otherwise, data from foliar material (**Chapter 3**) and from soil extracts (**Chapter 5**) were subjected to conceptually similar statistical workflows (Figs. 2.2 and 2.3, respectively). For both experiments, global differences in metabolic signals between treatment/point combinations was visualised for anions (ESI^-) and cations (ESI^+) separately by principal component analysis (PCA), using MetaboAnalyst online (v. 3.0; http://www.metaboanalyst.ca; Xia et al., 2015) on median-normalised, cube-root-transformed and Pareto-scaled data.

To select ions in foliar material (**Chapter 3**) that are either directly induced by *sa*CO_2, or primed by *sa*CO_2 for augmented induction following *Hpa* inoculation, ESI^- and ESI^+ datasets were analysed separately for statistically significant differences between all CO_2/treatment/time-point combinations by one-way ANOVA ($P < 0.01$ + Benjamini-Hochberg false discovery rate correction, FDR; see Fig. S6), using MarVis (v. 1.0; http://marvis.gobics.de; Kaever et al., 2012). From each ionization mode, 133 statistically significant markers were combined into one dataset of 266 markers for successive 2-way ANOVA ($P < 0.01$), using MeV (v. 4.9.0; http://mev.tm4.org). Heatmaps project TIC-normalised ion current values (NIC), relative to the average and standard deviation of the NIC values across all samples: Value = (NIC – mean)/ SD. For each time-point (24 and 72 hpi), this analysis resulted in 3 subsets of markers, whose intensity was statistically influenced by CO_2, *Hpa*, or for which the CO_2 x *Hpa* interaction was statistically significant (See **Chapter 3** for more details; Fig. 2.2). Hierarchal clustering (Pearson's correlation; MeV) allowed visual selection of ion clusters that are induced directly by *sa*CO_2 or primed for augmented induction after *Hpa* inoculation.

For quantification of the number of ions showing quantitative differences between rhizosphere and bulk soil (**Chapter 5**), volcano plots were created on median normalised, pareto-scaled and cube-root transformed data, with a cut-off value of > 2 fold-change (Log2 > 1) and a statistically significant threshold of $P < 0.05$ (Welch's *t*-test; MetaboAnalyst; Fig. 2.3). To study the composition of rhizosphere metabolites whose increased abundance in plant-containing soil

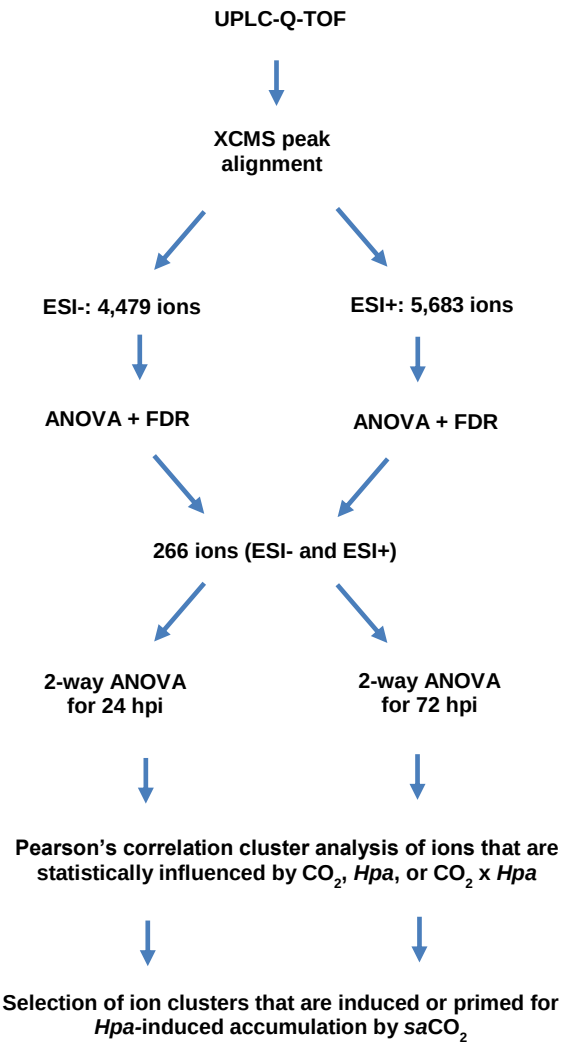

Figure 2.2 Schematic pipeline of the selection procedure for ions induced or primed for *Hpa*-induced accumulation by *sa*CO_2.

depends on the atmospheric CO_2 concentration, the combined set of ions 2,692 anions (ESI^-) and 5,578 cations (ESI^+) were analysed by ANOVA (Benjamini-Hochman false discovery rate (FDR) correction for multiple hypothesis testing (Hochberg and Benjamini, 1990); $P < 0.05$) for statistically significant differences between all CO_2/soil combinations, using MarVis, 3.2 (Fig. 2.3). This filter selected 498 differentially abundant ions, which were then subjected to 2-way ANOVA to select 174 ions with a statistically significant CO_2 x soil type interaction. ($P < 0.05$; see **Chapter 5** for details). Subsequent Pearson correlation analysis (MeV software, v. 4.9) was used to select 59 marker ions that show enrichment in plant-containing soil that varies between CO_2 conditions. To visualize the abundance patterns of this ion selection across all different CO_2/soil type combinations, heatmaps were created to project the average TIC-normalised ion current values (NIC) values for each condition, relative to the average and

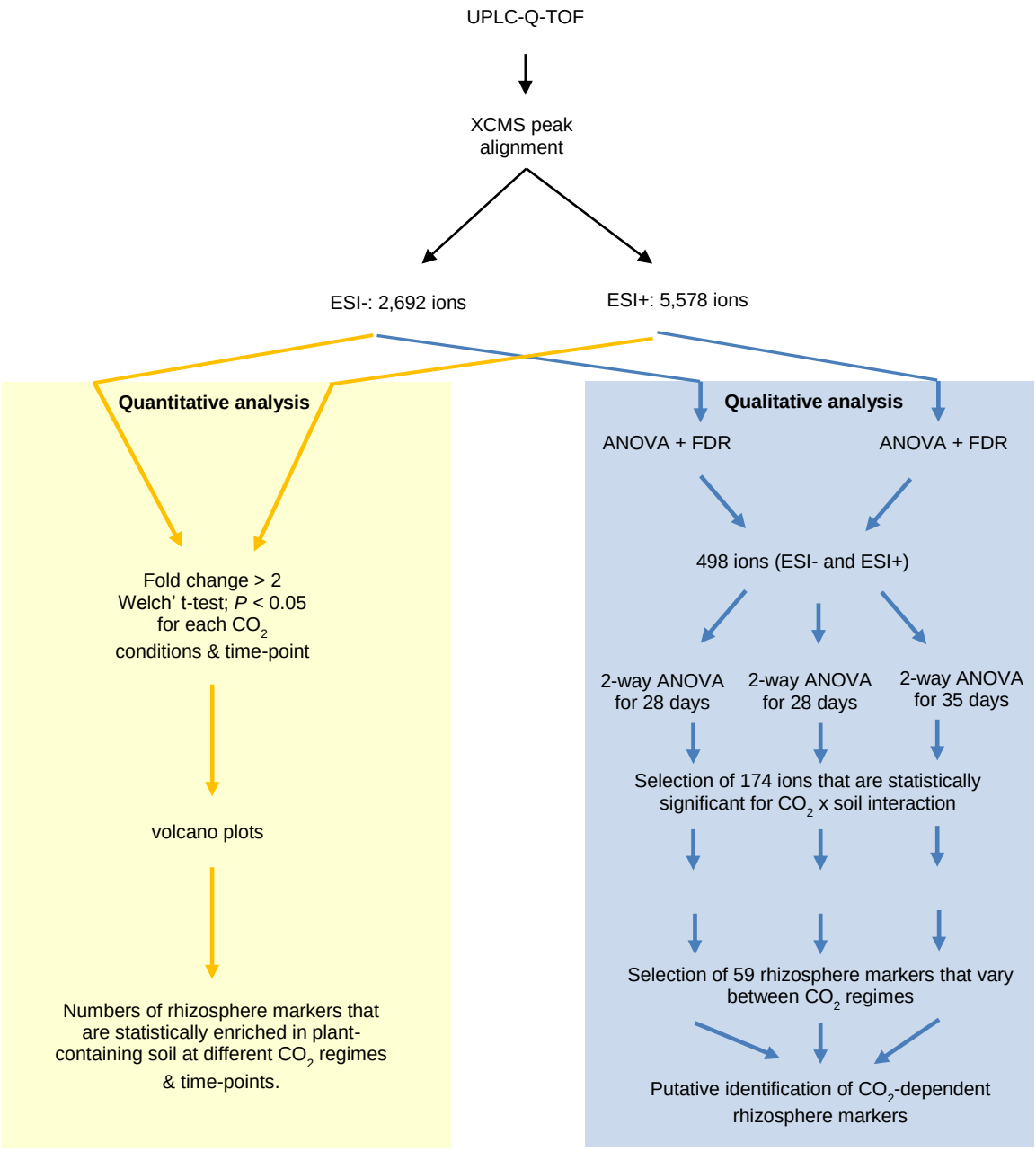

Figure 2.3 Schematic of the statistical selection procedures to study quantitative and qualitative impacts of CO_2 on rhizosphere chemistry. The approach involves various statistical filters to determine the numbers of rhizoshere ions that are statistically enriched in plant-containing soil (left; yellow) and to profile the composition of rhizosphere ions that vary between CO_2 concentrations (right; blue).

standard deviation of the NIC values across all samples (Value = (NIC – mean)/ SD). Putative identities of the selected ion markers were based on *m/z* values at stringent accuracy (< 30 ppm), the using METLIN chemical database (Smith et al., 2005a; https://metlin.scripps.edu). PubChem was used to check the predicted pathway/class annotation (https://pubchem.ncbi.nlm.nih.gov/).

2.15 Determining soil carbon (C) and nitrogen (N) concentrations.

C and N concentrations in soil types (**Chapter 4**) were determined for both nutrient poor and rich soils in *a*CO_2, using the complete combustion method followed by gas chromatography, using an ANCA GSL 20-20 Mass Spectrometer (Sercon PDZ Europa; Cheshire).

2.13 Soil inoculation with Pseudomonas simiae WCS417 and Pseudomonas putida KT2440.

To determine CO_2 impacts on colonisation of rhizosphere bacteria, yellow fluorescent protein (YFP) labelled *P. simiae* WCS417 (Berendsen et al., 2012) was cultivated on solid Lysogeny broth (LB) with selective antibiotics, 5 µg mL^{-1} tetracycline and 25 µg.mL^{-1} rifampicin. One fluorescent colony was selected for propagation in an overnight culture of liquid LB, containing the same selective concentrations of tetracycline and rifampicin. The medium was incubated in an orbital shaking incubator for 16 hours at 28 °C at 200 revolutions per minute (rpm). A similar method was employed for the cultivation of a green fluorescent protein (GFP)-tagged *P. putida* KT2440, which carries a stable chromosome-inserted $PA_{1/04/03}$-RBSII-*gfp*mut3*-T0-T1 transposon at a negligible metabolic cost (Dechesne and Bertolla, 2005). However, in this case, the bacteria were grown on minimal solid media (M9), after which one GFP-fluorescent colony was selected for propagation in LB liquid medium in the absence of selective antibiotics. Seeds were planted on bacterised soil. Soils were inoculated with either WCS417 or KT2240 by adding a bacterial suspension in 10 mM MgSO4 at 5 X 10^7 CFU.g^{-1}. Four weeks after germination, samples of rhizosphere/root adhering soil, or control soil (~2 g) were collected. These samples were serially diluted and stamp-plated, using a 96-well Replica plater (Sigma-Aldrich, R2383) onto LB agar containing selective tetracycline and rifampicin for WSC417, and M9 for KT2240. Fluorescent colonies were enumerated using a Dark Reader DR195M Transilluminator (Clare Chemical) and corrected for sample weight. A repeat of this experiment showed comparable results.

Application of DC for belowground experiments (**Chapter 4**) was based on the same method as described above for the aboveground experiments (**Chapter 3**), but the soil was inoculated with either WCS417 or KT2440 ten days prior to

sampling. Soil inoculation was performed by syringe injection of 6 mL 5 x 10^8 CFU.mL^{-1} into 60 mL pots, resulting in a final soil density of 5 X 10^7 CFU.g^{-1}, equivalent to the soil densities used for non-DC experiments.

2.14 Induced systemic resistance assays.

To establish the induced systemic resistance (ISR) ability of *P. simiae* WCS417, 5-week old plants, grown in 'standard' pots, using soil pre-inoculated with WC417 (as described in section 2.16), were challenged with *Pc* (as described in section 2.06). Lesion diameters were enumerated at 8 and 13 dpi and analysed using Student's test ($P < 0.05$).

2.15 Bacterial community profiling by terminal-restriction fragment length polymorphism analysis.

Bacterial communities were profiled by terminal-restriction fragment length polymorphism (T-RFLP), which relies on the polymorphisms within variable regions of an otherwise highly-conserved sequences (Osborn et al., 2000). As such, digestion of these sequences by (a) restriction enzyme(s) results in discriminatory fragment sizes (terminal restriction fragments; T-RFs), which can be used as an indication of the composition of the bacterial community. DNA was extracted from 0.25 g of roots plus adhering rhizosphere soil (Arabidopsis-rhizosphere samples) or 0.25 g of bulk soil (from control samples; n = 5), using a MoBio DNeasy PowerSoil extraction kit (Qiagen, UK), following the manufacturer's instructions. DNA quality and quantity were assessed, using a Nanodrop ND-1000 spectrophotometer (Thermo Scientific, UK). PCR was used to amplify the V5-V6-V7 variable regions of the *16S* rRNA gene, using primers 799F (5'-AAC MGG ATT AGA TAC CCK G-3') and 1193R (5'-ACG TCA TCC CCA CCT TCC- 3'). These primers had been designed to amplify a broad range of bacterial taxa and allow for the assessment and removal (if necessary) of co-amplified plant plastid derived sequences (the bacterial amplicon is ~400 - 500bp; whereas the amplicon from mitochondria/chloroplasts is ~800bp; Chelius & Triplett, 2001; Bodenhausen *et al.*, 2013). MyTaq DNA polymerase (Bioline, UK) was used to amplify *16s* rRNA gene sequences by using 1 µl of template, following the manufacture's details. An optimised PCR protocol of 30 cycles (30 s denaturation at 94°C; 30 s hybridisation at 57.5°C; 45 s elongation at 72°C),

provided the strongest *16s* amplification without visible amplification of plastid-derived plant DNA. Gel electrophoresis of PCR amplicons was performed on 1% agarose (with Tris acetate EDTA, TAE, buffer) to verify the approximate band size and ascertain the absence of plastid-derived plant DNA. Subsequently, DNA samples were amplified, using the optimised PCR protocol with a 6-fluorescein amidite (6-FAM) labelled fluorescent probe (Sigma-Aldrich, UK) ligated to the aforementioned forward 799F primer in combination with an unlabelled 1193R primer. The resultant PCR amplicons were purified, using a QIAquick PCR purification kit (Qiagen, UK), after which 5 µL of purified amplicons were digested in a reaction mixture containing 1 U Alu-I, 1.5 µL of 1 x Buffer B, 0.2 µL of bovine serum albumin in a final volume of 10 µL. Restriction reactions were incubated for 2 hours at 37 °C. Aliquots of 5 µL from the purified digested product were desalted by ethanol precipitation, using 0.25 µL glycogen (20 $mg.mL^{-1}$), 0.5 µL 3M sodium acetate and 13 µL ice-cold 70% ethanol. After gentle mixing, the samples were centrifuged at 18,000 *g* for 20 minutes, at 4 °C. Subsequently, the supernatant was discarded and pellets were washed twice in 70% ethanol (18, 000 *g* for 10 minutes). Finally, pellets were air-dried and re-suspended in 5µl of nuclease free water for T-RFLP analysis. Size and intensity of the T-RFs were quantified by capillary gel electrophoresis. To this end, 1 µL aliquots of digested and desalted samples were denatured in 10 µL hi-di formamide and spiked with GeneScan 500 ROX (ThermoScientific, UK) size standards. Samples were denatured at 94 °C for 5 minutes and cooled on ice prior to analysis on the ABI 3730 PRISM capillary DNA analyser (Applied Biosystems), using a denaturing polymer at injection times of 10 and 20 seconds and a 2kV injection voltage.

2.16 Community diversity and composition.

The electrophenograms generated were analysed using Genemapper v.4 (ThermoScientific, UK) to determine fragment sizes of T-RFs, relative to the ROX internal standards. To reduce noise, only peaks with a height greater than 50 fluorescent units were analysed, whereas peaks corresponding to T-RFs smaller than 40 nucleotides (nt) were discarded. Relative abundances of T-RFs were assessed by peak areas and the profiles were aligned using T-align (Smith et al., 2005b), a web-based alignment tool that expresses values as a proportion of the

total peak area, with a confidence interval of 0.5 nt. Any T-RF with a peak area less than 0.5% of the total peak area were excluded from analysis to eliminate noise. The software package PRIMER 6 (v6.1.13) was used to analyse the aligned T-RF profiles. Data were square-root transformed and Bray-Curtis similarity matrices were generated to allow similarity measures of the bacterial community structure. Metrics to assess diversity of microbial profiles were based on species richness (*i.e.* the number of T-RFs per sample) and the Shannon index. Samples were expressed as relative abundance, as discussed in Blackwood *et al.*, 2007. To evaluate similarity between samples, non-parametric multi-dimensional scaling (nMDS) was used. Kruskal stress values (*e*; shown in the MDS plots) are indicative of how well the data are represented by this analysis with $e \leq 0.10$ being a good fit, $0.20 > e > 0.10$ urging caution and verify separation by alternative cluster analysis, and $e \geq 0.2$ being a poor fit. With *e* stress values exceeding 0.1, differences were verified using hierarchical clustering analysis with SIMPROF evaluation.

2.17 Analysis of dissimilarity in T-RFLP patterns between samples.

Analysis of similarity (ANOSIM) was used to statistically evaluate the differences in microbial rhizosphere effects between CO_2 conditions and over 3 different time-points. The microbial rhizosphere effect was estimated by the difference in T-RFLP pattern between root plus rhizosphere samples and bulk soil samples. ANOSIM uses Bray-Curtis similarity measures to calculate a global R value, which indicates the difference between data groups (0 = no difference and 1 = totally different); the *P* value indicates if R is statistically significant. For each time-point, dissimilarity percentages between samples were calculated using SIMPER analysis, which uses Bray-Curtis distances to generate quantitative measures of similarity. This analysis also provided information on which T-RFs were most responsible for contributing to this dissimilarity, to a threshold set at an arbitrarily level of 60%.

Chapter 3: Mechanisms of glacial-to-future atmospheric CO_2 effects on plant immunity (adapted from Williams et al., 2018)*

3.1 Abstract

Impacts of rising atmospheric CO_2 concentrations on plant disease have received much attention recently. Nonetheless, evidence regarding the direct mechanisms by which CO_2 shapes plant immunity remains fragmented and controversial. Furthermore, the impact of sub-ambient CO_2 concentrations, which plants have experienced consistently over the past 800,000 years, has been largely overlooked. Using a combination of gene expression analysis, phenotypic characterisation of mutants and mass spectrometry-based metabolic profiling, I investigated development-independent effects of sub-ambient CO_2 (*sa*CO_2) and elevated CO_2 (*e*CO_2) on Arabidopsis immunity to two different pathogens. Resistance to the necrotrophic fungus *Plectosphaerella cucumerina* (*Pc*) was repressed at *sa*CO_2 and enhanced at *e*CO_2. This CO_2-dependent resistance was associated with priming of jasmonic acid (JA)-dependent gene expression and required intact JA biosynthesis and signalling. Resistance to the biotrophic oomycete *Hyaloperonospora arabidopsidis* (*Hpa*) increased at both *e*CO_2 and *sa*CO_2. Although *e*CO_2 primed salicylic acid (SA)-dependent gene expression, mutations affecting SA signalling only partially suppressed *Hpa* resistance at *e*CO_2, suggesting additional mechanisms are involved. Induced production of intracellular reactive oxygen species (ROS) at *sa*CO_2 corresponded to a loss of resistance in glycolate oxidase (GOX) mutants and increased transcription of the peroxisomal catalase gene *CAT2,* unveiling a mechanism by which photorespiration-derived ROS determined *Hpa* resistance at *sa*CO_2. Separating indirect developmental impacts from direct immunological effects, facilitated the discovery of distinct mechanisms by which CO_2 shapes plant immunity. Their evolutionary significance is discussed.

*****Williams, Alex, Pierre Pétriacq, Roland E. Schwarzenbacher, David J. Beerling, and Jurriaan Ton, 2018. "Mechanisms of Glacial-to-Future Atmospheric CO_2 Effects on Plant Immunity." *New Phytologist* 218 (2): 752–61. doi:10.1111/nph.15018.

3.2 Introduction

Past and future changes in atmospheric CO_2 directly impact plant metabolism (Temme et al., 2015), with feedbacks on a wide range of processes, including resistance to pests and diseases (Strengbom and Reich, 2006; Lake and Wade, 2009; Vaughan et al., 2014; Váry et al., 2015; Zhang et al., 2015; Mhamdi and Noctor, 2016). Although numerous effects of elevated CO_2 (eCO_2) on disease resistance have been reported, there is little consistency between studies. While some studies report decreased disease resistance at eCO_2 (Lake and Wade, 2009; Vaughan et al., 2014; Váry et al., 2015), others report no, or stimulatory effects, of eCO_2 on disease resistance (Strengbom and Reich, 2006; Riikonen et al., 2008; Pugliese et al., 2012; Zhang et al., 2015; Mhamdi and Noctor, 2016). These discrepancies may arise from differences in the eCO_2 concentrations studied, the duration of eCO_2 exposure, the method of disease quantification, species-specific adaptations to CO_2, or a combination of all these factors. Furthermore, biotrophic and necrotrophic pathogens are rarely compared within the same study, providing limited information on how distinct components of the plant immune system respond to eCO_2.

To date, various mechanisms by which CO_2 alters disease resistance have been proposed, ranging from changes in leaf nutrition (Strengbom and Reich, 2006), stomatal density (Lake and Wade, 2009) and pathogen-specific adaptations to altered host metabolism (Váry et al., 2015). Recent evidence suggests a mechanism whereby eCO_2 primes pathogen-induced production of defence regulatory hormones, such as salicylic acid (SA) and jasmonic acid (JA; Zhang et al., 2015; Mhamdi and Noctor, 2016), which control defences against biotrophic and necrotrophic pathogens, respectively (Thomma et al., 1998). Surprisingly, however, most studies do not take into account the stimulatory effects of CO_2 on plant development (Temme et al., 2015), despite evidence that the developmental stage can have a profound impact on SA-dependent and ethylene-dependent defences (Kus et al., 2002; Shibata et al., 2010).

Knowledge on the effects of *sa*CO_2 on plant immunity is limited and may offer valuable insights about the evolution of plant defence metabolism at typically low atmospheric CO_2 (below 200 ppm) during glacial periods over the past 800,000 years (Temme et al., 2015; Galbraith and Eggleston, 2017). While stomatal immunity has been implicated in defence at *sa*CO_2 (Zhou et al., 2017), the contribution of *sa*CO_2 towards post-invasive plant defence has not yet been established. At *sa*CO_2, the net photosynthetic rate decreases as a consequence of photorespiration, along with increased stomatal conductance, increased foliar nitrogen and lower water use efficiency (Temme et al., 2013; Li et al., 2014c). Although it remains unclear whether these physiological changes influence disease resistance, a transcriptome study at *sa*CO_2 revealed enhanced activity of peroxisomal processes, which correlated with changes in expression of defence-related genes (Li et al., 2014c). For instance, peroxisomal metabolism was stimulated at *sa*CO_2 (Li et al., 2014c), which can boost defence through changes in cellular redox homeostasis (Sørhagen et al., 2013). The photorespiratory machinery is a major source of intracellular hydrogen peroxide (H_2O_2), which plays an important signalling role in plant defence (Chaouch et al., 2010). This is further highlighted by the CATALASE-deficient *cat2* mutant, which is impaired in scavenging of peroxisomal H_2O_2 and expresses a constitutive defence phenotype (Chaouch et al., 2010). Therefore, it is plausible that *sa*CO_2 influences plant resistance, but the extent, specificity, and regulatory mechanisms remain unknown.

In this study, the direct impacts of *sa*CO_2 (200 ppm), *a*CO_2 (400 ppm) and *e*CO_2 (1200 ppm) on plant immunity were examined, by eliminating confounding effects of CO_2 on plant development. Using a plant development correction, we show that CO_2 has differential impacts on resistance against the biotrophic oomycete *Hyaloperonospora arabidopsidis* (*Hpa*) and the necrotrophic fungus *Plectosphaerella cucumerina* (*Pc*). Subsequent molecular and biochemical characterization of CO_2-dependent resistance phenotypes uncovered differing mechanisms by which CO_2 shapes the plant immune system. Apart from priming effects of *e*CO_2 on hormone-dependent defences, we provide evidence for a critical role of photorespiration in plant defence at *sa*CO_2 and discuss possible evolutionary implications.

3.3 Results

Plant development biases the assessment of CO_2-dependent disease resistance.

To determine the impacts of plant development on CO_2-dependent resistance, the growth response of Arabidopsis to CO_2 in different atmospheric CO_2 concentrations, ranging from 200 ppm (*sa*CO_2), 400 ppm (ambient CO_2; *a*CO_2) to 1200 ppm (*e*CO_2), were characterised. Using the number of leaves as a marker for developmental stage (Boyes et al., 2001), both 3- and 4.5-week old plants showed enhanced development at *e*CO_2, and reduced development at *sa*CO_2, compared to *a*CO_2 (Fig. 3.1 a). To determine whether these developmental effects influence disease resistance, resistance phenotypes

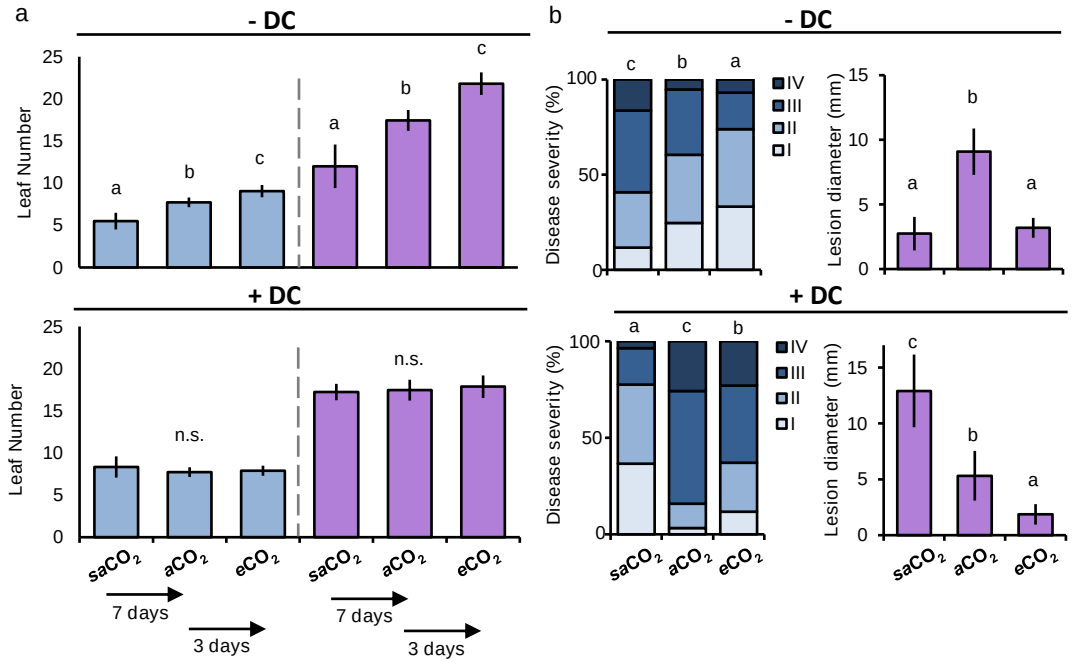

Figure 3.1 Plant development correction (DC) separates immunological effects of CO_2 from indirect developmental effects on Arabidopsis resistance. **a.** Effect of developmental correction (DC) on average leaf numbers in Arabidopsis (Col-0) at sub-ambient (*sa*CO_2; 200 ppm), ambient (*a*CO_2; 400 ppm) and elevated CO_2 (*e*CO_2; 1200 ppm). DC for *sa*CO_2 was performed by planting seeds 7 days earlier than at *a*CO_2; DC for *e*CO_2 was achieved by planting seeds 3 days later than at *a*CO_2. Upper panel: leaf numbers of 3- (left) and 4.5- (right) week old plants without DC. Lower panel: leaf numbers after DC. Data represent mean leaf numbers (± SD, n = 10-18) and are representative of two independent experiments. n.s.: not significant. **b.** Effect of DC on basal resistance against biotrophic *Hyaloperonospora arabidopsidis* (*Hpa*; left) and necrotrophic *Plectosphaerella cucumerina* (*Pc*; right). Shown are relative numbers of leaves (n > 50) in *Hpa* colonization classes of increasing severity (I–IV) at 6 days post inoculation (dpi), or average lesion diameters (± SD; n = 8) by *Pc* at 13 dpi. Different letters indicate statistically significant differences (Fisher's exact test; ANOVA with Tukey HSD post hoc analysis; $P < 0.05$). Pathogenicity assays with Col-0 were repeated several times with comparable outcomes.

against biotrophic *Hpa* and necrotrophic *Pc*, with and without correction for plant developmental stage, were compared. This development correction (DC) was achieved by delaying sowing at *e*CO_2 by 3 days in comparison to plants at *a*CO_2, while starting plant cultivation at *sa*CO_2 7 days earlier compared to plants at *a*CO_2 (Fig. S3.1; see **Chapter 2**). DC resulted in equal numbers of leaves at all CO_2 regimes at the time of pathogen inoculation (8-leaf stage for *Hpa* and 18-leaf stage for *Pc*; Fig. 3.1 a, bottom panel). Without DC, 3-week old plants showed increasing levels of *Hpa* resistance at rising CO_2 concentrations (Fig. 3.1 b, top left), whereas 4.5-week old plants showed enhanced *Pc* resistance at both *e*CO_2 and *sa*CO_2 (Fig. 3.1 b). This pattern of CO_2-dependent resistance phenotypes changed upon DC application. While 8-leaf plants showed enhanced *Hpa* resistance at both *sa*CO_2 and *e*CO_2 (Fig. 3.1 b), 18-leaf plants showed increasing levels of *Pc* resistance with rising CO_2 concentrations (Fig. 3.1 b). To confirm the development-independent effects of CO_2 on disease resistance, levels of *Hpa* and *Pc* colonization were quantified in an independent DC experiment by qPCR analysis of pathogen-specific DNA (Fig. S3.2). The impact of DC on resistance phenotypes at *sa*CO_2 and *e*CO_2 indicates that differences in plant development bias assessment of CO_2-dependent disease resistance against both biotrophic and necrotrophic pathogens. Accordingly, all subsequent experiments were conducted after application of DC.

Development-independent effects of e*CO_2 on SA- and JA-dependent resistance.*

SA and JA play important roles in plant defence against biotrophic and necrotrophic pathogens, respectively (Thomma et al., 1998). To examine the direct (development-independent) effects of *e*CO_2 on defence signalling hormones, ultra-performance liquid chromatography (UPLC) coupled to tandem mass spectrometry, was used to quantify SA and JA levels (**Chapter 2**). In comparison to plants at *a*CO_2, plants at *e*CO_2 showed a 69.3% and 69.4% increase in accumulation of SA and JA, respectively (Fig. 3.2 a). While increases in hormone levels were not sufficient to induce transcription of the SA-inducible marker gene *PR1* and the JA-inducible marker gene *VSP2* directly (Fig. 3.2 b), it

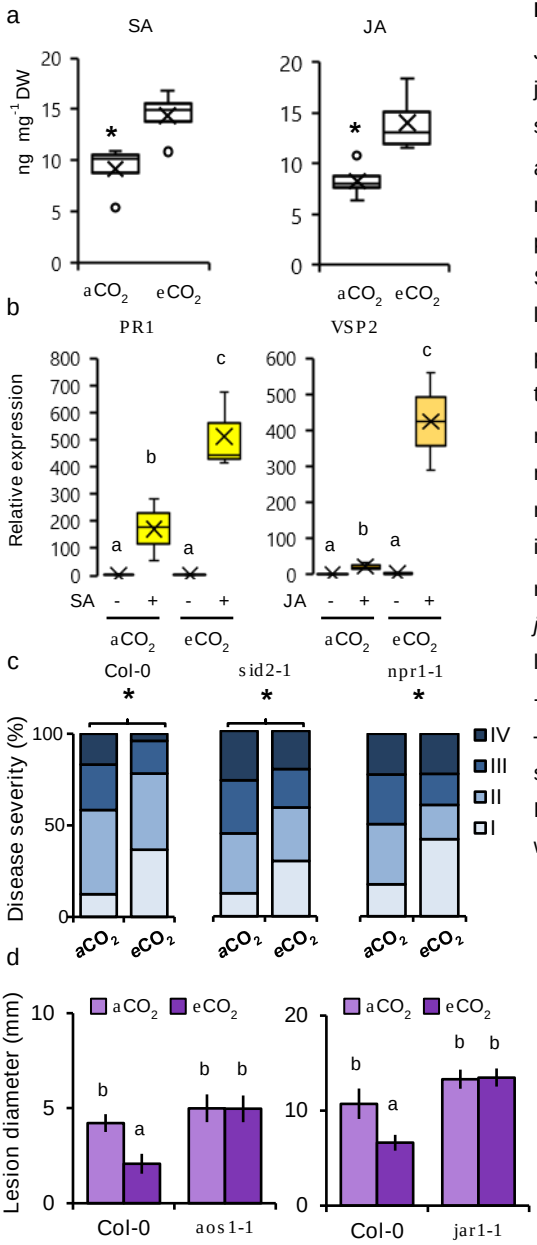

Fig. 3.2 Development-independent effects of *e*CO_2 on SA- and JA-dependent defence. **a.** Accumulation of salicylic- (SA) and jasmonic- (JA) acids in plants (Col-0) of similar developmental stage (8-leaf) at *a*CO_2 (400 ppm) and *e*CO_2 (1200 ppm). Shown are box plots of replicated metabolite quantifications (n = 5; means are indicated by X, outliers outside the 2.5 - 97.5 percentile interval are indicated by O). **b.** Responsiveness of SA- and JA-inducible genes (*PR1* and *VSP2*, respectively) in 8-leaf stage plants (Col-0) at *a*CO_2 and *e*CO_2. Shown are box plots of relative transcript levels at 8 and 24 hours after treatment (n = 3; X indicates means). **c.** Effects of *e*CO_2 on *Hpa* resistance in Col-0, the SA synthesis mutant *sid2-1* and the SA response mutant *npr1-1* at the 8-leaf stage. Shown are relative numbers of leaves (n > 50) in *Hpa* colonization classes of increasing severity (I – IV) at 6 dpi. **d.** Effects of *e*CO_2 on *Pc* resistance in Col-0, the JA production mutant *aos1-1* and the *jar1-1* response mutant at the 18-leaf stage. Shown are average lesion diameters per plant (± SD; n = 8) of *Pc* at 13 dpi. Asterisks - (**a**), Welch's t-test; (**c**), Fisher's exact test - or different letters – (**b**) & (**d**), ANOVA with Tukey HSD post hoc analysis - indicate significant differences between conditions (P < 0.05). Pathogenicity assays with *sid2-1*, *npr1-1*, *aos1-1* and *jar1-1* were repeated once with similar results.

was sufficient to prime augmented induction of *PR1* and *VSP2* after exogenous application of 0.5 mM SA and 0.1 mM JA, respectively (Fig. 3.2 b). To determine the contribution of priming of SA-dependent defence to *e*CO_2-induced resistance against *Hpa*, resistance phenotypes of Arabidopsis mutants impaired in SA production (*sid2-1*) or response (*npr1-1*) were analysed. Although less pronounced than in wild-type plants (Col-0), both *sid2-1* and *npr1-1* expressed statistically significant levels of *e*CO_2-induced resistance against *Hpa* (Fig. 3.2 c). Hence, priming of SA-dependent defence is not solely responsible for *e*CO_2-induced resistance against *Hpa*. To determine the contribution of priming of JA-dependent defence to *e*CO_2-induced resistance against *Pc*, resistance phenotypes of mutants in JA production (*aos1-1*) or sensitivity (*jar1-1*) were

analysed. In contrast to Col-0, both *aos1-1* and *jar1-1* failed to express elevated *Pc* resistance at *e*CO_2 (Fig. 3.2 d), indicating that priming of JA-inducible defence is critically important for *e*CO_2-induced resistance against *Pc*.

Development-independent resistance at sa*CO_2 is dependent on photorespiration-derived ROS.*

Basal resistance against *Hpa* was enhanced at both *e*CO_2 and *sa*CO_2 (Fig. 3.1 c). This non-linear relationship between CO_2 and *Hpa* resistance suggests involvement of different defence mechanisms at *e*CO_2 and *sa*CO_2. Unlike *e*CO_2 (Fig. 3.2 b), *sa*CO_2 did not alter basal and SA-induced *PR1* gene expression (Fig. S3.3 a). Moreover, despite the enhanced disease susceptibility phenotypes of the SA signalling mutants *sid2-1* and *nrp1-1* in comparison to the wild-type, both mutants displayed a statistically significant increase in *Hpa* resistance at *sa*CO_2 compared to the same mutant background at *a*CO_2 (Fig. S3.3 b). Hence, the SA-dependent defence pathway does not have a critical contribution to *sa*CO_2-induced resistance against *Hpa*. To search for alternative mechanisms, untargeted metabolite profiling of mock- and *Hpa*-inoculated plants at 24 and 72 hours post inoculation (hpi), was performed using UPLC-Q-TOF mass spectrometry (Pétriacq et al., 2016b). Unsupervised principal component analysis displayed global metabolic responses, which were affected by both *Hpa* and CO_2 concentration (Fig. S3.4). To identify ion markers of *sa*CO_2-induced resistance, a stringent pipeline was applied (**Chapter 2***;* Fig. 2.2) which selected for ions that were significantly influenced by CO_2, *Hpa*, or the interaction thereof (Fig. S3.5). Subsequent hierarchical clustering identified ion clusters that were either induced by *sa*CO_2, or primed by *sa*CO_2 for augmented induction after subsequent *Hpa* inoculation (Fig. 3.3). Putative ion marker identification by accurate mass/charge (*m/z*) detection revealed enrichment of metabolites involved in cellular redox regulation (nicotinamide adenine dinucleotide – NAD - metabolism, secondary antioxidant metabolites) and/or defence (glucosinolates, flavonoids, coumarins, alkaloids; Table S3.1). The cluster containing *sa*CO_2-primed markers also included traces of oxidised amino acids (Stadtman and Levine, 2003). Together, these metabolic profiles suggest that plants at *sa*CO_2 are exposed to

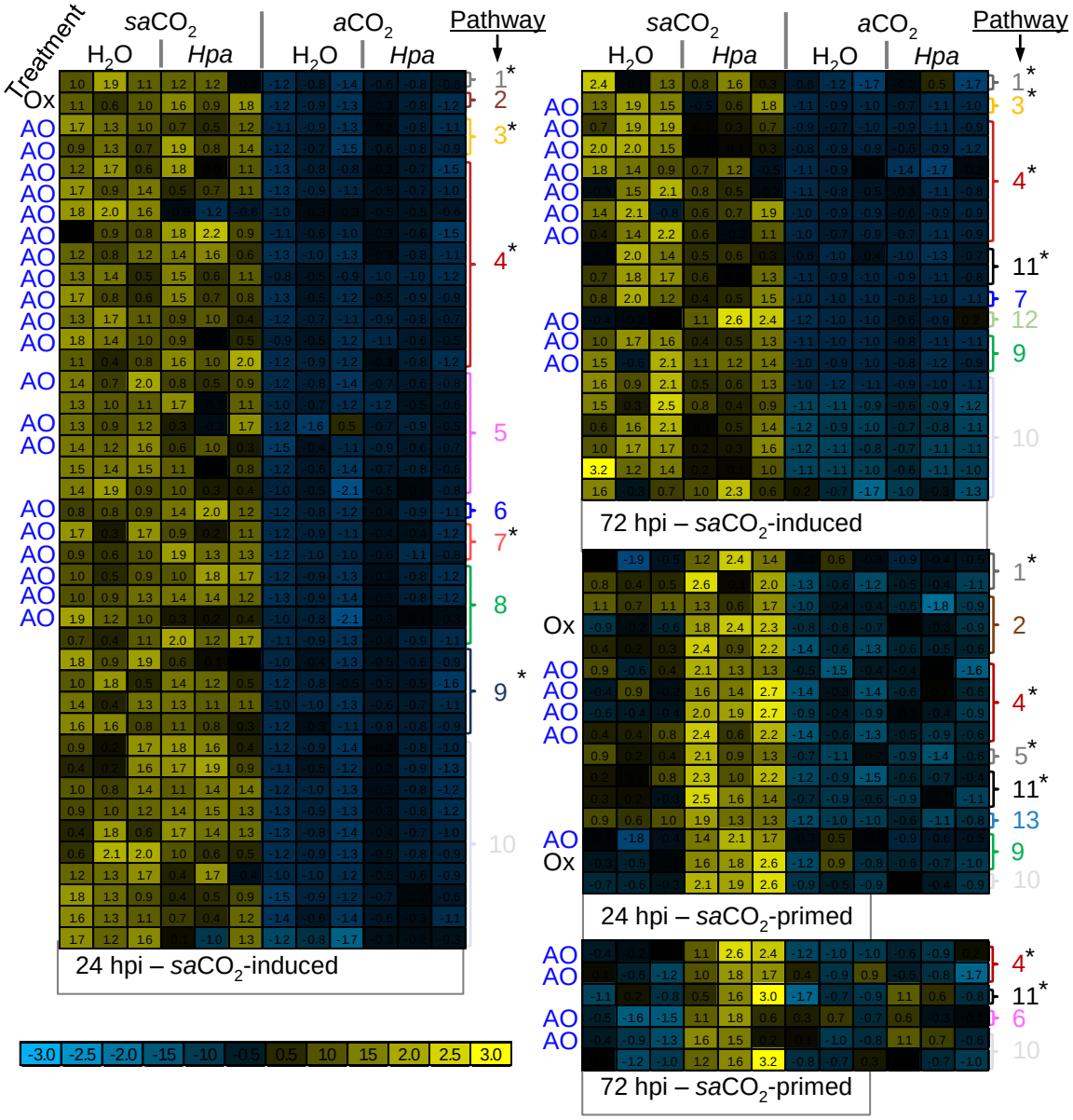

Figure 3.3 Metabolic profiling of mock- and *Hpa*-inoculated Arabidopsis leaves of similar developmental stage at *sa*CO_2 and *a*CO_2. Plants of 8-leaf stage (Col-0) grow at *sa*CO_2 (200 ppm) and *a*CO_2 (400 ppm) were mock- or *Hpa*-inoculated. Methanol extracts from leaves at 24 and 72 hpi were analysed by UPLC-Q-TOF in negative and positive ionization mode. Normalised ion intensities were filtered for statistically significant differences between treatments, using ANOVA ($P < 0.01$ + Benjamini-Hochberg false discovery rate correction), followed by 2-way ANOVA ($P < 0.01$) to select for ion markers that are significantly influenced by CO_2, *Hpa*, or the interaction thereof, at 24 and 72 hpi. Selected markers were subjected to hierarchical clustering (Pearson's correlation). Shown are sub-clusters of markers showing either enhanced accumulation at *sa*CO_2, or priming for augmented induction by *Hpa* at *sa*CO_2. Coloured heat-maps show normalized ion intensities relative to the average and standard deviation across all samples. Pathways corresponding to putative ion identities are shown on the right of the heat-maps; antioxidant properties of putative metabolites are indicated by 'AO' while putative oxidation products are indicated by 'Ox'. Pathways with defence properties are marked with an asterisk. Pathway designations are as follows; 1 – Alkaloids; 2 – Amino acids; 3 – Coumarins; 4 – Flavonoids; 5 – Lipids; 6 – Photorespiration; 7 – Polyphenols; 8 – Redox; 9 – Terpenoids; 10 – Unknown; 11 – Glucosinolates; 12 – Polyamines; 13 – Phytohormones

enhanced oxidative stress, potentially due to increased production of reactive oxygen species (ROS).

As ROS is involved in defence signalling in plants (Torres et al., 2002), we next investigated a possible role for ROS in *sa*CO_2-induced resistance. To this end, mock- and *Hpa*-inoculated leaves were stained at 48 hpi with 3,3'-diaminobenzidine (DAB), which predominantly marks extracellular ROS production, since most DAB substrate is immediately oxidized after leaf infiltration by apoplastic H_2O_2 and peroxidases (Daudi and O'Brien, 2012; **Chapter 2**). Although *Hpa*-inoculated leaves showed increased DAB staining intensity, there were differences observed in extracellular ROS intensities between *sa*CO_2 and *a*CO_2 conditions (Fig. S3.6 a), which was further illustrated upon DAB quantification (Fig. S3.6 b). Furthermore, the respiratory burst oxidase (RBOH) double mutant *rbohD/F*, which is impaired in stress-induced production of extracellular ROS (Torres et al., 2002), was unaffected in *sa*CO_2-induced resistance (Fig. S3.6 c). Hence, extracellular ROS do not play a role in *sa*CO_2-induced resistance. Subsequently, accumulation of intracellular ROS was tested by staining mock- and *Hpa*-inoculated leaves with 2',7'-dichlorofluorescein diacetate (DCFH-DA), which is hydrolysed by intracellular esterases to generate DCF that reacts with intracellular ROS, generating a fluorescent signal (Sandalio et al., 2008)**.** Although *sa*CO_2 did not increase intracellular ROS accumulation in mock-inoculated plants, *Hpa*-inoculated plants at *sa*CO_2 did show augmented ROS accumulation in comparison to *Hpa*-inoculated plants at *a*CO_2 (Fig. 3.4 a). Thus, *sa*CO_2 primes pathogen-induced accumulation of intracellular ROS.

A major source of intracellular ROS is photorespiration, which involves production of hydrogen peroxide from oxidation of glycolate by glycolate oxidases (GOX; Chaouch et al., 2010; Rojas et al., 2012). Loss-of-function mutations in photorespiration causes dramatic growth reduction or lethality at *a*CO_2 conditions (Timm and Bauwe, 2013), making them unsuitable for evaluation of resistance phenotypes at *a*CO_2 and *sa*CO_2. Therefore, single 'knock-down' mutants with T-DNA insertions in the promotors of *GOX* or *HAOX* (*gox1-2* and *haox1-2,* Fig. S3.7 a), which have previously been implicated in Arabidopsis resistance (Rojas et al., 2012), were selected. Despite the fact that these mutations reduced *GOX1* and

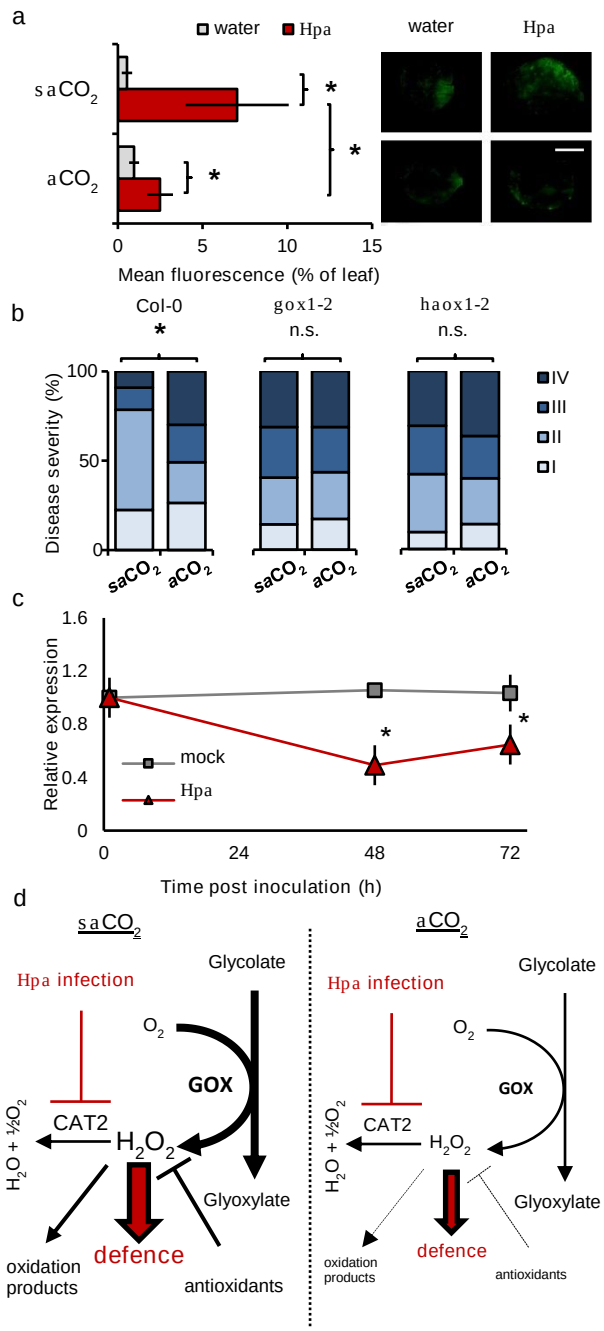

Figure 3.4 Role of photorespiration in *sa*CO_2-induced resistance against *Hpa*. a. Quantification of intracellular H_2O_2 by DCFH-DA staining in plants (Col-0) of similar developmental stage (8-leaf) at *sa*CO_2 (200 ppm) and *a*CO_2 (400 ppm). Shown are mean values of the fluorescent proportion of the leaf area (± SD, n = 8-10) at 48 hpi with water mock or *Hpa*. Insets show representative staining intensities. **b.** Quantification of *Hpa* resistance at *sa*CO_2 and *a*CO_2 in wild-type plants (Col-0) and glycolate oxidase knock-down mutants *gox1-2* and *haox1-2* at the 8-leaf stage. Shown are relative numbers of leaves (n > 50) in *Hpa* colonization classes of increasing severity (I–IV) at 7 dpi. The experiment was repeated with comparable results. **c.** Impacts of *Hpa* inoculation on *CAT2* gene expression in 3-week old Col-0 at *a*CO_2 (8-leaf stage). Shown are mean values of relative transcript abundance (± SD, n = 5) at different times post water or *Hpa* inoculation. Asterisks indicate statistically significant differences (Welch's t-test; Fisher's exact test; $P < 0.05$). The experiment was repeated at both *sa*CO_2 and *a*CO_2, yielding comparable results (Fig. S3.8). **d.** Model explaining the role of photorespiration in priming of ROS-dependent defence at *sa*CO_2. Enhanced photorespiratory activity at *sa*CO_2 causes increased production of H_2O_2 by glycolate oxidase (GOX), which is scavenged by CAT2 and antioxidant metabolites in healthy plants. *Hpa* infection represses transcription of the *CAT2* gene, causing augmented accumulation of GOX-derived H_2O_2 at *sa*CO_2. Impacts of photorespiration on intracellular H_2O_2 are indicated by black arrows. Impacts of *Hpa* on H_2O_2-dependent defence are indicated by red arrows.

HAOX1 expression by 42.6% and 75.4%, respectively (Fig. S3.7 b), *gox1-2* and *haox1-2* showed wild-type growth phenotypes at *sa*CO_2 (Fig. S3.7 c). However, unlike wild-type plants (Col-0), both mutants failed to express *sa*CO_2-induced resistance against *Hpa* (Fig. 3.4 b), indicating a critical role for ROS-generating GOX function.

In un-stressed Arabidopsis plants, GOX-derived ROS are largely scavenged by the peroxisomal catalase enzyme CAT2 (Chaouch et al., 2010). To test whether the augmentation in *Hpa*-induced ROS production at *sa*CO_2 (Fig. 3.4 a) is related to changes in *CAT2* expression, *CAT2* transcript accumulation

was profiled at different time-points after mock and *Hpa* inoculation. At both 48 and 72 hpi, *Hpa*-inoculated plants showed a statistically significant reduction in *CAT2* expression (Fig. 3.4 c), which was apparent at both *a*CO_2 and *sa*CO_2 conditions (Fig. S3.8). Since *sa*CO_2 boosts photorespiration (Li et al., 2014c), these results indicate that *Hpa*-induced *CAT2* repression triggers augmented accumulation of GOX-derived ROS during infection, which in turn results in enhanced resistance at *sa*CO_2 (Fig. 3.4 c).

3.4 Discussion

By eliminating bias from the indirect developmental effects of CO_2 on disease resistance, we have identified distinct mechanisms by which CO_2 shapes plant immunity. There is ample evidence that plant development influences immunity through age-related resistance (ARR; Kus et al., 2002). ARR in Arabidopsis is effective against (hemi)biotrophic pathogens, including *Pseudomonas syringae* pv. *tomato* (*Pst*) and *Hpa* (Kus et al., 2002; McDowell et al., 2005). When experiments were conducted without development correction (DC), *Hpa* resistance intensified with increasing CO_2 concentrations (Fig. 3.1). DC changed this pattern, revealing that plants of a similar developmental stage expressed higher levels of *Hpa* resistance at both *e*CO_2 and *sa*CO_2. These results suggest that, in the absence of DC, the resistance-enhancing effect of *sa*CO_2 against *Hpa* is masked by low ARR of under-developed plants. Interestingly, DC had an opposite effect on CO_2-dependent resistance against *Pc*. Without DC, plants showed enhanced resistance at both *sa*CO_2 and *e*CO_2, whereas plants of a similar developmental stage (*i.e*. after DC) displayed increasing levels of *Pc* resistance with rising CO_2 concentrations. Thus, without DC, assessment of CO_2-dependent resistance against *Pc* is biased by defence mechanisms that are more active at earlier developmental stages. Glucosinolates are known to accumulate to higher levels in younger plants (Petersen et al., 2002; Brown et al., 2003) and are effective against *Pc* (Frerigmann et al., 2016). Alternatively, age-dependent regulation of the JA response could play a role, which is primed in younger plants due to miR156-dependent repression of JAZ6-stabilizing SPL protein (Mao et al., 2017). Taken together, the results suggest

that DC is an effective method to eliminate bias from developmental effects of CO_2 on disease resistance, enabling a more accurate assessment of mechanisms by which CO_2 shapes plant immunity.

Previous studies have reported that *e*CO_2 can enhance, or prime, phytohormone-dependent plant defence (Zhang et al., 2015; Mhamdi and Noctor, 2016). However, none of these studies applied DC to eliminate bias from ARR. While some studies transferred plants of similar developmental age from *a*CO_2 to *e*CO_2 before pathogen inoculation (Zhang et al., 2015), I opted against this method, given it can cause abrupt, and potentially confounding, changes in carbon flux. Furthermore, transferring plants from *a*CO_2 to *e*CO_2 before pathogen challenge may neglect the full extent by which *e*CO_2 affects defence hormone production (Mhamdi and Noctor, 2016). Using DC, it was confirmed that *e*CO_2 enhances basal production of SA and JA (Fig. 3.2 a), causing priming of JA- and SA-dependent gene expression, respectively (Fig. 3.2 b). The JA signalling mutants *aos1-1* and *jar1-1* were impaired in expression of *e*CO_2-induced resistance against *Pc* (Fig. 3.2 d), indicating a critical contribution of JA-dependent defence signalling. Conversely, the SA signalling mutants *sid2-1* and *npr1-1* were only partially affected in *e*CO_2-induced resistance against *Hpa* (Fig. 3.2 c), indicating that priming of SA-dependent defence is not solely responsible for *Hpa* resistance at *e*CO_2. This is consistent with previous conclusions regarding *e*CO_2-induced resistance against hemi-biotrophic *Pseudomonas syringae* pv. *tomato* (*Pst;* Zhang et al., 2015; Mhamdi and Noctor, 2016). Furthermore, Mhamdi and Noctor reported that *e*CO_2-induced resistance to *Pst* is associated with changes in primary metabolism and increased pools of total and oxidised glutathione, while Arabidopsis mutants in glutathione regulation and NADPH-generating enzymes were affected in *Pst* resistance at *e*CO_2 (Mhamdi and Noctor, 2016). Although it is unclear whether these mutants were similarly affected in basal resistance at *a*CO_2, the study concluded that oxidative pathways controlling primary metabolism played a role in *e*CO_2-induced resistance. Since carbohydrate metabolism and signalling can boost SA-dependent and SA-independent defence (Tauzin and Giardina, 2014) by augmenting redox signalling (Morkunas and Ratajczak, 2014), it is tempting to speculate that *e*CO_2-

induced resistance in *Hpa* resistance is a consequence of changes in carbohydrate metabolism.

So far, the effects of *sa*CO_2 on plant disease resistance have received limited attention. The DC experiments presented in this chapter revealed that Arabidopsis expressed enhanced *Hpa* resistance at *sa*CO_2 (Fig. 3.1 b). Untargeted UPLC-Q-TOF analysis revealed that this *sa*CO_2-induced resistance was associated with ion clusters displaying constitutively enhanced accumulation and/or primed accumulation after subsequent *Hpa* infection at *sa*CO_2 (Fig. 3.3). As these ion clusters were enriched with putative metabolites involved in redox regulation, the importance of ROS in *sa*CO_2-induced resistance was explored. While a role for extracellular ROS was excluded (Fig. S3.6), plants at *sa*CO_2 showed augmented production of intracellular ROS after *Hpa* inoculation (Fig. 3.4 a). Glycolate oxidation by GOX is a major source of intracellular H_2O_2 (Chaouch et al., 2010), which likely increases at *sa*CO_2 due to enhanced photorespiration (Temme et al., 2013; Li et al., 2014c). Moreover, GOX-derived ROS have been linked to resistance against non-host pathogens in both Arabidopsis and *Nicotiana benthamiana* (Rojas et al., 2012). Indeed, *knock-down* mutants with reduced transcription of two separate *GOX* genes failed to express enhanced *Hpa* resistance at *sa*CO_2, indicating a crucial role for photorespiratory ROS. The peroxisomal catalase enzyme, CAT2, scavenges GOX-derived H_2O_2 to mitigate oxidative damage during photorespiration (Chaouch et al., 2010). Interestingly, transcriptional profiling of the *CAT2* gene revealed that Arabidopsis reduced *CAT2* expression after *Hpa* inoculation (Fig. 3.4 c; Fig. S3.8). Since CAT2 suppresses plant defence (Polidoros et al., 2001; Chaouch et al., 2010), this pathogen-induced *CAT2* repression likely reflects an innate immune response to generate defence-inducing ROS during infection. In this context, I propose that stimulation of photorespiration-related GOX activity at *sa*CO_2 primes pathogen-induced accumulation of intracellular ROS. Subsequent repression of *CAT2* expression following *Hpa* attack results in augmented accumulation of intracellular ROS, which mediates an augmented SA-independent defence response in comparison to *a*CO_2-exposed plants (Fig. 3.4 d).

It is plausible that photorespiration-derived ROS were key to survival when plants adapted to glacial periods with low atmospheric CO_2. Reduced growth and plant fecundity at glacial CO_2 conditions required longer life cycles to maintain reproductive fitness (Ward and Kelly, 2004). Additionally, reduced investment in foliar defence compounds at *sa*CO_2 would have consequently put plants at a higher risk of pathogen attack (Quirk et al., 2013), creating selective pressure for a primed immune system. Potentially, C3 plants benefitted from increased levels of photorespiration-derived ROS to prime their immune system. Along with limiting 2-PG toxicity, this hypothesis may explain why certain C4 plants (*e.g.* maize) have retained levels of photorespiration and GOX activity (Peterhansel and Maurino, 2011). This work has uncovered a specific link between *sa*CO_2, GOX-derived ROS and enhanced immunity. This evidence supports the notion that plants have utilised photorespiratory defence signalling over glacial periods to maintain elevated levels of adaptive broad-spectrum disease resistance. This may be especially pertinent to Arabidopsis which evolved under the CO_2 limited atmosphere of the Miocene epoch (Beilstein et al., 2010). In this context, future initiatives to replace C3 metabolism with C4 metabolism in major food crops may require careful consideration of the contribution of photorespiration to plant defence.

3.5 Supporting figures

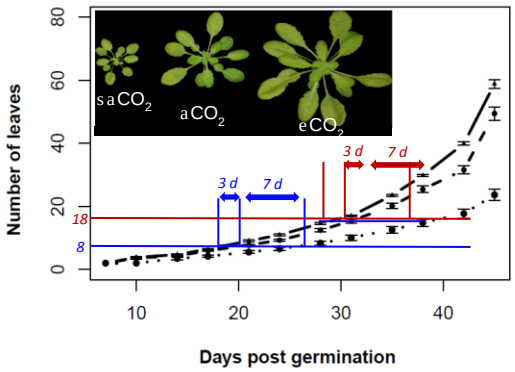

Figure S3.1 Effects of CO_2 on plant development. Data represent average leaf numbers (± SE; n = 8) plotted against time (days) at ambient CO_2 (*a*CO_2; 400 ppm; dashed line), subambient CO_2 (*sa*CO_2; 200 ppm; dotted line) and elevated CO_2 (*e*CO_2; 1200 ppm; straight line). Inserts show typical rosette sizes of 4.5-week old plants. Red and blue lines illustrate differences in absolute age at the 8- and 18-leaf stage, respectively. Shown are results from a representative experiment that was repeated twice.

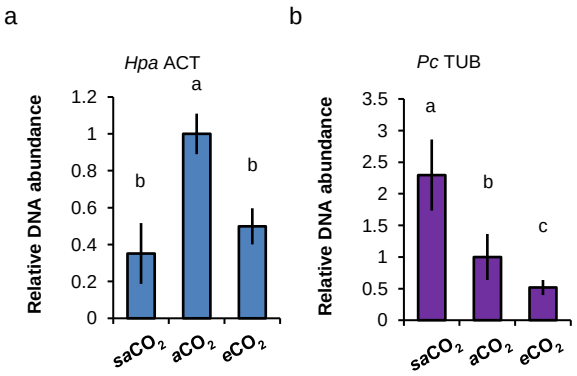

Figure S3.2 qPCR-based quantification of pathogen biomass to confirm the development-independent effects of CO_2 on resistance against *Hpa* and *Pc*. a. Relative quantification of *Hpa* DNA was based on the *Hpa* actin gene (ID: 807716). **b.** Relative quantification of *Pc* DNA was based on the *Pc* β-tubulin gene. Data represent relative DNA quantities normalized to Arabidopsis *ACT2* (At3g18780; ± SD, n = 4). Letters indicate statistical differences (ANOVA + Tukey post-hoc analysis; $P < 0.05$). For details about DC and timing of pathogen inoculation, see legend to Fig. 1.

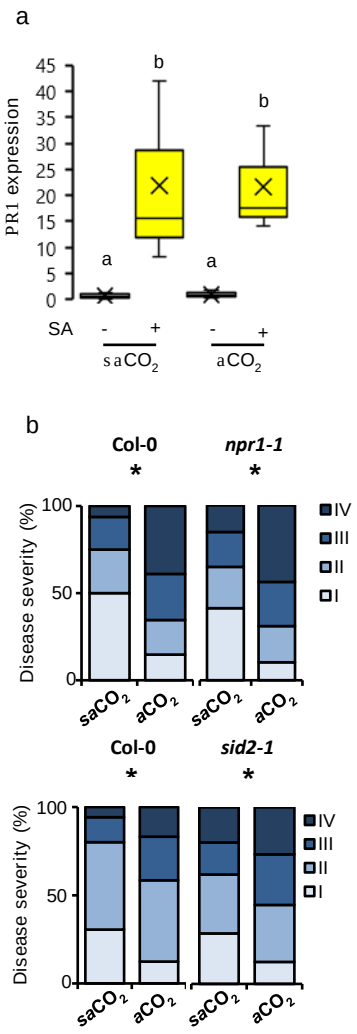

Fig. S3.3 SA signalling in *sa*CO_2-induced resistance against *Hpa*. **a.** Levels of SA-inducible *PR1* gene expression in 8-leaf Col-0 at *sa*CO_2 (200 ppm) and *a*CO_2 (400 ppm). Shown are box plots of relative transcript values (n = 3; X indicates means) at 24 hours after treatment. **b.** Quantification of *Hpa* resistance at *sa*CO_2 and *a*CO_2 in Col-0, the SA insensitive *npr1-1* mutant, and the SA production mutant *sid2-1* at the 8-leaf stage. Shown are relative numbers of leaves (n > 50) in *Hpa* colonization classes of increasing severity (I–IV) at 7 dpi. Letters - (**a**) ANOVA with Tukey HSD post hoc analysis - or asterisks - (**b**) Fisher's exact test - indicate statistically significant differences between conditions (P < 0.05). The pathogenicity assays with *sid2-1* and *npr1-1* were repeated with similar results.

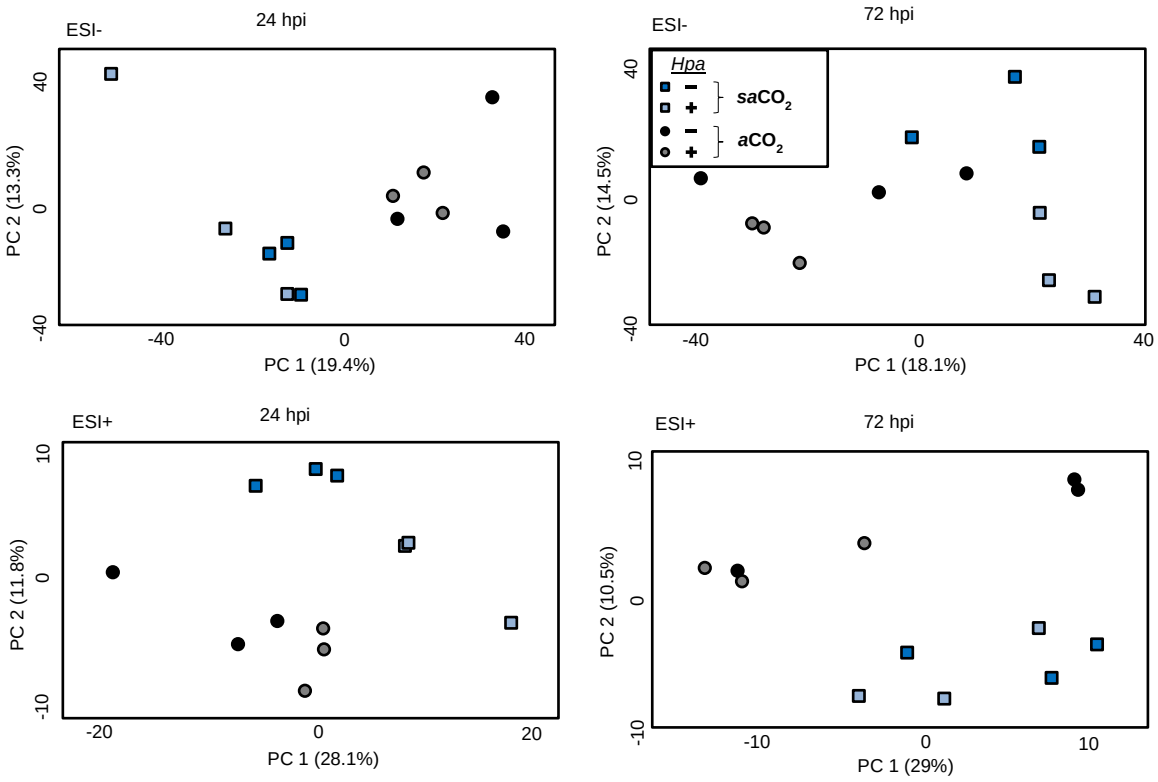

Figure S3.4 Global metabolic signatures of mock- and *Hpa*-inoculated Arabidopsis (Col-0) at the 8-leaf growth stage at *sa*CO_2 (200 ppm) and *a*CO_2 (400 ppm). Shown are principal component analysis (PCA) plots of negative (ESI^-; 4497 ions) and positive (ESI^+; 5683 ions) ionizations, obtained by UPLC-Q-TOF analysis of methanol extracts from leaf tissue at 24 and 72 hpi. Samples from plants grown at *sa*CO_2 are indicated by circles; samples from plants at *a*CO_2 are indicated by squares. Black/blue symbols indicate mock-inoculated plants; grey/ light blue symbols indicate samples from *Hpa*-inoculated plants.

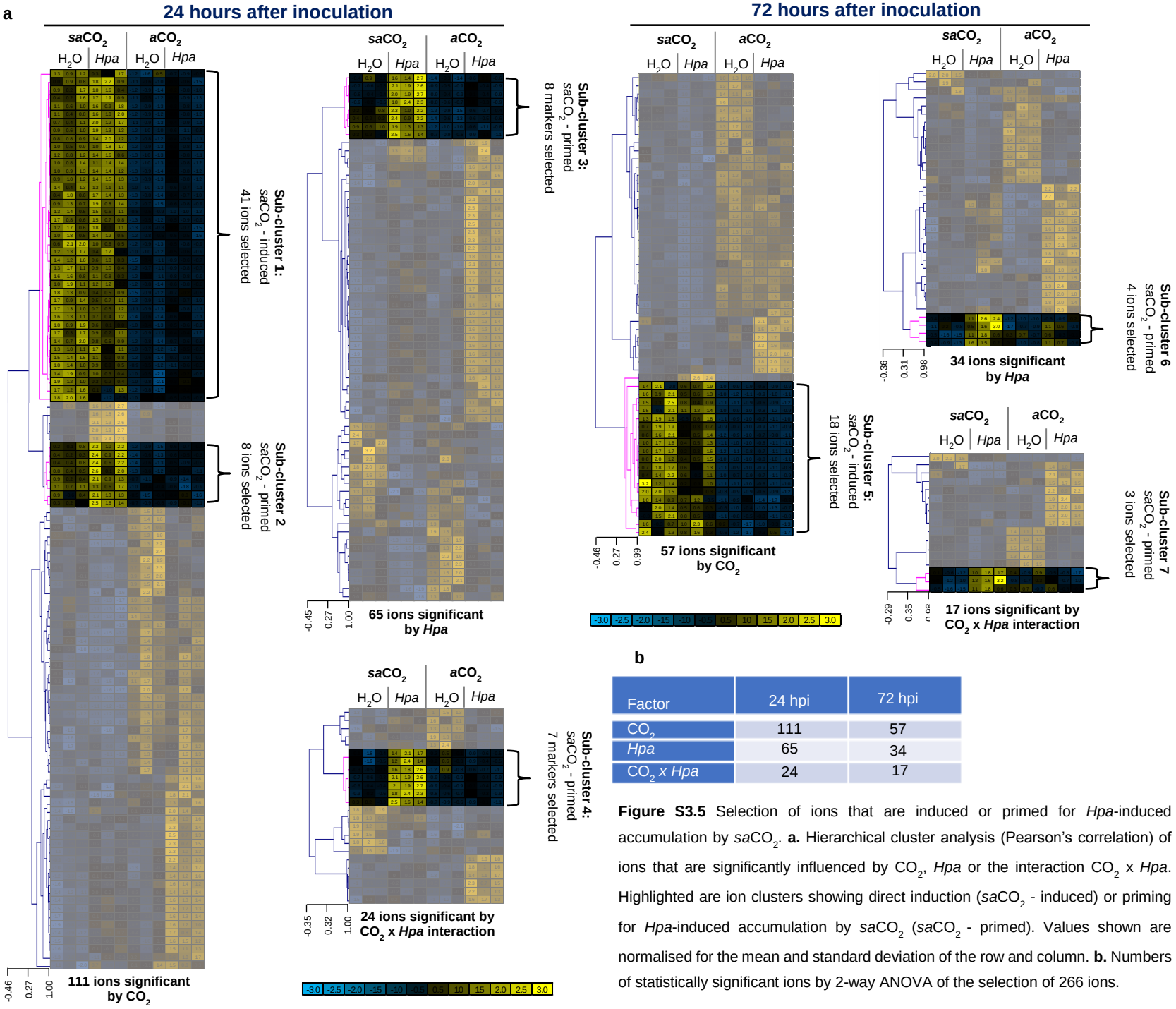

b

Factor	24 hpi	72 hpi
CO_2	111	57
Hpa	65	34
CO_2 *x Hpa*	24	17

Figure S3.5 Selection of ions that are induced or primed for *Hpa*-induced accumulation by *sa*CO_2. **a.** Hierarchical cluster analysis (Pearson's correlation) of ions that are significantly influenced by CO_2, *Hpa* or the interaction CO_2 x *Hpa*. Highlighted are ion clusters showing direct induction (*sa*CO_2 - induced) or priming for *Hpa*-induced accumulation by *sa*CO_2 (*sa*CO_2 - primed). Values shown are normalised for the mean and standard deviation of the row and column. **b.** Numbers of statistically significant ions by 2-way ANOVA of the selection of 266 ions.

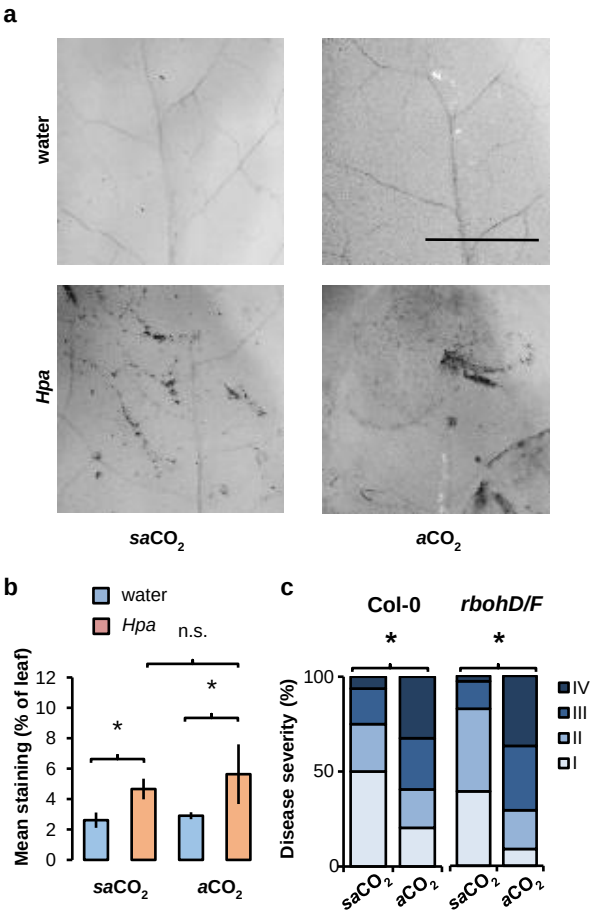

Figure S3.6 Extracellular H_2O_2 in *sa*CO_2-induced resistance against *Hpa*. **a.** Visualization of extracellular H_2O_2 accumulation in leaves of Arabidopsis (Col-0) at *a*CO_2 (400 ppm) and *sa*CO_2 (200 ppm). Shown are 3,3′-diaminobenzidine (DAB)-stained leaves at 48 hours after mock (water) or *Hpa* inoculation. Bar = 1 mm. **b.** Quantification of DAB staining signal by image analysis. Shown are mean values of the stained proportion of the leaf area (± SD, n = 5). **c.** Evaluation of *Hpa* resistance at *a*CO_2 and *sa*CO_2 in Col-0 and *rbohD/F* plants at the 8-leaf stage. The *rbohD/F* double mutant is impaired in production of extracellular H_2O_2 by NADP-dependent oxidase. Shown are relative numbers of leaves (n > 50) in *Hpa* colonization classes of increasing severity (I–IV) at 7 dpi. Asterisks indicate statistically significant differences between CO_2 conditions (Fisher's exact test; $P < 0.05$).

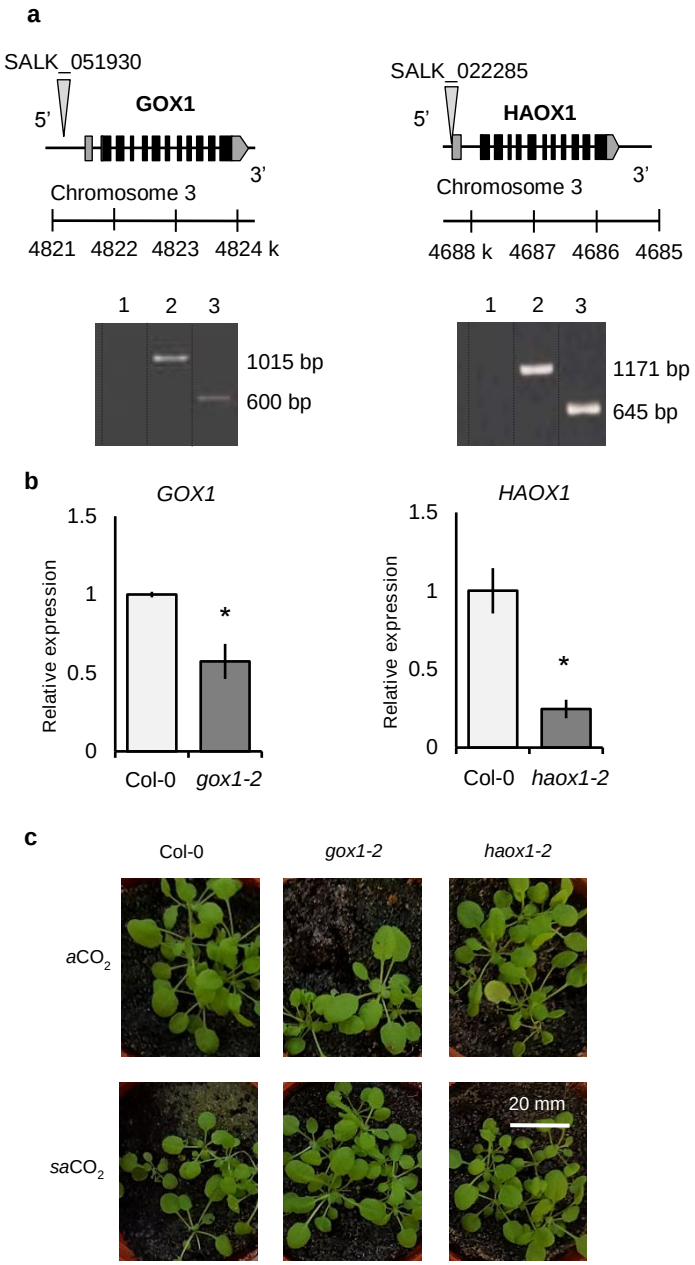

Figure S3.7. Selection of *gox1-2* (SALK_051930) and *haox1-2* (SALK_022285) *knock-down* mutants. **a.** PCR confirmation of homozygous T-DNA insertions. Gene models show locations of T-DNA insertions in promoter regions of *GOX1* and *HAOX1*. Images show PCR products from 1) mutant DNA with LP + RP primers (no band); 2) Col-0 DNA with LP + RP primers, and 3), mutant DNA with LBb1.3 + RP primers. **b.** Impacts of *knock-down* mutations on transcription of *GOX1* and *HAOX1* in *gox1-2* and *haox1-2* plants, respectively. Shown are mean values of relative transcript levels (± SD; n = 5) in shoot tissues of 3-week old plants. Asterisks indicate statistically significant reductions in relative transcript level compared to wild-type plants (Col-0; Student's t-test, $P < 0.05$). The experiment was repeated with similar results. **c.** Growth phenotypes of 3-week old Col-0, *gox1-2* and *haox1-2* at *a*CO_2 and *sa*CO_2 conditions.

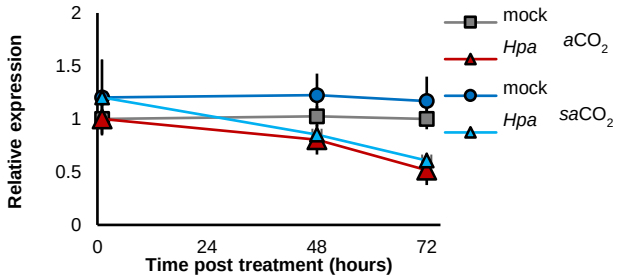

Fig. S3.8. Impacts of *Hpa* inoculation on *CAT2* gene expression in 8-leaf Col-0 plants at *sa*CO_2 (200 ppm) and *a*CO_2 (400 ppm). Shown are mean values of relative transcript abundance (± SD, n = 5) at different hours post mock (water) or *Hpa* inoculation.

Table S3.1 Putative identification of metabolic markers detected by UPLC-Q-TOF

Treatment [a]	*P* value [b]	Detected *m/z* [c]	RT (min) [c]	Adducts [d]	Predicted mass [d]	Error (ppm) [d]	Putative compound [d]	Predicted formula [d]	Pathways [e]
24 hours	1.2E-03	351.992	4.4	*[M+K]+*	313.021	19	Eudistomin H	C15H12BrN3	Alkaloids
	6.0E-03	422.166	1.6	*[M-H]-*	423.168	13	N-Methyl-2,3,7,8-tetramethoxy-5,6-dihydrobenzophenathridine-6-ethanoic acid	C24H25NO6	Alkaloids
	6.6E-03	482.067	1.8	*[M+Cl]-*	447.108	22	Pigment A aglycone	C25H19O8	Anthocyanins
	1.0E-03	244.027	1.5	*[M+K-2H]-*	207.081	11	Anthocyanidins	C15H11O	Anthocyanins
	2.2E-04	933.074	1.1	*[M-H]-*	934.071	10	Vescalagin	C41H26O26	Anthocyanins
	2.2E-04	391.066	1.1	*[M+Na-2H]-*	370.090	4	5-Hydroxy-6-methoxycoumarin 7-glucoside	C16H18O10	Coumarin
	2.2E-04	457.133	2.9	*[M-H]-*	458.142	5	cis-p-Coumaric acid 4-[apiosyl-(1->2)-glucoside]	C20H26O12	Coumarin
	5.3E-03	427.124	1.5	*[M+Na]+*	404.126	20	Calomelanol C	C24H20O6	Flavonoids
	1.3E-03	329.008	4.4	*[M+2Na-H]+*	284.032	13	7,4\',5\'-Trihydroxy-5,2\'-oxido-4-phenylcoumarin	C15H8O6	Flavonoids
	6.0E-03	639.161	3.0	*[M-H]-*	640.164	6	Laricitrin 3-rutinoside	C28H32O17	Flavonoids
	9.0E-03	932.246	2.8	*[M-H]-*	933.266	14	Pelargonidin 3-O-[b-D-Glucopyranosyl-(1->2)-[4-hydroxy-3-methoxy-(E)-cinnamoyl-(->6)]-b-D-glucopyranoside] 5-O-b-D-glucopyranoside	C43H49O23	Flavonoids
	2.5E-03	421.163	1.6	*[M-H]-*	422.173	6	Euchrenone b10	C25H26O6	Flavonoids
	5.6E-03	487.123	2.7	*[M-H]-*	488.132	3	Acacetin 7-(2\'\'-acetylglucoside)	C24H24O11	Flavonoids
	1.4E-03	667.080	3.4	*[M+2Na-H]+*	622.117	12	Apigenin 7-glucuronosyl-(1->2)-glucuronide	C27H26O17	Flavonoids
	3.4E-03	603.292	1.6	*[M-H]-*	604.288	10	Cerbertin	C32H44O11	Glucosides
	7.8E-04	199.097	2.5	*[M-H]-*	200.105	2	Decenedioic acid	C10H16O4	Lipids
	8.2E-03	453.209	3.0	*[M+Na-2H]-*	432.236	2	Glucosyl (2E,6E,10x)-10,11-dihydroxy-2,6-farnesadienoate	C21H36O9	Lipids
	8.4E-03	869.480	5.5	*[M+Cl]-*	833.521	20	PS (18:1(9Z)/22:6(4Z,7Z,10Z,13Z,16Z,19Z))	C46H76NO10P	Lipids
	6.0E-03	603.289	1.6	*[M+Cl]-*	567.317	8	PS (10:0/10:0)	C26H50NO10P	Lipids
	4.2E-03	449.190	1.6	*[M+K-2H]-*	411.239	10	PC (O-8:0/2:0)	C18H38NO7P	Lipids
	8.3E-03	431.196	1.6	*[M+Cl]-*	397.223	7	PE (12:0/0:0)	C17H36NO7P	Lipids
	1.4E-03	251.003	4.4	*[M+H]+*	250.000	18	Glycerate	C6H10CaO8	Photorespiration
	3.9E-03	315.108	2.5	*[M-H]-*	316.116	3	Hydroxytyrosol 1-O-glucoside	C14H20O8	Polyphenol
	2.7E-04	249.112	3.4	*[M+H]+*	248.105	0	Prenyl caffeate	C14H16O4	Polyphenol
	1.2E-04	350.988	4.4	*[M+K]+*	312.022	7	Gamma-Glutamyl-Se-methylselenocysteine	C9H16N2O5Se	Redox
	4.4E-03	267.087	1.6	*[M-H]-*	268.088	21	Cysteinyl-Phenylalanine	C12H16N2O3S	Redox
	6.9E-04	665.080	3.3	*[M+H]+*	664.093	30	Deamino-NAD$^+$	C21H26N6O15P2	Redox
	1.1E-03	493.077	2.9	*[M+Na]+*	470.088	0	Phe4Cl-Tyr-OH	C23H19ClN2O7	Amino acids
	6.6E-03	423.159	1.6	*[M+Na-2H]-*	402.189	10	D-Linalool 3-(6''-malonylglucoside)	C19H30O9	Terpenoids
	5.1E-04	467.166	2.1	*[M-H]-*	468.178	11	Dukunolide D	C26H28O8	Terpenoids
	4.2E-03	431.192	1.6	*[M-H]-*	432.197	5	S-Furanopetasitin	C24H32O5S	Terpenoids
	1.1E-03	331.001	4.4						Unknown
	7.3E-03	330.987	4.4						Unknown
	1.1E-04	97.978	4.4						Unknown
	8.1E-03	330.957	4.4						Unknown
	3.0E-05	249.986	4.4						Unknown
	1.7E-03	997.443	2.9						Unknown
	7.4E-03	1001.458	2.8						Unknown
	8.2E-03	731.210	1.9						Unknown
	1.4E-03	1100.454	3.0						Unknown
	8.1E-03	1187.442	2.8						Unknown
72 hours	5.5E-03	634.415	6.2	*[M+NH4]+*	616.378	5	Tabernamine	C40H48N4O2	Alkaloids
	1.3E-03	329.008	4.4	*[M+2Na-H]+*	284.032	13	7,4\',5\'-Trihydroxy-5,2\'-oxido-4-phenylcoumarin	C15H8O6	Coumarin
	1.1E-03	493.077	2.9	*[M+2Na-H]+*	448.101	10	1,2,6,8-Tetrahydroxy-3-methylanthraquinone 2-O-b-D-glucoside	C21H20O11	Flavonoids
	2.2E-04	391.066	1.1	*[M-H]-*	392.074	2	5,7,3\',4\',5\'-Pentahydroxy-3,6,8-trimethoxyflavone	C18H16O10	Flavonoids
	5.3E-03	427.124	1.5	*[M+H-H2O]+*	444.121	13	Artomunoxanthentrione	C26H20O7	Flavonoids

	2.5E-03	421.163	1.6	*[M-H]-*	422.173	6	Euchrenone b10	C25H26O6	Flavonoids
	8.1E-03	348.991	4.4	*[M+2Na-H]+*	304.014	16	6-Chloroapigenin	C15H9ClO5	Flavonoids
	8.2E-03	730.203	1.9	*[M+NH4]+*	712.185	21	Syringetin 3-(,6\'\'\'-acetylglucosyl)(1->6)-galactoside	C31H36O19	Flavonoids
	1.0E-03	244.027	1.5	*[M+H+Na]2+*	464.056	1	4-Hydroxyglucobrassicin	C16H20N2O10S2	Glucosinolate
	1.4E-03	664.066	3.4	*[M+Na]+*	641.091	20	6-Sinapoylglucoraphenin	C23H31NO14S3	Glucosinolate
	1.4E-03	251.003	4.4	*[M+H]+*	250.000	18	Glycerate	C6H10CaO8	Photorespiration
	7.4E-03	301.119	1.7	*[M+Na-2H]-*	280.142	5	Feruloyl-2-hydroxyputrescine	C14H20N2O4	Polyamines
	1.2E-04	350.988	4.4	*[M+K]+*	312.022	7	Gamma-Glutamyl-Se-methylselenocysteine	C9H16N2O5Se	Redox
	6.9E-04	664.071	3.3	*[M+H]+*	663.109	68	NAD^+	C21H27N7O14P2	Redox
	1.1E-03	331.001	4.4						Unknown
	7.3E-03	330.987	4.4						Unknown
	1.2E-03	327.999	4.4						Unknown
	1.1E-04	97.978	4.4						Unknown
	3.0E-05	249.986	4.4						Unknown
	2.0E-04	992.945	8.7						Unknown
24 hours + *Hpa*	9.95E-03	165.080	0.8	*[M+H-2H2O]+*	200.095	16	Harmalol	C12H12N2O	Alkaloids
	9.9E-03	882.307	3.0	*[M-H]-*	883.290	27	Wilfordine	C43H49NO19	Alkaloids
	4.0E-05	293.100	1.3	*[M-H]-*	294.106	3	N-Glycosyl-L-asparagine	C10H18N2O8	Amino acids
	1.6E-03	416.105	2.3	*[M-H]-*	417.117	11	Asn-TyrMe-OH	C19H19N3O8	Amino acids
	5.3E-03	146.061	1.0	*[M+H-2H2O]+*	181.074	1	L-Tyrosine	C9H11NO3	Amino acids
	3.6E-03	778.169	2.3	*[M+Na-2H]-*	757.219	32	Pelargonidin 3-sophoroside 5-glucoside	C33H41O20	Flavonoids
	1.0E-05	189.074	1.8	*[M-H2O-H]-*	208.089	17	Chalcone	C15H12O	Flavonoids
	1.1E-03	417.107	2.3	*[M-H]-*	418.126	29	4\'-Hydroxy-3,5,6,7,3\',5\'-hexamethoxyflavone	C21H22O9	Flavonoids
	8.0E-03	557.298	2.9	*[M-H]-*	558.298	12	Denticulaflavonol	C35H42O6	Flavonoids
	1.7E-03	454.203	3.0	*[M-H]-*	455.212	2	5-Ribosylparomamine	C17H33N3O11	Glucosides
	6.4E-04	402.089	1.7	*[M-H]-*	403.097	1	3-Methylpentyl glucosinolate	C13H25NO9S2	Glucosinolates
	5.4E-03	448.069	1.7	*[M+2Na-H]+*	403.097	0	3-Methylpentyl glucosinolate	C13H25NO9S2	Glucosinolates
	2.7E-04	249.112	3.4	*[M+Na-2H]-*	228.136	5	(-)-11-hydroxy-9,10-dihydrojasmonic acid	C12H20O4	Phytohormones
	1.12E-03	119.074	0.8	*[M+H-H2O]+*	136.0749	15	Tetrahydropteridine	C6H8N4	Redox
	3.6E-03	221.983	0.4	*[M-H2O-H]-*	241.008	29	3-Mercaptolactate-cysteine disulfide	C6H11NO5S2	Thiols
	2.6E-04	1044.112	5.4						Unknown
72 hours + *Hpa*	7.4E-03	301.119	1.7	*[M-H]-*	302.115	36	2,4\'-Dihydroxy-4,6-dimethoxydihydrochalcone	C17H18O5	Flavonoids
	8.3E-03	543.245	4.3	*[M+Na-2H]-*	522.268	4	7,8-Dihydro-3b,6a-dihydroxy-alpha-ionol 9-[apiosyl-(1->6)-glucoside]	C24H42O12	Flavonoids
	5.4E-03	448.069	1.7	*[M+2Na-H]+*	403.097	1	3-Methylpentyl glucosinolate	C13H25NO9S2	Glucosides
	5.7E-03	525.353	5.8	*[M+H]+*	524.348	3	PG (P-20:0/0:0)	C26H53O8P	Lipids
	1.5E-03	547.590	6.2						Unknown
	1.8E-03	518.763	5.6						Unknown

[a] : conditions for which the metabolic markers showed a statistically significant accumulation between $saCO_2$ and aCO_2

[b] : *P* values indicate levels of significance from FDR adjusted ANOVA and subsequent two-factor ANOVA ($P < 0.01$)

[c] : accurate *m/z* values with their corresponding retention time (RT) detected by UPLC-qTOF-MS

[d] : predicted parameters from the METLIN database using the detected accurate *m/z. Adducts : type of ion generated by electrospray ionization; Δppm: difference between observed and theoretical monoisotopic masses.*

PC: Phosphatidylcholine; PE: Phosphatidylethanolamine; PG: Phosphoglycerol; PS: Phosphatidylserine.

[e] : putative metabolites and their corresponding pathways were validated by information from the PubMed chemical database

Chapter 4: Impacts of glacial-to-future atmospheric CO_2 on bacterial rhizosphere colonisation in relation to plant growth and systemic resistance responses.

4.1 Abstract

Concern over rising atmospheric CO_2 concentrations has led to growing interest in the effects of global change on plant-microbiome interactions. As a primary substrate of photosynthesis, atmospheric CO_2 determines plant metabolism and influences root exudation chemistry. Accordingly, I predict that changes in atmospheric CO_2 concentration affect rhizosphere signalling and colonisation by soil microbes. In this study, the effects of past-to-future CO_2 concentrations on Arabidopsis rhizosphere colonisation by the rhizobacterial species *Pseudomonas simiae* WCS417, and the saprophytic bacterial species *Pseudomonas putida* KT2440, in nutrient-poor and nutrient-rich soils were examined. Rhizosphere colonisation by saprophytic KT2440 was not influenced by atmospheric CO_2 in either soil substrate. Conversely, rhizosphere colonisation by the specialist WCS417 strain increased at rising CO_2 concentration, in nutrient-poor soil. Examination of host responses to WCS417 colonisation revealed that plant growth and systemic resistance varied according to atmospheric CO_2 concentration and soil type, ranging from growth promotion with induced susceptibility at sub-ambient CO_2, to growth repression with induced resistance at elevated CO_2. Collectively, these results demonstrate atmospheric CO_2 and soil nutritional status can influence the nature of plant-rhizobacteria interactions. This outcome illustrates that plant responses to soil microbes should be taken into account for predictions of plant performance in response to changes in global climate and soil quality.

4.2 Introduction

Atmospheric CO_2 influences microbial diversity and its biomass in the rhizosphere (Paterson et al., 1997). Soil CO_2 concentrations are typically much

higher than atmospheric CO_2 concentrations (ranging between 2000 and 38000 ppm in soil pore spaces; Drigo et al., 2008), and even large increases in atmospheric CO_2 are thought to have little direct impact on CO_2 concentrations in soils. Indeed, effects of atmospheric CO_2 on soil communities are much less apparent in the absence of plants (Wiemken et al., 2001; Montealegre et al., 2002), indicating a dominant, plant-mediated mechanism. The most plausible factor driving root/ microbe associations is the exudation of photosynthates, which are estimated to range between 5 and 40% of fixed carbon (Lynch and Whipps, 1990; Hinsinger et al., 2006; Marschner, 2012). Rhizodeposition via carbon (C) exudation is enhanced under elevated CO_2 (eCO_2; Phillips et al., 2009; Eisenhauer et al., 2012). As a result, rhizosphere colonisation by microfauna and microbes that rely on C from plant exudates will be influenced by atmospheric CO_2 concentrations (Lipson and Wilson, 2005; Kassem et al., 2008; Eisenhauer et al., 2012).

The extent to which elevated CO_2 (eCO_2) affects microbial interactions in the rhizosphere remains controversial. Using chloroform fumigation extraction (CFE) to estimate microbial biomass, studies have reported both positive and negative relationships with eCO_2 (Rice et al., 1994; Ross et al., 1995; Kassem et al., 2008; Eisenhauer et al., 2012). It also remains contentious in how far eCO_2 induces shifts between fungal or bacterial communities (Ross et al., 1995; Lipson and Wilson, 2005; Drigo et al., 2008). Nevertheless, it is clear that CO_2 alters overall microbial community composition across a range of different soil types (Montealegre et al., 2002; Janus et al., 2005). Relatively early studies, focusing on eCO_2 stimulation of plant growth and rhizosphere microbial taxa, suggested a possible relationship between eCO_2, plant growth and increases in plant growth-promoting rhizobacteria (PGPR; O'Neill et al., 1987). PGPR are more closely associated with plant roots than generalist saprophytic soil colonisers and should, therefore, be more reliant on plant-derived C (Denef et al., 2007). Surprisingly, however, while there is extensive evidence that plant-rhizobia and plant-mycorrhiza interactions change at eCO_2 (*e.g.* Rogers et al., 2009; Mohan et al., 2014), functional efficacy of PGPR in eCO_2 is scarcely studied (Drigo et al., 2008). Considering that PGPR modulate a range of agronomically important plant traits, including plant growth, abiotic stress tolerance and resistance to pests and

diseases (Lugtenberg and Kamilova, 2009), this knowledge gap limits our ability to predict how man-made climate change will impact crop production and food security.

Although eCO_2 effects on the abundance of plant root-associated microbes are well studied, comparisons across a range of CO_2 conditions, including sub-ambient CO_2 (*sa*CO_2), are rare (Field et al., 2012). Furthermore, the effects of a range of CO_2 concentrations on interactions with specific plant-beneficial rhizobacteria and corresponding plant responses remain unknown. In a CO_2 gradient study (200 ppm to 600 ppm), microbial mass and soil respiration from a grassland ecosystem failed to detect a clear relationship to CO_2 concentration (Gill et al., 2006). By contrast, analysis of fungal communities, using pyrosequencing of internal transcribed spacer (ITS) sequences, revealed a positive relationship between operational taxonomic unit (OTU) richness and CO_2 concentration that was soil-type dependent (Procter et al., 2014). While these studies suggest that atmospheric CO_2 impacts plant-beneficial bacteria and fungi in the rhizosphere, it remains difficult to ascertain the underpinning mechanisms, or predict outcomes of plant responses to altered colonisation by these microbes. Most studies regarding the effect of atmospheric CO_2 gradients on rhizosphere microbes involved field experiments, which are prone to environmental variability, such as nutrient availability, soil moisture, temperature, soil pH, and plant species present (Freeman et al., 2004; Castro et al., 2010; Classen et al., 2015; Dam et al., 2017).

In this chapter, I employed controlled environmental conditions to study impacts of *sa*CO_2 and *e*CO_2 on rhizosphere colonisation by two well-characterised soil bacteria: the generalist saprophytic soil coloniser *P. putida* KT2440 and the specialist rhizosphere coloniser *P. simiae* WCS417. Strains with distinctly different life-styles were selected to investigate how CO_2 stimulates colonisation of the specialist rhizosphere strain in soil of relatively poor nutrient quality. My hypothesis was that the bacteria less associated with the plant roots, Kt2440, would be less affected by changing CO_2 concentration. Furthermore, I hypothesised that the bacteria that forms a closer association with the root, WCS417, could be affected in its ability to promote growth and ISR when carbon input is altered. Interestingly, increased colonisation was associated with

contrasting growth and systemic resistance responses in the host plant, demonstrating that changes in atmospheric CO_2 have profound and counterintuitive outcomes on plant production and resistance via indirect impacts on rhizosphere interactions.

4.3 Results

Impacts of atmospheric CO_2 on rhizosphere colonisation by soil bacteria depends on soil quality and bacterial species.

C and N content are markers for soil quality (Gil-Sotres et al., 2005), which directly alters the performance of PGPR (*e.g.* Egamberdiyeva, 2007; Agbodjato et al., 2015). To examine the importance of soil quality on rhizosphere colonisation by two well-studied soil bacteria, Arabidopsis was cultivated either in artificial nutrient-poor soil (1:9 sand:compost; v/v) with low C- and N-contents, or in nutrient-rich soil (2:3 sand:compost; v/v) with relatively high C and N content (Table 4.1). Soils were inoculated with 5 x 10^7 CFU.g^{-1} soil of *Pseudomonas simiae* WCS417, a specialist rhizosphere coloniser (Rainey, 1999; Zamioudis et al., 2014), or *Pseudomonas putida* KT2 440, a more generalist saprophytic soil coloniser (Weinel et al., 2002). Plants, or non-planted control soil, were subsequently left for 4 weeks before sampling for bacterial colonisation through enumeration of CFUs on selective agar medium. As expected, the specialist rhizosphere coloniser WCS417 showed poor colonisation in bulk soil, but performed exceptionally well in rhizosphere soil, which was clear for both soil types (Fig. 4.1). By contrast, the generalist saprophytic coloniser KT2440 colonised rhizosphere and bulk soil from both soil types with equal efficiencies, although its levels of rhizosphere colonisation remained orders of magnitude lower than that of WCS417.

Table 4.1 Determination of C and N concentrations in nutrient rich and poor soil

	Carbon (C)		Nitrogen (N)		C:N
Nutrient poor	2.58%	(0.15)	0.21%	(0.01)	12.29
Nutrient rich	18.78%	(0.48)	0.37%	(0.03)	51.02

To examine if atmospheric CO_2 alters rhizosphere colonisation by WCS417 and KT2440, Arabidopsis (accession Col-0) was cultivated for 4 weeks in both soil types at *sa*CO_2 (200 ppm), ambient CO_2 (*a*CO_2; 400 ppm) or *e*CO_2 (1200 ppm) before quantification of rhizosphere colonisation. Interestingly, in

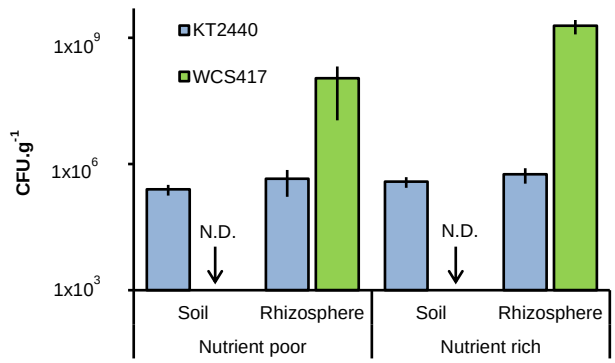

Figure 4.1. Effects of soil nutritional status on colonisation by *P. simiae* WCS417 and *P. putida* KT2440. Bacteria were introduced into nutrient-poor soil or nutrient-rich soil at $5x10^7$ CFU.g^{-1}. Colony forming units (CFU.g^{-1}) of KT2400 (blue) and WCS417 (green) were determined after 4 weeks. Samples were taken from root-associated rhizosphere soil (Rhizosphere), or bulk soil without plants (Soil). Data represent mean CFU.g^{-1} values (± SE, n = 8). N.D.: not detected.

nutrient-poor soil, the levels of rhizosphere colonisation by WCS417 were proportional to atmospheric CO_2 (Fig. 4.2 a), whereas rhizosphere colonisation by KT2440 was not influenced by CO_2 (Fig. 4.2 b). Furthermore, WCS417 colonisation was not statistically significant between CO_2 conditions for plants cultivated on nutrient-rich soil (Fig. 4.2 a). Hence, the stimulatory impacts of atmospheric CO_2 on rhizosphere colonisation by soil bacteria depend on soil quality and bacterial species.

Correction for CO_2 root development does not influence CO_2-dependent rhizosphere colonisation by P. simiae WCS417

As described in **Chapter 3**, atmospheric CO_2 directly influences plant development, which in turn influences aboveground interactions with microbes. Moreover, Staddon et al. (1998) reported that enhanced colonisation of *Plantago lanceolata* and *eCO_2* as confounded by larger root systems (Staddon et al., 1998). To correct for possible confounding effects of root development on WCS417 rhizosphere colonisation, developmental correction was applied as described in **Chapter 2** (Fig. 4.3 a), resulting in equal amounts of root dry weight at the time of sampling for nutrient-poor soils (Fig. 4.3 b). Furthermore, to prevent bias due to differences in colonisation time of WCS417, the bacteria were applied simultaneously at 10 days prior to sampling for all three CO_2 conditions, which was achieved by injecting 6 mL of a bacterial suspension at 5 x 10^8 CFU.mL (10 mM MgSO4) into the 60-mL pots. As had been observed in the absence of DC (Fig. 4.2 a), increasing concentrations of atmospheric CO_2 stimulated WCS417 colonisation of roots of equal size (Fig. 4.3 c). It can thus be concluded that the CO_2-dependent colonisation pattern of WCS417 occurs independently of the developmental stage of the root systems. Accordingly, subsequent experiments

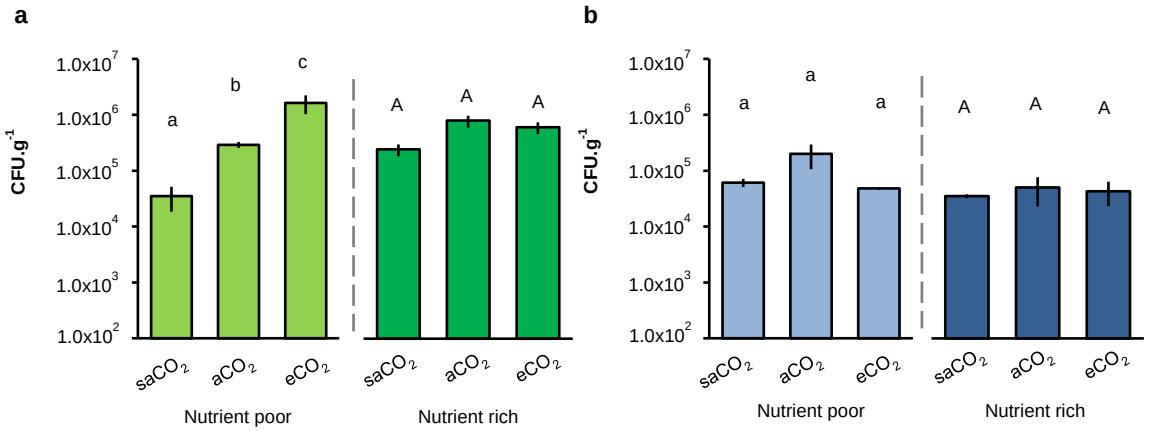

Figure 4.2. Impacts of atmospheric CO_2 and soil type on Arabidopsis rhizosphere colonisation by *P. simiae* WCS417 (**a**) and *P. putida* KT2440 (**b**)**.** Bacteria were introduced at $5x10^7$ CFU/g into nutrient-poor (left panels) or nutrient-rich (right panels) soil prior to planning Arabidopsis seeds. Rhizosphere colonisation was determined after 4 weeks of growth at sub-ambient CO_2 (200 ppm), ambient CO_2 (400 ppm), or elevated CO_2 (1200 ppm). Data shown represent mean $CFU.g^{-1}$ (± SE, n = 10). Letters indicate statistical differences (Student's t-test and ANOVA with Tukey multiple comparison, respectively; $P < 0.05$).

to address plant responses to WCS417 under different CO_2 regimes were conducted in the absence of DC.

Atmospheric CO_2 influences plant growth responses to P. simiae *WCS417 on nutrient-poor soil.*

To assess the influence of CO_2 on plant growth responses to rhizobacteria, control- and WCS417-inoculated plants were examined for rosette areas after 5 weeks of growth. In the absence of WCS417, plant growth was positively correlated with CO_2 concentration in both nutrient poor and rich soil (Fig. 4.4 a). Application of WCS417 did not influence growth of plants on nutrient-rich soil. Conversely, on nutrient-poor soil, WCS417 had a stimulatory effect on average rosette area at *sa*CO_2 and *a*CO_2, which was statistically significant at *a*CO_2 (Fig. 4.4 a). By contrast, WCS417 induced statistically significantly repression of mean rosette area at *e*CO_2 (Fig. 4.4 a). Since PGPR have been reported to affect root and shoot growth differentially through impacts on auxin and cytokinin levels (Vacheron et al., 2013), root biomass was determined in plants grown on nutrient-poor soil. As is shown in Fig. 4.4 b, root dry weights reflected aboveground growth patterns: apart from a positive effect of CO_2 on root dry weight in the absence of WCS417, inoculation of nutrient-poor soil with WCS417 increased root dry weights at *sa*CO_2 and *a*CO_2, while it repressed root dry weight at *e*CO_2. Together,

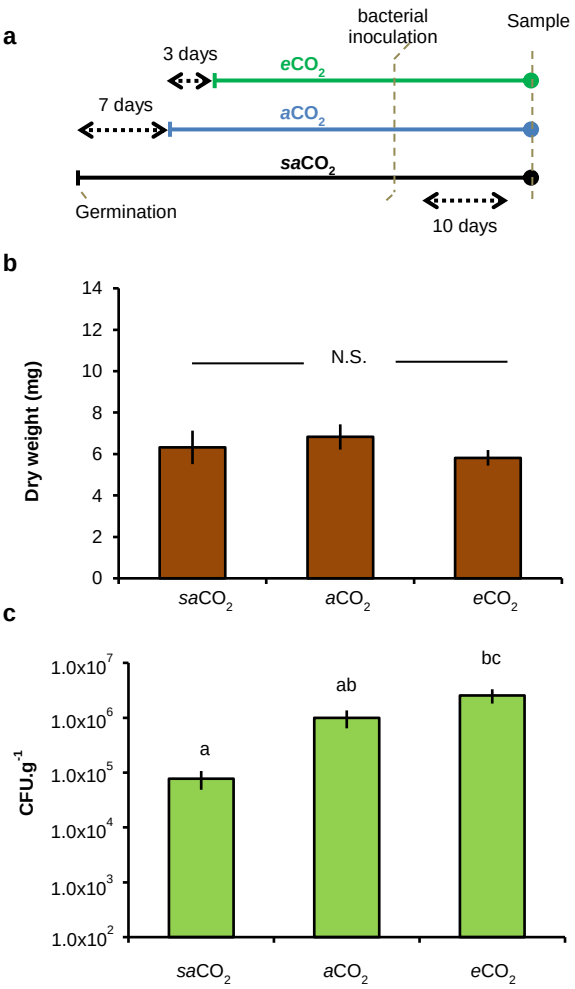

Figure 4.3. Developmental correction (DC) for CO_2-dependent differences in root growth do not affect CO_2-dependent colonisation by *P. simiae* WCS417. **a.** Schematic of germination offset to achieve DC at the time of sampling. Grey dashed vertical lines indicate time-points of bacterial inoculation and sampling. Inoculation was achieved by injecting 60-mL pots with 6 mL bacterial suspension (5 x 10^8 CFU/mL). WCS417 colonisation was determined 10 days after inoculation by enumeration of CFU on selective agar plates. **b.** Effects of DC on Arabidopsis root biomass at the time of sampling. Data represent mean dry root weight values (± SE, n = 10). n.s.: not statistically significant. **c.** Effects of increasing atmospheric CO2 on WCS417 rhizosphere colonisation from roots of similar developmental stage. Shown are Data shown represent mean CFU.g^{-1} (± SE, n = 10). Letters indicate statistical differences (Student's t-test and ANOVA with Tukey multiple comparison, respectively; $P < 0.05$).

these results suggest that WCS417 has a plant growth-promoting effect at *sa*CO_2 and *a*CO_2, but that it acts detrimentally to growth at *e*CO_2.

Atmospheric CO_2 influences systemic resistance responses to P. simiae WCS417 on both nutrient-poor and nutrient-rich soil.

Induced systemic resistance (ISR) occurs in the presence of WCS417 in Arabidopsis (Pieterse et al., 1996). As colonisation of WCS417 was CO_2 dependent, ISR responses were examined by challenging leaves of control- and WCS417-inoculated plants with the necrotrophic fungus *Plectosphaerella cucumerina*. Disease progression was examined at 8 and 13 days post inoculation (dpi). As described in **Chapter 3**, plants (grown on both nutrient-poor and nutrient-rich types) generally showed enhanced levels of basal resistance to *P. cucumerina* at *e*CO_2 (Fig. 4.5). Surprisingly, inoculation of nutrient-poor soil with WCS417 resulted in increased lesion diameters at *sa*CO_2. This induced systemic susceptibility at *sa*CO_2 was not present on nutrient-rich soil, where

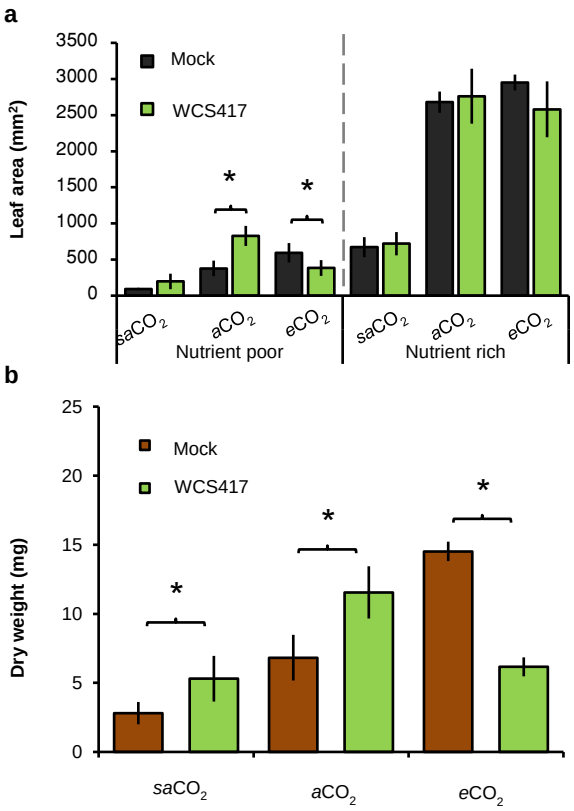

Figure 4.4. Effects of atmospheric CO_2 and soil nutritional status on plant growth responses to *P. simiae* WCS417. **a.** Effects of WCS417 on total leaf area of Arabidopsis at increased CO_2 concentrations in nutrient-poor (left) and nutrient-rich (right) soils. WCS417 bacteria were introduced into the soils prior to planting ($5x10^7$ CFU.g^{-1} soil). Leaf area was quantified by image analysis after 4 weeks of growth. Shown are mean leaf areas (± SE, n = 10). Asterisks indicate statistically significant differences to mock-treated control soils (Student's t-test; $P < 0.05$). **b**. Effects of WCS417 root biomass at increased CO_2 concentrations and in nutrient-poor soil. Data represent mean dry root weight values (± SE, n = 10).

WCS417 inoculation failed to influence lesion development by *P. cucumerina* in the leaves (Fig. 4.5) Furthermore, WCS417 reduced lesion development in leaves at *a*CO_2 and *e*CO_2, which was statistically significant in both nutrient-poor and nutrient-rich soils at least at one time-point after inoculation (Fig. 4.5). Hence, WCS417 driven systemic responses against *P. cucumerina* vary from induced susceptibility to induced resistance, depending on atmospheric CO_2 concentration and soil nutritional status.

4.4 Discussion

In this study, two strains of *Pseudomonas* were compared for their ability to colonise the Arabidopsis rhizosphere in response to changes in atmospheric CO_2. KT2440 is derived from a isolate that was extracted from benzene-contaminated soils in Japan (Nakazawa and Yokota, 1973). Accordingly, it survives well in root-free bulk soils, but it can also colonise the rhizosphere of plants, in particular grasses (Molina et al., 2000). The capacity of KT2440 to metabolise aromatic compounds offers an explanation of its preference for the maize rhizosphere, which contains relatively high concentrations of aromatic

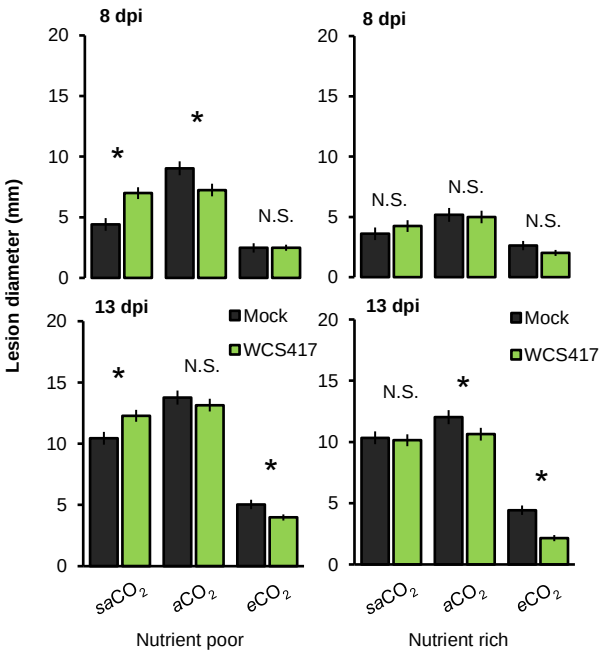

Figure 4.5. Effects of atmospheric CO_2 and soil nutritional status on systemic resistance responses of Arabidopsis to *P. simiae* WCS417. Bacteria were introduced into the soils prior to planting ($5x10^7$ CFU.g^{-1} soil). To quantify systemic resistance effects, 4-week-old plants were challenge-inoculated with *P. cucumerina* by applying 5-uL droplets of $5x10^6$ spores.mL^{-1} onto 4 fully expanded leaves per plant. Data shown are mean lesion diameters (± SE, n = 10) at 8 and 13 days post inoculation (dpi). Asterisks indicate statistical differences (Student's t-test; $P < 0.05$).

benzoxazinoids (Neal et al., 2012). It was shown that KT2440 is highly tolerant to the antimicrobial activity of benzoxazinoids and that it responds to these compounds with positive chemotaxis (Neal et al., 2012). As demonstrated in Fig. 4.1, KT2440 did not show increased colonisation of the Arabidopsis rhizosphere in comparison to control soil, suggesting that KT2440 is not specifically attracted to semiochemicals in the rhizosphere of Arabidopsis. Conversely, WCS417 showed relatively high levels of colonisation in the Arabidopsis rhizosphere, but failed to sustain colonies in bulk soil (Fig. 4.1). This colonisation pattern is typical for specialist rhizosphere colonisers. Indeed, *P. simiae* WCS417 was originally isolated from the rhizosphere of wheat (Lamers et al., 1988) and has since been reported to colonise the rhizosphere of a wide range of plant species (Berendsen et al., 2015). Whether this rhizosphere-specific colonisation is determined by selected semiochemicals, biocidal chemicals that recruit or select WCS417 bacteria, or whether this strain is better at competing for plant-derived C and/ or limiting rhizosphere nutrients, requires further investigation.

Although the effects of *sa*CO_2 on PGPR colonisation have not been studied previously, there is evidence that *e*CO_2 increases bacterial biomass in the rhizosphere (Kassem et al., 2008). Proctor et al. (2014) reported an increase in fungal species richness and enhanced relative abundance of selected fungi with *e*CO_2, which varied according to soil type (Procter et al., 2014). Furthermore,

a grassland free air CO_2 enrichment (FACE) experiment revealed that initial C accumulation occurred predominantly in arbuscular mycorrhizal fungi (AMF; Denef et al., 2007), which are specialist symbiotic fungi that rely on host-derived carbon (*e.g.* Lindahl et al., 2010). It is thus plausible that increased carbon deposition at *e*CO_2 will be more significant in carbon-poor soil types, where specialist rhizosphere microbes rely more heavily on plant-derived carbon. Indeed, although the generalist KT2440 strain was unaffected by *e*CO_2, the specialist rhizosphere strain WCS417 showed increasing levels of rhizosphere colonisation at rising CO_2 concentrations, which was most pronounced in nutrient-poor soil (Fig. 4.2). Moreover, the differential effects of CO_2 on KT2440 and WCS417 indicate that atmospheric CO_2 has profound repercussions on microbial composition in the rhizosphere. Accordingly, it is plausible that rising atmospheric CO_2 may induce shifts in rhizosphere community structure, via changes in plant exudation and rhizosphere chemistry. Exactly what these community shifts are, and which changes in rhizosphere chemistry drive these changes, requires a novel approach to measure exuded chemicals in non-sterile rhizosphere soil (See **Chapter 5**).

The plant-growth promoting ability of CO_2 can have an indirect effect on plant-microbe interactions. It is conceivable that age-dependent root exudation chemistry alters interactions with belowground rhizosphere microbes. In support of this, growth stage has been shown to influence root exudation patterns (Calvo et al., 2017), which correlated with higher and lower abundances of *Cyanobacteria* and *Acidobacteria*, respectively (Chaparro et al., 2013). Furthermore, a study investigating the effects of *e*CO_2 on colonisation of *Plantago lanceolata* and *Trifolium repens* by the AMF *Glomus mosseae* revealed that the level of AMF colonisation is confounded by larger root systems under *e*CO_2 conditions (Staddon et al., 1998). Nonetheless, correction for CO_2-induced differences in root growth did not change the CO_2-dependent colonisation by WCS417 bacteria (Fig. 4.3), indicating that this rhizosphere response is not majorly influenced by root development. It should be noted, however, that the developmental correction (DC) itself may have an influence on the outcome of the experiment. To avoid bias from differences in time of bacterial colonisation, the WCS417 bacteria were introduced through soil injection at a time window in

which the plant developmental stage is comparable between CO_2 conditions (**Chapter 3**; Fig. S3.1). Application of such high bacterial titres to fully developed roots is artificial and could induce acute MAMP-triggered responses that would not occur during gradual colonisation from the onset of germination (Zamioudis and Pieterse, 2012). Furthermore, as shown in Fig. 4.4 b, WCS417 itself has a profound impact on root development, which in turn could interact with root growth responses to CO_2. Therefore, to avoid potentially confounding effects of DC on the bioassay, subsequent analyses of plant responses to WCS417 were conducted in the absence of DC.

Rhizosphere colonisation by PGPRs promotes shoot and root development through different mechanisms (Lugtenberg and Kamilova, 2009). For instance, *Pseudomonas fluorescens* WCS365 has been shown to convert exuded tryptophan into the plant growth hormone auxin (Kamilova et al., 2006). In nutrient-poor soil, growth promotion by WCS417 was apparent under both *sa*CO_2 and *a*CO_2 (Fig. 4.4). However, WCS417 repressed plant growth at *e*CO_2 (Fig. 4.4), indicating potentially pathogenic activity. This hypothesis is supported by the colonisation data, which revealed >10 fold higher colonisation of WCS417 at *e*CO_2 compared to that at *a*CO_2. It is tempting to speculate that such high densities at the root surface are perceived as hostile by the host immune system, triggering a growth-repressing immune response. The continuum between mutualism and pathogenic lifestyles is a recognised phenomenon for fungal endophytes (Schulz and Boyle, 2005) and other root colonisers (Bever et al., 2012). Interestingly, this plasticity is partially driven by environmental factors, including CO_2 (Anderson et al., 2004; Schulz and Boyle, 2005). Although the relationship between plant-microbial mutualism and environmental factors remains complex (Garrett et al., 2006; Johnson and Gehring, 2007; Garrett et al., 2011), the conversion to plant growth-repression by WCS417 at *e*CO_2 coincided with the relatively high levels of resistance against *P. cucumerina* (Fig. 4.5). While this disease protection appears to be an additive result of *e*CO_2-induced resistance (**Chapter 3**; Fig. 3.1) and ISR, it is likely that these high levels of resistance come with costs to plant growth, which only become apparent under nutrient-limiting conditions. ISR has been associated with priming of JA and ET-controlled defences (Pieterse et al., 2002). Even though priming is generally

considered to be a low-cost defence strategy (van Hulten et al., 2006), the additive effect of *e*CO_2 and ISR may result in constitutive up-regulation of inducible defences that incur a detectable cost on plant growth under nutrient-limiting conditions. This hypothesis gains support from the observation that WCS417 only represses growth at *e*CO_2 in nutrient-poor soil (Fig. 4.4).

The results presented in this Chapter show that two well-characterised soil bacteria display different rhizosphere behaviour in response to changes in atmospheric CO_2. Moreover, the plant responses to colonisation by a specialist rhizobacterial strain revealed a range of outcomes growth and systemic resistance phenotypes, including growth repression and induced susceptibly. These findings demonstrate that predictions about impacts of climate change and soil quality on crop performance need to take into consideration the complex interactions taking place in the rhizosphere. This highlights the need for further research on the impacts of future climate change and soil processes on rhizosphere chemistry and microbial community structures.

Chapter 5: Impacts of glacial-to-future concentrations of atmospheric CO_2 on the bacterial community structure and chemical profile of the Arabidopsis rhizosphere.

5.1 Abstract

The rhizosphere effect is defined as the change in microbial community structure resulting from the biochemical influence of plant roots. Over recent years, various studies have shown that elevated atmospheric CO_2 concentrations affect rhizosphere microbial biomass and composition. However, the chemical signals mediating these CO_2 impacts remain unknown, which is partially due to the lack of a suitable experimental system for global analysis of rhizosphere chemistry. In this Chapter, the impacts of sub-ambient CO_2 (*sa*CO_2) and elevated CO_2 (*e*CO_2) on rhizosphere chemistry have been investigated in Arabidopsis, using an experimental approach that allows for untargeted metabolic profiling of non-sterile rhizosphere soil (Appendix 1). First, the global effects of *sa*CO_2 and *e*CO_2 on soil bacterial communities were determined at different time-points of Arabidopsis development, using T-RFLP analysis. While CO_2 had no significant impact on the bacterial community structure of plant-free soil, the diversity of the root-associated community increased with rising CO_2 concentrations. Similarly, the difference in community structure between root-associated bacteria and soil-based bacteria (*i.e.* the 'microbial rhizosphere effect') increased with rising CO_2 concentrations. Subsequent analysis of rhizosphere chemistry revealed that the impacts of CO_2 on the rhizosphere bacteria correlated with both quantitative and qualitative differences in rhizosphere chemistry. Qualitative changes in rhizosphere chemistry at *sa*CO_2 were predominantly associated with increased (phospho)lipids. Conversely, the changes in rhizosphere chemistry at *e*CO_2 were associated with a wider range of primary and secondary metabolites, including lipids, terpenoids, and phenolic compounds, such as flavonoids, coumarins and alkaloids. The results in this Chapter provide a first insight into the biochemical mechanisms by which changes in atmospheric CO_2 concentration shape microbial rhizosphere communities.

5.2 Introduction

CO_2 has long been known to play an important role in shaping the microbial composition of the rhizosphere. Rhizosphere microbes largely rely on plant-derived carbon as their primary food source (Drigo et al., 2008). Changes in atmospheric CO_2 can change carbon allocation to roots and exert a selective pressure on rhizosphere-inhabiting micro-organisms (King, 2011). These CO_2 effects have been documented for soil-borne archaea, bacteria, fungi, and fauna (*e.g.* Coûteaux and Bolger, 2000; Hayden et al., 2012). Yet, the chemical signals that influence these processes remain poorly understood. This is mostly because the effects of CO_2 on the composition of plant-exuded chemicals and the rhizosphere have received little attention (Calvo et al., 2017). While increasing concentrations of atmospheric CO_2 have been shown to enhance rhizo-deposition of plant-derived primary metabolites, such as sugars and amino acids (Drigo et al., 2009; Phillips et al., 2009; Fransson and Johansson, 2010; Li et al., 2014a), comprehensive analyses of CO_2-dependent changes in the chemical composition of root exudates or the rhizosphere soil remain rare (Jin et al., 2015).

Primary metabolites in root exudates, such as sugars and organic acids, promote root colonisation by beneficial microorganisms. For instance, exudation of malic acid boosts colonisation of plant growth-promoting *Pseudomonas fluorescens* WCS365 and *Bacillus subtilis* in tomato and Arabidopsis, respectively (de Weert et al., 2002; Rudrappa et al., 2008). Since concentrations of primary metabolites in root exudates increase at *e*CO_2 (Drigo et al., 2009), it is commonly assumed that the eCO_2 has a stimulatory effect on the rhizosphere microbiome through increased deposition of primary metabolites. However, secondary metabolites in root exudates can have an equally important role in shaping rhizosphere communities (Badri et al., 2009; van Dam and Bouwmeester, 2016). The response of soil bacteria to these signalling compounds is complex and often involves direct biocidal activity (Buchan et al., 2010). For instance, the phenylpropanoid-derived compound rosmaric acid from basil (Bais et al., 2002), as well as the tryptophan-derived benzoxazinoid 2,4-dihydroxy-7-methoxy-2H-1,4-benzoxazin-3(4H)-one (DIMBOA) from maize, can repress soil-based pathogens through their biocidal effects (Neal et al., 2012).

However, these chemicals can also serve as chemo-attractants to other rhizosphere microbes, such as plant-beneficial *Pseudomonas putida* KT2440 (Neal et al., 2012). These examples highlight the multifaceted mode of action by plant-derived secondary metabolites in the rhizosphere.

The study and identification of rhizosphere semiochemcials is complicated by a variety of factors. Firstly, the chemical composition of root exudates and the rhizosphere is constantly influenced by a range of fluctuating environmental factors, such as light intensity, humidity and temperature (Badri and Vivanco, 2009; Classen et al., 2015). Secondly, the developmental stage of the plant can have a profound impact on root exudation chemistry. For instance, chemical exudation profiles of Arabidopsis are not only genotype-dependent (Micallef et al., 2009b), but they also often change throughout plant development (Micallef et al., 2009a; Chaparro et al., 2013). Since CO_2 directly influences plant development (Mhamdi and Noctor, 2016; **Chapter 3**), effects of CO_2 on rhizosphere chemistry and microbial rhizosphere composition may partially be caused by plant development-dependent changes in root exudation chemistry. Indeed, Staddon et al. (1998) showed that the CO_2-dependent increases in root colonisation by *Glomus mosseae* in *Plantago lanceolata* and *Trifolium repens* are confounded by larger root systems under *e*CO_2 conditions. On the other hand, developmental correction for root biomass did not alter the CO_2-dependent pattern of colonization by *Pseudomonas simiae* WCS417 in Arabidopsis (**Chapter 4**).

In addition to variation in environmental conditions and plant development, the identification of new rhizosphere signals has been complicated by the lack of an experimental system that allows comprehensive analysis of non-sterile rhizosphere soil. Historically, studies of root exudation chemistry rely on the use of sterile hydroponically grown roots (van Dam and Bouwmeester, 2016). While such systems allow for precise quantification of plant-derived exudates without bias from degradation by microbial activity (Kuijken et al., 2014; Strehmel et al., 2014), hydroponic systems do not allow plant roots to develop naturally (Mattiello et al., 2010; Sgherri et al., 2010). Hydroponic systems can also introduce artificially high stress tolerance, as exemplified in hydroponically grown barley

whose salinity tolerance is greater than soil grown controls (Tavakkoli et al., 2010). Moreover, microbial degradation products of root exudates, rather than root-exuded plant metabolites themselves, might act as rhizosphere signals. For instance, benzoxazinoids in root exudates from cereal roots can be converted into stable 2-aminophenoxazin-3-one, which displays strong antimicrobial and allelopathic activities (Atwal et al., 1992; Macías et al., 2005). Methods to collect root exudates from non-sterile roots often rely on physical extraction of roots from their natural growth substrate (*e.g.* Phillips et al., 2008), which can affect root integrity, induce stress responses and contaminate chemical profiles with cellular metabolites. To address these experimental shortcomings, a new collection system was developed (Appendix 1; Pétriacq et al., 2017), which relies on extraction buffers that collect polar and apolar chemicals without damaging root cells, hence preventing contamination of samples with cellular metabolites. Using untargeted mass spectrometry analysis (UPLC-Q-TOF) of extracts from plant-free soil and plant-containing soil, followed by statistical analysis of the differences between these extracts, this method enables identification of chemicals that are statistically enriched in the rhizosphere. For two different plant species (Arabidopsis and Maize) and two different soil types (as used in **Chapter 4**), this method allowed for the reconstruction of metabolic profiles that are enriched in non-sterile rhizosphere soil.

In this Chapter, the experimental system developed by Pétriacq et al. (2017; Appendix 1) was exploited to study changes in rhizosphere biochemistry and related microbial communities by *sa*CO_2 and *e*CO_2, at different stages of plant development. This chapter provides evidence that glacial-to-future CO_2 concentrations alter the diversity of rhizobacterial communities and increase the microbial rhizosphere effect at selected stages of plant development. These impacts of CO_2 on rhizobacterial communities are associated with qualitative changes in the biochemical profiles of the rhizosphere.

5.3 Results

Impacts of CO_2 on bacterial communities in the rhizosphere. Samples for analysis of bacterial communities were collected simultaneously with the samples

for analysis of rhizosphere chemistry from plant-containing and plant-free control tubes (Figs. 5.1 a and 5.1 b). Samples were collected at 24, 28 and 34 days after

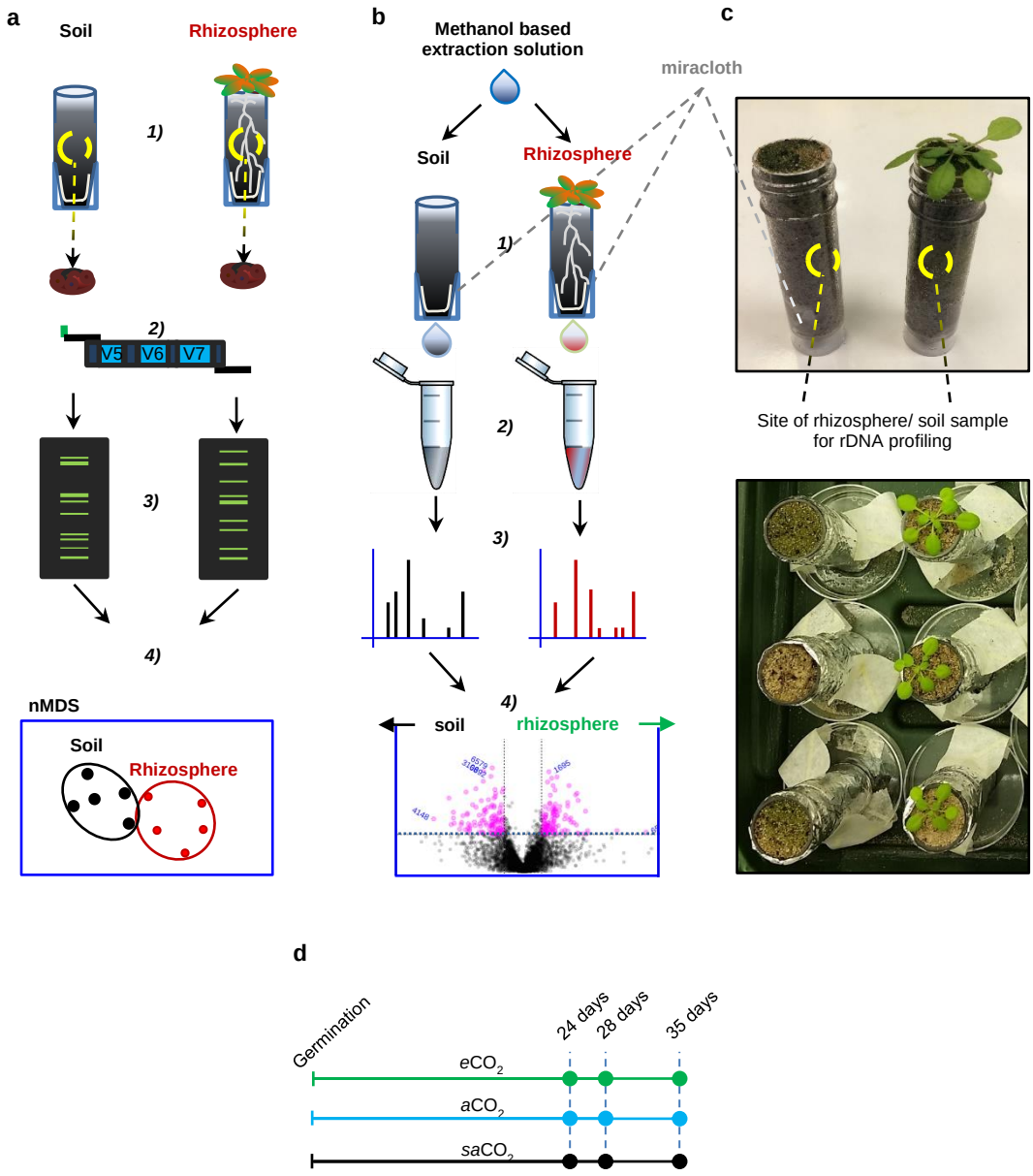

Figure 5.1. Experimental approach for comprehensive profiling of the microbial communities and chemistry of non-sterile rhizosphere soil. **a**, *1)* Samples from plant-free bulk soil and plant-containing soil were taken from collection tubes filled with a sand:compost mixture 9:1 (v/v). *2)* DNA extraction was performed on samples from bulk soil and roots plus adhering rhizosphere soil. Bacterial *16s* sequences were obtained by PCR amplification with T-RFLP primers. *3)* Amplified sequences were enzyme-digested and separated by electrophoresis, providing taxonomically variable community profiles. *4)* Multi-variate statistical analysis was applied to visualise and quantify the differences in T-RFLP patterns between samples. **b**, *1)* Samples were taken from the same experiment and experimental system as the samples for T-RFLP analysis. Five mL of extraction solution (50 : 49.99 : 0.01 Methanol : Water : formic acid) was applied on top of the collection tubes. *2)* Samples were collected for 1 min, centrifuged and freeze-dried. *3)* Concentrated samples were analysed by ultra-high-pressure liquid chromatography coupled to quadrupole time-of-flight mass spectrometry (UPLC-Q-TOF). *4)* Statistical filtering of ion intensities enabled detecting qualitative and quantitative differences between extracts from plant-free bulk soil and plant-containing soil and identifying putative metabolites that are enriched in the rhizosphere. **c**, Photographs of the experimental system. Top: tubes after 4.5 weeks of growth. Bottom: tubes after 3 weeks of growth taped onto petri-dishes to prevent cross contamination of metabolites and microbes. **d**, Schematic of the timing of sampling. Samples were collected simultaneously in *sa*CO_2 (black line), *a*CO_2 (blue line) and *e*CO_2 (green line) at each time point. Time points were selected to complement developmental collection (DC) timings of previous chapters.

planting to assess effects of growth stage on the microbial and chemical rhizosphere effects (Fig. 5.1 d). Samples for profiling of root-associated bacterial communities were collected by gently removing plants from the growth substrate and shaking them to eliminate loosely associated soil; samples for profiling of soil-based communities were collected from the centre of plant-free tubes at the approximate average depth of Arabidopsis roots (~350 mm; Fig. 5.1 c). Extracted DNA was used as a template for PCR amplification of the V5-V6-V7 region of the bacterial *16S* rRNA gene, using fluorescently labelled T-RFLP primers. Communities were profiled by terminal restriction fragment length polymorphism analysis (T-RFLP; Fig. 5.1a). Cluster analysis by Pearson correlation revealed a relatively high degree of variability between replicas for both the plant-associated

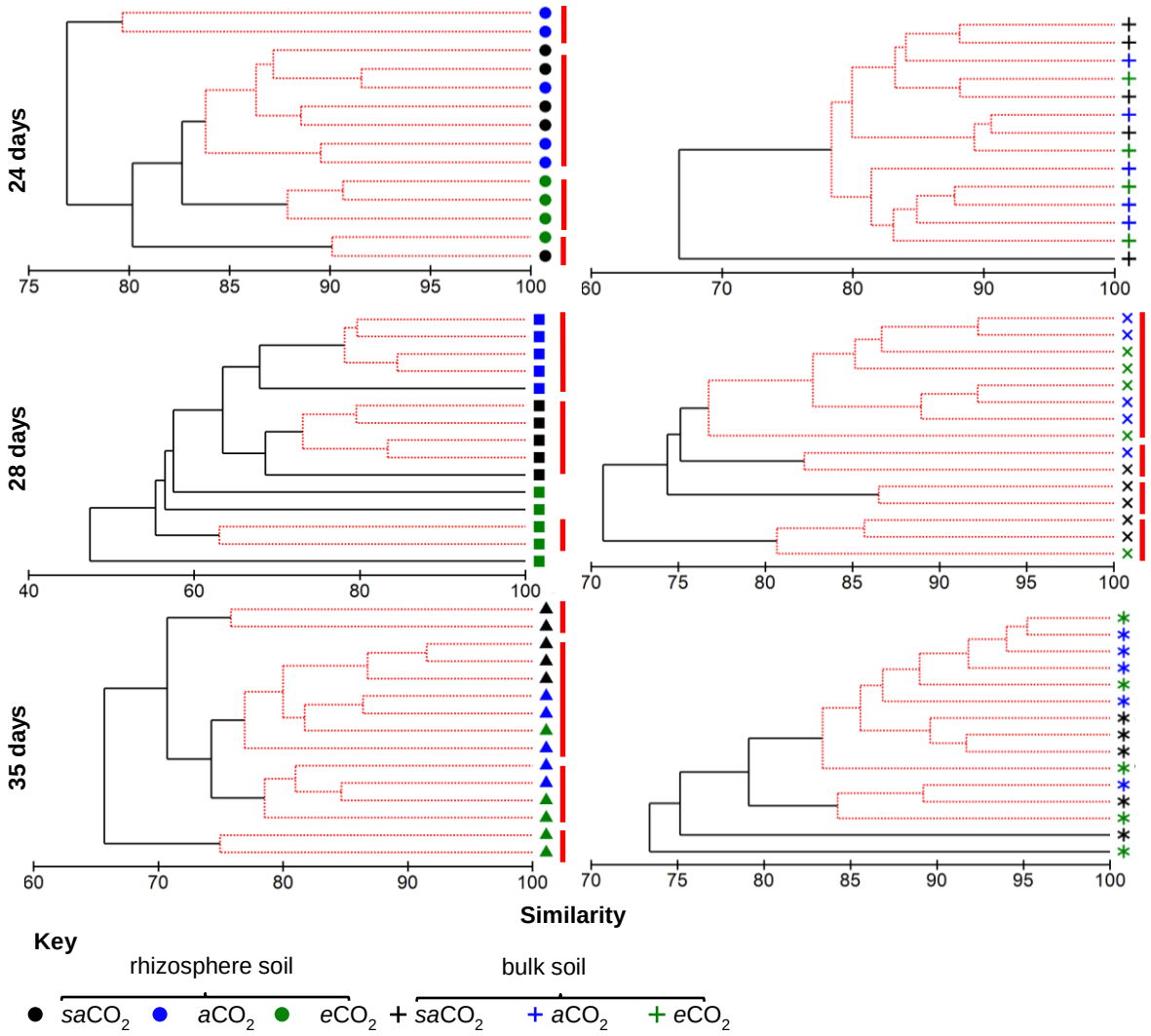

Figure 5.2 Impact of CO_2 on the T-RFLP community profiles of root (a) and soil-associated (b) bacterial communities. Samples were collected from plant-free and plant-containing tubes after 24 days, 28 days, and 35 days of growth under *sa*CO_2 *a*CO_2 or *sa*CO_2 conditions. Dendrograms were obtained by Pearson correlation cluster analysis of *16S* T-RFLP patterns. The obtained clusters were examined for statistical similarity by similarity profile analysis (SIMPROF). Red lines and bars indicate clusters that are statistically similar ($P < 0.05$).

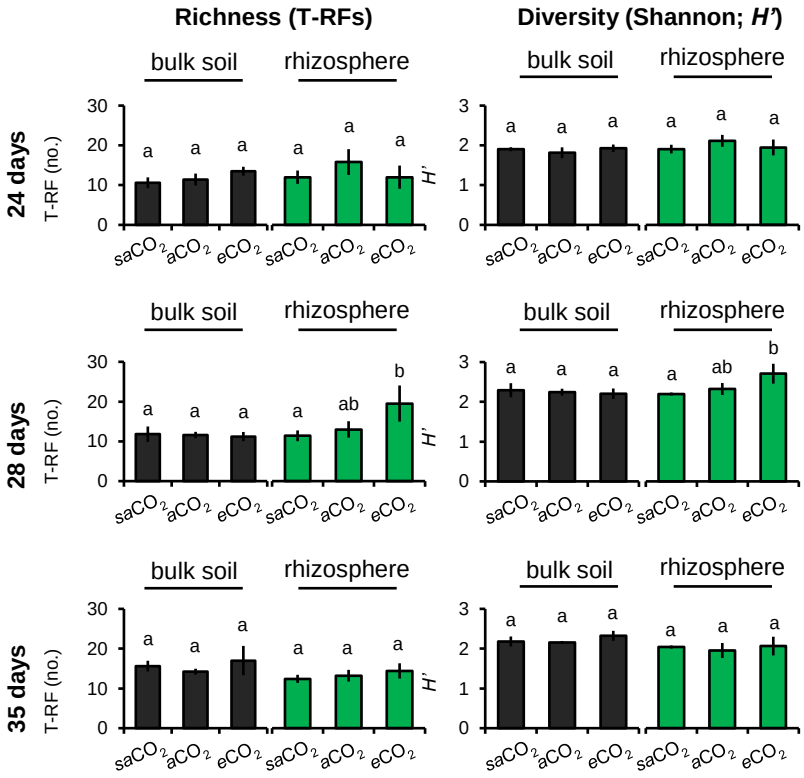

Figure 5.3. Impacts of atmospheric CO_2 on diversity of bacterial communities. Values shown represent average values (± SD; n = 4-6) of species richness (*i.e.* number of T-RFs) and the Shannon index. Analysis was performed in Arabidopsis at 24, 28 and 35 days post germination. Data from plant-free soil (bulk soil) are indicated in black; data from root-associated communities (rhizosphere) are shown in green. Letters indicate statistically significant differences (Student's T-test $P < 0.05$).

communities and the soil-based communities (Fig. 5.2). Nonetheless, the plant-associated communities showed a higher degree of clustering by atmospheric CO_2 concentration than soil-based communities, particularly at the second time-point after planting (28 days). Subsequent analysis of population diversity by species richness and Shannon index revealed that the root-associated communities at the second time-point displayed a statistically significant increase in diversity with rising CO_2 concentrations (Fig. 5.3). Conversely, CO_2 did not have an effect on species diversity metrics of soil-based bacterial communities at any of the three time-points analysed. Hence, atmospheric CO_2 has a measurable and statistically significant impact on root-associated bacterial communities, but does not influence the composition and diversity of bacterial soil communities.

To determine the impacts of CO_2 on the bacterial rhizosphere effect, *i.e.* the difference in community structure between root-associated and soil-based bacterial communities, non-parametric multidimensional scaling (nMDS) analysis was employed (Fig. 5.4 a). Subsequent statistical analysis of similarity (ANOSIM) was used to determine in how far distinct clustering patterns between root- and soil-based communities were significant (Fig. 5.4 a). At *sa*CO_2, the only

statistically significant rhizosphere effect was apparent at the third time-point (*P* = 0.016), whereas the rhizosphere effect at *a*CO_2 was statistically significant at all three time-points (*P* = 0.016, *P* = 0.008, *P* = 0.024, respectively). At *e*CO_2, the rhizosphere effect was borderline statistically significant at the first time-point (*P* = 0.14) and fully significant at the second and third time-point (*P* = 0.043, *P* = 0.008, respectively). The T-RFs that drive the top 60% of variation between these differences are summarised in Table S5.1. To determine the size of the microbial rhizosphere effect the percentage of dissimilarity was calculated by SIMPER (*Primer* software), which is based on the Bray-Curtis measure of similarity (Clarke, 1993). Root-and soil-associated communities showed an increased dissimilarity at rising CO_2 levels at the first and second time-point (Fig. 5.4 b), indicating that increasing atmospheric CO_2 enhance the microbial rhizosphere effect. At the final time-point, however, the level of dissimilarities converged to the same level for all CO_2 concentrations (Fig. 5.4 b). Overall, these results support the notion that changes in atmospheric CO_2 concentration have a quantitative and qualitative impact on microbial rhizosphere effect. These impacts likely involve changes in rhizosphere chemistry due to quantitative and qualitative changes in root exudation patterns. This hypothesis can be investigated by un-targeted chemical profiling of the rhizosphere soil at glacial-to-future CO_2 concentrations.

Impacts of CO_2 on the biochemical profiles of the rhizosphere. To analyse the impacts of CO_2 on rhizosphere chemistry, samples were extracted by flushing the tubes for 1 min. with 5 mL extraction solution, containing 50% methanol and 0.05% formic acid (Fig. 5.1 b). This extraction method does not lead to detectable damage of root cells, nor does it affect the viability of soil-based bacteria (Appendix 2; Petriacq et al., 2017). Analysis was performed using UPLC-Q-TOF MS in both ESI^- and ESI^+ modes, after which all ions were combined to assess the quantitative impacts of CO_2 on the chemical rhizosphere effect (*i.e.* the number of ions that are statistically enriched in plant-containing soil; **Chapter 2**, Fig. 2.2). To this end, volcano plots were generated for each time-point and CO_2 conditions (Fig. 5.5 a). These plots present statistical significance of each ion

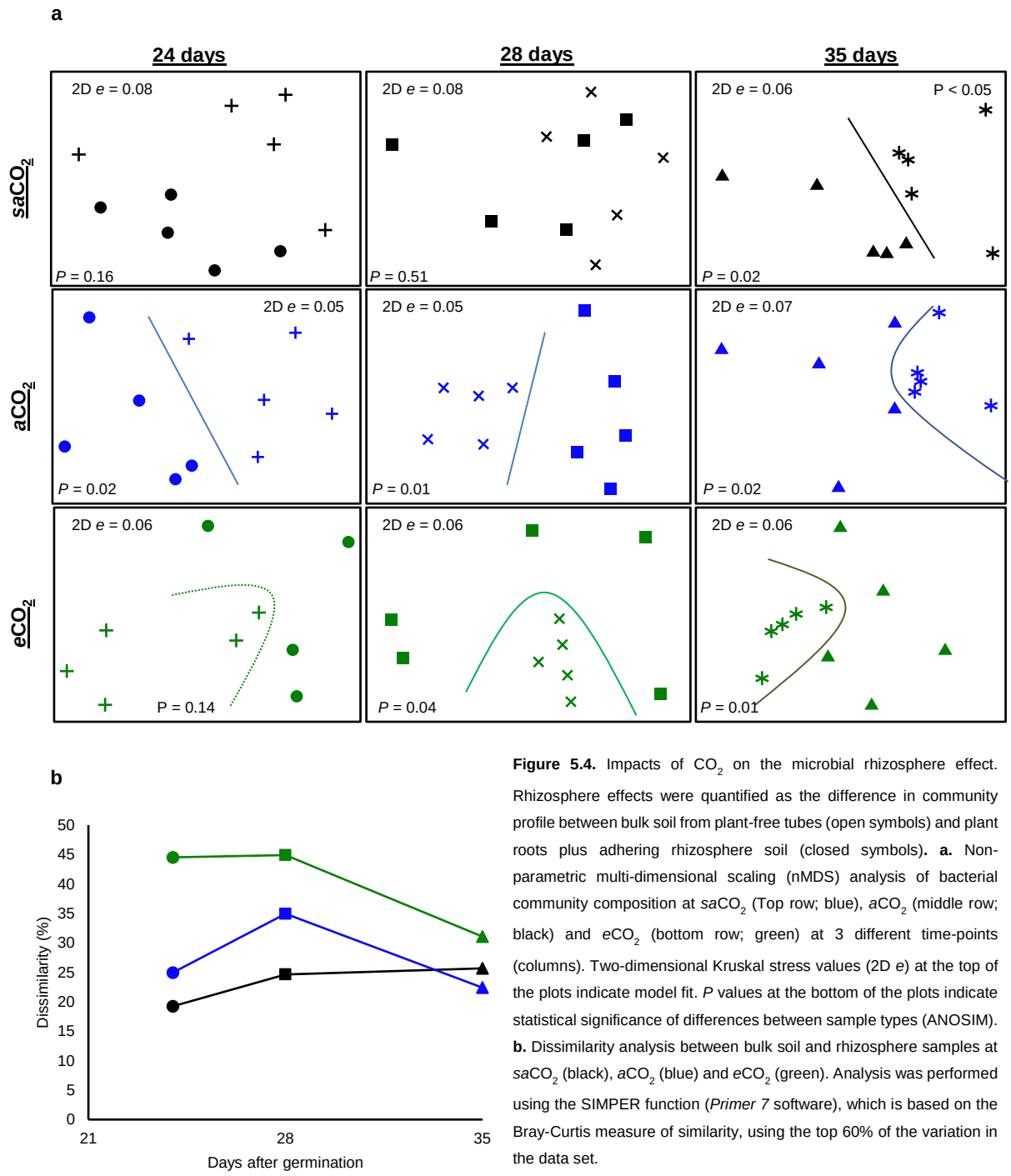

Figure 5.4. Impacts of CO_2 on the microbial rhizosphere effect. Rhizosphere effects were quantified as the difference in community profile between bulk soil from plant-free tubes (open symbols) and plant roots plus adhering rhizosphere soil (closed symbols)**. a.** Non-parametric multi-dimensional scaling (nMDS) analysis of bacterial community composition at *sa*CO_2 (Top row; blue), *a*CO_2 (middle row; black) and *e*CO_2 (bottom row; green) at 3 different time-points (columns). Two-dimensional Kruskal stress values (2D *e*) at the top of the plots indicate model fit. *P* values at the bottom of the plots indicate statistical significance of differences between sample types (ANOSIM). **b.** Dissimilarity analysis between bulk soil and rhizosphere samples at *sa*CO_2 (black), *a*CO_2 (blue) and *e*CO_2 (green). Analysis was performed using the SIMPER function (*Primer 7* software), which is based on the Bray-Curtis measure of similarity, using the top 60% of the variation in the data set.

marker as a function of their fold-change, thus visualising the quantitative differences in chemistry between soil from plant-free tubes and soil from plant-containing tubes. Using a statistical threshold of $P < 0.05$ (Welch's t-test) and a cut-off value of > 2 fold-change, the numbers of rhizosphere markers that were enriched in samples from plant-containing tubes varied between 148 (aCO_2, second time-point) to 403 (eCO_2 first time points; Fig. 5.5 b). At the first time-point (24 days), the numbers of statistically significant rhizosphere markers increased

with rising CO_2 concentrations. This relationship between the number of rhizosphere ions and CO_2 concentration was absent at the second time-point of sampling (28 days) and showed a negative correlation at the third time-point (35 days; Fig. 5.5 b). Thus, the quantitative impact of CO_2 on the biochemical rhizosphere effect varies according to the time-point of sampling.

To study the qualitative impacts of CO_2 on rhizosphere chemistry, the 2,692 anions (ESI^-) and 5,578 cations (ESI^+) of the entire dataset were re-

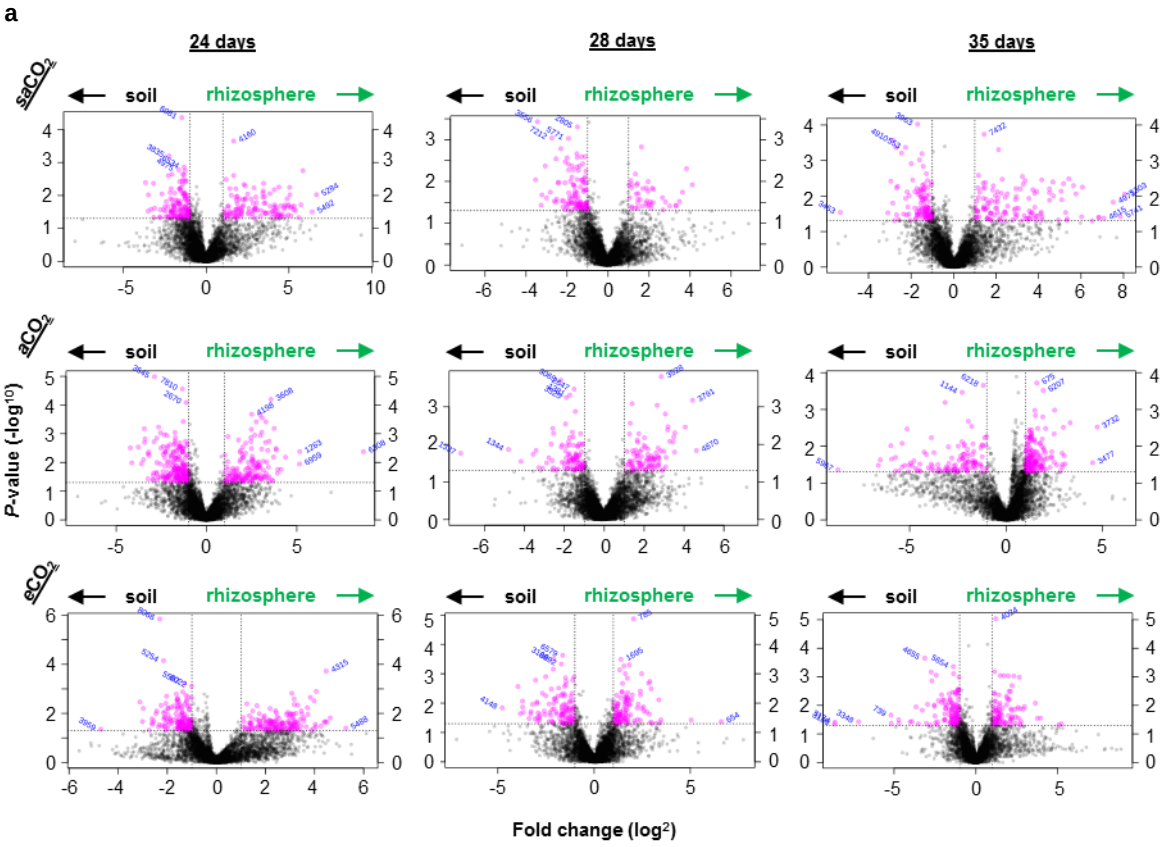

Figure 5.5. Quantitative impacts of CO_2 on the biochemical rhizosphere effect. Rhizosphere effects were quantified as the number of ions (UPLC-Q-TOF) showing a statistically significant increase in soil from plant-containing tubes compared to soil from plant-free tubes (Welch' T-test; $P < 0.05$; > 2-fold). **a**. Volcano plots expressing the statistical significance between samples as a function of fold-difference of average ion intensity at different time-points (columns) and atmospheric CO_2 concentrations (rows). Plots show values for the combined set of ions (both ESI^+ and ESI^-). Shown in pink are ions above the cut-off values ($P < 0.05$ and > 2-fold change). **b.** Numbers of ions enriched in plant-free bulk soil or plant-containing soil. Numbers are based on the statistical cut-off values of the volcano plots.

analysed for statistically significant differences between all CO_2/soil combinations, using ANOVA with Benjamini Hochman false discovery rate (FDR) correction (Fig. S5.1). This filter resulted in a total of 498 differentially abundant ions between all conditions (Appendix 3). For each time-point, this set of 498 ions was subjected to 2-way ANOVA, to select a subset of 174 ions that show a statistically significant interaction between CO_2 x soil type. Subsequent Pearson correlation analysis resulted in a final selection of 59 marker ions, which show enrichment in plant-containing soil that varies between CO_2 conditions (Fig. 5.6). These ions represent rhizosphere markers that are statistically influenced by atmospheric CO_2 concentration. Putative identification and allocation of these

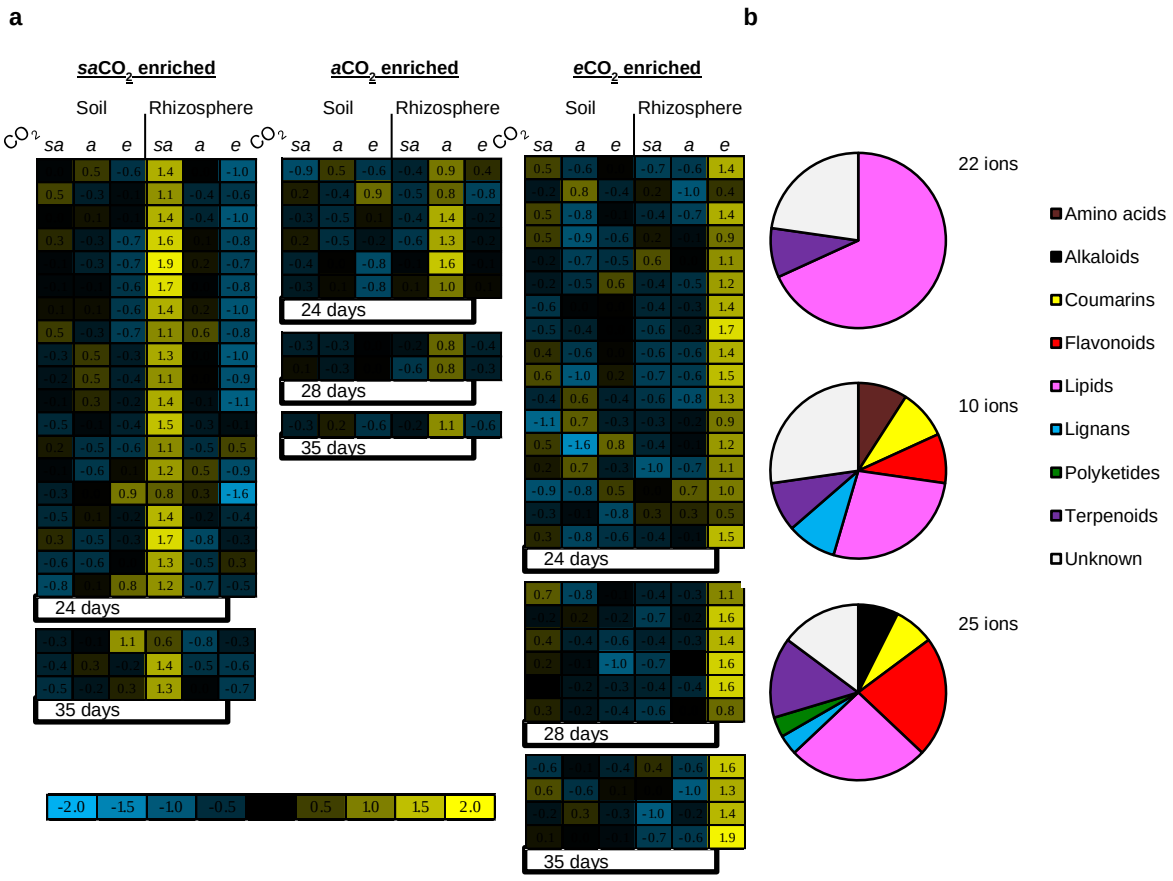

Figure 5.6. Qualitative impacts of CO_2 on the biochemical rhizosphere effect. After 1-way ANOVA ($P < 0.05$ + FDR) to select 498 ions showing statistically significant differences in abundance between all CO_2/time-point/soil-type combinations, 2-way ANOVA ($P < 0.05$) was performed to select 174 ions showing a statistically significant interaction between CO_2 x soil-type for all time-points. This selection was subjected to cluster analysis (Pearson correlation), resulting in a final selection of 59 ions that vary in rhizosphere abundance between CO_2 conditions. **a**, Heatmap projection of ion clusters showing statistically significant variation in rhizosphere abundance between *sa*CO_2, *a*CO_2 or *e*CO_2 conditions at the three different time-points. Projected ion intensities represent average expression values per CO_2/soil-type combination (n = 5), row-normalized to the average and standard deviation across all samples. **b.** Putative identification of CO_2-influenced rhizosphere ions and allocation to metabolite classes. Pie diagrams show distributions of selected ions over the different metabolite classes (right).

markers to metabolic classes revealed that CO_2 alters the biochemical composition of the rhizosphere in a concentration-dependent manner (Fig. 5.6; Table S5.2). While *sa*CO_2 changed the rhizosphere chemistry by an increase in putative (phospho)lipids and terpenoids, the changes induced by *a*CO_2 and *e*CO_2 involved enrichment with a wider range metabolite classes, including putative lipids, flavonoids, terpenoids, alkaloids, and coumarins (Fig. 5.5). These results indicate that increasing atmospheric CO_2 concentrations enhance the biochemical diversity of the rhizosphere.

5.4 Discussion

Root exudation chemistry drives the microbial diversity and function of the rhizosphere (Badri et al., 2009). Changes in atmospheric CO_2 can alter exudation chemistry, causing changes in rhizosphere chemistry and microbial communities (see **Chapter 4** for discussion). Over 60% of carbon exuded from roots can be degraded within hours of release (Uselman et al., 2000), which presents a challenge in verifying the origin of plant-exuded metabolites in non-sterile systems. Therefore, most studies of plant exudation chemistry are based on sterile hydroponic methods that limit bias from microbial metabolism (Kuijken et al., 2014; van Dam and Bouwmeester, 2016). While this allows accurate identification of plant exuded chemicals (Strehmel et al., 2014), these techniques neglect the contribution of microbe-derived chemical intermediates, which may be key to understanding the communication network between plants and rhizosphere microbes.

This chapter exploits a new experimental system developed to enable un-targeted profiling of rhizosphere chemistry from different plant-soil combinations (Pétriacq et al., 2017; Appendix 1). This experimental system was further adapted to investigate the effects of CO_2 on both chemical and microbial rhizosphere profiles in this study (Fig. 5.1). T-RFLP community profiling revealed that rising CO_2 concentrations increase the diversity of plant-associated bacterial communities (Fig. 5.2). Moreover, rising CO_2 increased the size of the bacterial rhizosphere effect, as quantified by the dissimilarity between root-associated and soil-based bacterial communities, which increased with rising CO_2 concentrations (Fig. 5.4). Using samples from the same experiment and experimental design,

analysis of rhizosphere chemistry revealed mostly qualitative differences, indicating an overall increase in biochemical diversity at increasing CO_2 concentrations (Fig. 5.5). Upon subsequent analysis, the ions contributing to CO_2-dependent changes in rhizosphere chemistry could putatively be identified and annotated to different metabolic classes, including alkaloids, flavonoids, coumarins, lipids and terpenoids. These types of metabolites are consistent with previously reported chemistry from Arabidopsis root exudates (Strehmel et al., 2014; Appendix 1). Together, these results show that atmospheric CO_2 concentrations shape the rhizosphere community of Arabidopsis, which coincides with qualitative changes in the rhizosphere chemistry.

The current study did not apply a developmental correction (DC), despite evidence that *i*) CO_2 directly influences Arabidopsis development (Mhamdi and Noctor, 2016; **Chapter 3**) and *ii*) that the developmental stage of Arabidopsis has profound impacts on root exudation chemistry (Micallef et al., 2009a; Chaparro et al., 2013). Accordingly, the observed impacts of increasing CO_2 concentrations on diversity of root-associated bacteria and the microbial rhizosphere effect, as well as the qualitative effects of CO_2 on rhizosphere chemistry, may be a consequence of differences in root development. In theory, the current dataset allows for DC by comparing the effects of CO_2 between time-point 1 (24 days) of the *e*CO_2 samples, time-point 2 (28 days) of the *a*CO_2 samples, and time-point 3 (35 days) of the *sa*CO_2 samples. However, differences in the timing of soil sampling were found to have major confounding effects on soil chemistry and related microbial communities (data not shown), which is why DC was not applied in this experiment. Alternatively, one could apply DC by offsetting the timing of germination. However, this type DC would risk introducing variation by differences in microbial and chemical composition of the soils at the start the incubation. Furthermore, this alternative DC would still not prevent differences in amount of time by which heterotrophic soil microbes condition the soil. Either way, the variation introduced by DC has a major confounding impact on microbial soil communities, thereby masking the true effects of CO_2 on the microbial and chemical composition of the rhizosphere.

The differential impact of *sa*CO_2 on rhizosphere chemistry could largely be attributed to (phosho)lipids. Exudation of fatty acids have been reported in maize roots (da Silva Lima et al., 2014) and Arabidopsis (Strehmel et al., 2014; Petriack et al. 2017; Appendix 1). The role of lipids in rhizosphere signalling is not fully understood. However, root-exuded phospholipid surfactants have been reported to benefit the plant by altering the physiochemical properties of the rhizosphere to increase soluble phosphorus (P) and retain water (Read et al., 2003). Lipid molecules have also been implicated in plant-rhizobia interactions. In *Medicago truncatula* lipid signalling are essential for the production of NOD factors by rhizobia and root nodule development (Franssen et al., 1992; Charron et al., 2004). Lipid signals also play an important role during interactions with mycorrhizal fungi (Drissner et al., 2007; Wang et al., 2012). Although Arabidopsis does not associate with rhizobia nor mycorrhiza, plant-derived lipids in the Arabidopsis rhizosphere could promote other, undescribed, symbiotic relationships, the importance of which may be exaggerated in *sa*CO_2. While the bacterial rhizosphere effect was less pronounced at *sa*CO_2 (Fig. 5.3), the T-RFLP data are not sensitive enough to provide information as to how specific rhizobacteiral taxa responded. Another possibility is that these lipids are not directly plant derived. A recently discovered lipid uptake system, which depends on the action of the epidermal aminosphospholipid ATPase10 (ALA10), indicates that plants can recover soil lipids (Poulsen et al., 2015). Whether ALA10 represents a mechanism to limit loss of energetically costly membrane lipids, or whether this uptake system enables plants to obtain C from rhizosphere lipids, is not known (Visser et al., 2010). As these lipids are rapidly metabolised, it is tempting to speculate that ALA10 in the roots recovers carbon from soil microbes under the carbon-limiting conditions of *sa*CO_2.

The differential impact of *e*CO_2 on rhizosphere chemistry involved a notable contribution of flavonoids (Fig. 5.5). An increase in flavonoid exudation has been reported previously under *e*CO_2 conditions. Haase et al. (2007) reported a 167% increase in exudation of phenolic compounds (predominantly flavonoids) from *Phaseolus vulgaris* at *e*CO_2 (Haase et al., 2007). Exuded flavonoids are best known for their chemotactic effects on beneficial rhizosphere-inhabiting bacteria, such as Rhizobia (Sugiyama and Yazaki, 2014). However,

flavonoids have also been reported to attract soil-borne pathogens. A classic example comes the dual attraction of Rhizobia and pathogenic *Phytophthora sojae* to isoflavonoids in root exudates from soybean (Morris et al., 1998). Flavonoids, such as the phytoalexin precursor naringenin, can also alter spore germination of *Fusarium*, which can play different roles in the rhizosphere, ranging from mutualistic to plant-pathogenic (Ruan et al., 1995). Hence, plant-derived flavonoids can act as powerful semio-chemicals in the rhizosphere. Flavonoids are often stored in plants as non-active glycosides in the vacuole of the plant cell (Aoki et al., 2000; Saito et al., 2013). Hydrolysation of glycosylated flavonoids often determines the fate and biological activity of the compound, which can occur pre- or post-exudation from roots through the action of plant or microbial beta-glycosidases, respectively (Shaw et al., 2006). Interestingly, the selection of CO_2-dependent rhizosphere markers putatively identified both glycosylated and non-glycosylated forms of flavonoids, which were mostly associated with *e*CO_2 (Table S5.2). Microbial conversion of plant-derived flavonoids and/or *de novo* synthesis of microbial flavonoids in the rhizosphere are considered to play an important role in soil ecology (Rao and Cooper, 1994). These dynamic processes may also explain why some rhizosphere-enriched flavonoids are not annotated as plant-derived (Table S5.2). Ultimately, differences in rhizo-deposition of flavonoids at *e*CO_2 may not only alter the selection, recruitment and maintenance of specific rhizobacterial taxa, they may also influence the activity of specialist rhizosphere microbes and modify their effects on plants. Indeed, **Chapter 4** of this thesis showed that Arabidopsis roots sustain higher levels of colonisation by the rhizobacterial strain *Pseudomonas simae* WCS417 at *e*CO_2, which was associated with a mildly pathogenic effect on plant growth.

While the T-RFLP profiling was sufficient to detect statistically significant changes in bacterial community structure by CO_2 (Figs. 5.3 and 5.4), the technique is based on a relatively small number of detected T-RFs (Fig. 5.2; Table S5.2). Since one single T-RF may represent many microbial taxa, the technique has limited sensitivity for detection of changes in microbial diversity (Dickie and Fitzjohn, 2007). This is supported by the fact that Illumina sequencing of the same *a*CO_2 samples from this experiment yielded over 3,800 bacterial

operational taxonomic units (Appendix 1; Petriacq et al. 2017). Moreover, the T-RFLP analysis does not reveal the identification of the taxa contributing to the observed community shifts. A more comprehensive impression of the CO_2-dependent changes in rhizobacterial community structure would require next-generation sequencing applications (Nesme et al., 2016). Apart from sequencing of *16S* rRNA genes (Appendix 2; Petriacq et al., 2017), recent meta-genomic applications would not only enable in depth analysis of taxonomic communities, but also detect quantitative changes in specific microbial genes and related microbial functions (Nesme et al., 2016). Furthermore, additional chemical profiling of the samples could increase the reliability of compound identification. For instance, the use of tandem MS analysis would allow for fragmentation of ions and potentially provide more certainty about the putative identities of single compounds (Sawada et al., 2012). Additional use of nuclear magnetic resonance (NMR) would enable structural validation of putative compounds (Leiss et al., 2011). Finally, metabolic flux analysis using carbon pulse labelling with $^{13}CO_2$ would enable inferring which rhizosphere compounds are derived from photosynthetic carbon (Allen, 2016). All these genomic and metabolomic techniques are compatible with the experimental design used on this study.

In conclusion, this Chapter provides proof-of-concept that the employed experimental system enables the linking of CO_2-induced changes in soil microbial community structure to changes in rhizosphere chemistry. Increasing the analytical power with the above-mentioned techniques could lead to the identification of novel semio-chemcials that drive these CO_2-dependent impacts on microbial soil communities.

Table S5.1 T-RF values that explain 60% of the dissimilarity between rhizosphere and control soil at a range of CO_2 concentrations and time-points

		24 days	28 days	35 days
Enriched in rhizosphere	*sa*CO_2	43.66, 285.05, 56.11, 412.6, 414.37, 51.34, 79.19	286.32, 75.59	73.84†
	aCO_2	285.05, 79.19, 40.44†, 43.66, 412.6, 414.37, 409.27	61.64, 285.05, 414.37†, 73.84†	61.64†, 75.59, 279.38†, 77.86
	eCO_2	76.49†, 79.19, 77.86, 285.05	286.32, 75.59, 61.64, 79.19, 283.24, 406.47, 56.11	414.37, 237.61†, 75.59, 287.83†, 286.32, 61.64†
Enriched in soil	*sa*CO_2	56.73*	61.64, 43.66, 79.19, 54.79, 283.24, 285.05, 56.11	79.19, 285.05, 286.32, 232.42*, 281.66, 283.24, 40.44, 412.6
	aCO_2	73.84*, 286.32, 75.59	283.24*, 75.59, 56.11, 281.66, 54.79	281.66, 409.27, 40.44, 56.11, 412.6
	eCO_2	72.74*, 75.59, 286.32, 73.84*	281.66, 285.05*, 76.49	285.05*, 412.6, 409.27, 40.44, 281.66, 56.11

* TRF absent in rhizosphere
† TRF absent in control soil

Table S5.1 Putative identification of rhizosphere ion markers (m/z values; UPLC-Q-TOF) that are statstically influenced by atmospheric CO_2

Treatment [a]	*P* value [b]	Detected *m/z* [c]	RT (min) [c]	Adducts [d]	Predicted mass [d]	Error (ppm) [d]	Putative compound [d]	Predicted formula [d]	Pathways [e]
saCO2	**24 days**								
	1.7E-03	663.454	4.6	*[M+H]+*	680.463	9	PG(12:0/17:0)	C35H69O10P	Lipid
	2.3E-04	648.551	3.8	*[M+H]+*	647.562	27	DG(19:0/0:0/19:0) (d5)	C41H75D5O5	Lipid
	2.7E-04	685.433	4.6	*[M+H-H2O]+*	702.447	17	PG(13:0/18:3(6Z,9Z,12Z))	C37H67O10P	Lipid
	0.0E+00	737.545	4.6	*[M+H]+*	736.525	16	PG(14:0/19:0)	C39H77O10P	Lipid
	0.0E+00	736.542	4.6	*[M+H]+*	735.541	9	PS(O-18:0/15:0)	C39H78NO9P	Lipid
	5.8E-04	764.522	4.6	*[M+H]+*	763.515	1	PE(16:0/22:6(4Z,7Z,10Z,13Z,16Z,19Z))	C43H74NO8P	Lipid
	2.5E-03	684.529	4.2	*[M+H]+*	683.525	5	1-tetradecanyl-2-(8-[3]-ladderane-octanyl)-sn-glycerophosphoethanolamine	C39H74NO6P	Lipid
	4.5E-03	656.422	4.2	*[M+H]+*	655.421	10	PE(12:0/18:4(6Z,9Z,12Z,15Z))	C35H62NO8P	Lipid
	8.1E-04	706.496	4.6	*[M+H]+*	705.495	8	PS(O-16:0/15:1(9Z))	C37H72NO9	Lipid
	1.7E-03	707.499	4.6	*[M+H]+*	706.479	18	PG(17:0/14:1(9Z))	C37H71O10P	Lipid
	4.2E-02	763.517	4.6	*[M+H]+*	762.520	13	PE(19:0/22:6(4Z,7Z,10Z,13Z,16Z,19Z))	C44H75O8P	Lipid
	2.6E-02	706.496	5.2	*[M+H]+*	705.495	8	PS(O-16:0/15:1(9Z))	C37H72NO9	Lipid
	2.9E-02	466.274	2.6	*[M+H-2H2O]+*	501.286	2	PE(20:4(5Z,8Z,11Z,14Z)/0:0)	C25H44NO7P	Lipid
	4.1E-03	765.560	5.2	*[M+H]+*	764.557	4	PG(13:0/22:0)	C41H81O10P	Lipid
	3.2E-02	632.454	4.2	*[M+H-2H2O]+*	667.455	19	PG(14:0/14:0)	C34H68O10P	Lipid
	2.9E-02	664.459	4.6	*[M+H]+*	663.448	5	PS(P-16:0/12:0)	C34H66NO9P	Lipid
	3.1E-11	251.128	2.6	*[M+H]+*	250.121	0	Ubiquinone-1	C14H18O4	Redox
	1.5E-03	565.216	2.2						Unknown
	3.2E-02	946.103	0.8						Unknown
	35 days								
	8.6E-03	1016.212	1.0						Unknown
	4.9E-02	562.237	2.7						Unknown
	3.3E-02	922.407	2.4						Unknown
aCO2	**24 days**								
	6.4E-06	325.186	4.4	*[M-H]-*	326.1882	15	AA861	C21H26O3	Quinone
	8.2E-04	333.157	5.2	*[M+H]+*	332.149	2	Glutaminyl-Tryptophan	C16H20N4O4	Amino acid
	4.2E-02	301.140	1.9	*[M+H]+*	300.136	10	4'-Hydroxy-5,7-dimethoxy-8-methylflavan	C18H20O4	Flavonoid
	7.4E-03	438.186	1.7	*[M+H-H2O]+*	455.192	6	PS(6:0/6:0)	C18H34NO10P	Lipid
	1.6E-02	393.175	3.7	*[M-H]-*	394.184	5	cis-3-Hexenyl b-primeveroside	C17H30O10	Lipid
	4.2E-02	326.189	4.4						Unknown
	28 days								
	8.0E-03	499.242	1.2	*[M-H]-*	500.241	16	Tigloylgomicin H	C28H36O8	Lignan
	2.0E-03	703.376	3.6	*[M+Na]+*	680.398	16	Gingerglycolipid C	C33H60O14	Lipid
	35 days								
	6.6E-04	357.148	3.5	*[M+H-2H2O]+*	392.162	4	6-Butyryl-5,7-dihydroxy-8-(3',3'-dimethylallyl)-4-phenylcoumarin	C24H24O5	Coumarin
eCO2	**24 days**								
	6.12E+02	612.387	3.7	*[M+H]+*	611.3683	17	Zizyphine A	C33H49N5O6	Alkaloid
	9.1E+02	906.230	1.8	*[M-H]-*	905.235	13	Cyanidin 3-O-(2''-xylosyl-6''-(6''-caffeoyl-glucosyl)-galactoside)	C41H45O23	Flavonoid
	2.8E+02	275.150	1.8	*[M-H]-*	276.159	3	p-Coumaroylagmatine	C14H20N4O2	Coumarin
	5.3E+02	534.292	2.3	*[M+NH4]+*	516.257	2	Eriojaposide B	C25H40O11	Terpenoid
	3.7E+02	371.157	3.8	*[M-H]-*	372.157	19	6,7-dihydroxy Bergamottin	C21H24O6	Coumarin
	4.2E+02	421.264	3.2	*[M+H]+*	818.531	12	PI(P-16:0/18:2(9Z,12Z))	C43H79O12P	Lipid
	8.7E+02	873.303	2.5	*[M-H2O-H]-*	892.300	24	Sempervirenoside A	C42H52O21	Flavonoid
	5.1E+02	514.220	2.1	*[M+H]+*	513.207	11	trans-Zeatin-O-glucoside riboside	C21H31N5O10	Terpenoid
	6.1E+02	612.915	3.7	*[M+2H]2+*	1223.812	2	KDNalpha2-3Galbeta1-4Glcbeta-Cer(d18:1/24:0)	C63H117NO21	Lipid

2.9E+02	289.165	2.1	*[M+Na-2H]-*	268.183	25	4-[1-Ethyl-2-(4-methylphenyl)butyl]phenol	C19H24O	Polyketide
9.7E+02	972.645	3.4	*[M+H]+*	971.631	7	MIPC(d18:0/18:0)	C48H94NO16P	Lipid
9.3E+02	928.623	3.4	*[M+Na]+*	905.626	8	C24:1-OH Sulfatide	C48H91NO12S	Lipid
4.9E+02	494.317	3.2	*[M+H]+*	493.304	11	Zygadenine	C27H43NO7	Alkaloid
5.06E+02	506.319	3.1	*[M+H]+*	505.3168	10	PC(17:2(9Z,12Z)/0:0)	C25H48NO7P	Lipid
2.9E+02	285.168	4.0	*[M+2Na+H]3+*	852.479	3	PI(14:1(9Z)/22:6(4Z,7Z,10Z,13Z,16Z,19Z))	C45H73O1	Lipid
3.3E+02	331.250	3.3						Unknown
3.3E+02	331.214	2.6						Unknown
28 days								
3.3E-02	922.407	2.4	*[M+H-H2O]+*	939.391	19	Lyciumin D	C45H64CoN6O12	Lignan
3.0E-02	202.181	0.6	*[M+H]+*	201.173	1	11-amino-undecanoic acid	C11H23NO2	Lipid
3.9E-04	617.197	1.4	*[M-H2O-H]-*	636.205	15	Linoside B	C30H36O15	Flavonoid
9.3E-03	789.182	1.6	*[M+CH3COO]-*	730.175	8	Isorientin 4'-O-glucoside 2''-O-p-hydroxybenzoagte	C34H34O18	Flavonoid
4.2E-02	301.140	1.9	*[M+H]+*	300.136	10	4'-Hydroxy-5,7-dimethoxy-8-methylflavan	C18H20O4	Flavonoid
2.9E-02	710.306	2.4	*[M+2Na]2+*	1374.630	2	Agavoside G	C62H102O33	Terpenoid
35 days								
1.21E-02	287.062212	0.7	[M-H2O-H]-	306.074	23	(+)-Gallocatechin	C15H14O7	Flavonoid
1.63E-03	213.145422	2.1	[M+H]+	212.1412	14	12-oxo-10E-dodecenoic acid	C12H20O3	Lipid
2.23E-02	657.28663	2.7	[M+H-H2O]+	674.2938	6	Trichilin A	C35H46O13	Terpenoid
2.46E-02	970.209516	1.4						Unknown

[a] : conditions for which the metabolic markers showed a statistically significant accumulation between *saCO₂* and *aCO₂*

[b] : *P* values indicate levels of significance from FDR adjusted ANOVA and subsequent two-factor ANOVA ($P < 0.01$)

[c] : accurate *m/z* values with their corresponding retention time (RT) detected by UPLC-qTOF-MS

[d] : predicted parameters from the METLIN database using the detected accurate *m/z. Adducts : type of ion generated by electrospray ionization; Δppm: difference between observed and theoretical monoisotopic masses.*

[e] : putative metabolites and their corresponding pathways were validated by information from the PubMed chemical database

DG: Diradylglycerols; MIPC: mannosyl inositol phosphorylceramide; PC: Phosphatidylcholine; PE: Phosphatidylethanolamine; PG: Phosphoglycerol; PI: phosphatidylinositol; PS: Phosphatidylserine

Chapter 6: Final Discussion

6.1 Summary of findings

This thesis aimed to explore the extent to which CO_2 concentration in the atmosphere influences the interactions of Arabidopsis with pathogenic and beneficial microbes. I have demonstrated that changes in atmospheric CO_2 concentration alter the defence-related metabolome in leaves and change the chemical profile of the rhizosphere. The impacts of these changes are summarised in Fig. 6.1, which integrates the results throughout this thesis to demonstrate the mechanisms by which microbial interactions are affected by CO_2 concentration.

By monitoring growth of Arabidopsis at *sa*CO_2, aCO_2 and *e*CO_2, I was able to implement a plant developmental correction (DC), which eliminates the indirect effects of CO_2 concentration on development that cause age-related resistance. Consequently, DC allowed me to address the direct effects of CO_2 concentration on the immune system of Arabidopsis and subsequent resistance against pathogens with contrasting infection strategies. As described in **Chapter 3,** *e*CO_2 increased resistance to both biotrophic *Hyaloperonospora arabidopsidis* (*Hpa*) and necrotrophic *Plectosphaerella cucumerina* (*Pc*; Fig. 6.1 b). These resistance phenotypes were associated with an upregulation of the phytohormones SA and JA. Subsequent mutant analysis revealed that the *e*CO_2-induced resistance to *Pc* is fully dependent on JA signalling, whereas *e*CO_2-induced resistance to *Hpa* involves additional mechanisms than SA-dependent defences alone. Thus, after elimination of age-related resistance, *e*CO_2 directly boosts phytohormonal-dependent defence signalling, contributing to enhanced resistance against both necrotrophic and biotrophic pathogens. Further DC experiments in **Chapter 3** revealed that development-independent resistance to *Hpa* at *sa*CO_2 was not dependent on SA signalling, but associated with enhanced accumulation of metabolites that regulate cellular redox status. Subsequent experiments uncovered a role for intracellular ROS in *sa*CO_2-induced resistance to *Hpa*, which are derived from the photo-respiration enzyme glycolate oxidase (GOX). This study is one of the first of its kind. Critically, it is the only study that has removed bias from differences in plant developmental stage. This thesis has also provided

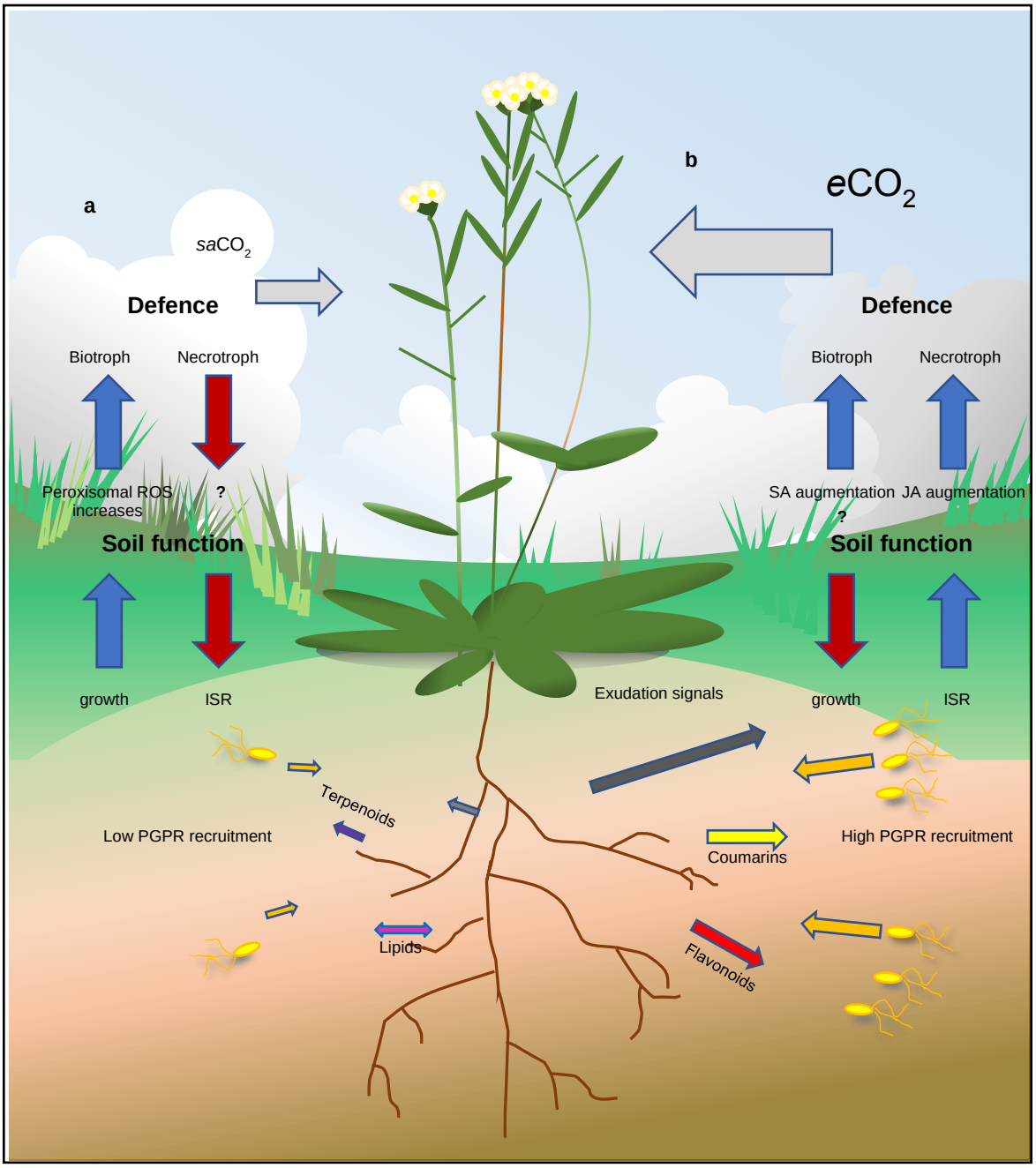

Figure 6.1 Model of CO_2-dependent plant-microbe interactions. **a.** *sa*CO_2 has differential impacts on plant defence, microbial interactions and changes in the function of soil microbes through changes in plant-mediated rhizosphere chemistry. These effects are illustrated with arrows and summarised in the figure. **b.** *e*CO_2 enhances plant defence through changes in phytohormone physiology, changes in the function of soil microbes, and through altered plant-mediated rhizosphere chemistry. Changing interactions are illustrated with arrows and summarised in the figure. Key; JA – jasmonic acid; SA – salicylic acid; ROS – reactive oxygen species; ISR – induced systemic resistance; PGPR – plant growth promoting rhizobacteria.

new insight into the mechanisms by which C_3 plants at *sa*CO_2 glacial environments have responded to pathogen challenge.

Chapter 4 explored the impacts of atmospheric CO_2 on colonisation by two beneficial soil bacteria and corresponding plant responses. This study

revealed that colonisation of the specialist rhizosphere coloniser *Pseudomonas simiae* WCS417 increased with rising CO_2 concentrations, whereas rhizosphere colonization by the saprophytic *Pseudomonas putida* KT2440 strain was unaffected by *sa*CO_2 and *e*CO_2. DC appeared to have no effect on the CO_2-depedendent colonization by WCS417 bacteria. Interestingly, depending on the nutritional status of the soil, the CO_2-dependent colonisation by WCS417 was associated with changes in WCS417-induced growth and resistance responses. In combination, this study has shown that CO_2 not only influences the colonisation of selected rhizobacteria, but also affects the host plant response to these bacteria (Fig. 6.1).

Finally, **Chapter 5** addressed the global impacts of CO_2 on microbial and biochemical rhizosphere composition, using a novel experimental system, which I helped develop (Appendix 1; Pétriacq et al. 2017). The changes observed in chemical rhizosphere profiles at *e*CO_2 was based on increased abundance of secondary metabolites, such as alkaloids, coumarins and flavonoids. Changes in bacterial community profiles at *sa*CO_2 were related to an increased presence of lipids and terpenoids in the rhizosphere. Together these results indicate clear impacts of CO_2 on the microbial and biochemical rhizosphere effect (Fig. 6.1).

While specific limitations of each approach have been considered in the discussion section of each experimental Chapter, a major outcome of this PhD study is the emerging need to address how distinct variables of global change, such as increased temperature and drought stress, may interact with the effects of eCO_2 on plant-microbe interactions. Another important discussion point emerging from this PhD study is how CO_2 influences the interaction between above- and below-ground plant responses to other organisms, including rhizosphere microbes, leaf pathogens, herbivorous arthropods and pollinators.

6.1 Interactions between below- and above-ground plant defences

In light of the data presented in this thesis, an emerging theory is that the modified immune status of above-ground tissues at *e*CO_2 or *sa*CO_2 are in part due to the impacts of CO_2 on ISR-eliciting rhizosphere microbes. It is evident that

eCO_2 increases root colonisation by PGPR (as seen in **Chapter 4**). If certain native soil microbes respond to *e*CO_2 by increased rhizosphere colonisation, this could result in increased levels of ISR, which may in turn explain the changes in responsiveness to JA and SA, that results in broad-spectrum resistance against necrotroph and biotrophic pathogens (**Chapter 3**). While *P. simiae* WCS417-mediated ISR was still detectable at *e*CO_2 against *Pc* (Figure 4.5), the relatively high basal resistance against *Pc* made it difficult to assess whether ISR was enhanced in comparison to *a*CO_2. If the soil microbiome is responsible for enhanced *Pc* resistance at *e*CO_2, this could explain possible disparities within the literature about the effects of CO_2 on aboveground disease resistance (**Chapter 1**). As was shown in **Chapter 4** (Fig. 4.5), ISR not only depends on atmospheric CO_2 concentration, but it also depends on the nutritional status of the soil. Furthermore, in studies where *e*CO_2 repressed plant immunity, it is plausible that some normally commensal or beneficial rhizosphere microbes become detrimental to the host plant, weakening plant development and resistance against aboveground diseases. Indeed, under conditions of *e*CO_2 and nutrient-poor soil, *P. simiae* WS417 not only displayed strongly increased rhizosphere colonisation, but it also repressed plant growth (**Chapter 4**; Fig. 4.4).

Soil processes are rarely considered in studies regarding the impacts of *e*CO_2 on above-ground disease resistance. Repeating the experiments described in **Chapter 3** in a sterile growth system would help to address the contribution of the rhizosphere microbiome to *e*CO_2-induced resistance in the leaves. This is relevant as functional changes in the soil will be dependent on other environmental factors, such as soil nutrient availability and other environmental stresses that are likely going to become more prevalent due to man-made global change (O_3, temperature, drought, extreme weather events and nutrient limitations). Furthermore, some symbiotic relationships, such as plant-mycorrhiza interactions, are able to mitigate environmental plant stress (Rodriguez et al., 2004). In that context, it is plausible that improved recruitment of beneficial soil microbes under *e*CO_2 could enhance crop tolerance against climate change-related environmental stresses and resist newly emerging diseases (Fig. 6.1 b).

Plant responses to infection under *sa*CO_2 conditions are rarely studied. Interestingly, plants grown at *sa*CO_2 expressed increased resistance to the

biotrophic pathogen *Hpa*, while basal defence against the necrotrophic fungus *Pc* was greatly diminished (**Chapter 3**). Even more surprisingly, *P. simiae* WCS417 induced susceptibility against *Pc* at *sa*CO_2 (**Chapter 4**). Resistance against *Hpa* was associated with increased peroxisomal ROS production, suggesting that photorespiration plays a major role in augmenting defence in a CO_2-limited environment (Fig. 6.1 a). Transcription of photorespiration-related genes is increased at *sa*CO_2 (Li et al., 2014c), and photorespiration has been shown to play a role in non-host resistance at *a*CO_2 (Rojas et al., 2012). Due to the repeated exposure of plants to *sa*CO_2 in recent evolutionary history, C_4 photosynthesis has developed as a strategy to maximise growth under CO_2-limited conditions (Edwards and Ogburn, 2012; Li et al., 2014c). Plants that did not develop C_4 may have retained photorespiration to provide a competitive advantage in environments of high biotic stress. Indeed, investment in defence metabolites is higher in C_3 plants at *sa*CO_2 (Forkelova et al., 2016; Huang et al., 2017) and transcription of many defence-related genes is constitutively higher (Li et al., 2014c). This advantage would only manifest itself in certain habitats, where biotrophic but not necrotrophic pathogens are prevalent, for instance at moderate temperatures and relatively high humidity. The fact that plants at *sa*CO_2 were more susceptible to *Pc* (**Chapter 3**; Fig. 3.1) which became even more pronounced after root colonisation *P. simiae* (**Chapter 4;** Fig. 4.5), suggests that there was a cost to GOX-dependent *sa*CO_2-induced resistance.

Communication with beneficial rhizobacteria requires targeted defence signalling (Zamioudis and Pieterse, 2012), as does defence against necrotrophic pathogens (Antico et al., 2012). In light of the results presented in **Chapter 4**, simultaneous management of both above- and below-ground interactions at *sa*CO_2 may be incompatible. In this respect, it would be useful to assess the impacts of *sa*CO_2 on plant interactions with PGPR and necrotrophic leaf pathogens, and assess whether the observed additive effects of *sa*CO_2 on Arabidopsis susceptibility to *Pc* are i) specific to *P. simiae* and ii) specific to *Pc*.

6.2 Impacts of interactions between eCO_2 and other environmental variables on plant-microbe interactions.

Generally, increases in atmospheric CO_2 have positive impacts on plant development. However, abiotic stresses associated with global change, such as increases in temperature, ozone (O_3) and drought stress tend to lessen the beneficial effects of eCO_2 on plant growth (Shaw et al., 2002; Eastburn et al., 2010, although see Tiedemann 2000). As many global change-associated factors occur concurrently, it is important to understand their interactions, particularly in relation to disease interactions. However, multi-factor studies increase the variability of already complicated datasets, making inference on interactive effects problematic. For instance, concurrent exposure to heat and drought stress profoundly changes the transcriptomic responses of plants to viral infection (Prasch and Sonnewald, 2013). This thesis has described and characterised several effects CO_2 on the physiology of Arabidopsis, and the consequences thereof, on interactions with pathogens and rhizosphere microbes. Future research needs to focus on how these eCO_2 responses manifest themselves in interaction with other climate change-related environmental stresses.

6.2.1 Elevated Ozone

Trophospheric Ozone (O_3) concentration has risen from pre-industrial levels of 10 ppb to 40 ppb (Stevenson et al., 2006). Tropospheric O_3 has a substantial contribution to global warming, both as a greenhouse gas (GHG) and a regulator of other GHGs (IPCC, 2013). O_3 also causes oxidative damage in plants, reduces carbon assimilation and impairs RuBisCO activity (Iriti and Faoro, 2008). The extent by which O_3 damages plants depends on the plant species (Krupa et al., 2000; Tai et al., 2014), making it challenging to generalise impacts of O_3 on global agricultural production. However, it has been estimated that O_3 pollution already causes substantial losses in major crop species, including winter wheat, rice, maize and soybean (Wang et al., 2007; Van Dingenen et al., 2009; Avnery et al., 2011). These adverse effects of O_3 are projected to get worse under future climate scenarios (Van Dingenen et al., 2009; Avnery et al., 2011).

Like eCO_2, O_3 can have both positive and negative impacts on disease severity. This variability may be due to the fact that O_3 is directly toxic to many

pathogens, such as fungal spores or bacteria (Hibben and Stotzky, 1969; Manning and v. Tiedemann, 1995; Paul et al., 2002). In addition, O_3 affects plants, potentially altering their ability to resist pests and diseases (Krupa et al., 2000). Furthermore, *e*O_3 can reduce the CO_2 fertilisation effect and lessen the defence-enhancing effects of *e*CO_2 on plants (Eastburn et al., 2011). For example, in conjunction with *e*O_3, the positive effects of *e*CO_2 on spring wheat resistance to *Puccinia recondita* rust were reduced (Tiedemann and Firsching, 2000). Enhanced resistance in potato against *Phytophthora infestans* at *e*CO_2 was also reversed by simultaneous exposure to *e*O_3 (Plessl et al., 2007). In barley, positive effects of both *e*CO_2 and *e*O_3 on downy mildew resistance were lost when the two were combined (Mikkelsen et al., 2014), suggesting complex mechanistic interactions. Conversely, in soybean, the defence-enhancing effects of *e*CO_2 against downy mildew remained unaffected by *e*O_3, further highlighting the pathosystem-specific nature of these interactive effects (Eastburn et al., 2010). While it should be noted that O_3 is one of the more widely studied factors of global climate change, the exact mechanisms by which it influences disease resistance remain poorly understood.

Belowground, *e*O_3 has been reported to stimulate C rhizodeposition (McCrady and Andersen, 2000). As discussed in **Chapters 4** and **5**, rhizodeposition of C is increased at *e*CO_2. While various studies have shown that *e*O_3 has limited impacts on microbial soil communities (Dohrmann and Tebbe, 2005; Dohrmann and Tebbe, 2006), effects on community structure and C utilisation by rhizosphere microbes have been recorded, such as in a rice paddy system (Chen et al., 2010). Furthermore, Li et al. (2013) failed to find changes in the microbial rhizosphere community of wheat at *e*O_3, but they did find changes in the abundance of functional genes in the rhizosphere through transcriptomic analysis (Li et al., 2013), suggesting that the microbial soil function is not necessarily dependent on community structure alone. Indeed, early work on the effects of *e*O_3 on soil microbes revealed that phosphatase activity of specialised bacteria is influenced by O_3 concentration, while other bacteria remained largely unaffected (Shafer, 1988). O_3 also changes microbial soil activities in conjunction with *e*CO_2. For instance, in aspen and birch rhizospheres, enhanced microbial respiration at *e*CO_2 was abolished by *e*O_3 (Phillips et al., 2002). Similar effects

were reported for cellulose digesting activity (Larson et al., 2002). Clearly, more research is required to identify *i*) the role of plants in O_3-induced effects on soil microbes and *ii*) the impacts of interactions between *e*CO_2 and *e*O_3 on the taxonomic structure and activity of the soil microbiome.

6.2.2 Elevated temperature

While moderate increases in temperature can change the developmental rate and seasonality of plants (Korner and Basler, 2010), extreme temperature events, which are predicted to occur more widely and frequently due to climate change (Luber and McGeehin, 2008), are almost always detrimental to plant production (Bauweraerts et al., 2013; Hatfield and Prueger, 2015). It is estimated that global crop production will decrease around 10% by 2050 due to global warming alone (Tai et al., 2014). Elevated temperature (*e*Temp) favours infection by fungal pathogens, such as *Fusarium verticillioides* (Murillo-Williams and Munkvold, 2008), although quantitative effects of *e*Temp on plant disease depends on the plant- pathogen interaction in question (Luck et al., 2011). Increased temperatures may intensify disease pressure, (Sharma et al., 2007; Evans et al., 2008), and increase pathogen virulence (Laine, 2008). Host defence responses are attenuated at higher temperatures, resulting in greater disease symptoms (Wang et al., 2008), due to inhibited effector recognition by temperature-sensitive resistance (R) genes (Zhu et al., 2010). In contrast, some R genes, such as Xa7 in rice, are more effective at *e*Temp (Webb et al., 2010). Hence, *e*Temp can have wide-ranging impacts on plant diseases, which depends on the nature of the interaction (McElrone et al., 2010; Melloy et al., 2014), but the majority of studies points to an increase in disease severity by *e*Temp (Eastburn et al., 2010; Shin and Yun, 2010; Pugliese et al., 2012; Ferrocino et al., 2013; Mikkelsen et al., 2014).

Although *e*CO_2 alone can increase host-pathogen resistance (**Chapter 3**), this can be countered by *e*Temp. To date, most studies examining combined exposure to *e*CO_2 and *e*Temp report contrasting impacts on plant disease. For instance, *e*CO_2 was unable to mitigate *e*Temp-induced susceptibility to *Fusarium* wilt resistance in lettuce (Ferrocino et al., 2013), whereas *e*CO_2 can mitigate the negative effects of *e*Temp on resistance of barley against spot blotch disease

(Mikkelsen et al., 2014). Furthermore, *e*CO_2 and *e*Temp can have synergistic and/or additive effects on disease. For instance, combined exposure of zucchini to *e*Temp and *e*CO_2 increased *Podosphaera* powdery mildew growth and virulence (Pugliese et al., 2012). On the other hand, synergic and/or additive effects of combined *e*CO_2 and *e*Temp exposure on disease resistance have been recorded as well, as was the case for the tobacco - potato virus X interaction (Aguilar et al., 2015). In some cases, increased disease at *e*CO_2 was mitigated by *e*Temp. For example, *e*Temp countered *e*CO_2 induced resistance against *Fusarium* crown rot in wheat, which was related to developmental plant stage (Melloy et al., 2014). A similar interaction has been reported between sweetgum and *Cercospora* (McElrone et al., 2010). Overall these data suggest a range of different effects with a range of different outcomes, depending on the host-pathogen interaction. Clearly, further study regarding the interactive effects of *e*Temp and *e*CO_2 is required to predict the combined impacts on agricultural systems and develop effective control strategies. In this context, it would help to study pathogens with different lifestyles, as is addressed in **Chapters 3** and **4**. Comparing pathogens of different lifestyles may help to increase our understanding of the mechanisms by which the plant immune system is affected by combined *e*Temp and *e*CO_2 conditions.

Temperature also influences microbial abundance and activity in rhizosphere soil. For instance, fungal abundance in a C_3 grass dominated field system increased at *e*Temp, while bacterial abundance decreased under these circumstances (Castro et al., 2010). Interestingly, combined exposure to *e*CO_2 and *e*Temp resulted in increased bacterial abundance. In a different grassland ecosystem, similar patterns were observed where fungal communities were strongly impacted by *e*Temp, resulting in greater soil respiration and N mineralisation (Briones et al., 2009). Exposure to *e*Temp are predicted to result in greater soil respiration and soil organic matter decomposition (Zogg et al., 1997), which may decrease the availability of soil organic C in the soil. Interestingly, this effect has been demonstrated to be greater in plant-free bulk soil than in rhizosphere soil (Hartley et al., 2007). Since *e*CO_2 have qualitative and quantitative impacts on root exudates (**Chapter 5**), which largely determine organic matter in the rhizosphere (Zhu and Cheng, 2011), it is difficult to predict

the combined impacts of *e*Temp and CO_2 on agricultural soils. Certainly, autotrophic (plant-related) and heterotrophic (soil organism-related) CO_2 effluxes are dependent on temperature (Schindlbacher et al., 2008). Together, these studies suggest C capture in soil could be reduced in warmer environments, turning soil from C sinks to C sources, and further increasing atmospheric CO_2 (Jones et al., 2003). Moreover, these processes are seasonally dependent, suggesting greater effects of warming on respiration outside of the growing season (Hartley et al., 2007; Suseela and Dukes, 2013). Soil respiration is likely to be dependent on soil moisture. For instance, respiration in grasslands was only increased by *e*Temp and *e*CO_2 when water availability was high. At lower water availability, respiration was decreased during the growing season, but increased over winter (Wan et al., 2007). As CO_2 enhances C rhizodeposition, *e*CO_2 might offset the negative effects of *e*Temp on C capture. Equally, *e*CO_2 might exacerbate C emissions through further stimulation of soil respiration (Pendall et al., 2004). However, the short-term nature of many of these studies may overstate potential C-cycle feedbacks as they ignore plant acclimation to warming (Luo et al., 2001). The method developed by Petriacq et al. (2017; Appendix 1), which allows for *in situ* profiling of rhizosphere chemistry in relation to microbial communities (**Chapter 5)**, would be very suitable to determine the metabolic contents and fluxes into the rhizosphere under combined exposure to *e*Temp and *e*CO_2.

6.2.1 Increased drought

Due to global warming, agriculture will experience increasing levels of drought stress (IPCC, 2013). Drought induces stomatal closure, which limits photosynthesis and antagonizes the growth-promoting effects of *e*CO_2 (*e.g.* (Warren et al., 2017). At the same time, drought can increase pre-invasive resistance to leaf pathogens through reduced stomatal aperture (Liu et al., 2009) (Pennypacker et al., 1991; Melotto et al., 2008), but reduce post-invasive resistance through drought-induced ABA signalling that antagonises SA-dependent and JA-disease resistance via repressive signalling cross-talk (Ton et al., 2009). Although the role of the defence regulatory phytohormones JA and SA in *e*CO_2-induced disease resistance has been characterised in **Chapter 3** of this thesis, the effects of *e*CO_2 on ABA signalling remained unexplored. Recently,

however, it was reported that *e*CO_2-induced susceptibility of Arabidopsis to *Pseudomonas syringae* pv. *tomato* (*Pst*) DC3000 involves ABA signalling (Zhou et al., 2017). Such studies suggest that enhanced ABA activity at *e*CO_2 can indeed counter SA-dependent resistance. This repressive effect might become more prevalent under conditions of (mild) drought stress. Indeed, drought stress in a normally resistant cultivar of wheat has been reported to induce susceptibility to *Fusarium* at *e*CO_2 (Melloy et al., 2010). Fungal pathogens are generally more tolerant to water deprivation than their hosts (Desprez-Loustau et al., 2006), explaining why some pathogens, such as *Botrytis cinerea*, have evolved the ability to produce ABA as a virulence factor (Siewers et al., 2006). Conversely, preventing drought stress at *e*CO_2 by increased watering has been associated with increased susceptibility to downy mildew (Eastburn et al., 2010). Similar observations have been made for leaf spot in two *Eucalyptus* species (McElrone et al., 2010). To date, these are the only reports of interactive effects between water availability and *e*CO_2. Again, more research is needed to obtain a better understanding of the mechanisms underpinning interactions between drought stress and *e*CO_2, particularly in relation to stomatal development, stomatal aperture and defence signalling interactions between SA, JA (as performed in **Chapter 3**) and ABA.

Drought is known to alter soil bacterial communities. Exposure of soil to drought has been shown to trigger tolerance-inducing activities in soil bacteria (Chen and Alexander, 1973; Evans and Wallenstein, 2014). Interestingly, some plant species increase drought tolerance in response to root treatment with PGPR or AMF (Kohler et al., 2009). Moreover, Timmusk et al. (2014) demonstrated that inoculation with bacteria that had been isolated from water-deprived soils induced drought tolerance (Timmusk et al., 2014). Although limited, these studies suggest that rhizosphere interactions could be exploited to mitigate drought stress in future climate scenarios. However, the mechanisms by which these rhizosphere interactions improve drought tolerance remains largely unknown, making it difficult to select for soil practices and/or crop varieties that allow for the establishment of drought-mitigating rhizosphere communities.

6.2.3 Changing Nutrient availability

Soil nutrient concentrations are subject to anthropogenic change because of intensive agriculture, such as habitual and wide-scale application of N and P fertilisers to improve yield. N is arguably the nutrient that has the greatest influence on crop yield growth and is, therefore, most studied (Lawlor et al., 2001). Importantly, nutrient availability is a key element in disease resistance (Dordas, 2008). Biochemically, many secondary defence metabolites contain N (alkaloids) and S (glucosinolates). Nutrition can also increase structural defences. For instance, K fertilisation has been demonstrated to improve plant resistance by promoting the formation of thick secondary cell walls (Dordas, 2008). The effects of N limitation are more complex, resulting in either increased susceptibility or increased resistance, which in part depend on the nutritional requirements of the pathogen (Dordas, 2008). Since CO_2 affects growth and nutrient uptake by the plant (Leakey et al., 2009), it can change the availability of soil nutrients. The nutritional status of the host plant, both in terms of macro- and micro elements, is critically important for pathogenic interactions (Divon and Fluhr, 2007). For example, Si has been shown to counter *e*CO_2-induced susceptibility to herbivory by decreasing leaf palatability (Frew et al., 2017). Furthermore, N fertilisation reduces *Fusarium* infection in beech trees at *e*CO_2 (Fleischmann et al., 2010). In this thesis, the use of nutrient-poor soil in **Chapter 4** did not result in statistically significant changes in disease severity of *Pc* at *e*CO_2 (Fig. 4.4) However, other studies have shown that leaf palatability decreases at *e*CO_2 due to lower C:N (Mcelrone et al., 2005; Matros et al., 2006; Kretzschmar et al., 2009; Eastburn et al., 2010; Mathur et al., 2013; dos Santos et al., 2013; Ghini et al., 2014). Hence, N availability could make leaves more vulnerable for parasitism by pests and diseases, as was demonstrated in a grass FACE experiment, where fungal infection at *e*CO_2 only increased when N was supplemented (Mitchell et al., 2003). To date, these are the only studies that have investigated the interactive effects of nutrient availability and *e*CO_2 on disease resistance. Accordingly, there is a pressing need to study the impacts of other nutrients, such as P, K, Si and Fe, in interaction with *e*CO_2.

Nutrition is an important factor in the rhizosphere, where nutrient limitations can be decisive for the outcome of plant-microbe and microbe-microbe

interactions. Ample examples can be drawn from the impacts of P on plant-mycorrhiza interactions, N acquisition by rhizobia, and the effects of Fe on microbial competition in the rhizosphere (Van Der Heijden et al., 2008; Berendsen et al., 2012). Plants are major players in nutritional homeostasis of the rhizosphere, where they exert particular influence over microbial biomass and metabolic rates of nutrient-poor soils (Hartman and Richardson, 2013). These impacts can be exaggerated under *e*CO_2 (Jin et al., 2015), which in turn can have unexpected outcomes on the performance of the host plant. For instance, in nutrient poor soil, **Chapter 4** revealed that increased colonisation by *P. simiae* WCS417 at *e*CO_2 turns a normally growth-promoting interaction into a growth-repressing interaction (Figs. 4.2 and 4.4). Conversely, sulphur acquisition by oak is significantly greater in mycorrhizal plants at *e*CO_2, resulting in stronger growth-promoting effects. Hence, *e*CO_2 can increase the symbiotic benefits for plants (Seegmuller et al., 1996). Whether these interactive effects of *e*CO_2 and soil nutrition result in positive or negative changes in soil function may depend on the nutrient that is limiting, the host plant in question, and the prevailing environmental conditions.

6.2.4 Temporal considerations and growth-stage effects.

Further to environmental factors, plant autonomous factors, such as plant development, may add to the effects of eCO_2 on plant-microbe interactions. As discussed in **Chapter 5**, root exudation patterns are highly dependent on the developmental stage of the plant (Calvo et al., 2017), which in turn can influence microbial community structures. For instance, higher and lower abundances of *Cyanobacteria* and *Acidobacteria*, respectively, have been reported as the host plant ages (Chaparro et al., 2013). Furthermore, as has been shown in **Chapter 3**, CO_2-dependent development has an impact on disease via age-related resistance (Kus et al., 2002). Controlling for developmental effects has been a concern in CO_2 research for decades, but has rarely been addressed. The exception is Staddon et al. (1998), who applied a developmental correction (DC) to *Plantago lanceolata* and *Trifolium repens* to study CO_2-dependent effects on colonisation by the arbuscular mycorrhizal fungus (AMF) *Glomus mosseae*. Revealingly, they demonstrated that AMF colonisation was strongly confounded by larger root systems in *e*CO_2 (Staddon et al., 1998). Until this thesis, such

corrections have not been applied again. Clear differences in Arabidopsis disease were established when growth effects of CO_2 were controlled for (**Chapter 3**). By contrast, these effects of plant development were less clear for the below-ground interactions – albeit these are arguably more difficult to measure. As CO_2 has both direct and indirect effects on plant-microbe interactions, addressing the mechanisms by which CO_2 influences plant immunity requires elimination of the indirect effects. However, from a more ecological point of view, this may be less informative or even impossible. For instance, the presence of beneficial rhizosphere microbes can stimulate plant development itself, which in turn effect the colonisation and behaviour of these microbes, as was essentially demonstrated in **Chapter 4**. Accordingly, controlling for differences in CO_2-dependent plant development in the presence and absence of growth-promoting soil microbes is impractical.

A final consideration for future work is the sensitivity of plant-rhizosphere systems to temporal factors. For instance, soil bacterial communities have repeatedly been found to show temporal plasticity in their response to CO_2 (Zak et al., 2000; Dunbar et al., 2014). This PhD thesis describes relatively short-term studies over a single plant generation to investigate the impacts of CO_2 on microbial interactions. Furthermore, this work was undertaken in a highly controlled environment, free of the influences of litter degradation and environmental fluctuations. Although single generation studies are sufficient to reveal effects of CO_2 on below-ground microorganisms, these effects tend to lessen over time and are less apparent in field studies than controlled environments (Blankinship et al., 2011). This suggests that CEF and short-term experiments may over-estimate the effects of CO_2 on rhizocommunity traits. For instance, the accumulated effects of altered rhizodeposition and litter degradation can only be postulated over years and multiple plant generations (Blankinship et al., 2011; Dunbar et al., 2014). However, short-term effects of CO_2 are biologically relevant, especially in the context of agricultural practise, where crop systems are predominantly annual (*e.g.* cereals, pulses, root crops). It currently remains unclear how plant-PGPR interactions in the rhizosphere are affected over longer time scales and multiple plant generations.

Resistance responses to pathogens may trigger trans-generational adaptive responses in plants (Pieterse et al. 2012), for instance beech seedlings that survive severe *Phytophthora* infection at *e*CO_2 are more resilient during subsequent infections (Fleischmann et al., 2010), which may translate to their progeny. Furthermore, the outcome of host/pathogen interactions are dynamic over generations, and virulence of pathogens, such as *Fusarium*, have been demonstrated to increase over generations at *e*CO_2, even in the absence of a host (Váry et al., 2015). Such transgenerational variability is likely to increase further due to the interactive complexity between plant species, soil type, plant community diversity, other biotic interactions, prevailing climatic conditions, and potential agricultural inputs as well as the extent to which all of these factors are present within the system (Philippot et al., 2013). Exploring *sa*CO_2 in these contexts may help to tease apart the effects of CO_2 from other interacting variables and add a further dimension to the findings summarised in Fig. 6.1.

All of the factors and interactions discussed above indicate the importance of an integrated investigative approach to map out potential impacts of climate change on agricultural production systems. It is expected that these factors will impact many of the processes highlighted throughout this thesis. While some factors may play a greater role in shaping plant-microbe interactions than others, it is clear from this discussion that the interactive affects are important to consider. In many cases, CO_2 is able to mitigate some of the damaging effects from *e*O_3, temperature, drought and soil nutritional stress. Future analysis of the impacts of climate change on plant-microbe interactions should aim to consider all potential interactions, in order to develop appropriate disease management strategies.

6.3 Outlook

The interdisciplinary research presented in this thesis has contributed to both molecular plant pathology and soil microbial ecology. This thesis provides novel insights into the physiological and chemical mechanisms behind the effects of CO_2 concentration on plant-microbe interactions. The work presented in **Chapter 3** may be important to make researchers aware of the importance of indirect developmental effects of CO_2 on plant-microbe interactions. Coupled with knowledge about how plants in relatively recent geological pasts adapted to

saCO_2, this study could help to inform potential agricultural policy concerning the future of farming in light of the ever increasing atmospheric concentrations of CO_2. Furthermore, the findings in **Chapters 4** and **5,** concerning below-ground interactions, demonstrate that a better understanding of the chemical and microbial composition of the rhizosphere is essential to better predict the impacts of *e*CO_2. Using novel analytical methods that allow for *in situ* profiling of rhizosphere chemistry in relation to microbial community structures (Appendix 1) will be essential to design novel soil management practices. Ultimately, this PhD thesis clearly demonstrates the need for future research to consider the impacts of interactions between *e*CO_2 and other climate change factors, such as extreme weather events.

Overall, this PhD thesis offers a better understanding of the impacts of atmospheric CO_2 on plant immunity, rhizosphere biology and soil chemistry, and has shown that plant developmental stage is an important factor in determining some of these interactions. The knowledge generated may prove valuable for future management, or mitigation, of crop disease epidemics. In addition, this study could aid the development of protective soil management practices and direct breeding strategies for new crop varieties that produce greater amounts of rhizosphere-active root exudation chemistry. In practice, this knowledge may help to make global food production more resilient against the detrimental consequences of future climate change.

Reference list

Abramovitch RB, Janjusevic R, Stebbins CE, Martin GB (2006) Type III effector AvrPtoB requires intrinsic E3 ubiquitin ligase activity to suppress plant cell death and immunity. Proc Natl Acad Sci U S A **103**: 2851–2856

Agbodjato NA., Noumavo PA., Baba-Moussa F., Salami HA., Sina H., Sèzan A., Bankolé H., Adjanohoun A., Baba-Moussa L. (2015) Characterization of potential plant growth promoting rhizobacteria isolated from Maize (Zea mays L.) in central and Northern Benin (West Africa). Appl Environ Soil Sci **2015**: 1–9

Aguilar E, Allende L, del Toro FJ, Chung B-N, Canto T, Tenllado F (2015) Effects of Elevated CO $_2$ and Temperature on Pathogenicity Determinants and Virulence of *Potato virus X* /Potyvirus-Associated Synergism. Mol Plant-Microbe Interact **28**: 1364–1373

Ahmad F, Ahmad I, Khan MS (2005) Indole Acetic Acid Production by the Indigenous Isolates of Azotobacter and Fluorescent Pseudomonas in the Presence and Absence of Tryptophan. Turk J Biol **29**: 29–34

Ainsworth E a, Rogers A (2007) The response of photosynthesis and stomatal conductance to rising [CO2]: mechanisms and environmental interactions. Plant Cell Environ **30**: 258–70

Ainsworth EA, Davey PA, Bernacchi CJ, Dermody OC, Heaton EA, Moore DJ, Morgan PB, Naidu SL, Ra HSY, Zhu XG, et al (2002) A meta-analysis of elevated [CO2] effects on soybean (Glycine max) physiology, growth and yield. Glob Chang Biol **8**: 695–709

Allen DK (2016) Quantifying plant phenotypes with isotopic labeling & metabolic flux analysis. Curr Opin Biotechnol **37**: 45–52

Alonso JM, Stepanova AN, Leisse TJ, Kim CJ, Chen H, Shinn P, Stevenson DK, Zimmerman J, Barajas P, Cheuk R, et al (2003) Genome-Wide Insertional Mutagenesis of Arabidopsis thaliana. Science (80-) **301**: 653–657

Amthor JS (2001) Effects of atmospheric CO2 concentration on wheat yield: review of results from experiments using various approaches to control CO2 concentration. F Crop Res **73**: 1–34

Anderson PK, Cunningham AA, Patel NG, Morales FJ, Epstein PR, Daszak P (2004) Emerging infectious diseases of plants: Pathogen pollution, climate change and agrotechnology drivers. Trends Ecol Evol **19**: 535–544

Antico CJ, Colon C, Banks T, Ramonell KM (2012) Insights into the role of jasmonic acid-mediated defenses against necrotrophic and biotrophic fungal pathogens. Front Biol (Beijing) **7**: 48–56

Aoki T, Akashi T, Ayabe S (2000) Flavonoids of Leguminous Plants: Structure, Biological Activity, and Biosynthesis. J Plant Res **113**: 475–488

Archer D, Eby M, Brovkin V, Ridgwell A, Cao L, Mikolajewicz U, Caldeira K, Matsumoto K, Munhoven G, Montenegro A, et al (2009) Atmospheric Lifetime of Fossil Fuel Carbon Dioxide. Annu Rev Earth Planet Sci **37**: 117–134

Atwal AS, Teather RM, Liss SN, Collins FW (1992) Antimicrobial activity of 2-aminophenoxazin-3-one under anaerobic conditions. Can J Microbiol **38**: 1084–1088

Avnery S, Mauzerall DL, Liu J, Horowitz LW (2011) Global crop yield reductions due to surface ozone exposure: 1. Year 2000 crop production losses and economic damage. Atmos Environ **45**: 2284–2296

Badr A, El-Shazly H (2012) Molecular approaches to origin, ancestry and domestication history of crop plants: Barley and clover as examples. J Genet Eng Biotechnol **10**: 1–12

Badri D V., Vivanco JM (2009) Regulation and function of root exudates. Plant Cell Environ **32**: 666–681

Badri D V., Weir TL, van der Lelie D, Vivanco JM (2009) Rhizosphere chemical dialogues:

plant-microbe interactions. Curr Opin Biotechnol **20**: 642–650

Bais HP, Walker TS, Schweizer HP, Vivanco JM (2002) Root specific elicitation and antimicrobial activity of rosmarinic acid in hairy root cultures of Ocimum basilicum. Plant Physiol Biochem **40**: 983–995

Bais HP, Weir TL, Perry LG, Gilroy S, Vivanco JM (2006) The role of root exudates in rhizosphere interactions with plants and other organisms. Annu Rev Plant Biol **57**: 233–266

Bakker P a HM, Berendsen RL, Doornbos RF, Wintermans PC a, Pieterse CMJ (2013) The rhizosphere revisited: root microbiomics. Front Plant Sci **4**: 165

Barbour WM, Hattermann DR, Stacey G (1991) Chemotaxis of Bradyrhizobium japonicum to soybeen exudates. Appl Env Microbiol **57**: 2635–2639

Bari R, Jones JDG (2009) Role of plant hormones in plant defence responses. Plant Mol Biol **69**: 473–488

Bauweraerts I, Wertin TM, Ameye M, Mcguire MA, Teskey RO, Steppe K (2013) The effect of heat waves, elevated [CO2] and low soil water availability on northern red oak (Quercus rubra L.) seedlings. Glob Chang Biol **19**: 517–528

Beerling DJ, Kelly CK (1997) Stomatal density responses of temperate woodland plants over the past seven decades of CO2 increase: A comparison of salisbury (1927) with contemporary data. Am J Bot **84**: 1572–1583

Beerling DJ, Royer DL (2011) Convergent Cenozoic CO2 history. Nat Geosci **4**: 418–420

Beilstein M, Nagalingum N, Clements M, Manchesterb S, Mathews S (2010) Dated molecular phylogenies indicate a Miocene origin for Arabidopsis thaliana. Proc Natl Acad Sci U S A **107**: 18724–18728

Berendsen RL, Pieterse CMJ, Bakker P a HM (2012) The rhizosphere microbiome and plant health. Trends Plant Sci **17**: 478–86

Berendsen RL, van Verk MC, Stringlis IA, Zamioudis C, Tommassen J, Pieterse CMJ, Bakker PAHM (2015) Unearthing the genomes of plant-beneficial Pseudomonas model strains WCS358, WCS374 and WCS417. BMC Genomics **16**: 539

Berg G, Smalla K (2009) Plant species and soil type cooperatively shape the structure and function of microbial communities in the rhizosphere. FEMS Microbiol Ecol **68**: 1–13

Berger S, Sinha AK, Roitsch T (2007) Plant physiology meets phytopathology: plant primary metabolism and plant-pathogen interactions. J Exp Bot **58**: 4019–4026

Bettarini I, Vaccari FP, Miglietta F (1998) Elevated CO2 concentrations and stomatal density: observations from 17 plant species growing in a CO2 spring in central Italy. Glob Chang Biol **4**: 17–22

Bever JD, Platt TG, Morton ER (2012) Microbial population and community dynamics on plant roots and their feedbacks in plant communities. Annu Rev Microbiol **66**: 265–283

Blackwood CB, Hudleston D, Zak DR, Buyer JS (2007) Interpreting ecological diversity indices applied to terminal restriction fragment length polymorphism data: Insights from Simulated Microbial Communities. Appl Environ Microbiol **73**: 5276–5283

Blankinship JC, Niklaus PA, Hungate BA (2011) A meta-analysis of responses of soil biota to global change. Oecologia **165**: 553–565

Block A, Schmelz E, Jones JB, Klee HJ (2005) Coronatine and salicylic acid: The battle between Arabidopsis and Pseudomonas for phytohormone control. Mol Plant Pathol **6**: 79–83

Bodenhausen N, Horton MW, Bergelson J (2013) Bacterial Communities Associated with the Leaves and the Roots of Arabidopsis thaliana. PLoS One **8**: e56329

Boege K, Marquis RJ (2005) Facing herbivory as you grow up: The ontogeny of resistance in plants. Trends Ecol Evol **20**: 441–448

Boller T, Felix G (2009) A renaissance of elicitors: perception of microbe-associated molecular patterns and danger signals by pattern-recognition receptors. Annu Rev Plant Biol **60**: 379–406

Bolwerk A, Lagopodi AL, Wijfjes AHM, Lamers GEM, Chin-A-Woeng TFC, Lugtenberg BJJ, Bloemberg G V (2003) Interactions in the tomato rhizosphere of two Pseudomonas biocontrol strains with the phytopathogenic fungus Fusarium oxysporum f. sp. radicis-lycopersici. Mol Plant Microbe Interact **16**: 983–993

Boyer JS (1995) Biochemical and biophysical aspects of water deficits and the predisposition to disease. Annu Rev Phytopathol **33**: 251–274

Boyes DC, Zayed a M, Ascenzi R, McCaskill a J, Hoffman NE, Davis KR, Görlach J (2001) Growth stage-based phenotypic analysis of Arabidopsis: a model for high throughput functional genomics in plants. Plant Cell **13**: 1499–510

Braga MR, Aidar MPM, Marabesi MA, de Godoy JRL (2006) Effects of elevated CO2 on the phytoalexin production of two soybean cultivars differing in the resistance to stem canker disease. Environ Exp Bot **58**: 85–92

Briones MJI, Ostle NJ, McNamara NP, Poskitt J (2009) Functional shifts of grassland soil communities in response to soil warming. Soil Biol Biochem **41**: 315–322

Brooks JR, Flanagan LB, Varney GT, Ehleringer JR (1997) Vertical gradients in photosynthetic gas exchange characteristics and refixation of respired CO2 within boreal forest canopies. Tree Physiol **17**: 1–12

Brown PD, Tokuhisa JG, Reichelt M, Gershenzon J (2003) Variation of glucosinolate accumulation among different organs and developmental stages of Arabidopsis thaliana. Phytochemistry **62**: 471–481

Buchan A, Crombie B, Alexandre GM (2010) Temporal dynamics and genetic diversity of chemotactic-competent microbial populations in the rhizosphere. Environ Microbiol **12**: 3171–3184

Calvo OC, Franzaring J, Schmid I, Müller M, Brohon N, Fangmeier A (2017) Atmospheric CO 2 enrichment and drought stress modify root exudation of barley. Glob Chang Biol **23**: 1292–1304

Cao H, Glazebrook J, Clarke JD, Volko S, Dong X (1997) The Arabidopsis NPR1 gene that controls systemic acquired resistance encodes a novel protein containing ankyrin repeats. Cell **88**: 57–63

Carvalhais LC, Dennis PG, Badri D V., Tyson GW, Vivanco JM, Schenk PM (2013) Activation of the Jasmonic Acid Plant Defence Pathway Alters the Composition of Rhizosphere Bacterial Communities. PLoS One **8**: 1–5

Castro HF, Classen AT, Austin EE, Norby RJ, Schadt CW (2010) Soil microbial community responses to multiple experimental climate change drivers. Appl Environ Microbiol **76**: 999–1007

Chakraborty S, Datta S (2003) How will plant pathogens adapt to host plant resistance at elevated CO2 under a changing climate? New Phytol **159**: 733–742

Chakraborty S, Newton AC (2011) Climate change, plant diseases and food security: An overview. Plant Pathol **60**: 2–14

Chakraborty S, Tiedemann a V, Teng PS (2000) Climate change: potential impact on plant diseases. Environ Pollut **108**: 317–26

Chaouch S, Queval G, Vanderauwera S, Mhamdi A, Vandorpe M, Langlois-Meurinne M, Van Breusegem F, Saindrenan P, Noctor G (2010) Peroxisomal hydrogen peroxide is coupled to biotic defense responses by ISOCHORISMATE SYNTHASE1 in a daylength-related manner. Plant Physiol **153**: 1692–1705

Chaparro JM, Badri D V, Vivanco JM (2013) Rhizosphere microbiome assemblage is affected by plant development. ISME J **8**: 790–803

Charron D, Pingret J, Chabaud M, Journet E, Barker DG (2004) Pharmacological Evidence

That Multiple Phospholipid Signaling Pathways Link Rhizobium Nodulation Factor Perception in Medicago truncatula Root Hairs to Intracellular Responses, Including Ca2+ Spiking and Specific ENOD Gene Expression. Geofocus **136**: 3582–3593

Chauvin A, Caldelari D, Wolfender JL, Farmer EE (2013) Four 13-lipoxygenases contribute to rapid jasmonate synthesis in wounded Arabidopsis thaliana leaves: A role for lipoxygenase 6 in responses to long-distance wound signals. New Phytol **197**: 566–575

Chelius MK, Triplett EW (2001) The Diversity of Archaea and Bacteria in Association with the Roots of Zea mays L. Microb Ecol **41**: 252–263

Chen M, Alexander M (1973) Survival of soil bacteria during prolonged desiccation. Soil Biol Biochem **5**: 213–221

Chen Z, Wang X, Yao F, Zheng F, Feng Z (2010) Elevated Ozone Changed Soil Microbial Community in a Rice Paddy. Soil Sci Soc Am J **74**: 829–387

Chinchilla D, Shan L, He P, de Vries S, Kemmerling B (2009) One for all: the receptor-associated kinase BAK1. Trends Plant Sci **14**: 535–541

Clarke KR (1993) Non-parametric multivariate analyses of changes in community structure. Aust J Ecol **18**: 117–143

Classen AT, Sundqvist MK, Henning JA, Newman GS, Moore JAM, Cregger MA, Moorhead LC, Patterson CM (2015) Direct and indirect effects of climate change on soil microbial and soil microbial-plant interactions: What lies ahead? Ecosphere **6**: art130

Compant S, Van Der Heijden MGA, Sessitsch A (2010) Climate change effects on beneficial plant-microorganism interactions. FEMS Microbiol Ecol **73**: 197–214

Conroy JP (1992) Influence of Elevated Atmospheric CO_2 Concentrations on Plant Nutrition. Aust J Bot **40**: 445–456

Cook J, Oreskes N, Doran PT, Anderegg WRL, Verheggen B, Maibach EW, Carlton JS, Lewandowsky S, Skuce AG, Green SA, et al (2016) Consensus on consensus: a synthesis of consensus estimates on human-caused global warming. Environ Res Lett **11**: art048002

Coûteaux M, Bolger T (2000) Interactions between atmospheric CO 2 enrichment and soil fauna. Plant Soil **224**: 123–134

Cui H, Xiang T, Zhou J-M (2009) Plant immunity: a lesson from pathogenic bacterial effector proteins. Cell Microbiol **11**: 1453–1461

Czechowski T, Stitt M, Altmann T, Udvardi MK, Scheible W-R (2005) Genome-wide identification and testing of superior reference genes for transcript normalization in Arabidopsis. Plant Physiol **139**: 5–17

Dam M, Bergmark L, Vestergård M (2017) Elevated CO2 increases fungal-based micro-foodwebs in soils of contrasting plant species. Plant Soil **415**: 549–561

van Dam NM, Bouwmeester HJ (2016) Metabolomics in the Rhizosphere: Tapping into Belowground Chemical Communication. Trends Plant Sci **21**: 256–265

Dangl JL, Jones JD (2001) Plant pathogens and integrated defence responses to infection. Nature **411**: 826–833

Daudi A, O'Brien JA (2012) Detection of Hydrogen Peroxide by DAB Staining in Arabidopsis Leaves. Bio-protocol **2**: 1–5

Dechesne A, Bertolla F (2005) Impact of the Microscale Distribution of a. Microbiology **71**: 8123–8131

DeLucia EH, Nabity PD, Zavala JA, Berenbaum MR (2012) Climate Change: Resetting Plant-Insect Interactions. Plant Physiol **160**: 1677–1685

Denef K, Bubenheim H, Lenhart K, Vermeulen J, Van Cleemput O, Boeckx P, Müller C (2007) Community shifts and carbon translocation within metabolically-active rhizosphere microorganisms in grasslands under elevated CO2. Biogeosciences **4**: 769–779

Department of Energy and Climate Change (2011) The Carbon Plan: Delivering our low carbon future. Energy 218

Desprez-Loustau M, Marcais B, Nageleisen L, Piou D, Vannini A (2006) Interactive effects of drought and pathogens in forest trees. Ann For Sci **63**: 597–612

Dey SK, Chakrabarti B, Prasanna R, Pratap D, Singh SD, Purakayastha TJ, Pathak H (2017) Elevated carbon dioxide level along with phosphorus application and cyanobacterial inoculation enhances nitrogen fixation and uptake in cowpea crop. Arch Agron Soil Sci **63**: 1927–1937

Dharmatilake A, Bauer W (1992) Chemotaxis of Rhizobium meliloti towards Alfalfa Roots Chemotaxis of Rhizobium meliloti towards Nodulation Gene- Inducing Compounds from Alfalfa Roots. Appl Environ Microbiol **58**: 1153–1158

Dickie IA, Fitzjohn RG (2007) Using terminal restriction fragment length polymorphism (T-RFLP) to identify mycorrhizal fungi: A methods review. Mycorrhiza **17**: 259–270

Van Dingenen R, Dentener FJ, Raes F, Krol MC, Emberson L, Cofala J (2009) The global impact of ozone on agricultural crop yields under current and future air quality legislation. Atmos Environ **43**: 604–618

Divon HH, Fluhr R (2007) Nutrition acquisition strategies during fungal infection of plants. FEMS Microbiol Lett **266**: 65–74

Dohrmann AB, Tebbe CC (2006) Genetic profiling of bacterial communities from the rhizospheres of ozone damaged Malva sylvestris (Malvaceae). Eur J Soil Biol **42**: 191–199

Dohrmann AB, Tebbe CC (2005) Effect of Elevated Tropospheric Ozone on the Structure of Bacterial Communities Inhabiting the Rhizosphere of Herbaceous Plants Native to Germany Effect of Elevated Tropospheric Ozone on the Structure of Bacterial Communities Inhabiting the Rhizosphere of. Appl Environ Microbiol **71**: 7750–7758

Donohoe A, Armour KC, Pendergrass AG, Battisti DS (2014) Shortwave and longwave radiative contributions to global warming under increasing CO_2. Proc Natl Acad Sci **111**: 16700–16705

Dordas C (2008) Role of Nutrients in Controlling Plant Diseases in Sustainable Agriculture : A Review Role of Nutrients in Controlling Plant Diseases in Sustainable Agriculture : A Review. Agron Sustain Dev **28**: 33–46

Drigo B, Kowalchuk GA, Van Veen JA (2008) Climate change goes underground: Effects of elevated atmospheric CO 2 on microbial community structure and activities in the rhizosphere. Biol Fertil Soils **44**: 667–679

Drigo B, van Veen JA, Kowalchuk GA (2009) Specific rhizosphere bacterial and fungal groups respond differently to elevated atmospheric CO2. ISME J **3**: 1204–1217

Drissner D, Kunze G, Callewaert N, Gehrig P, Tamasloukht MB, Boller T, Felix G, Amrhein N, Bucher M (2007) Lyso-Phosphatidylcholine Is a Signal in the Arbuscular Mycorrhizal Symbiosis. **318**: 265–268

Dunbar J, Gallegos-Graves LV, Steven B, Mueller R, Hesse C, Zak DR, Kuske CR (2014) Surface soil fungal and bacterial communities in aspen stands are resilient to eleven years of elevated CO2 and O3. Soil Biol Biochem **76**: 227–234

Eastburn DM, Degennaro MM, Delucia EH, Dermody O, Mcelrone AJ (2010) Elevated atmospheric carbon dioxide and ozone alter soybean diseases at SoyFACE. Glob Chang Biol **16**: 320–330

Eastburn DM, McElrone a. J, Bilgin DD (2011) Influence of atmospheric and climatic change on plant-pathogen interactions. Plant Pathol **60**: 54–69

Edwards EJ, Ogburn RM (2012) Angiosperm Responses to a Low-CO_2 World: CAM and C_4 Photosynthesis as Parallel Evolutionary Trajectories. Int J Plant Sci **173**: 724–733

Egamberdiyeva D (2007) The effect of plant growth promoting bacteria on growth and nutrient uptake of maize in two different soils. Appl Soil Ecol **36**: 184–189

Eisenhauer N, Cesarz S, Koller R, Worm K, Reich PB (2012) Global change belowground: Impacts of elevated CO 2, nitrogen, and summer drought on soil food webs and biodiversity. Glob Chang Biol **18**: 435–447

Van der Ent S, Van Wees SCM, Pieterse CMJ (2009) Jasmonate signaling in plant interactions with resistance-inducing beneficial microbes. Phytochemistry **70**: 1581–8

Estiarte M, Penuelas J, Kimball B, Idso S, LaMorte R, Pinter P, Wall G, Garcia R (1994) Elevated CO2 effects on stomatal density of wheat and sour orange trees. J Exp Bot **45**: 1665–1668

EU (2005) Climate Change: - Medium and longer term emission reduction strategies, including targets. 1–5

Evans N, Baierl A, Semenov MA, Gladders P, Fitt BD. (2008) Range and severity of a plant disease increased by global warming. J R Soc Interface **5**: 525–531

Evans SE, Wallenstein MD (2014) Climate change alters ecological strategies of soil bacteria. Ecol Lett **17**: 155–164

Farooq M, Wahid A, Kobayashi N, Fujita D, Basra SMA (2009) Plant drought stress : effects , mechanisms and management. Agron Sustain Dev **29**: 185–212

Felix G, Duran JD, Volko S, Boller T (1999) Plants have a sensitive perception system for the most conserved domain of bacterial flagellin. Plant J **18**: 265–76

Ferrocino I, Chitarra W, Pugliese M, Gilardi G, Gullino ML, Garibaldi A (2013) Effect of elevated atmospheric CO2 and temperature on disease severity of Fusarium oxysporum f.sp. lactucae on lettuce plants. Appl Soil Ecol **72**: 1–6

Field KJ, Cameron DD, Leake JR, Tille S, Bidartondo MI, Beerling DJ (2012) Contrasting arbuscular mycorrhizal responses of vascular and non-vascular plants to a simulated Palaeozoic CO_2 decline. Nat Commun **3**: art835

Fischer G, Shah M, Tubiello FN, van Velhuizen H (2005) Socio-economic and climate change impacts on agriculture: an integrated assessment, 1990-2080. Philos Trans R Soc Lond B Biol Sci **360**: 2067–83

Fleischmann F, Raidl S, Oßwald WF (2010) Changes in susceptibility of beech (Fagus sylvatica) seedlings towards Phytophthora citricola under the influence of elevated atmospheric CO2 and nitrogen fertilization. Environ Pollut **158**: 1051–1060

Forkelova L, Unsicker S, Forkel M, Huang J, Trumbore S (2016) Carbon limitation reveals allocation priority to defense compounds in peppermint. Geophys. Res. Abstr. 18:

Franssen HJ, Vijn I, Yang WC, Bisseling T (1992) Developmental aspects of the Rhizobium-legume symbiosis. Plant Mol Biol **19**: 89–107

Fransson PMA, Johansson EM (2010) Elevated CO2 and nitrogen influence exudation of soluble organic compounds by ectomycorrhizal root systems. FEMS Microbiol Ecol **71**: 186–196

Freeman C, Kim SY, Lee SH, Kang H (2004) Effects of elevated atmospheric CO2 concentrations on soil microorganisms. J Microbiol **42**: 267–277

Frerigmann H, Piślewska-Bednarek M, Sánchez-Vallet A, Molina A, Glawischnig E, Gigolashvili T, Bednarek P (2016) Regulation of Pathogen-Triggered Tryptophan Metabolism in Arabidopsis thaliana by MYB Transcription Factors and Indole Glucosinolate Conversion Products. Mol Plant **9**: 682–695

Frew A, Allsopp PG, Gherlenda AN, Johnson SN (2017) Increased root herbivory under elevated atmospheric carbon dioxide concentrations is reversed by silicon-based plant defences. J Appl Ecol **54**: 1310–1319

Fu ZQ, Guo M, Jeong B, Tian F, Elthon TE, Cerny RL, Staiger D, Alfano JR (2007) A type III effector ADP-ribosylates RNA-binding proteins and quells plant immunity. Nature **447**: 284–288

Galbraith ED, Eggleston S (2017) A lower limit to atmospheric CO2 concentrations over the

past 800,000 years. Nat Geosci **10**: 295–299

Ganopolski A, Calov R (2011) The role of orbital forcing, carbon dioxide and regolith in 100 kyr glacial cycles. Clim Past **7**: 1415–1425

Garcia-Ruiz H, Murphy JF (2001) Age-related Resistance in Bell Pepper to Cucumber mosaic virus. Ann Appl Biol **139**: 307–317

Garcia de Salamone I, Hynes K, Nelson L (2001) Cytokinin production by plant growth promoting rhizobacteria and selected mutants. Can J Microbiol **47**: 404–411

Garrett K a, Dendy SP, Frank EE, Rouse MN, Travers SE (2006) Climate change effects on plant disease: genomes to ecosystems. Annu Rev Phytopathol **44**: 489–509

Garrett KA, Forbes GA, Savary S, Skelsey P, Sparks AH, Valdivia C, Van Bruggen AHC, Willocquet L, Djurle A, Duveiller E, et al (2011) Complexity in climate-change impacts: An analytical framework for effects mediated by plant disease. Plant Pathol **60**: 15–30

Ghini R, Leod RE de O Mac, Torre Neto A, Cardoso DC, Bettiol W, de Morais LAS, Vique B (2014) Increased atmospheric carbon dioxide concentration: Effects on eucalypt rust (Puccinia psidii), C: N ratio and essential oils in eucalypt clonal plantlets. For Pathol **44**: 409–416

Ghini R, Torre-Neto A, Dentzien AFM, Guerreiro-Filho O, Iost R, Patrício FR a., Prado JSM, Thomaziello R a., Bettiol W, DaMatta FM (2015) Coffee growth, pest and yield responses to free-air CO2 enrichment. Clim Change **132**: 307–320

Gil-Sotres F, Trasar-Cepeda C, Leirós MC, Seoane S (2005) Different approaches to evaluating soil quality using biochemical properties. Soil Biol Biochem **37**: 877–887

Gilardi G, Gisi U, Garibaldi A, Gullino ML (2017) Effect of elevated atmospheric CO2 and temperature on the chemical and biological control of powdery mildew of zucchini and the Phoma leaf spot of leaf beet. Eur J Plant Pathol **148**: 229–236

Gill RA, Anderson LJ, Polley HW, Johnson HB, Jackson RB (2006) Potential nitrogen contraints on soil carbon sequestration under low and elevated atmospheric CO2. Ecology **87**: 41–52

Glazebrook J (2005) Contrasting mechanisms of defense against biotrophic and necrotrophic pathogens. Annu Rev Phytopathol **43**: 205–227

Glazebrook J, Chen W, Estes B, Chang H-S, Nawrath C, Métraux J-P, Zhu T, Katagiri F (2003) Topology of the network integrating salicylate and jasmonate signal transduction derived from global expression phenotyping. Plant J **34**: 217–28

Glick BR, Cheng Z, Czarny J, Duan J (2007) Promotion of plant growth by ACC deaminase-producing soil bacteria. Eur J Plant Pathol **119**: 329–339

Goldemberg J (2006) The promise of clean energy. Energy Policy **34**: 2185–2190

Gray J (1993) Major Paleozoic land plant evolutionary bio-events. Palaeogeogr Palaeoclimatol Palaeoecol **104**: 153–169

Gray JE, Holroyd GH, van der Lee FM, Bahrami a R, Sijmons PC, Woodward FI, Schuch W, Hetherington a M (2000) The HIC signalling pathway links CO2 perception to stomatal development. Nature **408**: 713–716

Gray SB, Brady SM (2016) Plant developmental responses to climate change. Dev Biol **419**: 64–77

Greenberg JT (1997) Programmed Cell Death in Plant-Pathogen Interactions. Annu Rev Plant Physiol Plant Mol Biol **48**: 525–545

Gregory PJ (2007) The Rhizosphere. Plant Roots. Springer-Verlag, Berlin, pp 216–252

Gschwendtner S, Leberecht M, Engel M, Kublik S, Dannenmann M, Polle A, Schloter M (2015) Effects of Elevated Atmospheric CO2 on Microbial Community Structure at the Plant-Soil Interface of Young Beech Trees (Fagus sylvatica L.) Grown at Two Sites with Contrasting Climatic Conditions. Microb Ecol **69**: 867–878

Guo B, Zhang Y, Li S, Lai T, Yang L, Chen J, Ding W (2016) Extract from Maize (Zea mays L.): Antibacterial Activity of DIMBOA and Its Derivatives against Ralstonia solanacearum. Molecules **21**: art1397

Guo J, Feng R, Ding Y, Wang R (2014) Applying carbon dioxide, plant growth-promoting rhizobacterium and EDTA can enhance the phytoremediation efficiency of ryegrass in a soil polluted with zinc, arsenic, cadmium and lead. J Environ Manage **141**: 1–8

Haase S, Neumann G, Kania A, Kuzyakov Y, Romheld V, Kandeler E (2007) Elevation of atmospheric CO2 and N-nutritional status modify nodulation, nodule-carbon supply, and root exudation of Phaseolus vulgaris L. Soil Biol Biochem **39**: 2208–2221

Haldar S, Sengupta S (2015) Plant-microbe Cross-talk in the Rhizosphere: Insight and Biotechnological Potential. Open Microbiol J **9**: 1–7

Hanjra MA, Qureshi ME (2010) Global water crisis and future food security in an era of climate change. Food Policy **35**: 365–377

Hansen J, Sato M, Kharecha P, Beerling D, Berner R, Masson-Delmotte V, Pagani M, Raymo M, Royer D, Zachos J (2008) Target atmospheric CO2: Where should humanity aim? Open Atmos Sci J **2**: 217–231

Hansen J, Sato M, Kharecha P, Russell G, Lea DW, Siddall M (2007a) Climate change and trace gases. Philos Trans A Math Phys Eng Sci **365**: 1925–54

Hansen J, Sato M, Ruedy R (2012) Perception of climate change. Proc Natl Acad Sci **109**: 2415–2423

Hansen J, Sato M, Ruedy R, Kharecha P, Lacis a., Miller R, Nazarenko L, Lo K, Schmidt G a., Russell G, et al (2007b) Dangerous human-made interference with climate: a GISS modelE study. Atmos Chem Phys **7**: 2287–2312

Hartley IP, Heinemeyer A, Evans SP, Ineson P (2007) The effect of soil warming on bulk soil vs. rhizosphere respiration. Glob Chang Biol **13**: 2654–2667

Hartman WH, Richardson CJ (2013) Differential Nutrient Limitation of Soil Microbial Biomass and Metabolic Quotients (qCO2): Is There a Biological Stoichiometry of Soil Microbes? PLoS One. doi: 10.1371/journal.pone.0057127

Hatfield JL, Prueger JH (2015) Temperature extremes: Effect on plant growth and development. Weather Clim Extrem **10**: 4–10

Hayden HL, Mele PM, Bougoure DS, Allan CY, Norng S, Piceno YM, Brodie EL, Desantis TZ, Andersen GL, Williams AL, et al (2012) Changes in the microbial community structure of bacteria, archaea and fungi in response to elevated CO2 and warming in an Australian native grassland soil. Environ Microbiol **14**: 3081–3096

Van Der Heijden MGA, Bardgett RD, Van Straalen NM (2008) The unseen majority: Soil microbes as drivers of plant diversity and productivity in terrestrial ecosystems. Ecol Lett **11**: 296–310

Heil M (2002) Induced Systemic Resistance (ISR) Against Pathogens in the Context of Induced Plant Defences. Ann Bot **89**: 503–512

Herms DA, Mattson WJ (1992) The Dilemma of Plants: To Grow or Defend. Q Rev Biol **67**: 283–335

Hibben CR, Stotzky G (1969) Effects of ozone on the germination of fungus spores. Can J Microbiol **15**: 1187–1196

Hibberd JM, Whitbread R, Farrar JF (1996a) Effect of elevated concentrations of CO 2 on infection of barley by Erysiphe graminis. Physiol Mol Plant Pathol **48**: 37–53

Hibberd JM, Whitbread R, Farrar JF (1996b) Effect of 700 µmol mol− 1CO2 and infection with powdery mildew on the growth and carbon partitioning of barley. New Phytol **134**: 309–315

Hinsinger P, Plassard C, Jaillard B (2006) Rhizosphere: A new frontier for soil biogeochemistry. J Geochemical Explor **88**: 210–213

Hochberg Y, Benjamini Y (1990) More powerful procedures for multiple significance testing.

Stat Med **9**: 811–818

Houterman PM, Ma L, van Ooijen G, de Vroomen MJ, Cornelissen BJC, Takken FLW, Rep M (2009) The effector protein Avr2 of the xylem-colonizing fungus Fusarium oxysporum activates the tomato resistance protein I-2 intracellularly. Plant J **58**: 970–8

Hovenden MJ, Williams AL (2010) The impacts of rising CO2 concentrations on Australian terrestrial species and ecosystems. Austral Ecol **35**: 665–684

Huang J, Hammerbacher A, Forkelová L, Hartmann H (2017) Release of resource constraints allows greater carbon allocation to secondary metabolites and storage in winter wheat. Plant Cell Environ **40**: 672–685

Huang L, Ren Q, Sun Y, Ye L, Cao H, Ge F (2012) Lower incidence and severity of tomato virus in elevated CO2 is accompanied by modulated plant induced defence in tomato. Plant Biol **14**: 905–913

van Hulten M, Pelser M, van Loon LC, Pieterse CMJ, Ton J (2006) Costs and benefits of priming for defense in Arabidopsis. Proc Natl Acad Sci U S A **103**: 5602–5607

IPCC (2013) Working Group I Contribution to the IPCC Fifth Assessment Report - Summary for Policymakers. Clim. Chang. 2013 Phys. Sci. Basis. pp 1–36

Iriti M, Faoro F (2008) Oxidative stress, the paradigm of ozone toxicity in plants and animals. Water Air Soil Pollut **187**: 285–301

Jablonski LM, Wang X, Curtis PS (2002) Plant reproduction under elevated CO2 conditions: A meta-analysis of reports on 79 crop and wild species. New Phytol **156**: 9–26

Janus LR, Angeloni NL, McCormack J, Rier ST, Tuchman NC, Kelly JJ (2005) Elevated atmospheric CO2 alters soil microbial communities associated with trembling aspen (Populus tremuloides) roots. Microb Ecol **50**: 102–109

Jin J, Tang C, Sale P (2015) The impact of elevated carbon dioxide on the phosphorus nutrition of plants: A review. Ann Bot **116**: 987–999

Johnson NC, Gehring CA (2007) Mycorrhizas: Symbiotic Mediators of Rhizosphere and Ecosystem Processes. *In* JLBT-TR Whitbeck, ed,Academic Press, Burlington, pp 73–100

Jones CD, Cox P, Huntingford C, Centre H, Office M (2003) Uncertainty in climate – carbon-cycle projections associated with the sensitivity of soil respiration to temperature. Tellus **55B**: 642–648

Jones JDG, Dangl JL (2006) The plant immune system. Nature **444**: 323–9

Jordá L, Sopeña-Torres S, Escudero V, Nuñez-Corcuera B, Delgado-Cerezo M, Torii KU, Molina A (2016) ERECTA and BAK1 Receptor Like Kinases Interact to Regulate Immune Responses in Arabidopsis. Front Plant Sci **7**: 1–15

Jung SC, Martinez-Medina A, Lopez-Raez J a, Pozo MJ (2012) Mycorrhiza-induced resistance and priming of plant defenses. J Chem Ecol **38**: 651–64

Jwa N-S, Walling LL (2001) Influence of elevated CO2 concentration on disease development in tomato. New Phytol **149**: 509–518

Kaever A, Landesfeind M, Possienke M, Feussner K, Feussner I, Meinicke P (2012) MarVis-Filter: ranking, filtering, adduct and isotope correction of mass spectrometry data. J Biomed Biotechnol **2012**: 263910

Kamilova F, Kravchenko L V, Shaposhnikov AI, Makarova N, Lugtenberg B (2006) Effects of the tomato pathogen Fusarium oxysporum f. sp. radicis-lycopersici and of the biocontrol bacterium Pseudomonas fluorescens WCS365 on the composition of organic acids and sugars in tomato root exudate. Mol Plant Microbe Interact **19**: 1121–1126

Kamilova F, Leveau JHJ, Lugtenberg B (2007) Collimonas fungivorans, an unpredicted in vitro but efficient in vivo biocontrol agent for the suppression of tomato foot and root rot. Environ Microbiol **9**: 1597–603

Kape R, Parniske M, Brandt S, Werner D (1992) Isoliquiritigenin, a strong nod gene- and glyceollin resistance-inducing flavonoid from soybean root exudate. Appl Environ Microbiol

58: 1705–1710

Karnosky D, Percy K, Xiang B, Callan B, Noormets A, Mankovska B, Hopkin A, Sober J, Jones W, Dickson R, et al (2002) Interacting elevated CO2 and tropospheric O3 predisposes aspen (Populus tremuloides Michx.) to infection by rust (Melampsora medusae f. sp. tremuloidae). Glob Chang Biol **8**: 329–338

Kassem II, Joshi P, Sigler V, Heckathorn S, Wang Q (2008) Effect of elevated CO2 and drought on soil microbial communities associated with Andropogon gerardii. J Integr Plant Biol **50**: 1406–1415

Kenrick P, Crane PR (1997) The origin and early evolution of plants on land. Nature **389**: 33–39

Keunen E, Peshev D, Vangronsveld J, Van Den Ende W, Cuypers A (2013) Plant sugars are crucial players in the oxidative challenge during abiotic stress: Extending the traditional concept. Plant, Cell Environ **36**: 1242–1255

Khalid A, Tahir S, Arshad M, Zahir ZA (2004) Relative efficiency of rhizobacteria for auxin biosynthesis in rhizosphere and non-rhizosphere soils. Soil Res **42**: 921–926

Khudhair M, Melloy P, Lorenz DJ, Obanor F, Aitken E, Datta S, Luck J, Fitzgerald G, Chakraborty S (2014) Fusarium crown rot under continuous cropping of susceptible and partially resistant wheat in microcosms at elevated CO2. Plant Pathol **63**: 1033–1043

King GM (2011) Enhancing soil carbon storage for carbon remediation: Potential contributions and constraints by microbes. Trends Microbiol **19**: 75–84

Kobayashi T, Ishiguro K, Nakajima T, Kim HY, Okada M, Kobayashi K (2006) Effects of Elevated Atmospheric CO(2) Concentration on the Infection of Rice Blast and Sheath Blight. Phytopathology **96**: 425–431

Kohler J, Caravaca F, Roldán A (2009) Effect of drought on the stability of rhizosphere soil aggregates of Lactuca sativa grown in a degraded soil inoculated with PGPR and AM fungi. Appl Soil Ecol **42**: 160–165

Koornneef A, Leon-Reyes A, Ritsema T, Verhage A, Den Otter FC, Van Loon LC, Pieterse CMJ (2008) Kinetics of salicylate-mediated suppression of jasmonate signaling reveal a role for redox modulation. Plant Physiol **147**: 1358–1368

Korner C, Basler D (2010) Phenology Under Global Warming. Science (80-) **327**: 1461–1462

Kretzschmar F dos S, Aidar MPM, Salgado I, Braga MR (2009) Elevated CO2 atmosphere enhances production of defense-related flavonoids in soybean elicited by NO and a fungal elicitor. Environ Exp Bot **65**: 319–329

Krupa S, Mcgrath MT, Andersen CP, Booker FL, Burkey KO, Chappelka AH, Chevone BI, Pell EJ, Zilinskas B a (2000) Ambient ozone and plant health. Plant Dis **85**: 4–12

Kuijken RCP, Snel JFH, Heddes MM, Bouwmeester HJ, Marcelis LFM (2014) The importance of a sterile rhizosphere when phenotyping for root exudation. Plant Soil **387**: 131–142

Kuokkanen K, Julkunen-Tiitto R, Keinänen M, Niemelä P, Tahvanainen J (2001) The effect of elevated CO2 and temperature on the secondary chemistry of Betula pendula seedlings. Trees **15**: 378–384

Kus J V, Zaton K, Sarkar R, Cameron RK (2002) Age-related resistance in Arabidopsis is a developmentally regulated defense response to Pseudomonas syringae. Plant Cell **14**: 479–90

Lacis A a, Schmidt G a, Rind D, Ruedy R a (2010) Atmospheric CO2: principal control knob governing Earth's temperature. Science (80-) **330**: 356–359

Laine AL (2008) Temperature-mediated patterns of local adaptation in a natural plant-pathogen metapopulation. Ecol Lett **11**: 327–337

Lake JA, Wade RN (2009) Plant-pathogen interactions and elevated CO2: morphological changes in favour of pathogens. J Exp Bot **60**: 3123–31

Lakshmanan V, Castaneda R, Rudrappa T, Bais HP (2013) Root transcriptome analysis of Arabidopsis thaliana exposed to beneficial Bacillus subtilis FB17 rhizobacteria revealed genes for bacterial recruitment and plant defense independent of malate efflux. Planta **238**: 657–668

Lamers JG, Schippers B, Geels FP (1988) Soil-borne diseases of wheat in the Netherlands and results of seed bacterization with pseudomonads against Gaeumannomyces graminis var. tritici, associated with disease resistance. Cereal Breed Relat to Integr Cereal Prod 134–139

Larson JL, Zak DR, Sinsabaugh RL (2002) Extracellular Enzyme Activity Beneath Temperate Trees Growing Under Elevated Carbon Dioxide and Ozone. Soil Sci Soc Am J **66**: 1848–56

Lau JA, Strengbom J, Stone LR, Reich PB, Tiffin P (2008) Direct and indirect effects of CO2, nitrogen, and community diversity on plant-enemy interactions. Ecology **89**: 226–236

Lavola A, Julkunen-Tiitto R, de la Rosa TM, Lehto T, Aphalo PJ (2000) Allocation of carbon to growth and secondary metabolites in birch seedlings under UV-B radiation and CO2 exposure. Physiol Plant **109**: 260–267

Lawlor DW, Lemaire G, Gastal F (2001) Nitrogen, Plant Growth and Crop Yield. *In* PJ Lea, J-F Morot-Gaudry, eds, Plant Nitrogen. Springer Berlin Heidelberg, Berlin, Heidelberg, pp 343–367

Leakey ADB, Ainsworth E a, Bernacchi CJ, Rogers A, Long SP, Ort DR (2009) Elevated CO2 effects on plant carbon, nitrogen, and water relations: six important lessons from FACE. J Exp Bot **60**: 2859–2876

Leiss KA, Choi YH, Verpoorte R, Klinkhamer PGL (2011) An overview of NMR-based metabolomics to identify secondary plant compounds involved in host plant resistance. Phytochem Rev **10**: 205–216

Lepinay C, Rigaud T, Salon C, Lemanceau P, Mougel C (2012) Interaction between Medicago truncatula and Pseudomonas fluorescens: Evaluation of Costs and Benefits across an Elevated Atmospheric CO2. PLoS One **7**: e45740

Li X, Ahammed GJ, Li Z, Tang M, Yan P, Han W (2016) Decreased Biosynthesis of Jasmonic Acid via Lipoxygenase Pathway Compromised Caffeine-Induced Resistance to Colletotrichum gloeosporioides Under Elevated CO2 in Tea Seedlings. Phytopathology **106**: 1270–1277

Li X, Chu W, Dong J, Duan Z (2014a) An Improved High-performance Liquid Chromatographic Method for the Determination of Soluble Sugars in Root Exudates of Greenhouse Cucumber Grown under CO2 Enrichment. J Am Soc Hortic Sci **139**: 356–363

Li X, Deng Y, Li Q, Lu C, Wang J, Zhang H, Zhu J, Zhou J, He Z (2013) Shifts of functional gene representation in wheat rhizosphere microbial communities under elevated ozone. ISME J **7**: 660–671

Li X, Sun Z, Shao S, Zhang S, Ahammed GJ, Zhang G, Jiang Y, Zhou J, Xia X, Zhou Y, et al (2014b) Tomato-Pseudomonas syringae interactions under elevated CO2 concentration: the role of stomata. J Exp Bot **66**: 307–316

Li Y, Xu J, Haq NU, Zhang H, Zhu X-G (2014c) Was low CO2 a driving force of C4 evolution: Arabidopsis responses to long-term low CO2 stress. J Exp Bot **65**: 3657–3667

Lin Y-H, Xu J-L, Hu J, Wang L-H, Ong SL, Leadbetter JR, Zhang L-H (2003) Acyl-homoserine lactone acylase from Ralstonia strain XJ12B represents a novel and potent class of quorum-quenching enzymes. Mol Microbiol **47**: 849–860

Lindahl BD, de Boer W, Finlay RD (2010) Disruption of root carbon transport into forest humus stimulates fungal opportunists at the expense of mycorrhizal fungi. ISME J **4**: 872–881

Lipson D, Wilson R (2005) Effects of elevated atmospheric CO2 on soil microbial biomass, activity, and diversity in a chaparral ecosystem. Appl Environ **71**: 8573–8580

Liu J, Elmore JM, Fuglsang AT, Palmgren MG, Staskawicz BJ, Coaker G (2009) RIN4

functions with plasma membrane H+-ATPases to regulate stomatal apertures during pathogen attack. PLoS Biol **7**: e1000139

Liu W-X, Zhang F-C, Zhang W-Z, Song L-F, Wu W-H, Chen Y-F (2013) Arabidopsis Di19 Functions as a Transcription Factor and Modulates PR1, PR2, and PR5 Expression in Response to Drought Stress. Mol Plant **6**: 1487–1502

Lobell DB, Field CB (2007) Global scale climate–crop yield relationships and the impacts of recent warming. Environ Res Lett **2**: art14002

Long SP, Ainsworth EA, Leakey ADB, Ort DR, No J (2006) Food for Thought : Lower-Than-. **312**: 1918–1922

van Loon L, Bakker P, Pieterse C (1998) Systemic resistance induced by rhizosphere bacteria. Annu Rev Phytopathol **36**: 453–483

López Sánchez A, Stassen JHM, Furci L, Smith LM, Ton J (2016) The role of DNA (de)methylation in immune responsiveness of Arabidopsis. Plant J **88**: 361–374

Luber G, McGeehin M (2008) Climate Change and Extreme Heat Events. Am J Prev Med **35**: 429–435

Luck J, Spackman M, Freeman A, TreBicki P, Griffiths W, Finlay K, Chakraborty S (2011) Climate change and diseases of food crops. Plant Pathol **60**: 113–121

Lugtenberg B, Kamilova F (2009) Plant-growth-promoting rhizobacteria. Annu Rev Microbiol **63**: 541–56

Luna E, Bruce TJ a, Roberts MR, Flors V, Ton J (2012) Next-generation systemic acquired resistance. Plant Physiol **158**: 844–853

Luna E, Pastor V, Robert J, Flors V, Mauch-Mani B, Ton J (2011) Callose deposition: a multifaceted plant defense response. Mol Plant Microbe Interact **24**: 183–93

Luo Q (2011) Temperature thresholds and crop production: A review. Clim Change **109**: 583–598

Luo Y, Wan S, Hui D, Wallace LL (2001) Acclimatization of soil respiration to warming in a tall grass prairie. Nature **413**: 622–625

Lynch JM, Whipps JM (1990) Substrate flow in the rhizosphere. Plant Soil **129**: 1–10

Macías FA, Marín D, Oliveros-Bastidas A, Castellano D, Simonet AM, Molinillo JMG (2005) Structure-activity relationships (SAR) studies of benzoxazinones, their degradation products and analogues. Phytotoxicity on standard target species (STS). J Agric Food Chem **53**: 538–548

Manning WJ, v. Tiedemann A (1995) Climate change: Potential effects of increased atmospheric Carbon dioxide (CO2), ozone (O3), and ultraviolet-B (UV-B) radiation on plant diseases. Environ Pollut **88**: 219–245

Mao Y-B, Liu Y-Q, Chen D-Y, Chen F-Y, Fang X, Hong G-J, Wang L-J, Wang J-W, Chen X-Y (2017) Jasmonate response decay and defense metabolite accumulation contributes to age-regulated dynamics of plant insect resistance. Nat Commun **8**: 13925

Marschner H (2012) Mineral Nutrition of Higher Plants, 3rd ed. Academic Press, London

Masui T, Matsumoto K, Hijioka Y, Kinoshita T, Nozawa T, Ishiwatari S, Kato E, Shukla PR, Yamagata Y, Kainuma M (2011) An emission pathway for stabilization at 6 Wm-2 radiative forcing. Clim Change **109**: 59–76

Mathur P, Sharma E, Singh SD, Bhatnagar AK, Singh VP, Kapoor R (2013) Effect of elevated CO2 on infection of three foliar diseases in oilseed Brassica juncea. J Plant Pathol **95**: 135–144

Matilla M a, Ramos JL, Bakker P a HM, Doornbos R, Badri D V, Vivanco JM, Ramos-González MI (2010) Pseudomonas putida KT2440 causes induced systemic resistance and changes in Arabidopsis root exudation. Environ Microbiol Rep **2**: 381–388

Matros A, Amme S, Kettig B, Buck-Sorlin GH, Sonnewald U, Mock H-P (2006) Growth at

elevated CO2 concentrations leads to modified profiles of secondary metabolites in tobacco cv. SamsunNN and to increased resistance against infection with potato virus Y. Plant Cell Environ **29**: 126–37

Mattiello L, Kirst M, da Silva FR, Jorge RA, Menossi M (2010) Transcriptional profile of maize roots under acid soil growth. BMC Plant Biol **10**: 196

Maunoury N, Redondo-Nieto M, Bourcy M, Van de Velde W, Alunni B, Laporte P, Durand P, Agier N, Marisa L, Vaubert D, et al (2010) Differentiation of symbiotic cells and endosymbionts in Medicago truncatula nodulation are coupled to two transcriptome-switches. PLoS One **5**: e9519

McCrady JK, Andersen CP (2000) The effect of ozone on below-ground carbon allocation in wheat. Environ Pollut **107**: 465–472

McDowell JM, Williams SG, Funderburg NT, Eulgem T, Dangl JL (2005) Genetic analysis of developmentally regulated resistance to downy mildew (Hyaloperonospora parasitica) in Arabidopsis thaliana. Mol Plant Microbe Interact **18**: 1226–1234

McDowell JM, Woffenden BJ (2003) Plant disease resistance genes: recent insights and potential applications. Trends Biotechnol **21**: 178–183

Mcelrone A, Reid C, Hoye K, Hart E, Jackson RB (2005) Elevated CO2 reduces disease incidence and severity of a red maple fungal pathogen via changes in host physiology and leaf chemistry. Glob Chang Biol **11**: 1828–1836

McElrone AJ, Hamilton JG, Krafnick AJ, Aldea M, Knepp RG, DeLucia EH (2010) Combined effects of elevated CO2 and natural climatic variation on leaf spot diseases of redbud and sweetgum trees. Environ Pollut **158**: 108–114

Melloy P, Aitken E, Luck J, Chakraborty S, Obanor F (2014) The influence of increasing temperature and CO2 on Fusarium crown rot susceptibility of wheat genotypes at key growth stages. Eur J Plant Pathol **140**: 19–37

Melloy P, Hollaway G, Luck J, Norton R, Aitken E, Chakraborty S (2010) Production and fitness of Fusarium pseudograminearum inoculum at elevated carbon dioxide in FACE. Glob Chang Biol **16**: 3363–3373

Melotto M, Underwood W, He SY (2008) Role of stomata in plant innate immunity and foliar bacterial diseases. Annu Rev Phytopathol **46**: 101–22

Melotto M, Underwood W, Koczan J, Nomura K, He SY (2006) Plant stomata function in innate immunity against bacterial invasion. Cell **126**: 969–980

Mhamdi A, Noctor G (2016) High CO2 primes plant biotic stress defences through redox-linked pathways. Plant Physiol **172**: 929–942

Micallef SA, Channer S, Shiaris MP, Colón-Carmona A (2009a) Plant age and genotype impact the progression of bacterial community succession in the Arabidopsis rhizosphere. Plant Signal Behav **4**: 777–780

Micallef SA, Shiaris MP, Colón-Carmona A (2009b) Influence of Arabidopsis thaliana accessions on rhizobacterial communities and natural variation in root exudates. J Exp Bot **60**: 1729–1742

Mikkelsen BL, Jørgensen RB, Lyngkjær MF (2014) Complex interplay of future climate levels of CO2, ozone and temperature on susceptibility to fungal diseases in barley. Plant Pathol **64**: 319–327

Millet Y a, Danna CH, Clay NK, Songnuan W, Simon MD, Werck-Reichhart D, Ausubel FM (2010) Innate immune responses activated in Arabidopsis roots by microbe-associated molecular patterns. Plant Cell **22**: 973–990

Miri HR, Rastegar A, Bagheri AR (2012) The impact of elevated CO 2 on growth and competitiveness of C 3 and C 4 crops and weeds. Eur J Exp Biol **2**: 1144–1150

Mitchell C, Reich P, Tilman D, Groth J (2003) Effects of elevated CO2, nitrogen deposition, and decreased species diversity on foliar fungal plant disease. Glob Chang Biol **9**: 438–451

Moeder W, Ung H, Mosher S, Yoshioka K (2010) SA-ABA antagonism in defense responses. Plant Signal Behav **5**: 1231–1233

Mohan JE, Cowden CC, Baas P, Dawadi A, Frankson PT, Helmick K, Hughes E, Khan S, Lang A, Machmuller M, et al (2014) Mycorrhizal fungi mediation of terrestrial ecosystem responses to global change: Mini-review. Fungal Ecol **10**: 3–19

Molina LÁ, Ramos C, Duque E, Ronchel MC, García JM, Wyke L, Ramos JL (2000) Survival of Pseudomonas putida KT2440 in soil and in the rhizosphere of plants under greenhouse and environmental conditions. Soil Biol Biochem **32**: 315–321

Montealegre CM, Kessel C Van, Russelle MP, Sadowsky MJ (2002) Changes in microbial activity and composition in a pasture ecosystem exposed to elevated atmospheric carbon dioxide. Plant Soil **243**: 197–207

Morkunas I, Ratajczak L (2014) The role of sugar signaling in plant defense responses against fungal pathogens. Acta Physiol Plant **36**: 1607–1619

Morris PF, Bone E, Tyler BM (1998) Chemotropic and Contact Responses of Phytophthora sojae Hyphae to Soybean Isoflavonoids and Artificial Substrates1. Plant Physiol **117**: 1171–1178

Moshe A, Pfannstiel J, Yariv B, Kolot M, Sobol I, Czosnek H, Gorovits R (2012) Stress Responses to Tomato Yellow Leaf Curl Virus (TYLCV) Infection of Resistant and Susceptible Tomato Plants are Different. Metabolomics **1**: 1–13

Murillo-Williams a., Munkvold GP (2008) Systemic Infection by Fusarium verticillioides in Maize Plants Grown Under Three Temperature Regimes. Plant Dis **92**: 1695–1700

Nakagawa T, Kawaguchi M (2006) Shoot-applied MeJA suppresses root nodulation in Lotus japonicus. Plant Cell Physiol **47**: 176–180

Nakazawa T, Yokota T (1973) Benzoate metabolism in Pseudomonas putida(arvilla) mt 2: Demonstration of two benzoate pathways. J Bacteriol **115**: 262–267

Neal AL, Ahmad S, Gordon-Weeks R, Ton J (2012) Benzoxazinoids in root exudates of maize attract Pseudomonas putida to the rhizosphere. PLoS One **7**: e35498

Neal AL, Ton J (2013) Systemic defense priming by Pseudomonas putida KT2440 in maize depends on benzoxazinoid exudation from the roots. Plant Signal Behav **8**: e22655

Nelson EB (2004) Microbial Dynamics and Interactions in the Spermosphere. Annu Rev Phytopathol **42**: 271–309

Nesme J, Achouak W, Agathos SN, Bailey M, Baldrian P, Brunel D, Frostegård Å, Heulin T, Jansson JK, Jurkevitch E, et al (2016) Back to the future of soil metagenomics. Front Microbiol **7**: art73

Newton AC, Fitt BDL, Atkins SD, Walters DR, Daniell TJ (2010) Pathogenesis, parasitism and mutualism in the trophic space of microbe-plant interactions. Trends Microbiol **18**: 365–373

Nie M, Bell C, Wallenstein MD, Pendall E (2015) Increased plant productivity and decreased microbial respiratory C loss by plant growth-promoting rhizobacteria under elevated CO 2. Sci Rep **5**: 1–6

O'Neill EG, Luxmoore RJ, Norby RJ (1987) Elevated atmospheric CO2 effects on seedling growth, nutrient uptake, and rhizosphere bacterial populations of Liriodendron tulipifera L. Plant Soil **104**: 3–11

Obama B (2017) The irreversible momentum of clean energy. Science (80-) **355**: 126–129

Oehme V, Högy P, Franzaring J, Zebitz CPW, Fangmeier A (2013) Pest and disease abundance and dynamics in wheat and oilseed rape as affected by elevated atmospheric CO2 concentrations. Funct Plant Biol **40**: 125–136

Oka-Kira E, Kawaguchi M (2006) Long-distance signaling to control root nodule number. Curr Opin Plant Biol **9**: 496–502

Osborn AM, Moore ERB, Timmis KN (2000) An evaluation of terminal-restriction fragment

length polymorphism (T-RFLP) analysis for the study of microbial community structure and dynamics. Environ Microbiol **2**: 39–50

Pandya S, Iyer P, Gaitonde V, Parekh T, Desai A (1999) Chemotaxis of Rhizobium sp.S2 towards Cajanus cajan root exudate and its major components. Curr Microbiol **38**: 205–209

Pangga IB, Chakraborty S, Yates D (2004) Canopy Size and Induced Resistance in Stylosanthes scabra Determine Anthracnose Severity at High CO(2). Phytopathology **94**: 221–227

Paterson E, Hall JM, Rattray E a. S, Griffiths BS, Ritz K, Killham K (1997) Effect of elevated CO2 on rhizosphere carbon flow and soil microbial processes. Glob Chang Biol **3**: 363–377

Paul W, Mcdunn JE, Wentworth AD, Takeuchi C, Nieva J, Jones T, Bautista C, Ruedi JM, Gutierrez A, Janda KD, et al (2002) Evidence for Antibody-Catalyzed Ozone Formation in Bacterial Killing and Inflammation. Science (80-) **298**: 2195–9

Pendall E, Bridgham S, Hanson PJ, Hungate B, Kicklighter DW, Johnson DW, Law BE, Luo Y, Megonigal JP, Olsrud M, et al (2004) Below-ground process responses to elevated CO2 and temperature: A discussion of observations, measurement methods, and models. New Phytol **162**: 311–322

Pennypacker B, Leath K, Jr RH (1991) Impact of drought stress on the expression of resistance to Verticillium albo-atrum in alfalfa. Phytopathology **81**: 1014–1024

Penuelas J, Matamala R (1990) Changes in N and S leaf content, stomatal density and specific leaf area of 14 plant species during the last three centuries of CO2 increase. J Exp Bot **41**: 1119–1124

Percy K, Awmack C, Lindroth R, Kubiske M, Kopper B, Isebrands J, Pregitzer K, Hendrey G, Dickson R, Zak D, et al (2002) Altered performance of forest pests under atmospheres enriched by CO2 and O3. Nature **420**: 403–408

Peterhansel C, Maurino VG (2011) Photorespiration redesigned. Plant Physiol **155**: 49–55

Petersen BL, Chen S, Hansen CH, Olsen CE, Halkier BA (2002) Composition and content of glucosinolates in developing Arabidopsis thaliana. Planta **214**: 562–571

Petit JR, Jouzel J, Raynaud D, Barkov NI, Barnola JM, Basile I, Bender M, Chappellaz J, Davis M, Delaygue G, et al (1999) Climate and atmospheric history of the past 420,000 years from the Vostok ice core, Antarctica. Nature **399**: 429–436

Pétriacq P, Stassen J, Ton J (2016a) Spore density determines infection strategy by the plant-pathogenic fungus Plectosphaerella cucumerina. Plant Physiol **170**: 2325–2339

Pétriacq P, Ton J, Patrit O, Tcherkez G, Gakière B (2016b) NAD acts as an integral regulator of multiple defense layers. Plant Physiol **172**: 1465–1479

Pétriacq P, Williams A, Cotton A, McFarlane AE, Rolfe SA, Ton J (2017) Metabolite profiling of non-sterile rhizosphere soil. Plant J 147–162

Philippot L, Raaijmakers JM, Lemanceau P, van der Putten WH (2013) Going back to the roots: the microbial ecology of the rhizosphere. Nat Rev Microbiol **11**: 789–799

Phillips DA, Fox TC, Six J (2006) Root exudation (net efflux of amino acids) may increase rhizodeposition under elevated CO2. Glob Chang Biol **12**: 561–567

Phillips RL, Zak DR, Holmes WE, White DC (2002) Microbial community composition and function beneath temperate trees exposed to elevated atmospheric carbon dioxide and ozone. Oecologia **131**: 236–244

Phillips RP, Bernhardt ES, Schlesinger WH (2009) Elevated CO2 increases root exudation from loblolly pine (Pinus taeda) seedlings as an N-mediated response. Tree Physiol **29**: 1513–1523

Phillips RP, Erlitz Y, Bier R, Bernhardt ES (2008) New approach for capturing soluble root exudates in forest soils. Funct Ecol **22**: 990–999

Pielke RA (2005) Land use and climate change. Science (80-) **310**: 1625–1626

Pieterse C, Wees S, Ton J, Pelt JA, Loon LC (2002) Signalling in Rhizobacteria- Induced Systemic Resistance in Arabidopsis thaliana. Plant Biol **4**: 535–544

Pieterse C, van Wees SCM, Hoffland E, Pelt JA Van, van Loon L (1996) Systemic Resistance in Arabidopsis Induced by Biocontrol Bacteria Is Independent of Salicylic Acid Accumulation and Pathogenesis-Related Gene Expression. Plant Cell **8**: 1225–1237

Pieterse CMJ, Leon-Reyes A, Van der Ent S, Van Wees SCM (2009) Networking by small-molecule hormones in plant immunity. Nat Chem Biol **5**: 308–316

Pineda A, Zheng S-J, van Loon JJ a, Pieterse CMJ, Dicke M (2010) Helping plants to deal with insects: the role of beneficial soil-borne microbes. Trends Plant Sci **15**: 507–14

Ping L, Boland W (2004) Signals from the underground: bacterial volatiles promote growth in Arabidopsis. Trends Plant Sci **9**: 263–266

Plessl M, Elstner EF, Rennenberg H, Habermeyer J, Heiser I (2007) Influence of elevated CO2 and ozone concentrations on late blight resistance and growth of potato plants. Environ Exp Bot **60**: 447–457

Polidoros AN, Mylona P V., Scandalios JG (2001) Transgenic tobacco plants expressing the maize Cat2 gene have altered catalase levels that affect plant-pathogen interactions and resistance to oxidative stress. Transgenic Res **10**: 555–569

Poulsen LR, López-Marqués RL, Pedas PR, McDowell SC, Brown E, Kunze R, Harper JF, Pomorski TG, Palmgren M (2015) A phospholipid uptake system in the model plant Arabidopsis thaliana. Nat Commun **6**: art8649

Pozo MJ, Loon LC, Pieterse CMJ (2005) Jasmonates - Signals in Plant-Microbe Interactions. J Plant Growth Regul **23**: 211–222

Prasch CM, Sonnewald U (2013) Simultaneous Application of Heat, Drought, and Virus to Arabidopsis Plants Reveals Significant Shifts in Signaling Networks. Plant Physiol **162**: 1849–1866

Pritchard SG, Rogers HH, Prior SA, Peterson CM (1999) Elevated CO2 and plant structure: A review. Glob Chang Biol **5**: 807–837

Procter AC, Christopher Ellis J, Fay PA, Wayne Polley H, Jackson RB (2014) Fungal community responses to past and future atmospheric CO2 differ by soil type. Appl Environ Microbiol **80**: 7364–7377

Przybyla D, Göbel C, Imboden A, Hamberg M, Feussner I, Apel K (2008) Enzymatic, but not non-enzymatic, 1O2-mediated peroxidation of polyunsaturated fatty acids forms part of the EXECUTER1-dependent stress response program in the flu mutant of Arabidopsis thaliana. Plant J **54**: 236–248

Pugliese M, Liu J, Titone P, Garibaldi A, Gullino ML (2012) Effects of elevated CO 2 and temperature on interactions of zucchini and powdery mildew. Phytopathol Mediterr **51**: 480–487

Qiu YL, Lee J, Bernasconi-Quadroni F, Soltis DE, Soltis PS, Zanis M, Zimmer EA, Chen Z, Savolainen V, Chase MW (1999) The earliest angiosperms: Evidence from mitochondrial, plastid and nuclear genomes. Nature **402**: 404–407

Quirk J, McDowell NG, Leake JR, Hudson PJ, Beerling DJ (2013) Increased susceptibility to drought-induced mortality in Sequoia sempervirens (Cupressaceae) trees under Cenozoic atmospheric carbon dioxide starvation. Am J Bot **100**: 582–591

Rainey PB (1999) Adaptation of Pseudomonas fluorescens to the plant rhizosphere. Environ Microbiol **1**: 243–257

Rao JR, Cooper JE (1994) Rhizobia catabolize nod gene-inducing flavonoids via C-ring fission mechanisms. J Bacteriol **176**: 5409–5413

Read DB, Bengough AG, Gregory PJ, Crawford JW, Robinson D, Scrimgeour CM, Young IM, Zhang K, Zhang X (2003) Plant roots release phospholipid surfactants that modify the

physical and chemical properties of soil. New Phytol **157**: 315–326

REN 21 (2017) Renewables 2017: global status report. doi: 10.1016/j.rser.2016.09.082

Rengel Z, Marschner P (2005) Nutrient availability and management in the rhizosphere: Exploiting genotypic differences. New Phytol **168**: 305–312

Riahi K, Rao S, Krey V, Cho C, Chirkov V, Fischer G, Kindermann G, Nakicenovic N, Rafaj P (2011) RCP 8.5-A scenario of comparatively high greenhouse gas emissions. Clim Change **109**: 33–57

Rice CW, Garcia FO, Hampton CO, Owensby CE (1994) Soil microbial response in tallgrass prairie to elevated CO2. Plant Soil **165**: 67–74

Riikonen J, Syrjälä L, Tulva I, Mänd P, Oksanen E, Poteri M, Vapaavuori E (2008) Stomatal characteristics and infection biology of Pyrenopeziza betulicola in Betula pendula trees grown under elevated CO2 and O3. Environ Pollut **156**: 536–543

Robinson E a, Ryan GD, Newman J a (2012) A meta-analytical review of the effects of elevated CO 2 on plant – arthropod interactions highlights the importance of interacting environmental and biological variables. New Phytol **194**: 321–336

Rodriguez RJ, Redman RS, Henson JM (2004) The role of fungal symbioses in the adaptation of plants to high stress environments. Mitig Adapt Strateg Glob Chang **9**: 261–272

Rogers A, Ainsworth EA, Leakey ADB (2009) Will Elevated Carbon Dioxide Concentration Amplify the Benefits of Nitrogen Fixation in Legumes? Plant Physiol **151**: 1009–1016

Rojas CM, Senthil-Kumar M, Tzin V, Mysore KS (2014) Regulation of primary plant metabolism during plant-pathogen interactions and its contribution to plant defense. Front Plant Sci **5**: art17

Rojas CM, Senthil-Kumar M, Wang K, Ryu C-M, Kaundal A, Mysore KS (2012) Glycolate Oxidase Modulates Reactive Oxygen Species-Mediated Signal Transduction during Nonhost Resistance in Nicotiana benthamiana and Arabidopsis. Plant Cell **24**: 336–352

Rosenzweig C, Elliott J, Deryng D, Ruane AC, Müller C, Arneth A, Boote KJ, Folberth C, Glotter M, Khabarov N, et al (2014) Assessing agricultural risks of climate change in the 21st century in a global gridded crop model intercomparison. Proc Natl Acad Sci **111**: 3268–3273

Ross DJ, Tate KR, Newton P (1995) Elevated Co2 And Temperature Effects On Soil Carbon And Nitrogen Cycling In Ryegrass/White Clover Turves Of An Endoaquept Soil. Plant Soil **176**: 37–49

Royer DL (2001) Stomatal density and stomatal index as indicators of paleoatmospheric CO(2) concentration. Rev Palaeobot Palynol **114**: 1–28

Ruan Y, Kotraiah V, Straney D (1995) Flavonoids Stimulate Spore Germination in Fusarium solani Pathogenic on Legumes in a Manner Sensitive to Inhibitors of cAMP-Dependent Protein Kinase. Mol Plant-Microbe Interact **8**: 929–938

Rudrappa T, Czymmek KJ, Paré PW, Bais HP (2008) Root-secreted malic acid recruits beneficial soil bacteria. Plant Physiol **148**: 1547–56

Runion GB, Prior S a., Rogers HH, Mitchell RJ (2010) Effects of elevated atmospheric Co2 on two southern forest diseases. New For **39**: 275–285

Rusterucci C, Zhao Z, Haines K, Mellersh D, Neumann M, Cameron RK (2005) Age-related resistance to Pseudomonas syringae pv. tomato is associated with the transition to flowering in Arabidopsis and is effective against Peronospora parasitica. Physiol Mol Plant Pathol **66**: 222–231

Sah SK, Reddy KR, Li J (2016) Abscisic Acid and Abiotic Stress Tolerance in Crop Plants. Front Plant Sci **7**: art571

Saito K, Yonekura-Sakakibara K, Nakabayashi R, Higashi Y, Yamazaki M, Tohge T, Fernie AR (2013) The flavonoid biosynthetic pathway in Arabidopsis: Structural and genetic diversity. Plant Physiol Biochem **72**: 21–34

Sandalio LM, Rodríguez-Serrano M, Romero-Puertas MC, del Río LA (2008) Imaging of Reactive Oxygen Species and Nitric Oxide In Vivo in Plant Tissues. Methods Enzymol **440**: 397–409

dos Santos MS, Ghini R, Fernandes B V., Silva CA (2013) Increased carbon dioxide concentration in the air reduces the severity of Ceratocystis wilt in Eucalyptus clonal plantlets. Australas Plant Pathol **42**: 595–599

Sawada Y, Nakabayashi R, Yamada Y, Suzuki M, Sato M, Sakata A, Akiyama K, Sakurai T, Matsuda F, Aoki T, et al (2012) RIKEN tandem mass spectral database (ReSpect) for phytochemicals: A plant-specific MS/MS-based data resource and database. Phytochemistry **82**: 38–45

Sawinski K, Mersmann S, Robatzek S, Böhmer M (2013) Guarding the green: pathways to stomatal immunity. Mol Plant Microbe Interact **26**: 626–632

Schindlbacher A, Zechmeister-Boltenstern S, Kitzler B, Jandl R (2008) Experimental forest soil warming: Response of autotrophic and heterotrophic soil respiration to a short-term 10C temperature rise. Plant Soil **303**: 323–330

Schulz B, Boyle C (2005) The endophytic continuum. Mycol Res **109**: 661–686

Schulze-Lefert P, Vogel J (2000) Closing the ranks to attack by powdery mildew. Trends Plant Sci **5**: 343–348

Seegmuller S, Schulte M, Herschbach C, Rennenberg H (1996) Interactive effects of mycorrhization and elevated atmospheric CO2 on sulphur nutrition of young pedunculate oak {Quercus robur L.) trees. Plant Cell Environ **19**: 418–426

Seyfferth C, Tsuda K (2014) Salicylic acid signal transduction: the initiation of biosynthesis, perception and transcriptional reprogramming. Front Plant Sci **5**: art697

Sgherri C, Cecconami S, Pinzino C, Navari-Izzo F, Izzo R (2010) Levels of antioxidants and nutraceuticals in basil grown in hydroponics and soil. Food Chem **123**: 416–422

Shafer SR (1988) Influence of ozone and simulated acidic rain on microorganisms in the rhizosphere of Sorghum. Environ Pollut **51**: 131–152

Shakun JD, Clark PU, He F, Marcott SA, Mix AC, Liu Z, Otto-Bliesner B, Schmittner A, Bard E (2012) Global warming preceded by increasing carbon dioxide concentrations during the last deglaciation. Nature **484**: 49–54

Sharbel TF, Haubold B, Mitchell-Olds T (2000) Genetic isolation by distance in Arabidopsis thaliana: biogeography and postglacial colonization of Europe. Mol Ecol **9**: 2109–2118

Sharma M, Ghosh R, Tarafdar A, Telangre R (2015) An efficient method for zoospore production, infection and real-time quantification of Phytophthora cajani causing Phytophthora blight disease in pigeonpea under elevated atmospheric CO2. BMC Plant Biol **15**: art90

Sharma RC, Duveiller E, Ortiz-Ferrara G (2007) Progress and challenge towards reducing wheat spot blotch threat in the Eastern Gangetic Plains of South Asia: Is climate change already taking its toll? F Crop Res **103**: 109–118

Shaw LJ, Morris P, Hooker JE (2006) Perception and modification of plant flavonoid signals by rhizosphere microorganisms. Environ Microbiol **8**: 1867–1880

Shaw MR, Zavaleta ES, Chiariello NR, Cleland EE, Mooney H a, Field CB (2002) Grassland responses to global environmental changes suppressed by elevated CO2. Science (80-) **298**: 1987–90

Shibata Y, Kawakita K, Takemoto D (2010) Age-related resistance of Nicotiana benthamiana against hemibiotrophic pathogen Phytophthora infestans requires both ethylene- and salicylic acid-mediated signaling pathways. Mol Plant Microbe Interact **23**: 1130–1142

Shin JW, Yun SC (2010) Elevated CO2 and temperature effects on the incidence of four major chili pepper diseases. Plant Pathol J **26**: 178–184

Siewers V, Kokkelink L, Smedsgaard J, Tudzynski P (2006) Identification of an abscisic acid

gene cluster in the grey mold Botrytis cinerea. Appl Environ Microbiol **72**: 4619–4626

Silva CEO Da, Ghini R (2014) Plant growth and leaf-spot severity on eucalypt at different CO2 concentrations in the air. Pesqui Agropecuária Bras **49**: 232–235

da Silva Lima L, Olivares FL, Rodrigues de Oliveira R, Vega MRG, Aguiar NO, Canellas LP (2014) Root exudate profiling of maize seedlings inoculated with Herbaspirillum seropedicae and humic acids. Chem Biol Technol Agric **1**: 1–18

Smith A, O 'maille G, Want EJ, Qin C, Trauger SA, Brandon TR, Custodio DE, Abagyan R, Siuzdak G (2005a) METLIN A Metabolite Mass Spectral Database. Proc 9Th Int Congr Ther Drug Monit Clin Toxicol **27**: 747–751

Smith CA, Want EJ, O'Maille G, Abagyan R, Siuzdak G (2006) XCMS: Processing mass spectrometry data for metabolite profiling using nonlinear peak alignment, matching, and identification. Anal Chem **78**: 779–787

Smith CJ, Danilowicz BS, Clear AK, Costello FJ, Wilson B, Meijer WG (2005b) T-Align, a web-based tool for comparison of multiple terminal restriction fragment length polymorphism profiles. FEMS Microbiol Ecol **54**: 375–380

Song F, Han X, Zhu X, Herbert SJ (2012) Response to water stress of soil enzymes and root exudates from drought and non-drought tolerant corn hybrids at different growth stages. Can J Soil Sci **92**: 501–507

Sørhagen K, Laxa M, Peterhänsel C, Reumann S (2013) The emerging role of photorespiration and non-photorespiratory peroxisomal metabolism in pathogen defence. Plant Biol **15**: 723–736

Springer C, Ward J (2007) Flowering Time and Elevated Atmospheric $CO_2$2. New Phytol **176**: 243–255

Staddon PL, Graves JD, Fitter AH (1998) Effect of enhanced atmospheric CO2 on mycorrhizal colonization by Glomus mosseae in Plantago lanceolata and Trifolium repens. New Phytol **139**: 571–580

Stadtman ER, Levine RL (2003) Free radical-mediated oxidation of free amino acids and amino acid residues in proteins. Amino Acids **25**: 207–218

Staswick PE (2002) Jasmonate Response Locus JAR1 and Several Related Arabidopsis Genes Encode Enzymes of the Firefly Luciferase Superfamily That Show Activity on Jasmonic, Salicylic, and Indole-3-Acetic Acids in an Assay for Adenylation. Plant Cell **14**: 1405–1415

Steinkellner S, Lendzemo V, Langer I, Schweiger P, Khaosaad T, Toussaint J-P, Vierheilig H (2007) Flavonoids and strigolactones in root exudates as signals in symbiotic and pathogenic plant-fungus interactions. Molecules **12**: 1290–1306

Stevenson DS, Dentener FJ, Schultz MG, Ellingsen K, van Noije TPC, Wild O, Zeng G, Amann M, Atherton CS, Bell N, et al (2006) Multimodel ensemble simulations of present-day and near-future tropospheric ozone. J Geophys Res Atmos **111**: D08301

Strehmel N, Böttcher C, Schmidt S, Scheel D (2014) Profiling of secondary metabolites in root exudates of Arabidopsis thaliana. Phytochemistry **108**: 35–46

Strengbom J, Reich PB (2006) Elevated [CO2] and increased N supply reduce leaf disease and related photosynthetic impacts on Solidago rigida. Oecologia **149**: 519–25

Sugiyama A, Yazaki K (2014) Flavonoids in plant rhizospheres: Secretion, fate and their effects on biological communication. Plant Biotechnol **31**: 431–443

Suseela V, Dukes JS (2013) The responses of soil and rhizosphere respiration to simulated climatic changes vary by season. Ecology **94**: 403–413

Tai APK, Martin MV, Heald CL (2014) Threat to future global food security from climate change and ozone air pollution. Nat Clim Chang **4**: 817–821

Tang S, Liao S, Guo J, Song Z, Wang R, Zhou X (2011) Growth and cesium uptake responses of Phytolacca americana Linn. and Amaranthus cruentus L. grown on cesium

contaminated soil to elevated CO 2 or inoculation with a plant growth promoting rhizobacterium Burkholderia sp. D54, or in combination. J Hazard Mater **198**: 188–197

Taub DR, Wang X (2008) Why are nitrogen concentrations in plant tissues lower under elevated CO2? A critical examination of the hypotheses. J Integr Plant Biol **50**: 1365–1374

Tauzin AS, Giardina T (2014) Sucrose and invertases, a part of the plant defense response to the biotic stresses. Front Plant Sci **5**: art293

Tavakkoli E, Rengasamy P, McDonald GK (2010) The response of barley to salinity stress differs between hydroponic and soil systems. Funct Plant Biol **37**: 621–633

Temme AA, Cornwell WK, Cornelissen JHC, Aerts R (2013) Meta-analysis reveals profound responses of plant traits to glacial CO2 levels. Ecol Evol **3**: 4525–4535

Temme AA, Liu JC, Cornwell WK, Cornelissen JHC, Aerts R (2015) Winners always win: Growth of a wide range of plant species from low to future high CO2. Ecol Evol **5**: 4949–4961

Teng N, Jin B, Wang Q, Hao H, Ceulemans R, Kuang T, Lin J (2009) No detectable maternal effects of elevated CO2 on Arabidopsis thaliana over 15 generations. PLoS One **4**: e6035

Teng N, Wang J, Chen T, Wu X, Wang Y, Lin J (2006) Elevated CO2 induces physiological, biochemical and structural changes in leaves of Arabidopsis thaliana. New Phytol **172**: 92–103

Thomma BP, Eggermont K, Penninckx I a, Mauch-Mani B, Vogelsang R, Cammue BP, Broekaert WF (1998) Separate jasmonate-dependent and salicylate-dependent defense-response pathways in Arabidopsis are essential for resistance to distinct microbial pathogens. Proc Natl Acad Sci U S A **95**: 15107–15111

Thompson G (1993) The effects of host carbon dioxide, nitrogen and water supply on the infection of wheat by powdery mildew and aphids. Plant Cell Environ **16**: 687–694

Thompson GB, Drake BG (1994) Insects and fungi on a C3 sedge and a C4 grass exposed to elevated atmospheric CO2 concentrations in open-top chambers in the field. Plant, Cell Environ **17**: 1161–1167

Thomson AM, Calvin K V., Smith SJ, Kyle GP, Volke A, Patel P, Delgado-Arias S, Bond-Lamberty B, Wise MA, Clarke LE, et al (2011) RCP4.5: A pathway for stabilization of radiative forcing by 2100. Clim Change **109**: 77–94

Tiedemann A V., Firsching KH (2000) Interactive effects of elevated ozone and carbon dioxide on growth and yield of leaf rust-infected versus non-infected wheat. Environ. Pollut. pp 357–363

Timm S, Bauwe H (2013) The variety of photorespiratory phenotypes - employing the current status for future research directions on photorespiration. Plant Biol **15**: 737–747

Timmusk S, Abd El-Daim IA, Copolovici L, Tanilas T, Kännaste A, Behers L, Nevo E, Seisenbaeva G, Stenström E, Niinemets Ü (2014) Drought-Tolerance of Wheat Improved by Rhizosphere Bacteria from Harsh Environments: Enhanced Biomass Production and Reduced Emissions of Stress Volatiles. PLoS One **9**: e96086

Tkaczyk M, Sikora K, Nowakowska J a., Kubiak K, Oszako T (2014) Effect of CO2 enhancement on beech (Fagus sylvatica L.) seedling root rot due to Phytophthora plurivora and Phytophthora cactorum. Folia For Pol **56**: 149–156

Ton J, Flors V, Mauch-Mani B (2009) The multifaceted role of ABA in disease resistance. Trends Plant Sci **14**: 310–7

Torres MA, Dangl JL, Jones JDG (2002) Arabidopsis gp91phox homologues AtrbohD and AtrbohF are required for accumulation of reactive oxygen intermediates in the plant defense response. Proc Natl Acad Sci **99**: 517–522

Trębicki P, Nancarrow N, Cole E, Bosque-Pérez N a., Constable FE, Freeman AJ, Rodoni B, Yen AL, Luck JE, Fitzgerald GJ (2015) Virus disease in wheat predicted to increase with a changing climate. Glob Chang Biol **21**: 3511–3519

Treseder KK, Egerton-Warburton LM, Allen MF, Cheng Y, Oechel WC (2003) Alteration of Soil Carbon Pools and Communities of Mycorrhizal Fungi in Chaparral Exposed to Elevated Carbon Dioxide. Ecosystems **6**: 786–796

Turner JG, Ellis C, Devoto A (2002) The Jasmonate Signal Pathway. Plant Cell **14**: 153–164

United Nations (2015) United Nations Convention to Combat Desertification. 336

Uren NC (2007) Types, Amounts, and Possible Functions of Compounds released into the Rhizosphere by Soil- Grown Plants. *In* R Pinton, Z Varanini, P Nannipieri, eds, Rhizosph. Biochem. Org. Subst. Soil-Plant Interface. Dekker, M, New York, pp 1–21

Uselman SM, Qualls RG, Thomas RB (2000) Effects of increased atmospheric CO2 , temperature, and soil N availability on root exudation of dissolved organic carbon by a N-fixing tree (Robinia pseudoacacia L.). Plant Soil **222**: 191–202

Vacheron J, Desbrosses G, Bouffaud M-L, Touraine B, Moënne-Loccoz Y, Muller D, Legendre L, Wisniewski-Dyé F, Prigent-Combaret C (2013) Plant growth-promoting rhizobacteria and root system functioning. Front Plant Sci **4**: art356

Váry Z, Mullins E, McElwain JC, Doohan FM (2015) The severity of wheat diseases increases when plants and pathogens are acclimatized to elevated carbon dioxide. Glob Chang Biol **21**: 2661–2669

Vassilev N, Vassileva M, Nikolaeva I (2006) Simultaneous P-solubilizing and biocontrol activity of microorganisms: potentials and future trends. Appl Microbiol Biotechnol **71**: 137–144

Vaughan MM, Huffaker A, Schmelz E a., Dafoe NJ, Christensen S, Sims J, Martins VF, Swerbilow J, Romero M, Alborn HT, et al (2014) Effects of elevated [CO2] on maize defence against mycotoxigenic Fusarium verticillioides. Plant Cell Environ **37**: 2691–2706

Verhagen BWM, Glazebrook J, Zhu T, Chang H-S, van Loon LC, Pieterse CMJ (2004) The Transcriptome of Rhizobacteria-Induced Systemic Resistance in Arabidopsis. Mol Plant-Microbe Interact **17**: 895–908

Vessey J (2003) Plant growth promoting rhizobacteria as biofertilizers. Plant Soil **255**: 571–586

Visser B, Le Lann C, den Blanken FJ, Harvey JA, van Alphen JJM, Ellers J (2010) Loss of lipid synthesis as an evolutionary consequence of a parasitic lifestyle. Proc Natl Acad Sci **107**: 8677–8682

Vlot AC, Dempsey DA, Klessig DF (2009) Salicylic Acid, a Multifaceted Hormone to Combat Disease. Annu Rev Phytopathol **47**: 177–206

van Vuuren DP, Edmonds J, Kainuma M, Riahi K, Thomson A, Hibbard K, Hurtt GC, Kram T, Krey V, Lamarque JF, et al (2011a) The representative concentration pathways: An overview. Clim Change **109**: 5–31

van Vuuren DP, Stehfest E, den Elzen MGJ, Kram T, van Vliet J, Deetman S, Isaac M, Goldewijk KK, Hof A, Beltran AM, et al (2011b) RCP2.6: Exploring the possibility to keep global mean temperature increase below 2°C. Clim Change **109**: 95–116

Walters D, Heil M (2007) Costs and trade-offs associated with induced resistance. Physiol Mol Plant Pathol **71**: 3–17

Wan S, Norby RJ, Ledford J, Weltzin JF (2007) Responses of soil respiration to elevated CO2, air warming, and changing soil water availability in a model old-field grassland. Glob Chang Biol **13**: 2411–2424

Wang D, Heckathorn SA, Barua D, Joshi P, Hamilton EW, Lacroix JJ (2008) Effects of elevated CO 2 on the tolerance of photosynthesis to acute heat stress in C 3 , C 4 , and. **95**: 165–176

Wang E, Schornack S, Marsh JF, Gobbato E, Schwessinger B, Eastmond P, Schultze M, Kamoun S, Oldroyd GED (2012) A common signaling process that promotes mycorrhizal and oomycete colonization of plants. Curr Biol **22**: 2242–2246

Wang X, Manning W, Feng Z, Zhu Y (2007) Ground-level ozone in China: Distribution and

effects on crop yields. Environ Pollut **147**: 394–400

Ward JK, Gerhart LM (2010) Plant responses to low [CO2] of the past. New Phytol **188**: 674–695

Ward JK, Kelly JK (2004) Scaling up evolutionary responses to elevated CO2: Lessons from Arabidopsis. Ecol Lett **7**: 427–440

Warren JM, Norby RJ, Wullschleger SD (2017) Elevated CO 2 enhances leaf senescence during extreme drought in a temperate forest. 117–130

Wasternack C, Hause B (2013) Jasmonates: Biosynthesis, perception, signal transduction and action in plant stress response, growth and development. An update to the 2007 review in Annals of Botany. Ann Bot **111**: 1021–1058

Watanabe M, Kitaoka S, Eguchi N, Watanabe Y, Satomura T, Takagi K, Satoh F, Koike T (2014) Photosynthetic traits and growth of Quercus mongolica var. crispula sprouts attacked by powdery mildew under free-air CO2 enrichment. Eur J For Res **133**: 725–733

Webb KM, Oña I, Bai J, Garrett KA, Mew T, Vera Cruz CM, Leach JE (2010) A benefit of high temperature: Increased effectiveness of a rice bacterial blight disease resistance gene. New Phytol **185**: 568–576

de Weert S, Vermeiren H, Mulders IHM, Kuiper I, Hendrickx N, Bloemberg G V., Vanderleyden J, De Mot R, Lugtenberg BJJ (2002) Flagella-Driven Chemotaxis Towards Exudate Components Is an Important Trait for Tomato Root Colonization by *Pseudomonas fluorescens*. Mol Plant-Microbe Interact **15**: 1173–1180

Van Wees SCM, Van der Ent S, Pieterse CMJ (2008) Plant immune responses triggered by beneficial microbes. Curr Opin Plant Biol **11**: 443–8

Weinel C, Nelson KE, Tümmler B (2002) Global features of the Pseudomonas putida KT2440 genome sequence. Environ Microbiol **4**: 809–818

Wiemken V, Laczko E, Ineichen K, Boller T (2001) Effects of Elevated Carbon Dioxide and Nitrogen Fertilization on Mycorrhizal Fine Roots and the Soil Microbial Community in Beech-Spruce Ecosystems on Siliceous and Calcareous Soil. Microb Ecol **42**: 126–135

Wildermuth MC, Dewdney J, Wu G, Ausubel FM (2001) Isochorismate synthase is required to synthesize salicylic acid for plant defence. Nature **414**: 562–565

Williams A, Pétriacq P, Schwarzenbacher RE, Beerling DJ, Ton J (2018) Mechanisms of glacial-to-future atmospheric CO 2 effects on plant immunity. New Phytol **218**: 752–761

Woodward FI, Kelly CK (1995) The influence of CO2 concentration on stomatal density. New Phytol **131**: 311–327

Xia J, Sinelnikov I V., Han B, Wishart DS (2015) MetaboAnalyst 3.0-making metabolomics more meaningful. Nucleic Acids Res **43**: 251–257

Ye L, Fu X, Ge F (2010) Elevated CO2 alleviates damage from Potato virus Y infection in tobacco plants. Plant Sci **179**: 219–224

Zak DR, Pregitzer KS, Curtis PS, Holmes WE (2000) Atmospheric Co 2 and the Composition and Function of Soil Microbial Communities. Ecol Appl **10**: 47–59

Zamioudis C, Hanson J, Pieterse MJ (2014) b -Glucosidase BGLU42 is a MYB72-dependent key regulator of rhizobacteria-induced systemic resistance and modulates iron deficiency responses in Arabidopsis roots. New Phytol **204**: 368–379

Zamioudis C, Korteland J, Van Pelt JA, Van Hamersveld M, Dombrowski N, Bai Y, Hanson J, Van Verk MC, Ling HQ, Schulze-Lefert P, et al (2015) Rhizobacterial volatiles and photosynthesis-related signals coordinate MYB72 expression in Arabidopsis roots during onset of induced systemic resistance and iron-deficiency responses. Plant J **84**: 309–322

Zamioudis C, Pieterse CMJ (2012) Modulation of host immunity by beneficial microbes. Mol Plant Microbe Interact **25**: 139–150

Zavala JA, Casteel CL, DeLucia EH, Berenbaum MR (2008) Anthropogenic increase in carbon dioxide compromises plant defense against invasive insects. Proc Natl Acad Sci

105: 5129–5133

Zhang H, Xie X, Kim M-S, Kornyeyev D a, Holaday S, Paré PW (2008) Soil bacteria augment Arabidopsis photosynthesis by decreasing glucose sensing and abscisic acid levels in planta. Plant J **56**: 264–73

Zhang S, Li X, Sun Z, Shao S, Hu L, Ye M, Zhou Y, Xia X, Yu J, Shi K (2015) Antagonism between phytohormone signalling underlies the variation in disease susceptibility of tomato plants under elevated CO2. J Exp Bot **66**: 1951–1963

Zhou Y, Vroegop-Vos I, Schuurink RC, Pieterse CMJ, Van Wees SCM (2017) Atmospheric CO2 Alters Resistance of Arabidopsis to Pseudomonas syringae by Affecting Abscisic Acid Accumulation and Stomatal Responsiveness to Coronatine. Front Plant Sci **8**: art700

Zhu B, Cheng W (2011) Rhizosphere priming effect increases the temperature sensitivity of soil organic matter decomposition. Glob Chang Biol **17**: 2172–2183

Zhu Y, Qian W, Hua J (2010) Temperature modulates plant defense responses through NB-LRR proteins. PLoS Pathog **6**: e1000844

Zipfel C, Felix G (2005) Plants and animals: a different taste for microbes? Curr Opin Plant Biol **8**: 353–60

Ziska L., Bunce J. (1997) The role of temperature in determining the stimulation of CO2 assimilation at elevated carbon dioxide concentration in soybean seedlings. Physiol Plant **100**: 126–132

Zogg GP, Zak DR, Ringelberg DB, White DC, MacDonald NW, Pregitzer KS (1997) Compositional and Functional Shifts in Microbial Communities Due to Soil Warming. Soil Sci Soc Am J **61**: 475–481

The Plant Journal (2017) 92, 147–162 doi: 10.1111/tpj.13639

Appendix 1

Metabolite profiling of non-sterile rhizosphere soil

Pierre Pétriacq[1,2,3,*] , Alex Williams[3], Anne Cotton[3], Alexander E. McFarlane[3], Stephen A. Rolfe[1,3] and Jurriaan Ton[1,3,*]

[1]*Plant Production and Protection (P3) Institute for Translational Plant & Soil Biology, Department of Animal and Plant Sciences, The University of Sheffield, Sheffield S10 2TN, UK,*
[2]*biOMICS Facility, Department of Animal and Plant Sciences, The University of Sheffield, Sheffield S10 2TN, UK, and*
[3]*Department of Animal and Plant Sciences, The University of Sheffield, Sheffield S10 2TN, UK*

Received 29 April 2016; revised 11 July 2017; accepted 12 July 2017; published online 25 July 2017.
*For correspondence (e-mails p.petriacq@sheffield.ac.uk; j.ton@sheffield.ac.uk).

SUMMARY

Rhizosphere chemistry is the sum of root exudation chemicals, their breakdown products and the microbial products of soil-derived chemicals. To date, most studies about root exudation chemistry are based on sterile cultivation systems, which limits the discovery of microbial breakdown products that act as semiochemicals and shape microbial rhizosphere communities. Here, we present a method for untargeted metabolic profiling of non-sterile rhizosphere soil. We have developed an experimental growth system that enables the collection and analysis of rhizosphere chemicals from different plant species. High-throughput sequencing of 16S rRNA genes demonstrated that plants in the growth system support a microbial rhizosphere effect. To collect a range of (a)polar chemicals from the system, we developed extraction methods that do not cause detectable damage to root cells or soil-inhabiting microbes, thus preventing contamination with cellular metabolites. Untargeted metabolite profiling by UPLC-Q-TOF mass spectrometry, followed by uni- and multivariate statistical analyses, identified a wide range of secondary metabolites that are enriched in plant-containing soil, compared with control soil without roots. We show that the method is suitable for profiling the rhizosphere chemistry of Zea mays (maize) in agricultural soil, thereby demonstrating the applicability to different plant–soil combinations. Our study provides a robust method for the comprehensive metabolite profiling of non-sterile rhizosphere soil, which represents a technical advance towards the establishment of causal relationships between the chemistry and microbial composition of the rhizosphere.

Keywords: rhizosphere chemistry, rhizosphere microbiome, root exudates, metabolomics, Arabidopsis thaliana, maize, soil, benzoxazinoids, technical advance.

INTRODUCTION

Plant roots convert their associated soil into complex mesotrophic environments that support a highly diverse microbial community (Dessaux *et al.,* 2016). This so-called rhizosphere effect is mediated by the exudation of plant metabolites from roots (Badri and Vivanco, 2009; van Dam and Bouwmeester, 2016; Oburger and Schmidt, 2016). The chemical composition of these root exudates and their microbial breakdown products plays a crucial role in rhizosphere interactions between plants and beneficial soil microbes (Oburger and Schmidt, 2016). Although developments in sequencing technology have revolutionized our ability to characterize rhizosphere microbial communities (van Dam and Bouwmeester, 2016; Oburger and Schmidt, 2016), the chemical diversity of the rhizosphere remains largely unexplored. This knowledge gap mostly arises from a lack of suitable methods to collect and comprehensively analyse metabolites from non-sterile rhizosphere soil.

It has been estimated that plants exude up to 21% of their carbon through their roots, where it is metabolized by the microbial community in the rhizosphere (Hinsinger *et al.,* 2006; Badri and Vivanco, 2009; Neumann *et al.,* 2009). Hence, plant roots drive multitrophic interactions in the rhizosphere via root exudation chemistry. Apart from serving as a primary carbon source for rhizosphere microbes, root exudates can influence rhizosphere interactions via selective biocidal and/or signalling activity (Berendsen *et al.,* 2012). Both polar and apolar compounds have been reported to influence rhizosphere interactions. In addition to polar primary metabolites, such as organic and amino acids (Rudrappa *et al.,* 2008; Ziegler *et al.,* 2015; van Dam and Bouwmeester, 2016), more complex apolar secondary metabolites, like flavonoids, coumarins and benzoxazinoids (Hassan and Mathesius, 2012; Neal *et al.,* 2012; Ziegler *et al.,* 2015; Szoboszlay *et al.,* 2016), have been reported to play an important role in influencing rhizosphere microbes. For instance, the benzoxazinoid DIMBOA, which is exuded by roots of maize seedlings, has chemotactic properties on Pseudomonas putida KT2440 (Neal *et al.,* 2012), a rhizobacterial strain that primes host defences against herbivores (Neal and Ton, 2013). Likewise, the release of malic acid from Arabidopsis thaliana (Arabidopsis) roots attracts the Gram-positive rhizobacteria Bacillus subtilis, which in turn induces disease resistance against Pseudomonas syringae pv. tomato (Rudrappa *et al.,* 2008). Furthermore, it was shown recently that plantderived flavonoids have profound effects on the structure of soil bacterial communities (Szoboszlay *et*

al., 2016). Although these studies illustrate the importance of specific classes of root-derived chemicals in rhizosphere interactions, untargeted metabolome studies of root exudation products remain scarce, thereby limiting the scope for discoveries of important rhizosphere signals (Lakshmanan *et al.,* 2012; Neal *et al.,* 2012).

In addition to plant genotype and nutrition, various other factors can influence root exudation chemistry, such as plant developmental stage, temperature, humidity and physiochemical soil properties (Boyes *et al.,* 2001; Uren, 2007; Badri and Vivanco, 2009; Zhang *et al.,* 2016). The environmental effects of root exudation chemistry have been studied mostly in (semi)sterile hydroponic systems (Song *et al.,* 2012; Vranova *et al.,* 2013; da Silva Lima *et al.,* 2014). An important justification for the use of such soil-free growth conditions is that they allow for the tight maintenance of environmental variables (Ziegler *et al.,* 2015; Bowsher *et al.,* 2016). In addition, hydroponic growth systems prevent sorption of metabolites to soil particles and microbial degradation. A recent study made a compelling case for the use of sterile root systems for studying root exudation chemistry by demonstrating that root exudates collected from non-sterile systems underestimated the quantity and diversity of carbon-containing metabolites resulting from microbial breakdown (Kuijken *et al.,* 2014). Using hydroponically grown roots under sterile conditions, Strehmel et al. (2014) reported wide-ranging chemical diversity in root exudates of Arabidopsis, including mostly secondary metabolites such as (deoxy)nucleosides, anabolites and catabolites of glucosinolates, derivatives of phytohormones (e.g. salicylic acid, SA; jasmonic acid, JA; and oxylipins) and phenylpropanoids (e.g. coumarins and hydroxynammic acids). Nonetheless, there are disadvantages to hydroponically grown, sterile root systems. Hydroponically cultivated roots often develop root morphologies that differ from those of soil-grown roots, which probably reflects an underlying difference in physiology that may affect exudation chemistry (Sgherri *et al.,* 2010; Tavakkoli *et al.,* 2010). Furthermore, microbial degradation products of root exudates, rather than the root exuded plant metabolites themselves, might act as potent rhizosphere signals. For instance, benzoxazinoids exuded from cereal roots can be converted into stable 2-aminophenoxazin- 3-one, which has strong antimicrobial and allelopathic activities (Atwal *et al.,* 1992; Macıas *et al.,* 2005). In addition, it is plausible that certain root exudation products stimulate the production of signalling and/or biocidal compounds by rhizosphere microbes (Cameron *et al.,* 2013). Therefore, ignoring the rhizosphere microbiome by studying sterile root systems limits the identification of novel semiochemicals that can shape microbial communities and their activities in the rhizosphere (Prithiviraj *et al.,* 2007).

To date, various methods have been described to collect root exudates from non-sterile rhizosphere soil. These methods have been used mostly to determine total organic carbon and/or nitrogen content (Phillips *et al.,* 2008; Yin *et al.,* 2014), or to assay for biological response activity (Khan *et al.,* 2002). Some of these studies revealed biological activities by amino acids, organic acids and other extractable elements (Haase *et al.,* 2008; Chaignon *et al.,* 2009; Bravin *et al.,* 2010; Shi *et al.,* 2011; Oburger *et al.,* 2013); however, the lack of comprehensive metabolic analyses of non-sterile rhizosphere soil limits our ability to establish relationships between microbial community structure and rhizosphere chemistry. Here, we describe a method for untargeted metabolite profiling from non-sterile rhizosphere soil with high microbial diversity. We have developed methods for extraction of polar and apolar metabolites that do not cause detectable levels of damage to root cells, nor affect the viability of soil- and rhizosphere-inhabiting microbes. Using UPLC-Q-TOF mass spectrometry followed by uni- and multivariate statistical analyses, we demonstrate quantitative and qualitative differences in metabolite profiles between soil without plants and soil with plants, and putatively identify the rhizosphere metabolites that are enriched in extracts from soil hosting Arabidopsis and Zea mays (maize). We discuss the potential of this technique for discovering semiochemicals that shape microbial community structure and activity in the rhizosphere.

RESULTS

Development of a plant cultivation system for the extraction of rhizosphere chemicals We used the model plant species A. thaliana (Arabidopsis) to develop a plant cultivation system that is suitable for the extraction of rhizosphere chemicals. Individual plants were grown for 5 weeks in 30-ml plastic tubes with drainage holes in the bottom (Figure 1). As Arabidopsis naturally grows in sandy soils (Lev-Yadun and Berleth, 2009), the tubes contained a homogenous 1 : 9 (v/v) mixture of fresh M3 compost and sand. Control tubes without plants were included for the extraction of chemicals from control soil. All tubes were placed in individual trays, in order to prevent any cross-contamination of microbes and chemicals (Figure 1). Each tube was watered once per week (5 ml) from the base, with a final watering 3 days before sampling (relative water content after sampling of 88 _ 4.5% per g). This watering regime provided reproducible levels of relative water content at the time of sampling. Under these conditions, flushing the tubes with 5 ml of water or extraction solution (see below) consistently yielded 4.0–4.5 ml collected volume after 1 min of incubation.

Microbial diversity of roots and rhizosphere soil, and rhizosphere effect

Root-derived chemicals mediate the rhizosphere effect (Jones *et al.,* 2009; Bakker *et al.,* 2013). To verify whether plants in our cultivation system showed a rhizosphere effect, we extracted DNA from control soil (without plants) and Arabidopsis roots plus adhering rhizosphere soil. Thus, the ‘root plus rhizosphere’ samples capture the microbial diversity of the rhizosphere, the rhizoplane and the root cortex. Paired-end

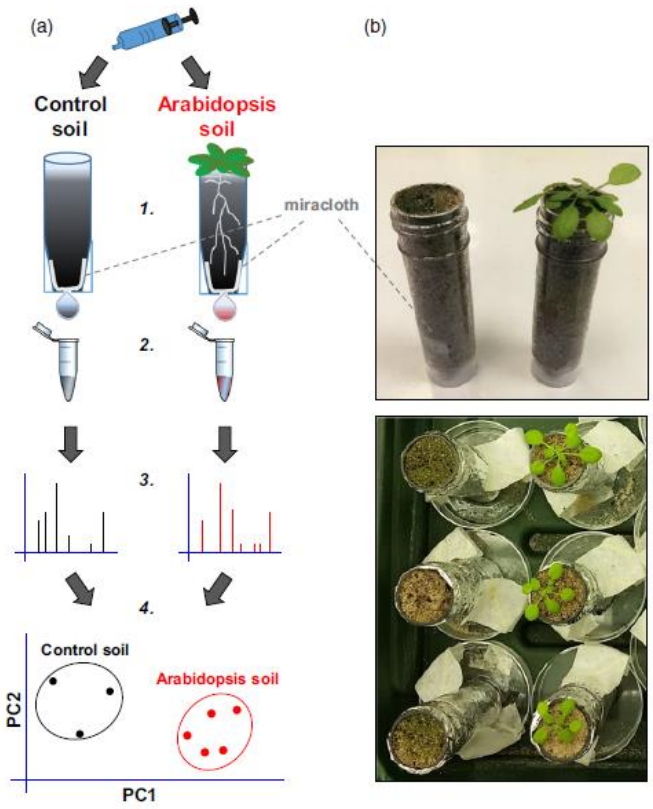

Figure 1. Experimental growth system and analytical approach for comprehensive chemical profiling of non-sterile rhizosphere soil. (a) 1. Collection tubes (30 mL) with holes in the bottom (7 mm) covered by Miracloth were filled with a sand : compost mixture (9 : 1, v/v) and wrapped in aluminium foil to prevent excess algal growth. Individual Arabidopsis plants (Col-0) were grown for 5 weeks in tubes. Additional tubes containing control soil without plants were maintained under similar conditions. 2. After the application of 5 mL of extraction solution, metabolite samples were collected for 1 min, centrifuged and freeze-dried. 3. Concentrated samples were analysed by ultra-high-pressure liquid chromatography coupled with quadrupole time-of-flight mass spectrometry (UPLC-Q-TOF). 4. Multi- and univariate statistical methods were used to determine qualitative and quantitative differences between extracts from control soil and Arabidopsis soil. The selection of ions by statistical difference and fold-change between soil types enabled the putative identification of metabolites that were enriched in non-sterile rhizosphere soil. (b) Photographs of the experimental system. Top: tubes after 4.5 weeks of growth. Bottom: tubes after 3 weeks of growth taped onto Petri dishes to prevent any cross contamination of metabolites and microbes.

250-bp MiSeq Illumina sequencing of amplified partial 16S rRNA genes was used to profile microbial communities. A total of 2 280 754 raw sequences were obtained with an average of 285 094 per sample. Of these, 1 693 274 reads passed quality controls, chimera removal and singleton removal. Operational taxonomic units (OTUs) were generated by clustering at 97% similarity, and were cross-referenced against the Greengenes 13.8 database (DeSantis *et al.,* 2006), yielding a total of 3863 OTUs. Rarefaction analysis (Figure S1) indicated sufficient sequencing depth to capture the majority of OTUs. Dominant bacterial taxa at the phylum level were Actinobacteria (10.0% across all samples) and Proteobacteria (87.8%), mostly comprising a-, b- and c-proteobacteria (17.1, 44.8 and 25.3%, respectively), whereas at the family level we detected Burkholderiaceae (16.6% across all samples), Oxalobacteraceae (16.4%), Pseudomonadaceae (14.6%) and Xanthomonadaceae (10.3%; Figure S2). In addition, we detected ten families of the Rhizobiales (9.1%), including Bradyrhizobiaceae (3.4%) and Rhizobiaceae (1.6%). Many of these phyla and families have previously been reported to be associated with plant roots (Lundberg *et al.,* 2012; Bulgarelli *et al.,* 2015), illustrating that the soil substrate of our cultivation system harbours a microbiome that is typical for microbe-rich soil. To investigate whether the growth system produced a rhizosphere effect by plant roots, we analysed samples for statistically significant differences in OTUs between 'root plus rhizosphere' samples and soil samples. To minimize confounding effects from low-abundance OTUs, data were filtered to include only sequences that appeared (i) more than five times across 30% of the samples, and (ii) more than 20 times across all samples, resulting in a final selection of 662 OTUs. Principal coordinate analysis (PCoA) using Uni-Frac distances revealed a difference in phylogenetic similarity (Figure 2a) between the 'root plus rhizosphere' samples and the control soil samples, which was confirmed by PERMANOVA analysis ($F_{1,6}$, P = 0.023). A total of 178 OTUs were found to differ significantly in relative abundance between 'root plus rhizosphere' and control soil samples, including an increased abundance of 17 Rhizobiales OTUs in root samples (e.g. Rhizobiaceae, Methylobacteriaceae, Hyphomicrobiaceae, Phyllobacteriaceae and Bradyrhizobiaceae; Figure 2b). Although the mean Shannon diversity index did not differ between soil and 'root plus rhizosphere' samples (3.58, SD = 0.001; 3.22, SD = 0.001, respectively; Student's t-test, t(3) = 0.92, P = 0.39), the mean OTU richness of 'root plus rhizosphere' samples (717, SD = 2.1) was significantly lower than that of control soil samples (1177, SD = 2.3; Student's t-test, t (3) = 3.51, P = 0.04; Figure S1), showing an influence of roots on the microbial communities. Hence, the presence of plant roots in our experimental system produces a statistically significant rhizosphere effect.

Selection of extraction solutions that do not cause detectable damage to root and microbial cells

Plant-derived metabolites range from polar/hydrophilic (e.g. organic and amino acids, nucleotides) to apolar/hydrophobic (e.g. lipids and phenylpropanoids). Consequently, comprehensive metabolic profiling of rhizosphere soil requires extraction solutions of different polarities; however, the extraction solution should not damage cells from roots or soil microbes, which could contaminate the extract with cellular metabolites

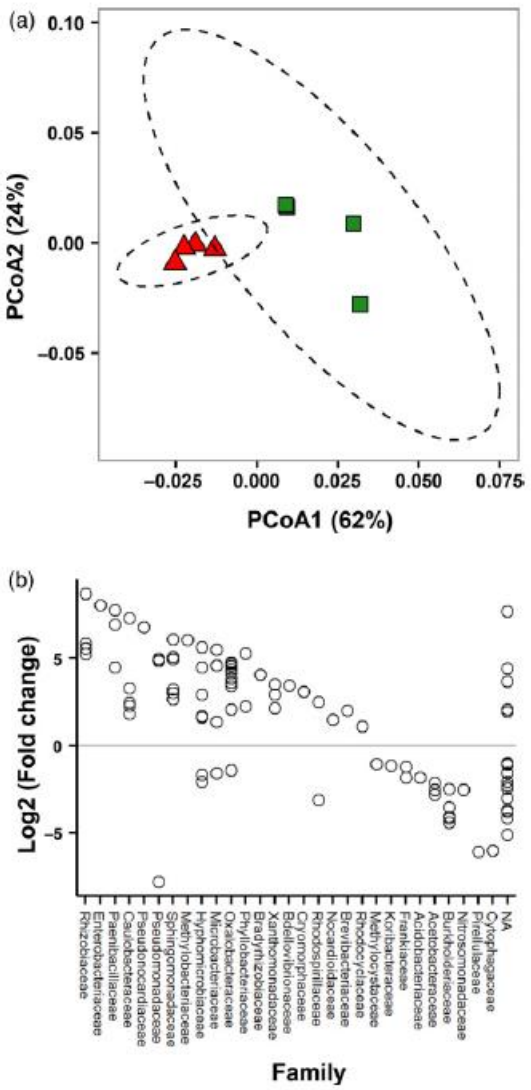

Figure 2. Rhizosphere effect of Arabidopsis in the cultivation system based on 16S rRNA gene sequencing Shown are comparisons of bacterial communities between samples from control soil (without roots) and root samples plus adhering rhizosphere soil. (a) Principal coordinate analysis of operational taxonomic units (OTUs) in root plus rhizosphere samples (red) and in control soil samples (green). Ordinations were performed using weighted UniFrac distances. PERMANOVA analysis showed that the root and control soil samples differed significantly (P = 0.023). (b) OTUs that differ in relative abundance between root plus rhizosphere samples and control soil samples. OTUs with positive fold changes are more abundant in the root plus rhizosphere samples than in the control samples. Results are plotted by family for OTUs that showed a significant difference in abundance as calculated using DESeq2, and corrected for false discovery. Only OTUs that have a mean count of ≥20 are shown for clarity. NA, taxonomy not available.

(for a conceptual model, see Figure S3). Although water-based solutions without organic solvents are unlikely to cause cellular damage, they are unsuitable for extracting apolar (hydrophobic) metabolites. Conversely, solutions containing organic solvents extract apolar compounds, but risk cell damage by destabilization of membrane lipids (Patra *et al.,* 2006). With a polarity index of 5.1, methanol (MeOH) is capable of extracting polar and apolar metabolites (Figure S3). Accordingly, we selected MeOH as the organic solvent in our extraction solutions.

To test whether exposure to the MeOH-containing extraction solutions has a damaging effect on plant roots, we incubated intact roots of Arabidopsis for 1 min in acidified extraction solutions with different MeOH concentrations [0, 50 and 95% (v/v) MeOH + 0.05% (v/v) formic acid]. As a negative control, tissues were incubated for 1 min in water. To minimize root damage prior to treatment, roots were collected from agar-grown plants. As a positive control for cell damage, tissues were wounded before incubation. After incubation, tissues were transferred to sterile water for the quantification of electrolyte leakage, which is a sensitive method to quantify cell damage in Arabidopsis (Pétriacq *et al.,* 2016a). As shown in Figure 3a, none of the extraction solutions increased the level of electrolyte leakage in comparison with water-incubated roots (Figure 3a). Hence, 1-min exposure to the MeOH-containing solutions does not induce ion leakage from the root cells of Arabidopsis.

To investigate further the potentially damaging effects of the MeOH-containing solutions on root cell integrity, we carried out microscopy studies. Based on the assumption that cell damage by MeOH would permeabilize root cells and cause the denaturation of cytoplasmic proteins, we used the fluorescence of a C-terminal fusion between the cytoplasmic aspartyl-tRNA synthetase IBI1 and YFP as a marker for root cell integrity (Luna *et al.,* 2014). Roots of 2-week-old 35S::IBI1:YFP plants were carefully removed from MS agar medium, incubated for 1 min in extraction solutions or water (negative control), and analysed for YFP fluorescence (Figure S4). As a positive control for cell damage, 35S::IBI1:YFP roots were incubated for 15 min in 100% MeOH. YFP fluorescence in roots incubated in acidified 0% MeOH and 50% MeOH solutions was similar to roots incubated for 1 min in water (negative control). Some roots incubated in acidified 95% MeOH showed a weaker YFP signal, although this reduction was less severe than the near complete loss of YFP fluorescence in roots after incubation for 15 min in 100% MeOH (positive control). Thus, 1-min exposure to the 0 and 50% MeOH solutions does not have detectable effects on root cell integrity, which is in line with our conductivity measurements (Figure 3).

To investigate whether the extraction solutions affect soil microbes, control and Arabidopsis soils were drenched for 1 min with the extraction solutions, and microbial viability was tested by dilution plating onto (non-)selective LB agar plates. The viability of culturable soil bacteria was quantified by colony counting on non-selective plates. To test impacts on specific rhizosphere-colonizing bacterial strains, the Gram-negative Pseudomonas (P.) simiae WCS417r (formally known as P. fluorescens WCS417r; Berendsen *et al.,* 2012) and the Gram-positive Bacillus (B.) subtilis 168 (Yi *et al.,* 2016) were introduced into separate

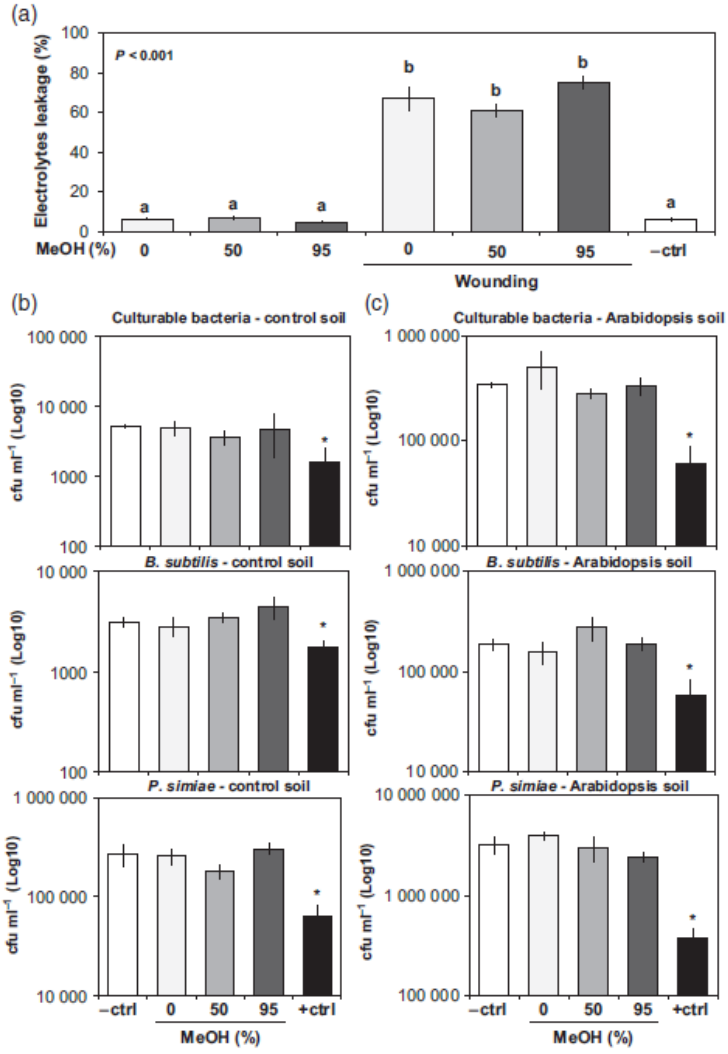

Figure 3. Effects of methanol (MeOH)-containing extraction solutions on electrolyte leakage from Arabidopsis roots (a) and viability of soil microbes (b, c). (a) Quantification of electrolyte leakage from Arabidopsis roots after incubation for 1 min in acidified extraction solutions containing 0, 50 or 95% MeOH (v/v) and 0.05% formic acid (v/v). The negative control treatment (–ctrl) refers to intact roots that had not been exposed to any extraction solution. As a positive control treatment for cell damage, wounding was inflicted prior to incubation by cutting roots with a razor blade. Shown are average levels of conductivity (n = 4, SEM), relative to the maximum level of conductivity after tissue lysis (set at 100%). Statistically significant differences between treatments were determined by a Welch's F-test for ranked data (P values indicated in the upper left corner), followed by Games–Howell posthoc tests (P < 0.05; different letters indicate statistically significant differences). (b, c) Effects of MeOH-containing extraction solutions on viability of soil (b) and rhizosphere (c) microbes. Shown are average values of colony forming units (CFUs) per g of soil for culturable soil bacteria, Bacillus subtilis 168 and Pseudomonas simiae WCS417r, from extraction solution-treated soils (n = 3, SEM). Asterisks indicate statistically significant differences between negative control (water-flushed soil) and the corresponding treatment (P < 0.05, Student's ttest). In all cases, only positive controls (i.e. incubation in 95% MeOH for 45 min) showed statistically significant differences.

tubes 2 days prior to treatment with extraction solution, and plated onto selective agar plates after the application of extraction solution. The CFUs from solution-treated soils were compared with water-treated soils (1 min; negative control), as well as soils that had been treated for 45 min with 95% MeOH (positive control for microbial cell damage). Whereas the 45-min incubation with 95% MeOH reduced bacterial counts by 10- to 100-fold, none of the acidified MeOH solutions had a statistically significant effect on CFU counts from either soil type in comparison with water-treated soil (Figure 3b,c).

In summary, our control experiments for cell damage show that 1-min extraction with the 0 and 50% MeOH solutions does not have detectable impacts on root cell integrity and viability of soil bacteria. Direct exposure of roots to acidified 95% MeOH solution does have a minor effect on root cell integrity, however, as evidenced by the faint loss of YFP fluorescence (Figure S4). Accordingly, we cannot exclude the possibility that metabolic profiles obtained with the 95% MeOH solution are contaminated with cellular metabolites from damaged root cells.

Untargeted metabolic profiling of control and Arabidopsis soil by UPLC-Q-TOF mass spectrometry

Soil samples were extracted with the three acidified solutions (0.05% formic acid, v/v), containing increasing MeOH concentrations (0, 50 and 95% MeOH). Chemical profiles were obtained by untargeted UPLC-Q-TOF mass spectrometry (MS), using MS^E profiling technology (Appendix S1), which enables the simultaneous acquisition of both intact parent ions and fragmented daughter ions (Glauser *et al.,* 2013; Gamir *et al.,* 2014a,b; Planchamp *et al.,* 2014; Pétriacq *et al.,* 2016a,b). Prior to statistical analysis, chemical profiles of ion intensity were aligned and integrated using XCMS (Smith *et al.,* 2006; Pétriacq *et al.,* 2016a,b). Similarities and differences in ion intensities from both positive (electrospray ionization source, ESI_+, 17 518 cations) and negative ($ESI_–$, 19 488 anions) ionization modes were first examined by multivariate data analysis, using METABOANALYST 3.0 (Xia *et al.,* 2015). Unsupervised three-dimensional principal component analysis (3D-PCA) separated samples from both soil types that had been extracted with the same solution (Figure 4a), indicating global metabolic differences between control and Arabidopsis soil. These differences were reproducible between three independent experiments (Figure S5). Extractions with the 95% MeOH

solution resulted in higher levels of variation than extractions with the 50% and 0% MeOH solutions (Figures 4a and S5). Cluster analysis (Pearson's correlation) revealed complete segregation between control soil samples and Arabidopsis soil samples analysed in positive ionization mode (ESI+), whereas samples analysed in negative ionization mode (ESI–) showed partial segregation between both these soil types. Although samples from the same extraction solution clustered relatively closely within the dendrogram, extracts from the 95% MeOH solution showed more variation than the other solutions (Figure 4b). Finally, we used supervised partial least squares discriminant analysis (PLS-DA) to compare metabolite profiles

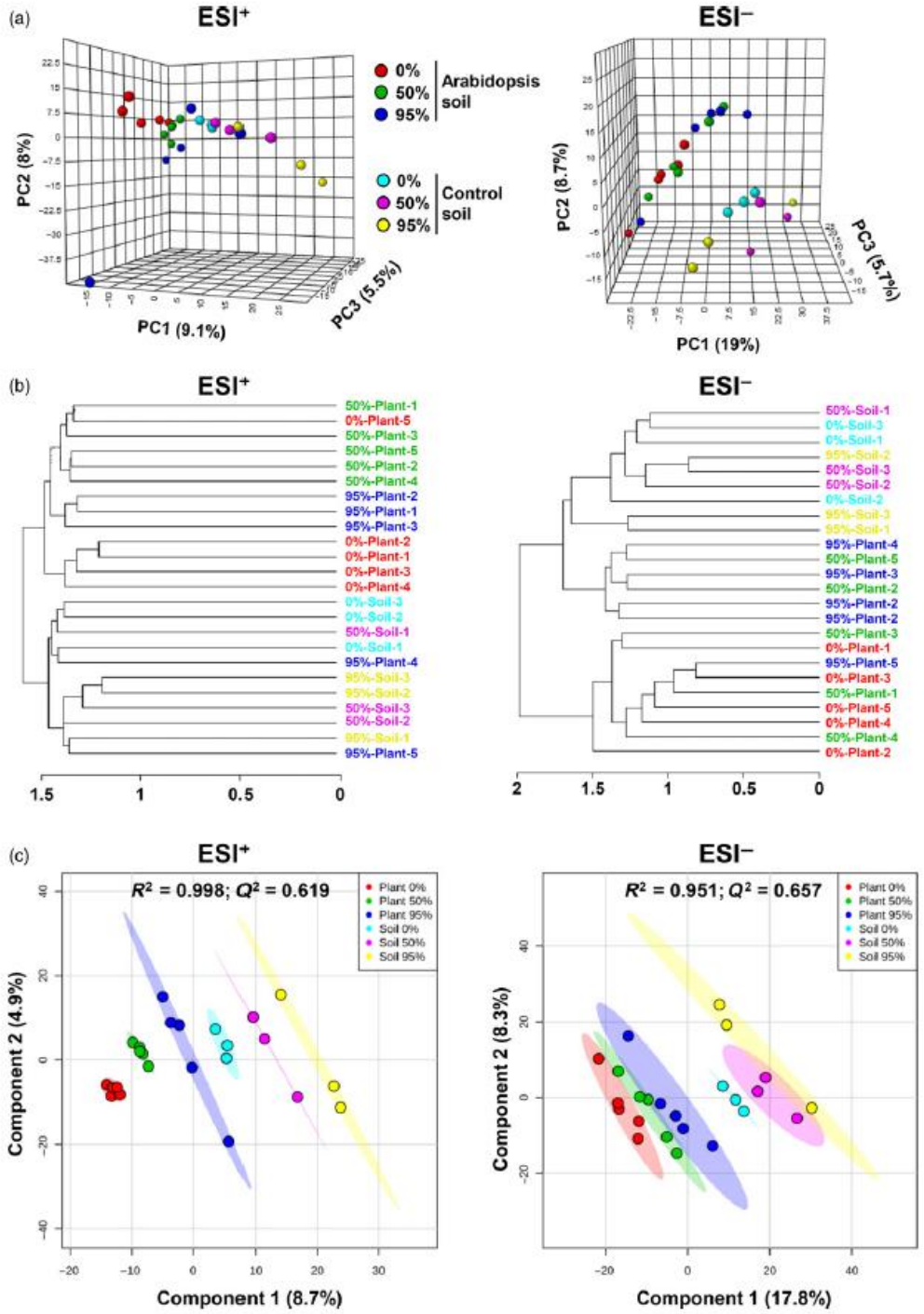

Figure 4. Global differences in metabolite profiles between extracts from control soil ('soil') and Arabidopsis soil ('plant'). Shown are multivariate and hierarchical cluster analyses of mass spectrometry data from extracts with different extraction solutions (indicated by % MeOH). Ions (m/z values) were obtained by UPLC-Q-TOF analysis in both positive (ESI+) and negative (ESI–) ionization mode. Prior to analysis, data were median-normalized, cube root-transformed and Pareto-scaled. (a) Unsupervised three-dimensional principal component analysis (3D-PCA). Shown in parentheses are the percentages of variation explained by each principal component (PC). (b) Cluster analysis (Pearson's correlation). (c) Supervised partial least squares discriminant analysis (PLS-DA). R2 and Q2 values indicate the correlation and predictability values of PLS-DA models, respectively.

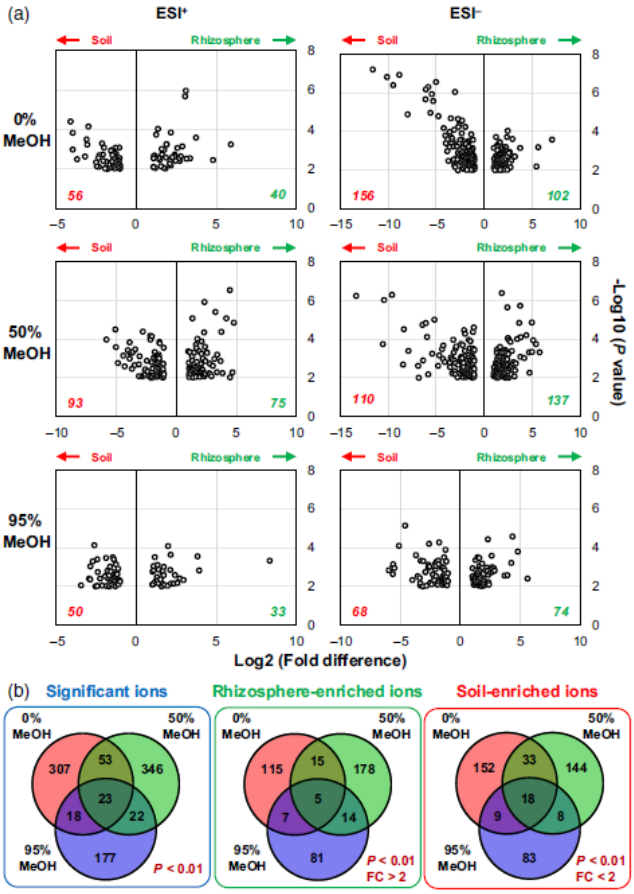

Figure 5. Quantitative differences in metabolite abundance between extracts from control soil and Arabidopsis soil. (a) Volcano plots expressing statistical enrichment of ions (Welch's t-test) as a function of fold difference in control soil (red; 'soil') and Arabidopsis soil (green; 'rhizosphere'). Data shown represent positive (ESI+) and negative (ESI–) ions from extractions with different solutions (indicated by % MeOH). Cut-off values were set at P < 0.01 (–Log10 = 2) and fold change > 2 (Log2 = 1). (b) Venn diagrams showing overlap in ions (cations and anions combined) that significantly differ between control and Arabidopsis soil samples (left panel; P < 0.01, Welch's t–test; without fold-change threshold), enriched in extracts from Arabidopsis soil (middle panel; >2-fold enrichment to soil at P < 0.01, Welch's t-test) and enriched in control soil (right panel; <2-fold enrichment to rhizosphere at P < 0.01, Welch's t-test).

between samples from control soil and Arabidopsis soil (Figure 4c). Comprehensive analysis of all samples revealed a clear separation between all different soil/ solution combinations, in both the ESI+ and ESI– data. The corresponding PLS-DA models displayed high levels of correlation (R2 ESI+ = 0.998; R2 ESI– = 0.951) and predictability (Q2 ESI+ = 0.619; Q2 ESI– = 0.657). Binary comparisons between control and Arabidopsis soil for each extraction solution confirmed these differences, each with high levels of correlation (R2 > 0.94) and predictability (Q2 > 0.59) of the PLS-DA models (Figure S6). As was also clear from 3D-PCA and Pearson's correlation analyses, however, samples extracted with the 95% MeOH solution were more variable than extracts obtained with the 0 and 50% MeOH solutions (Figure 4a–c). The enhanced variation between samples extracted with the 95% MeOH solution is consistent with our finding that direct exposure of roots to 95% MeOH solution causes minor cell damage (Figure S4). Together, our results show consistent differences in polar and apolar metabolite composition between control soil and Arabidopsis soil, indicating a global influence of roots on the chemical composition of the soil in our cultivation system.

Quantitative differences in metabolites between extractions from the rhizosphere and from control soil

Quantification of the total number of detected ions (m/z values) yielded marginally higher numbers from samples of control soil compared with that of Arabidopsis soil (Figure S7a). A substantial fraction could be detected in both soil types (66.9, 64.1 and 49.4% for the 0, 50 and 95% MeOH solutions, respectively; Figure S7a), indicating a large number of metabolites that were present in both rhizosphere and control soil. Ions that were uniquely present in one or more sample from Arabidopsis soil were most abundant in extractions with the 95% MeOH solution (6448), followed by the 50% MeOH solution (4362) and the 0% MeOH solution (3991; Figure S7a). To select for ions that were statistically over- or under-represented in Arabidopsis soil, we constructed volcano plots that expressed statistical significance of each ion (m/z value) against foldchange between both soil types (Figure 5a). Using a statistical threshold of P < 0.01 (Welch's t-test) and a cut-off value of greater than twofold change (Log2 > 1), the numbers of ions enriched in control soil were generally higher than those enriched in Arabidopsis soil (Figure 5a). Furthermore, there was relatively little overlap in differentially abundant ions between extraction solutions (P < 0.01, Welch's t-test, Figures 5b and S7). This pattern was equally clear for ions that were specifically enriched in either soil type (P < 0.01, Welch's t-test, greater than twofold change; Figures 5b and S7b, middle and right), illustrating the fact that the acidified solutions extracted different classes of metabolites. The 50% MeOH solution yielded the highest number of rhizosphere-enriched ions (178), followed by the 0% MeOH solution (115) and 95% MeOH solution (81). As the 50% MeOH solution also yielded relatively low levels of variability between

replicate samples (Figures 4 and S5), our results suggest that this solution is most suitable for the extraction of rhizosphere-enriched metabolites.

Composition of rhizosphere- and control soil-enriched metabolites

To study which metabolite classes drive the global differences between the rhizosphere and control soil (Figures 4 and 5), we pooled the top-20 ranking ions from each volcano plot, ranked by fold change and statistically significant difference between control and Arabidopsis soil, resulting in a total of 120 metabolic markers for each soil type. To enhance statistical stringency, ions were subsequently filtered by statistical significance between all soil/ solution combinations (ANOVA; $P < 0.01$), using a Benjamini–Hochberg correction for false-discovery rate (FDR). The final selection yielded a total of 76 rhizosphere enriched ions and 75 control soil-enriched ions. MARVIS (Kaever *et al.,* 2012) was used to correct for adducts and/or C isotopes (tolerance: m/z = 0.1 Da and retention time = 10 sec), after which the predicted masses were used for putative identification (Table S1), using METLIN, PubChem, MassBank, Lipid Bank, ChemSpider, Kegg, AraCyc and MetaCyc databases (Kaever *et al.,* 2009, 2012; Gamir *et al.,* 2014a,b; Pastor *et al.,* 2014; Pétriacq *et al.,* 2016a,b). To obtain a global profile of soil- and rhizosphere-enriched chemistry, putative compounds were assigned to different metabolite classes (Figure 6). Putative chemicals that are unlikely to accumulate as natural produ cts in (rhizosphere) soil, such as synthetic drugs or mammalian hormones, were excluded from these profiles (Table S1). In comparison with control soil, Arabidopsis soil was enriched with ions that putatively annotate to flavonoids (8 versus 2%), lipids (33 versus 6%) and alkaloids (5% in Arabidopsis soil only; Figures 6 and S8; Table S1), which supports the notion that rhizosphere soil is enriched with plant-derived metabolites. The global composition of control soil showed a higher fraction of metabolites that could not be annotated (Figures 6 and S8; Table S1), probably because of an under-representation of soil metabolites in publically available databases.

Applicability of the method to maize in agricultural soil

Having established that our method is suitable for detecting rhizosphere-enriched metabolites from Arabidopsis, we investigated whether the method could be applied to profile rhizosphere metabolites from a crop species (maize) in agricultural soil. To this end, the cultivation system was up-scaled to 50-ml tubes that were filled with a mixture of agricultural soil from arable farmland (Spen Farm, Leeds, UK) and perlite (75 : 25, v/v). The perlite was added to improve the drainage of the soil, which improved plant growth and ensured that sufficient solution was collected from the base of the tubes within 1 min of the application of extraction solution. Maize plants were grown for 17 days, and rhizosphere chemistry was extracted using the 50% MeOH solution (plus formic acid 0.05%, v/v). Further validation experiments showed that 1-min exposure of maize roots to this solution did not lead to increased electrolyte leakage (Figure 7a). Comparative analysis of metabolites by UPLC-Q-TOF identified a total of 6071 cations (ESI_+) and 9006 anions (ESI_-). 3D-PCA showed complete separation between samples from control (red) and maize (green) soil (Figure 7b). Quantitative differences were determined by volcano plots (Welch's t-test, $P < 0.01$: fold change > 2), revealing 287 cations (ESI_+) and 197 anions (ESI_-) that were statistically enriched in maize soil (Figure 7c). Cross-referencing the 100 most significant ions (top 50 anions plus top 50 cations) against public

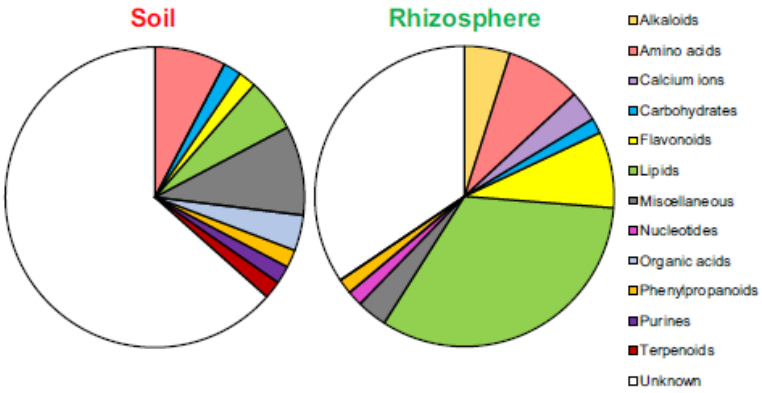

Figure 6. Composition of putative metabolites enriched in control soil (left) or Arabidopsis soil (right). Differentially abundant ions were selected from the top- 20 ranking ions of each volcano plot (Figure 5a) and filtered for statistical significance between all soil/extraction solution combinations (ANOVA with Benjamini–Hochberg FDR; $P < 0.01$). The resulting 76 rhizosphere-enriched ions and 75 control soil-enriched ions were corrected for adducts and/or C isotopes (tolerance: m/z = 0.1 Da and retention time = 10 sec), and cross-referenced against publicly available databases for putative identification. A comprehensive list of all rhizosphere- and soil-enriched markers is presented in Table S1. Multiple ions putatively annotating to the same metabolite were counted additively towards the metabolite classes in the pie charts. Putative metabolites that are unlikely to accumulate as natural products in (rhizosphere) soil (e.g. synthetic drugs or mammalian hormones) were not included in the final selection presented. Miscellaneous: putative metabolites that do not belong to any of the other metabolite classes listed. Unknown: ion markers that could not be assigned to any known compound.

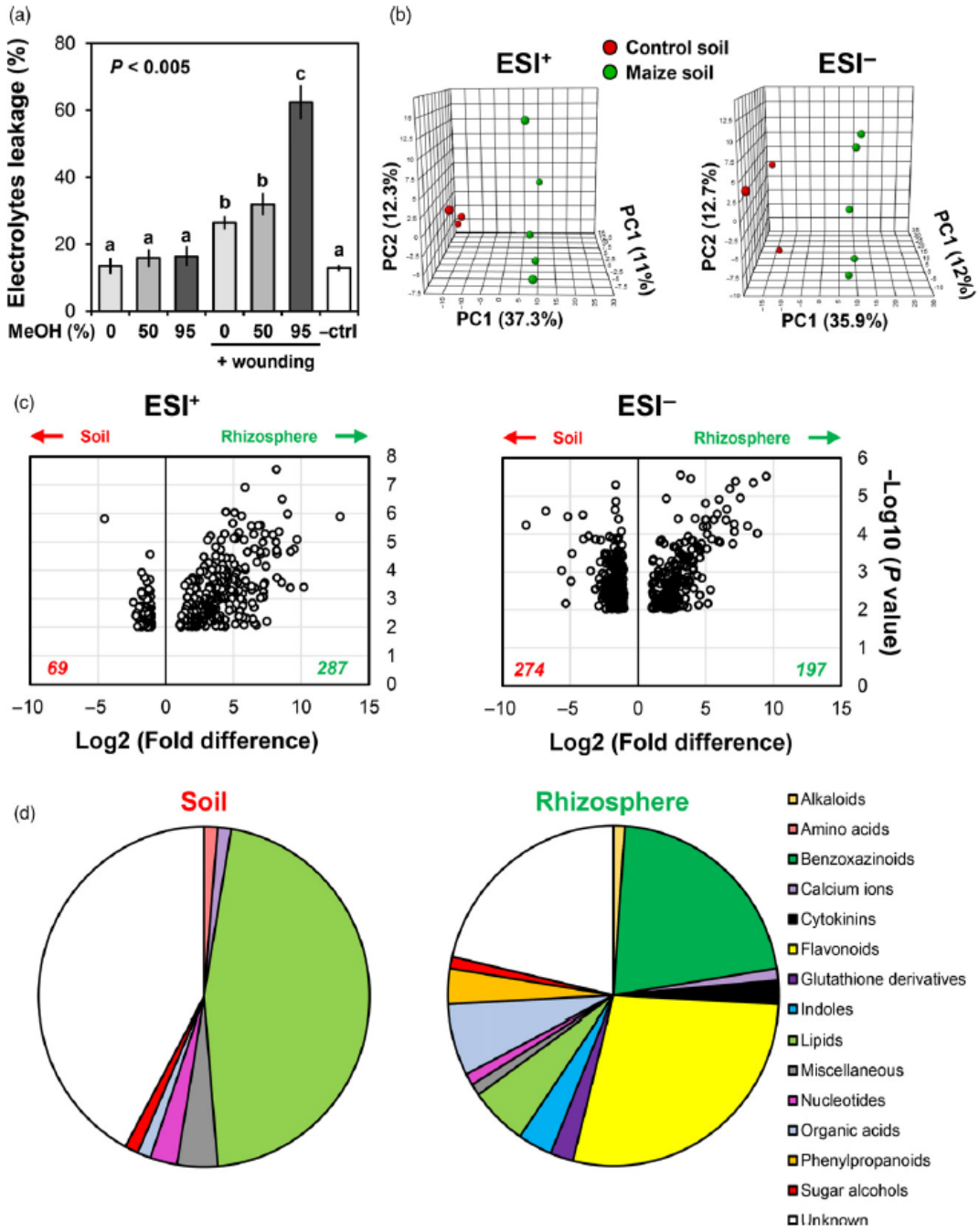

Figure 7. Applicability of the profiling method for maize in agricultural soil. The experimental system for extracting soil chemistry was based on 50-mL collection tubes filled with a mixture of agricultural soil from arable farmland and perlite (75 : 25, v/v). Samples were extracted with the 50% MeOH (v/v) solution 17 days after planting. (a) Quantification of maize root damage after direct exposure to the extraction solutions. Five-day-old maize roots were incubated for 1 min in acidified extraction solutions containing 0, 50 or 95% MeOH (v/v) and tested for electrolyte leakage by conductivity. For details, see the legend to Figure 3a. Shown are average levels of conductivity (n = 4, SEM), relative to the maximum level of conductivity after tissue lysis (set at 100%). Statistically significant differences between treatments were determined by a Welch's F-test for ranked data (P values indicated in the upper left corner of each panel), followed by Games–Howell post-hoc tests (P < 0.05; different letters indicate statistically significant differences). (b) Unsupervised 3D-PCA, showing global differences in metabolic profiles between control soil (red) and maize soil (green). Shown are data from extracts with the 50% MeOH (v/v) extraction solution. For further details, see the legend to Figure 4. (c) Volcano plots expressing statistical enrichment of ions (Welch's t-test) as a function of fold difference in control soil (red; 'soil') and maize soil (green; 'rhizosphere'). Cut-off values were set at P < 0.01 (–Log10 = 2) and fold change > 2 (Log2 = 1). (d) Relative composition of putative metabolite classes enriched in control soil (left) or maize soil (right). Differentially abundant metabolites were selected from the top-50 ranking ions of each volcano plot (ESI+ and ESI–; c), corrected for adducts and/or C isotopes (tolerance: m/z = 0.1 Da and retention time = 10 s), and cross-referenced against publicly available databases for putative identification. A comprehensive list of all rhizosphere- and soil-enriched markers is presented in Table S2. Putative metabolites that unlikely accumulate as natural products in (rhizosphere) soil (e.g. synthetic drugs or mammalian hormones) were not included in the final selection presented. For further details, see the legend to Figure 6.

samples. Most metabolic markers could be putatively identified (Table S2) and annotated to different metabolite classes (Figure 7d). As described for the profiling of the Arabidopsis rhizosphere (Figure 6), these final profiles did not include putative compounds that are unlikely to accumulate in (rhizosphere) soil, such as synthetic drugs (Table S2). Strikingly, a relatively large fraction of maize rhizosphere-enriched ions could be annotated to flavonoids (28%) and benzoxazinoids (21%), which mediate below-ground interactions (Neal *et al.,* 2012; Robert *et al.,* 2012; Neal and Ton, 2013) For instance, HBOA, DIBOA and HMBOA displayed strong rhizosphere enrichment in maize soil samples (Figure S8), and are known to be produced by maize roots (Marti *et al.,* 2013). Thus, our profiling method is sufficiently robust and sensitive to profile plant-derived rhizosphere chemicals from a crop species in agricultural soil.

Profiling chemistry in distal rhizosphere fractions

The rhizosphere was defined by Lorenz Hiltner in 1904 as 'the soil compartment influenced by the root' (Smalla *et al.,* 2006); however, many rhizosphere studies focus exclusively on soil that is closely associated with plant roots (after the removal of loosely associated soil), which may not encompass the total rhizosphere as more distal and loosely associated soil could still be influenced by root-derived chemistry. To investigate whether our profiling method detects chemical influences beyond soil that is closely associated with roots, we used an alternative growth system that separated roots from distal soil (Figure S9). Maize plants were grown in small, fine mesh bags within larger 150-ml tubes containing soil (see Appendix S1), which prevented outward root growth, yet allowed for the passage of root-derived chemicals and microbes into the distal soil. Similar plant-free tubes were constructed as no-plant controls. After 24 days of growth the mesh bags were carefully removed, and then metabolites were extracted from the remaining distal soil that had surrounded the mesh bags using the 50% MeOH extraction solution. As a control for whole-soil fractions, metabolites from empty and maize-containing tubes were extracted before removing the mesh bag from the tube, as described earlier. Thus, the experimental design allowed for comparison between four soil fractions: (i) distal soil surrounding mesh bags without roots; (ii) distal soil surrounding mesh bags with maize roots; (iii) whole soil from tubes containing mesh bags without roots; and (iv) whole soil from tubes containing mesh bags with maize roots. Extracts were analysed by UPLC-Q-TOF in ESI− (26 011 anions) and subjected to unsupervised PCA (Figure S9b). Comparison of whole-soil fractions confirmed a clear separation between plant-free and maize soil samples, illustrating the chemical rhizosphere effect of maize. Although less pronounced than the whole-soil fractions, PCA of the distal soil fractions still revealed separate clustering between plant-free and maize soil (Figure S9b), indicating that the chemical influence of the rhizosphere extended beyond the soil closely associated with roots. To verify this distant rhizosphere effect, we quantified levels of DIMBOA, which acts as a relatively stable rhizosphere semiochemical, influencing the behaviour of both rhizobacteria and arthropods (Neal *et al.,* 2012; Robert *et al.,* 2012). In comparison to both plant-free soil fractions, statistically higher quantities of DIMBOA were detected in both whole maize soil and distal maize soil (Figure S9c). Hence, DIMBOA acts as a mobile long-range rhizosphere signal that extends beyond soil that is closely associated with roots. Considering that maize roots contain high quantities of DIMBOA (Robert *et al.,* 2012), and that the distal soil was separated from the roots prior to chemical extraction with the 50% MeOH solution, this result also confirms that the 50% MeOH extraction solution does not have a damaging effect on maize roots, as exemplified by similar DIMBOA levels in whole maize soil and distal maize soil (Figure S9c).

DISCUSSION

Rhizosphere chemistry is a complex mixture of root exudation chemicals, their microbial breakdown products and the microbial breakdown products of soil-specific chemicals. Although it is known that microbial diversity in the rhizosphere can influence plant growth and health (Berendsen *et al.,* 2012), the chemical signals mediating these interactions remain poorly understood. The majority of root exudation studies are based on hydroponic and/or sterile growth systems Khorassani *et al.,* 2011; Kuijken *et al.,* 2014; Bowsher *et al.,* 2016). Although sterile growth systems are appropriate for the exact quantification of root-exuded plant chemicals (Kuijken *et al.,* 2014), these systems do not consider the importance of rhizosphere signals that are of microbial origin, such as microbial breakdown products of root exudates, or metabolites that are specifically produced by rhizosphere-inhabiting microbes. Consequently, linking rhizosphere chemistry with microbial communities and/or activities remains problematic when the biochemical diversity of the non-sterile rhizosphere is not considered (Oburger and Schmidt, 2016). Furthermore, although root exudation studies are increasingly relying on sensitive analytical methods (Khorassani *et al.,* 2011; Ziegler *et al.,* 2015; van Dam and Bouwmeester, 2016), the majority of these studies employ targeted analyses of specific compounds (e.g. organic and amino acids, coumarins) that do not address the biochemical diversity of rhizosphere soil. Recent advances in liquid chromatography, mass spectrometry, and uni- and multivariate data analysis have made it possible to conduct untargeted metabolic profiling of complex metabolite mixtures, such as root exudates and soil extracts (Khorassani *et al.,* 2011; Strehmel *et al.,* 2014; Swenson *et al.,* 2015; Ziegler *et al.,* 2015; van Dam and Bouwmeester, 2016). In this study, we employed untargeted UPLC-Q-TOF analysis of soil extracts, followed by uni- and multivariate data reduction to separate rhizosphere-specific chemistry from common soil chemistry. We show that this method is suitable to profile *in situ* rhizosphere chemistry from different plant species and soil types.

The microbial rhizosphere effect is driven by root exudation chemistry (Jones *et al.,* 2009). Accordingly, we verified whether our cultivation system supported the generation of a difference in microbial communities between control soil samples (without plant roots) and root samples plus adhering rhizosphere soil, using 16S rRNA gene sequencing. This analysis identified a total number of 3863 OTUs, which by rarefaction analysis appeared to be sufficient to cover the majority of dominant OTUs (Figure S1). Many of the taxa detected in our samples (e.g. Oxalobacteraceae, Pseudomonadaceae, Xanthomonadaceae and the Rhizobiaceae) are commonly associated with soil and/or plant roots (Lundberg *et al.,* 2012). Comparative analysis identified a range of OTUs with differential relative abundance between control soil and 'root plus rhizosphere' samples (Figure 2), which provided evidence for a rhizosphere effect in our experimental growth system. Many of the corresponding taxa have been linked to rhizosphere effects, such as an enhanced relative abundance of Oxalobacteraceae (Figures 2b and S2; Lundberg *et al.,* 2012; Bulgarelli *et al.,* 2015), as well as the Rhizobiales, which are commonly associated with plant roots (Hao *et al.,* 2016).

Our cultivation system was designed for the *in situ* extraction of chemicals from biologically complex nonsterile rhizosphere soils. The soil matrix for the Arabidopsis experiments consisted of a 9 : 1 (v/v) mixture of sand and compost, which is comparable with the sandy soil types of naturally occurring Arabidopsis accessions (Lev- Yadun and Berleth, 2009). This matrix also allowed relatively short collection times of the extracts (1 min), which was sufficient to recover 90% of the volume applied and prevents root damage through extended exposure to MeOH in the extraction solution. The soil matrix for the maize experiments contained agricultural soil from an arable farm field, which was supplemented with 25% (v/v) autoclaved perlite to prevent compaction, and allowed sufficient elution of metabolites over the 1-min extraction period. Using this system, we detected quantitative and qualitative differences in chemistry between extracts from control and maize soil (Figure 7), demonstrating that the method was applicable for the profiling of rhizosphere chemistry from a crop species in agricultural soil.

A major challenge for the *in situ* profiling of rhizosphere chemistry is to prevent damage of root cells and microbes during the extraction procedure that could otherwise contaminate the extract with metabolites that are not exuded from intact roots. Whereas water-based extraction solutions are unlikely to cause cellular damage, they are less suitable for the extraction of apolar metabolites. Conversely, solutions containing organic solvents extract apolar metabolites, but can damage cell membranes. With our limited understanding of root exudation chemistry in natural soil types, it remains difficult to distinguish between naturally exuded metabolites and metabolites leaking from damaged root tissues or lysed microbial cells. Therefore, we carried out a range of experiments to investigate whether the MeOH-containing extraction solutions caused cell damage: (i) quantification of root electrolyte leakage (Figure 3a); (ii) epifluorescence microscopy, to assess root cell integrity (Figure S4); (iii) dilution plating, to assess the viability of soil- and rhizosphere-colonising bacteria after incubation of the soil in extraction solutions (Figure 3b, c); and (iv) detection of plant-derived chemicals in root-free soil fractions (Figure S9). Firstly, exposure of both Arabidopsis and maize roots to the MeOH-containing solutions did not increase electrolyte leakage for the duration of the extraction procedure (1 min; Figures 3 and 7). Secondly, microscopic analysis of root cells from YFP-expressing Arabidopsis roots did not reveal any loss of cell integrity after 1 min of exposure to 0 and 50% MeOH-containing solutions (Figure S4). This assay did reveal a weak effect of the 95% MeOH solution, however, indicating that extraction of rhizosphere chemistry with this solution could affect root cell integrity. Thirdly, the extraction of control and Arabidopsis soil with the MeOH-containing extraction solutions did not reduce the viability of culturable soil microbes, nor did it affect the viability of the Gram-negative rhizobacterial strain P. simiae WCS417r and the Gram-positive rhizobacterial strain B. subtilis 168 (Figure 3b,c). Finally, using the 50% MeOH extraction solution and a compartmentalized growth system that separated maize roots from peripheral rhizosphere soil, we showed that the extraction of peripheral soil after the removal of maize roots yielded similar DIMBOA quantities as the extraction of soil containing maize roots (Figure S9c). As maize roots accumulate high quantities of DIMBOA (Robert *et al.,* 2012), this result further confirms that the 50% MeOH extraction solution does not damage maize roots in the soil. Accordingly, we conclude that 1 min of exposure to 0 or 50% MeOH extraction solution does not cause detectable levels of cell damage to roots and soil microbes that could contaminate the chemical profiles from the soils with intracellular metabolites.

Multivariate data analysis and clustering revealed that the variability between replicate extractions was lower for the 0 and 50% MeOH extraction solutions, compared with the 95% MeOH solution (Figure 4). This is consistent with our finding that direct exposure to this solution sometimes reduced YFP fluorescence in transgenic Arabidopsis roots (Figure S4). Data projection in volcano plots showed that extraction with the 50% MeOH solution yielded the highest number of rhizosphere-enriched ions, in comparison with other extraction solutions (Figure 5a). Hence, the 50% MeOH extraction solution performs best in terms of variability between extractions and total numbers of differentially detected ions. Quantitative analysis of MS profiles revealed slightly lower numbers of rhizosphere-enriched ions than control soil-enriched ions, which was apparent for both Arabidopsis (Figures 5 and S7) and maize (Figure 7). It is possible that this difference arises from the rhizosphere effect, which reduces bacterial richness (Figures S1 and S2), resulting in lower biochemical diversity in the rhizosphere (Prithiviraj *et al.,* 2007).

The sets of ions enriched in control and plant-containing soil differed substantially in composition (Figures 6 and 7). Interestingly, the number of ions annotated to putative metabolites from publicly available databases was higher for rhizosphere selection (Tables S1 and S2). We attribute this difference to the fact

that plant-containing soil is enriched with plant-derived metabolites, which are better represented in publicly available databases than soil-specific metabolites (Strehmel *et al.,* 2014; Swenson *et al.,* 2015). Indeed, the selection of putative rhizosphere metabolites from Arabidopsis contained a relatively high fraction of flavonoids, lipids and other amino acid-derived secondary metabolites, such as alkaloids and phenylpropanoids (Figure 6; Table S1), whereas the set of putative rhizosphere metabolites from maize included relatively large fractions of flavonoids and benzoxazinoids (Figure 7; Table S2). It should be noted, however, that the analytical method used in this study is limited by the putative identification of single ions. Unless the identity of a single metabolite is confirmed by subsequent targeted analyses, such as specific chromatographic retention time, fragmentation or NMR patterns, its annotation remains putative (i.e. inconclusive). The novelty of our method does not come from the applied mass spectrometry detection method, however, but from the combined use of the experimental design, extraction methods, mass spectrometry profiling and statistical techniques to deconstruct rhizosphere chemistry. Once a wider profile of rhizosphere chemistry has been established, targeted techniques can be used to confirm metabolite identities. Furthermore, where multiple putative metabolites annotate to the same metabolite class, a more reliable conclusion can be drawn about the involvement of this metabolite class. In our case, multiple rhizosphere ions could be annotated to the same plant metabolic pathways, suggesting that the overall rhizosphere profile is influenced by these plant metabolite classes. In support of this, previous studies have reported the presence of the same secondary compounds in plant root exudates (Hassan and Mathesius, 2012; Oburger *et al.,* 2013; Oburger and Schmidt, 2016; Szoboszlay *et al.,* 2016). Moreover, benzoxazinoids, such as DIMBOA, have previously been implicated to act as below-ground semiochemicals during maize–biotic interactions (Neal *et al.,* 2012; Robert *et al.,* 2012; Marti *et al.,* 2013). Hence, our method provides a new tool to explore rhizosphere semiochemicals for different plant species and soils.

Relatively few rhizosphere-enriched ions could be annotated to primary plant metabolites, such as proteinogenic amino acids or organic acids (Figures 6 and 7). Although these compounds are exuded in high quantities by roots (Rudrappa *et al.,* 2008; Ziegler *et al.,* 2015; van Dam and Bouwmeester, 2016), the microbial activity in the rhizosphere will quickly metabolize them, and the C18-UPLC separation is not optimal for the separation of (often very polar) primary metabolites. Above all, we stress that our method is not suitable for quantitative analysis of primary and secondary root exudates, for which sterile root cultivation systems are more appropriate (Kuijken *et al.,* 2014; Strehmel *et al.,* 2014). Our method should only be used for the profiling, identification and/or quantification of rhizosphere chemicals. These compounds can be microbial breakdown products of secondary metabolites in root exudates, but could equally well newly synthesized by rhizosphere-specific bacterial and fungal microbes. Using the experimental pipeline detailed in this paper, stable isotope labelling of plant root exudates via leaf exposure to $_{13}CO_2$ can potentially differentiate between these classes of rhizosphere metabolites, where plant-derived breakdown products are likely to retain higher levels of $_{13}C$ than newly synthesized microbial products. Furthermore, as is illustrated by our study, the method allows for the simultaneous assessment of rhizosphere chemistry and microbial composition, which can be used for genetic strategies that aim to establish a causal relationship between plant genotype, rhizosphere chemistry and microbial composition (Oburger and Schmidt, 2016). Such an approach would also advance studies on the effects of above-ground stimuli [such as light, atmospheric CO_2 and above-ground (a) biotic stresses] on below-ground plant–microbe interactions.

In summary, our study presents a straightforward method to obtain profiles of rhizosphere chemistry in nonsterile rhizosphere soil. The method is applicable to both model systems and soil-grown crops in agricultural soil. Considering that the microbial interactions in the rhizosphere can have both beneficial and detrimental effects on plant performance (Berendsen *et al.,* 2012; Cameron *et al.,* 2013), our method provides a powerful tool to advance rhizosphere biology and to decipher the chemistry driving plant–microbe interaction in complex non-sterile soils.

EXPERIMENTAL PROCEDURES

Chemicals and reagents All chemicals and solvents used for metabolomics were of mass spectrometry grade (Sigma-Aldrich, https://www.sigmaaldrich.c om). Other solvents were of analytical grade.

Experimental set-up of growth system Collection tubes for the Arabidopsis experiments were constructed by melting 7-mm holes in the base of 30-ml plastic tubes (Sterilin 128A; ThermoFisher Scientific, https://www.thermofisher.com), using a soldering iron (Figure 1). The drainage hole was covered with 4-cm_2 pieces of Millipore miracloth (pore size, 22–25 lm, VWR, https://uk.vwr.com) to avoid any loss of soil and to prevent outgrowth by roots. Tubes were filled with ~45 g of soil matrix, consisting of a homogenous 9 : 1 (v/v) mixture of sand (silica CH52) and dry compost (Levington M3), which is comparable with the sandy soil types of naturally occurring A. thaliana (Arabidopsis) accessions (Lev-Yadun and Berleth, 2009). To prevent cross contamination of rhizosphere microbes and chemicals between samples, each collection tube was placed onto an individual Petri dish (Nunclon™ Delta, 8.8 cm_2; ThermoFisher Scientific; Figure 1). Collection tubes were wrapped in aluminium foil to limit algal growth in the soil matrix. Seeds of Arabidopsis accession Columbia (Col-0) were stratified for 2 days in the dark in autoclaved water at 4°C. Three or four seeds were pipetted onto individual tubes and placed into a growth cabinet (Fitotron; SANYO, http://sanyo-av.com) with the following growth conditions: 8.5 h light/15.5 h dark at 21/19°C, with an average of 120 lmol m_{-2} s_{-1} photons at the top of the collection tubes and a relative humidity of 70%. Four days later seedlings were removed to leave one seedling per pot, which was grown for 5 weeks until sampling. All pots were watered twice per week by applying 5 ml of autoclaved distilled water to the Petri dishes, using a 5-ml pipette (Starlab, https://www.starlabgroup.com). The final watering date was set at 3 days before

sampling, which resulted in consistent soil water contents at the time of sampling. The relative water content (RWC) was determined by the ratio of soil weight (W) minus soil dry weight (DW), divided by water-saturated soil weight (SW) minus soil dry weight: RWC = (W ± DW)/ (SW ± DW).

The watering regime applied provided reproducible RWC values at the time of sampling (88 ± 4.5%). Although the RWC during the cultivation of plants was frequently lower, the relatively high RWC value at the time of sampling allowed for constant and relatively high recovery volumes (4–4.5 ml) from the soil matrix.

Collection tubes for the maize experiments were constructed by melting 7-mm holes in the base of 50-ml plastic tubes. Tubes were fitted with Miracloth at the bottom and filled with a water-saturated mixture of agricultural soil/autoclaved perlite (75 : 25; v/ v), in order to allow for a sufficient collection volume 1 min after the application of extraction solutions (see below). Soil was collected from an arable field (Spen Farm, Leeds, UK), air-dried, sieved to a maximum particle size of 4.75 mm and homogenized using a mixer. Maize seeds (Z. mays variety W22) were surface sterilized for 3 h by placing them in Petri dishes in an airtight container with 100 ml of bleach, to which 5 ml of concentrated HCl had been added. Seeds were imbibed overnight in autoclaved, sterile water before placing on Petri dishes containing sterile, damp filter paper in the dark at 23°C for 2 days. Germinated seeds were planted in filled collection tubes, 1.5 cm from the soil surface. Collection tubes were wrapped in foil, covered with black plastic beads and placed in a growth chamber with the following conditions: 12 h light/12 h dark at 25/20°C. The additional maize experiment to profile distal rhizosphere chemistry is described in Appendix S1.

Profiling of root associated microbial communities Details about DNA extraction, 16S rRNA gene sequencing and analysis of root-associated prokaryotic OTUs are presented in Appendix S1.

Metabolite extraction from control and Arabidopsis/maize soil Plant soil samples were collected from tubes containing one 5-week-old Arabidopsis plant or one 17-day-old maize plant. Plant soil chemistry was analysed from five replicated samples, whereas control soil chemistry was analysed from three replicated samples. All samples were collected at the same time. For the Arabidopsis system, cold extraction solution (5 ml) containing 0, 50 or 95% methanol (v/v) with 0.05% formic acid (v/v) was applied to the top of the tubes. After 1 min, 4.0–4.5 ml was collected from the drainage hole in 5-ml centrifuge tubes (Starlab). For the maize system, 15 ml of the 50% methanol solution (0.05% formic acid, v/v) was applied and flushed through the soil by applying pressure to the top of the pot, using a modified lid containing a syringe. After 1 min, 10 ml was collected in centrifuge tubes. For both cultivation systems, extracts were centrifuged to pellet soil residues (5 min, 3500 g), after which 4 ml of supernatant was transferred into a new centrifuge tube and flash-frozen in liquid nitrogen, freeze-dried for 48 h until complete dryness (Modulyo benchtop freeze dryer; Edwards, https://www.edwardsvacuum.com), and stored at -80°C. Dried aliquots were re-suspended in 100 ll of methanol : water : formic acid (50 : 49.9 : 0.1, v/v), sonicated at 4°C for 20 min, and vortexed and centrifuged (15 min, 14 000 g, 4°C) to remove potential particles that could block the UPLC column. Final supernatants (80 ll) were transferred into glass vials containing a glass insert prior to UPLC-Q-TOF analysis.

Assessment of cell damage by extraction solutions The effects of acidified extraction solutions on the integrity of root cells were determined by conductivity measurement from electrolyte leakage and epifluorescence microscopy of transgenic YFP-expressing roots, as detailed in Appendix S1. The effects of extraction solutions on culturable soil bacteria and introduced soil- and rhizosphere-colonising bacteria were determined by dilution plating, as described in Appendix S1.

UPLC-Q-TOF analysis of soil chemistry Details of the UPLC-Q-TOF analysis, including the targeted detection of DIMBOA, and uni- and multivariate data analyses to deconstruct rhizosphere chemistry, are presented in Appendix S1.

ACCESSION NUMBERS

The sequences used in this study can be found in the European Nucleotide Archive (http://www.ebi.ac.uk/ena) under accession number PRJEB17782.

ACKNOWLEDGEMENTS

The authors would like to thank Bob Turner for advice and feedback on assessing bacterial viability, and Choong-Min Ryu for providing the B. subtilis 168 strain. The research was supported by a consolidator grant from the European Research Council (ERC no. 309944 'Prime-A-Plant'), a Research Leadership Award from the Leverhulme Trust (no. RL-2012-042) and an ERA-CAPS BBSRC grant (BB/L027925/1, 'BENZEX') to Jurriaan Ton and Stephen Rolfe. The Plant Production and Protection (P3) centre of the University of Sheffield supported Pierre Pétriacq's work. The authors declare no conflicts of interest.

SUPPORTING INFORMATION

Additional Supporting Information may be found in the online version of this article.
Figure S1. Rarefaction curves of 16S rRNA operational taxonomic units (OTUs).
Figure S2. Relative abundance of bacterial taxa.
Figure S3. Solvent polarity and extraction of rhizosphere chemistry.
Figure S4. Epifluorescence microscopy analysis of Arabidopsis root cell damage.
Figure S5. Reproducibility of metabolite profiles between experiments.
Figure S6. Binary PLS-DA analysis of metabolite profiles.
Figure S7. Details of quantitative differences in metabolites.
Figure S8. Relative quantities of benzoxazinoids.
Figure S9. Profiling distal rhizosphere chemistry.
Table S1. Putative identification of Arabidopsis metabolic markers.
Table S2. Putative identification of maize metabolic markers.
Appendix S1. Supplementary experimental procedures.

REFERENCES

Atwal, A.S., Teather, R.M., Liss, S.N. and Collins, F.W. (1992) Antimicrobial activity of 2-aminophenoxazin-3-one under anaerobic conditions. Can. J. Microbiol. 38, 1084–1088.
Badri, D.V. and Vivanco, J.M. (2009) Regulation and function of root exudates. Plant, Cell Environ. 32, 666–681.
Bakker, P.A.H.M., Berendsen, R.L., Doornbos, R.F., Wintermans, P.C.A. and Pieterse, C.M.J. (2013) The rhizosphere revisited: root microbiomics. Front. Plant Sci. 4, 165.
Berendsen, R.L., Pieterse, C.M.J. and Bakker, P.A.H.M. (2012) The rhizosphere microbiome and plant health. Trends Plant Sci. 17, 478–486.
Bowsher, A.W., Ali, R., Harding, S.A., Tsai, C.-J. and Donovan, L.A. (2016) Evolutionary divergences in root exudate composition among ecologically-contrasting helianthus species. PLoS One, 11, e0148280.
Boyes, D.C., Zayed, A.M., Ascenzi, R., McCaskill, A.J., Hoffman, N.E., Davis, K.R. and G€orlach, J. (2001) Growth stage-based phenotypic analysis of Arabidopsis: a model for high throughput functional genomics in plants. Plant Cell, 13, 1499–1510.
Bravin, M.N., Michaud, A.M., Larabi, B. and Hinsinger, P. (2010) RHIZOtest: a plant-based biotest to account for rhizosphere processes when assessing copper bioavailability. Environ. Pollut. (Barking Essex 1987) 158,3330–3337.
Bulgarelli, D., Garrido-Oter, R., M€unch, P.C., Weiman, A., Dr€oge, J., Pan, Y., McHardy, A.C. and Schulze-Lefert, P. (2015) Structure and function of the bacterial root microbiota in wild and domesticated barley. Cell Host Microbe 17, 392–403.
Cameron, D.D., Neal, A.L., van Wees, S.C.M. and Ton, J. (2013) Mycorrhizainduced resistance: more than the sum of its parts? Trends Plant Sci. 18,539–545.
Chaignon, V., Quesnoit, M. and Hinsinger, P. (2009) Copper availability and bioavailability are controlled by rhizosphere pH in rape grown in an acidic Cu-contaminated soil. Environ. Pollut. (Barking Essex 1987) 157,3363–3369.
van Dam, N.M. and Bouwmeester, H.J. (2016) Metabolomics in the rhizosphere: tapping into belowground chemical communication. Trends Plant Sci. 21, 256–265.
DeSantis, T.Z., Hugenholtz, P., Larsen, N. et al. (2006) Greengenes, a chimera-checked 16S rRNA gene database and workbench compatible with ARB. Appl. Environ. Microbiol. 72, 5069–5072.
Dessaux, Y., Grandcl_ement, C. and Faure, D. (2016) Engineering the rhizosphere. Trends Plant Sci. 21, 566–578.
Gamir, J., Cerezo, M. and Flors, V. (2014a) The plasticity of priming phenomenon activates not only common metabolomic fingerprint but also specific responses against P. cucumerina. Plant Signal. Behav. 9, e28916.
Gamir, J., Pastor, V., Kaever, A., Cerezo, M. and Flors, V. (2014b) Targeting novel chemical and constitutive primed metabolites against Plectosphaerella cucumerina. Plant J. 78, 227–240.
Glauser, G., Veyrat, N., Rochat, B., Wolfender, J.-L. and Turlings, T.C.J. (2013) Ultra-high pressure liquid chromatography-mass spectrometry for plant metabolomics: a systematic comparison of high-resolution quadrupole-time-of-flight and single stage Orbitrap mass spectrometers. J. Chromatogr. A 1292, 151–159.
Haase, S., Rothe, A., Kania, A., Wasaki, J., R€omheld, V., Engels, C., Kandeler, E. and Neumann, G. (2008) Responses to iron limitation in Hordeum vulgare L. as affected by the atmospheric CO_2 concentration. J. Environ. Qual. 37, 1254–1262.
Hao, D.C., Song, S.M., Mu, J., Hu, W.L. and Xiao, P.G. (2016) Unearthing microbial diversity of Taxus rhizosphere via MiSeq high-throughput amplicon sequencing and isolate characterization. Sci. Rep. 6, 22006.
Hassan, S. and Mathesius, U. (2012) The role of flavonoids in root-rhizosphere signalling: opportunities and challenges for improving plantmicrobe interactions. J. Exp. Bot. 63, 3429–3444.
Hinsinger, P., Plassard, C. and Jaillard, B. (2006) Rhizosphere: a new frontier for soil biogeochemistry. J. Geochem. Explor. 88, 210–213.
Jones, D.L., Nguyen, C. and Finlay, R.D. (2009) Carbon flow in the rhizosphere: carbon trading at the soil–root interface. Plant Soil, 321, 5–33.
Kaever, A., Lingner, T., Feussner, K., G€obel, C., Feussner, I. and Meinicke, P. (2009) MarVis: a tool for clustering and visualization of metabolic biomarkers. BMC Bioinformatics, 10, 92.
Kaever, A., Landesfeind, M., Possienke, M., Feussner, K., Feussner, I. and Meinicke, P. (2012) MarVis-Filter: ranking, filtering, adduct and isotope correction of mass spectrometry data. J. Biomed. Biotechnol. 2012, 263910.
Khan, Z.R., Hassanali, A., Overholt, W., Khamis, T.M., Hooper, A.M., Pickett, J.A., Wadhams, L.J. and Woodcock, C.M. (2002) Control of witchweed Striga hermonthica by intercropping with Desmodium spp., and the mechanism defined as allelopathic. J. Chem. Ecol. 28, 1871–1885.
Khorassani, R., Hettwer, U., Ratzinger, A., Steingrobe, B., Karlovsky, P. and Claassen, N. (2011) Citramalic acid and salicylic acid in sugar beet root exudates solubilize soil phosphorus. BMC Plant Biol. 11, 121.
Kuijken, R.C.P., Snel, J.F.H., Heddes, M.M., Bouwmeester, H.J. and Marcelis, L.F.M. (2014) The importance of a sterile rhizosphere when phenotyping for root exudation. Plant Soil, 387, 131–142.
Lakshmanan, V., Kitto, S.L., Caplan, J.L., Hsueh, Y.-H., Kearns, D.B., Wu, Y.- S. and Bais, H.P. (2012) Microbe-associated molecular patterns-triggered root responses mediate beneficial rhizobacterial recruitment in Arabidopsis. Plant Physiol. 160, 1642–1661.
Lev-Yadun, S. and Berleth, T. (2009) Expanding ecological and evolutionary insights from wild Arabidopsis thaliana accessions. Plant Signal. Behav. 4, 796–797.
Luna, E., van Hulten, M., Zhang, Y. et al. (2014) Plant perception of b-aminobutyric acid is mediated by an aspartyl-tRNA synthetase. Nat. Chem. Biol. 10, 450–456.
Lundberg, D.S., Lebeis, S.L., Paredes, S.H. et al. (2012) Defining the core Arabidopsis thaliana root microbiome. Nature, 488, 86–90.
Mac_ıas, F.A., Mar_ın, D., Oliveros-Bastidas, A., Castellano, D., Simonet, A.M. and Molinillo, J.M.G. (2005) Structure-Activity Relationships (SAR) studies of benzoxazinones, their degradation products and analogues. Phytotoxicity on standard target species (STS). J. Agric. Food Chem. 53, 538–548.
Marti, G., Erb, M., Boccard, J. et al. (2013) Metabolomics reveals herbivore induced metabolites of resistance and susceptibility in maize leaves and roots. Plant, Cell Environ. 36, 621–639.
Neal, A.L. and Ton, J. (2013) Systemic defense priming by Pseudomonas putida KT2440 in maize depends on benzoxazinoid exudation from the roots. Plant Signal. Behav. 8, e22655.
Neal, A.L., Ahmad, S., Gordon-Weeks, R. and Ton, J. (2012) Benzoxazinoids in root exudates of maize attract Pseudomonas putida to the rhizosphere. PLoS One, 7, e35498.
Neumann, G., George, T.S. and Plassard, C. (2009) Strategies and methods for studying the rhizosphere—the plant science toolbox. Plant Soil, 321, 431–456.
Oburger, E. and Schmidt, H. (2016) New methods to unravel rhizosphere processes. Trends Plant Sci. 21, 243–255.
Oburger, E., Dell'mour, M., Hann, S., Wieshammer, G., Puschenreiter, M. and Wenzel, W.W. (2013) Evaluation of a novel tool for sampling root exudates from soil-grown plants compared to conventional techniques. Environ. Exp. Bot. 87, 235–247.
Pastor, V., Gamir, J., Cama~nes, G., Cerezo, M., S_anchez-Bel, P. and Flors, V. (2014) Disruption of the ammonium transporter AMT1.1 alters basal defenses generating resistance against Pseudomonas syringae and Plectosphaerella cucumerina. Front Plant Sci. 5, 231.
Patra, M., Salonen, E., Terama, E., Vattulainen, I., Faller, R., Lee, B.W., Holopainen, J. and Karttunen, M. (2006) Under the influence of alcohol: the effect of ethanol and methanol on lipid bilayers. Biophys. J . 90, 1121–1135.
Pétriacq, P., Stassen, J.H. and Ton, J. (2016a) Spore density determines infection strategy by the plant-pathogenic fungus Plectosphaerella cucumerina. Plant Physiol. 170, 2325–2339.
Pétriacq, P., Ton, J., Patrit, O., Tcherkez, G. and Gaki_ere, B. (2016b) NAD acts as an integral regulator of multiple defense layers. Plant Physiol. 172, 1465–1479.
Phillips, R.P., Erlitz, Y., Bier, R. and Bernhardt, E.S. (2008) New approach for capturing soluble root exudates in forest soils. Funct. Ecol. 22, 990– 999.
Planchamp, C., Glauser, G. and Mauch-Mani, B. (2014) Root inoculation with Pseudomonas putida KT2440 induces transcriptional and metabolic changes and systemic resistance in maize plants. Front. Plant Sci. 5, 719.
Prithiviraj, B., Paschke, M.W. and Vivanco, J.M. (2007) Root communication: the role of root exudates. Encycl. Plant Crop Sci. 1–4. https://doi.org/10. 1081/E-EPCS-120042072

Robert, C.A.M., Veyrat, N., Glauser, G. et al. (2012) A specialist root herbivore exploits defensive metabolites to locate nutritious tissues: a root herbivore exploits plant defences. Ecol. Lett. 15, 55–64.
Rudrappa, T., Czymmek, K.J., Par_e, P.W. and Bais, H.P. (2008) Root-secreted malic acid recruits beneficial soil bacteria. Plant Physiol. 148, 1547–1556.
Sgherri, C., Cecconami, S., Pinzino, C., Navari-Izzo, F. and Izzo, R. (2010) Levels of antioxidants and nutraceuticals in basil grown in hydroponics and soil. Food Chem. 123, 416–422.
Shi, S., Richardson, A.E., O'Callaghan, M., DeAngelis, K.M., Jones, E.E., Stewart, A., Firestone, M.K. and Condron, L.M. (2011) Effects of selected root exudate components on soil bacterial communities. FEMS Microbiol. Ecol. 77, 600–610.
da Silva Lima, L., Olivares, F.L., Rodrigues de Oliveira, R., Vega, M.R.G., Aguiar, N.O. and Canellas, L.P. (2014) Root exudate profiling of maize seedlings inoculated with Herbaspirillum seropedicae and humic acids. Chem. Biol. Technol. Agric. 1, 1–18.
Smalla, K., Sessitsch, A. and Hartmann, A. (2006) The rhizosphere: "soil compartment influenced by the root". FEMS Microbiol. Ecol. 56, 165.
Smith, C.A., Want, E.J., O'Maille, G., Abagyan, R. and Siuzdak, G. (2006) XCMS: processing mass spectrometry data for metabolite profiling using nonlinear peak alignment, matching, and identification. Anal. Chem. 78, 779–787.
Song, F., Han, X., Zhu, X. and Herbert, S.J. (2012) Response to water stress of soil enzymes and root exudates from drought and non-drought tolerant corn hybrids at different growth stages. Can. J. Soil Sci. 92, 501–507.
Strehmel, N., B€ottcher, C., Schmidt, S. and Scheel, D. (2014) Profiling of secondary metabolites in root exudates of Arabidopsis thaliana. Phytochemistry,108, 35–46.
Swenson, T.L., Jenkins, S., Bowen, B.P. and Northen, T.R. (2015) Untargeted soil metabolomics methods for analysis of extractable organic matter. Soil Biol. Biochem. 80, 189–198.
Szoboszlay, M., White-Monsant, A. and Moe, L.A. (2016) The effect of root exudate 7,4'-dihydroxyflavone and naringenin on soil bacterial community structure. PLoS One, 11, e0146555.
Tavakkoli, E., Rengasamy, P. and McDonald, G.K. (2010) The response of barley to salinity stress differs between hydroponic and soil systems. Funct. Plant Biol. 37, 621–633.
Uren, N. (2007) Types, amounts, and possible functions of compounds released into the rhizosphere by soil-grown plants. In The Rhizosphere: Biochemistry and Organic Substances at the Soil- Plant Interface (Pinton, R., Varanini, Z. and Nannipieri, P. eds). pp. 19–40. Marcel Dekker, Inc, New York, pp. 1–21.
Vranova, V., Rejsek, K., Skene, K.R., Janous, D. and Formanek, P. (2013) Methods of collection of plant root exudates in relation to plant metabolism and purpose: a review. J. Plant Nutr. Soil Sci. 176, 175–199.
Xia, J., Sinelnikov, I.V., Han, B. and Wishart, D.S. (2015) MetaboAnalyst 3.0 —making metabolomics more meaningful. Nucleic Acids Res. 43, 251– 257.
Yi, H.-S., Ahn, Y.-R., Song, G.C., Ghim, S.-Y., Lee, S., Lee, G. and Ryu, C.-M. (2016) Impact of a bacterial volatile 2,3-butanediol on Bacillus subtilis rhizosphere robustness. Front. Microbiol. 7, 993.
Yin, H., Wheeler, E. and Phillips, R.P. (2014) Root-induced changes in nutrient cycling in forests depend on exudation rates. Soil Biol. Biochem. 78, 213–221.
Zhang, D., Zhang, C., Tang, X., Li, H., Zhang, F., Rengel, Z., Whalley, W.R., Davies, W.J. and Shen, J. (2016) Increased soil phosphorus availability induced by faba bean root exudation stimulates root growth and phosphorus uptake in neighbouring maize. New Phytol. 209, 1–9.
Ziegler, J., Schmidt, S., Chutia, R., M€uller, J., B€ottcher, C., Strehmel, N., Scheel, D. and Abel, S. (2015) Non-targeted profiling of semi-polar metabolites in Arabidopsis root exudates uncovers a role for coumarin secretion and lignification during the local response to phosphate limitation. J. Exp. Bot. 67, 1421–1432.

Acknowledgements

Thanks to my people. Some words for those who inspired me;

Little Isaac, littler Sam & Rory – life is bigger than work. Never stop dreaming.

My friends; Emily, for staying my kindest friend, despite all the years. Jamie and Amy, for all the wine and for breaking my heart twice in 2 years! Carl and Max, for 10 years of trash-talk and excursions. Jim, for being my brother; we survived the tide. Katie, for the consistent support, exercise, milche and fun. Luke, for helping me to see the (Gerard) way. Dobbo, for being a bro. Carly and Speth, for all the tears, frowns, smiles and laughs. Mike, you hurricane.

Lou and Danny, for being family. Sarah, for being a second mum when mine no longer could. She'd be ever so grateful.

Thanks to my siblings – you keep me level-headed and always squash my delusions of grandeur. Nick, for (interrupted) games, Asian adventures and whisky; Rach, for bringing two gorgeous nephews, and one gorgeous lady, into my life; Fran, the greatest brother a boy could have (apart from Phil & Nick); Phil, for amusing and inspiring me with your writing; Marta for being there for Phil, the guy is hopeless; Dan, for being my hero; and Christen, for being my sister, friend, confidante and councillor. Finally, Dad, for being my unerring philosophical, theological, scientific and financial safety net.

To my colleagues; Anne, your jaded and humorous perspective on work makes me seriously ambivalent. Sarah, for the coffees and cheese when Pierre left me. Roland, for occasionally beating me at squash. David, for being a bloody handsome tech. My supervisors; Jurriaan, for having faith in me from the beginning and for teaching me that you don't need to sacrifice being a good person to be a good scientist. David, for your feedback. Finally, to Pierre, you stood by me and encouraged me through every part of my PhD. You take on so much but ask so little - your ability to balance the demands of academia with outrageous fun really motivating. Don't change!

Thanks to my co-pilot Kat, the most kind and magnanimous friend I could ever hope for, without you I'd have crashed long ago. We've suffered and laughed together and even in those ugliest of days I wouldn't change a moment. Words are never enough to explain how much your love and support (often undeserving) mean to me. No one is perfect, but the cracks in your flawlessness helped light my way.

Finally, I'd like to thank my mum, to whom this work is dedicated. She raised me into the man I am. She taught me see the beauty in the undeserving, and to love, even when my heart hurts. Her tenacity taught me the strength to strive and the grace to fail, although I never had her humility in doing so. I can only hope to emulate her qualities. And despite it all, she couldn't see her worth. To mum; I wish you could know how much I admire you and how inspiring you were to everyone who knew you. Our achievements were yours too.